

N O T I C E

THIS DOCUMENT HAS BEEN REPRODUCED FROM
MICROFICHE. ALTHOUGH IT IS RECOGNIZED THAT
CERTAIN PORTIONS ARE ILLEGIBLE, IT IS BEING RELEASED
IN THE INTEREST OF MAKING AVAILABLE AS MUCH
INFORMATION AS POSSIBLE

DOE/NASA/0147-1
NASA CR-165449

Low NO_x Heavy Fuel Combustor Concept Program

Phase I Final Report

Martin B. Cutrone
General Electric Company

(NASA-CR-165449) LOW NO_x HEAVY FUEL
COMBUSTOR CONCEPT PROGRAM, PHASE 1 Final
Report (General Electric Co.) 251 p
HC A12/MF A01

N82-24651

CSCI 10B

Unclass

G3/44 09977

October 1981

Prepared for
NATIONAL AERONAUTICS AND SPACE ADMINISTRATION
Lewis Research Center
Under Contract DEN 3-147

for
U.S. DEPARTMENT OF ENERGY
Fossil Energy
Office of Coal Utilization

Low NO_x Heavy Fuel Combustor Concept Program

Phase I Final Report

Martin B. Cutrone
GE Program Manager
General Electric Company
Schenectady, New York 12345

October 1981

Prepared for
National Aeronautics and Space Administration
Lewis Research Center
Cleveland, Ohio 44135
Under Contract DEN 3-147

for
U.S. DEPARTMENT OF ENERGY
Fossil Energy
Office of Coal Utilization
Washington, D.C. 20545
Under Interagency Agreement DE-AI01-77ET13111

TABLE OF CONTENTS

Section		Page
1	ABSTRACT	1-1
2	EXECUTIVE SUMMARY	2-1
	2.1 Background and Program Objectives	2-1
	2.2 Test Fuels	2-2
	2.3 Combustor Concepts Studied	2-3
	2.3.1 Rich/Lean Combustors	2-4
	2.3.2 Lean/Lean Combustors	2-5
	2.3.3 Catalytic Combustor Concept	2-7
	2.4 Combustion Test Results	2-7
	2.4.1 Rich/Lean Combustor Tests	2-7
	2.4.2 Lean/Lean Combustor Tests	2-12
	2.5 Conclusions and Recommendations	2-13
3	INTRODUCTION	3-1
	3.1 Background	3-1
	3.2 Program Objectives and Specific Goals	3-1
	3.3 Program Scope and Approach	3-2
	3.4 Report Contents	3-4
4	TEST FUELS	4-1
5	TEST FACILITIES	5-1
	5.1 Fuel-Handling System	5-1
	5.2 Air Supply System and A5 Test Facility	5-5
	5.3 Test Rig	5-6
	5.4 Instrumentation	5-9
	5.5 Emissions Measurement System	5-10
6	COMBUSTOR TEST CONDITIONS	6-1
7	COMBUSTOR CONCEPTS	7-1
	7.1 Rich/Lean Combustor Concepts	7-4
	7.1.1 Rich/Lean Combustor with Premixing, Concept 1A	7-5
	7.1.2 Rich/Lean Combustor with Multiple-Nozzle Dome, Concept 2	7-6
	7.1.3 Rich/Lean Combustor with Narrow Passage Quench, Concept 3	7-8
	7.2 Lean/Lean Combustor Concepts	7-9
	7.2.1 Series-Staged Lean/Lean Combustor, Concept 4	7-11

TABLE OF CONTENTS (CONT'D)

Section	Page
7.2.2 Series-Staged Lean/Lean Combustor with Premixed Main Stage, Concept 5	7-14
7.2.3 Parallel-Staged Lean/Lean Combustor, Concept 6	7-18
7.2.4 Summary	7-22
7.3 Lean Reaction Catalytic Combustor Concept	7-24
7.3.1 Overall Arrangement and Fuel/Air Scheduling	7-25
7.3.2 Fuel/Air Preparation	7-28
7.3.3 Catalytic Reactor Section	7-33
7.3.4 Downstream Pilot Stage Section	7-33
7.4 Fuel Nozzle Designs	7-33
 8 COMBUSTOR TEST RESULTS	 8-1
8.1 Rich/Lean Combustor Test Results	8-1
8.1.1 Rich/Lean Combustor with Premix, Concept 1A	8-1
8.1.2 Rich/Lean Combustor with Multiple Nozzle Dome, Concept 2	8-9
8.1.3 Rich/Lean Combustor with Narrow Passage Quench Zone, Concept 3	8-33
8.2 Lean/Lean Combustor Test Results	8-42
8.2.1 Series-Staged Lean/Lean Combustor, Concept 4	8-44
8.2.2 Series-Staged Lean/Lean Combustor with Premixed Main Stage, Concept 5	8-65
8.2.3 Parallel-Staged Lean/Lean Combustor, Concept 6	8-73
8.3 NO _x Yield from Fuel Nitrogen	8-81
8.4 Catalytic Combustor Test Results	8-88
 9 DATA EVALUATION AND CONCLUSIONS	 9-1
9.1 Rich/Lean Combustor Concepts	9-1
9.1.1 Data Correlations	9-1
9.1.2 Summary and Evaluation, Rich/Lean Combustors	9-6
9.1.3 Problem Areas/Required Development for Rich/Lean Combustors	9-12
9.1.4 Conclusions	9-13
9.2 Lean/Lean Combustor Concepts	9-13
9.2.1 Data Correlations	9-13
9.2.2 Summary and Conclusions, Lean/Lean Combustor Concepts	9-21
9.2.3 Problem Areas/Required Development for Lean/Lean Combustors	9-22

TABLE OF CONTENTS (CONT'D)

Section	Page
10 CONCEPTUAL DESIGNS OF PHASE II COMBUSTORS	
10.1 Rich/Lean Combustor Design Recommended for Phase II	
10.2 Conceptual Design of Lean/Lean Combustor for MS7001E Cycle	
10.2.1 Introduction	
10.2.2 Discussion	
10.3 Application of NASA/DOE Dry Low NO _x Heavy Fuels Program Results to Other Cycles	
10.3.1 Lean/Lean Concept 6 for the LM2500 Cycle	
10.3.2 Rich/Lean Concept 3 for the LM2500 Cycle	
10.3.3 Lean/Lean Combustor for LM5000 Application	
Appendix A—Low NO _x Heavy Fuel Combustor Concept Program Report—Preliminary Results on a Low NO _x Lean Burn Catalytic Combustion Concept	A-1
Appendix B—Analysis of Subscale Catalytic Reactor Test Series I	B-1
Appendix C—Low NO _x Heavy Fuel Combustor Concept Program Report—Further Results on a Low NO _x Lean Burn Catalytic Combustion Concept	C-1

Section 1

ABSTRACT

The Low NO_x Heavy Fuel Combustor Concept Program is part of the DOE/LeRC Advanced Conversion Technology Project (ACT), with funding provided by DOE and program management by NASA/LeRC. This report describes the results of the General Electric Phase I Program to evaluate the potential of several advanced combustor concepts for achieving dry low NO_x emissions with high nitrogen content fuels.

Combustion tests were completed with seven concepts, including three rich/lean concepts, three lean/lean concepts, and one catalytic combustor concept. Testing was conducted with ERBS petroleum distillate, petroleum residual, and SRC-II coal-derived liquid fuels over a range of operating conditions for the 12:1 pressure ratio General Electric MS7001E heavy-duty turbine. Blends of ERBS and SRC-II fuels were used to vary fuel properties over a wide range. In addition, pyridine was added to the ERBS and residual fuels to vary nitrogen level while holding other fuel properties constant.

Test results indicate that low levels of NO_x and fuel-bound nitrogen conversion can be achieved with the rich/lean combustor concepts for fuels with nitrogen contents up to 1.0% by weight. Multinozzle rich/lean Concept 2 demonstrated dry low NO_x emissions within 10%-15% of the EPA New Source Performance Standards goals for SRC-II fuel, with yields of approximately 15%, while meeting program goals for combustion efficiency, pressure drop, and exhaust gas temperature profile. Similar, if not superior, potential was demonstrated by Concept 3, which is a novel and promising rich/lean combustor design. This combustor formed the basis for the design of the combustor vehicle recommended for development to prototype level in Phase II for high-nitrogen coal-derived liquid fuels and low and intermediate heating value coal-derived gases.

Smoke emissions for the rich/lean combustors were higher than program goals, but a major improvement was achieved with only minor modification to the fuel nozzles, and further improvement can be expected. Liner metal temperatures were excessive when compared to current production combustor hardware and significant improvements were identified in the proposed Phase II conceptual combustor design.

Lean/lean combustor Concept 4 demonstrated performance which shows potential for achieving ultralow NO_x emissions (one-half NSPS limits) with petroleum distillate fuel, and meeting emissions goals dry with fuels containing up to 0.25 weight percent fuel nitrogen. Pressure drop, exhaust gas profile, and liner metal temperature goals were also met. Combustion efficiency goals were met over the bulk of the operating range, except at very load loads and at pilot/main stage crossover.

Subscale tests of the catalytic combustor reactor section demonstrated ultralow NO_x performance with clean fuels. A 20 cm (8 in.) diameter catalytic combustor was fabricated and will be tested with distillate and simulated low and intermediate heating value coal gases in the on-going Phase IA program.

Section 2

EXECUTIVE SUMMARY

2.1 BACKGROUND AND PROGRAM OBJECTIVES

A decline in the availability of petroleum fuels is projected to occur in the 1980s and accelerate throughout the 1990s. This is particularly true with regard to the petroleum distillate fuels currently used in many stationary power generation sources. Faced with declining supply, these are expected to be devoted to transportation and other consumer use. The availability decline will be accompanied by continued cost increases.

Fuel supplied for power generation equipment must thus move towards the utilization of petroleum products of lower cost and quality, and towards the combustion of coal-derived liquids (CDL) and gaseous fuels. Furthermore, because of the projected higher costs, increasingly stringent emissions requirements, and the uncertainty in the projected mix of fuels to be available, combustion systems for gas turbines must be efficient, environmentally acceptable, and have fuels flexibility. Lower quality petroleum residual fuels and CDLs have higher fuel-nitrogen content and lower hydrogen content requiring significant improvements in current production combustion technology to meet emissions and operational performance requirements.

Coal-derived gaseous fuels include both low Btu (LBTU) and intermediate Btu (IBTU) heating-value fuels. Although Phase I testing to date has been restricted to liquid fuels, the rich/lean combustion technology discussed in this report is applicable to LBTU gas and to IBTU gas, the latter generally characterized by high flame temperature and thus a tendency for high thermal NO_x , combined with the potential of organic nitrogen which can lead to organic NO_x .

Given these requirements, General Electric has completed the first phase (Phase I) of a multiphase program to develop dry low NO_x combustion technology under the sponsorship of the National Aeronautics and Space Administration (NASA). This report discusses the results of the Phase I work directed towards developing basic technology for low NO_x combustion of high-nitrogen liquid fuels. The on-going Phase IA effort will complete screening tests of the most promising Phase I combustor concepts with coal-derived gaseous fuels.

Current planning calls for completion of a Phase II effort to develop the detailed design of a machine combustor, with Phase III to accomplish a field demonstration of a low NO_x combustion system. The Phase I combustion technology data base has been used to generate the conceptual design of the combustor vehicle recommended for development in Phase II.

The objectives of the program described in this report were to develop low NO_x combustor technology to meet current U.S. EPA NSPS emissions requirements and operational performance standards for operation of the General Electric MS7001E tur-

bine with high-nitrogen fuels, and with fuels flexibility. A goal was established to meet these requirements dry, i.e., without the use of water injection for NO_x suppression. Dry operation leads to improved cycle efficiency to offset expected higher fuel costs, and to the elimination of investment and operating expenses associated with water injection systems. Furthermore, water and steam injection is successful in reducing thermal NO_x but actually increases NO_x from fuel-bound nitrogen sources.

2.2 TEST FUELS

SRC-II coal-derived middle-distillate liquid, ERBS petroleum distillate, petroleum residual fuels, and blends of these three fuels were used for combustion tests. In addition, pyridine was added in various percentages to increase the concentration of fuel nitrogen. The ERBS fuel was a middle-petroleum distillate with 12.95% hydrogen and essentially no fuel-bound nitrogen. The solvent-refined coal SRC-II fuel had only 9.07% hydrogen content and a high level of fuel-bound nitrogen at 0.87% by weight. The residual had a 294 K (70 °F) pour point and contained significant levels of vanadium and 0.23 weight percent fuel-bound nitrogen. Heated storage tanks and fuel supply lines were required when using this fuel. With the three types of fuel used, plus the blending and the pyridine doping, a very wide range of fuel properties was available for evaluating the combustor concepts. Table 2-1 presents the properties of the test fuels.

Table 2-1
FUEL PROPERTIES

	ERBS*	SRC II	Residual
Specific Gravity @ 298/298 K	0.8377	0.9796	0.9440
Hydrogen Content, Percent	12.95	9.07	11.52
Sulfur Content, Percent	0.085	0.20	0.49
Net Heat of Combustion, MJ/kg (Btu/lb)	42.5 (18,275)	38.1 (16,365)	41.3 (17,748)
Viscosity, M^2/S @ 311 K	1.36×10^{-6}	3.55×10^{-6}	1.345×10^{-3}
Nitrogen Content, Percent	0.0054	0.87	0.23
Surface Tension, N/m	—	—	3.29×10^{-2} @ 339 K
Surface Tension, N/m	—	—	3.06×10^{-2} @ 366 K
Pour Point, K (°F)	244 (−20)	255 (−55)	294 (70)
Vanadium	—	—	26 ppm

* Experimental Referee Broad Specification petroleum distillate fuel

† Supplier's data

Listed below are the two key properties to be accommodated in development of successful dry low NO_x combustors for application to nitrogen heavy fuels, i.e., hydrogen and organic nitrogen-content.

	<u>ERBS</u>	<u>RESIDUAL</u>	<u>SRC-III</u>
Weight Percent Nitrogen	0.0054	0.23	0.87
Weight Percent Hydrogen	12.9	11.52	9.07

Rich combustion is required to minimize the formation of NO_x from fuel-bound nitrogen. It may be noted that the increasing nitrogen content of these fuels has an associated decrease in hydrogen content. Low hydrogen content increases the tendency for smoke formation which further enhances the smoke potential associated with rich combustion. In addition, the low hydrogen content and resulting low H/C ratios produce more radiant flames which, with the special requirement of avoiding stoichiometric zones near the combustor walls that would be generated from film cooling in rich-stage liners, lead to concerns for adequate cooling of rich-stage liner walls. These combustion characteristics were the primary subjects of test investigation in this program.

2.3 COMBUSTOR CONCEPTS STUDIED

Six advanced combustor concepts were tested, including three rich/lean and three lean/lean staged combustors. Figure 2-1 shows the test hardware fabricated and subsequently tested. A lean-reaction catalytic combustor concept was also fabricated (see Figure 2-2) and will be tested on liquid fuel and simulated coal-derived LBTU and IBTU gases during the ongoing Phase IA test program, along with the most promising rich/lean and lean/lean combustors emerging from the Phase I effort, i.e., Concepts 2 and 4, respectively.

The combustor hardware was 20 cm (8 in.) in diameter and designed for tests at the General Electric MS7001E cycle conditions. The 20 cm (8 in.) combustors were scaled to preserve the mass flux inherent in the MS7001E 72 MWe machine. The large-scale test hardware, at MS7001E cycle conditions of 1358 K (1985 °F) firing

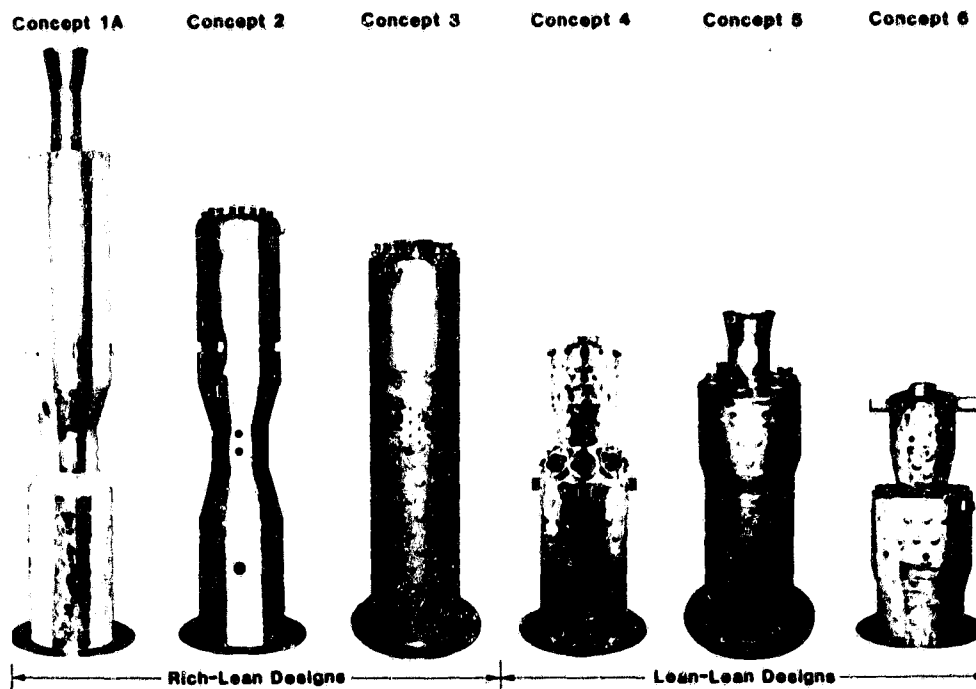


Figure 2-1. NASA DOE low NO_x heavy fuel combustor concepts

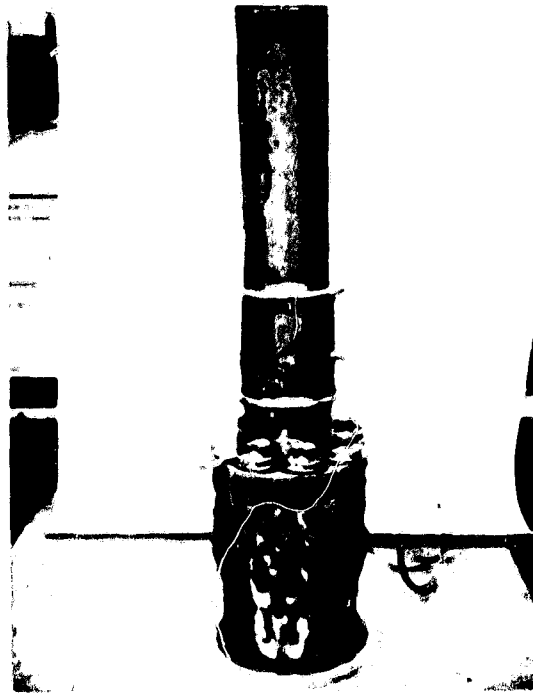


Figure 2-2. Catalytic combustor, Concept 8

temperature and 12:1 pressure ratio, includes combustor detail directly analogous to commercial combustors and has an energy output essentially equal to the 25 MWe General Electric MS5001 turbine. The large scale and realistic component detail were selected to minimize the effect of scaling the derived Phase I low NO_x test results to the 35.6 cm (14 in.) diameter full-scale size of the MS7001E combustion system.

2.3.1 Rich/Lean Combustors

Rich/lean combustion is required to achieve dry low NO_x emissions with the high-nitrogen fuels emphasized in the Phase I test program. In this combustion mode, a rich mixture of fuel and air ($\Phi = 1.7$) is burned in the first stage, producing incomplete combustion at lower flame temperatures in an oxygen-deficient environment. Under these conditions, little thermal NO_x is produced while fuel nitrogen is released with minimal conversion to NO_x . This incompletely combusted mixture is then mixed with additional combustion air in a low residence time quench zone to produce a lean mixture ($\Phi = 0.5$) with combustion completed in the lean second stage.

Rich/Lean Combustor with Premixing, Concept 1A

Concept 1A contains a single fuel nozzle and swirl cup in a premixing tube ahead of the rich stage. The premix tube should provide uniform mixing of fuel and air. Following the rich stage is a necked-down quench zone where secondary air is introduced and mixed with the products of combustion from the rich stage in minimum time. This shifts the stoichiometry from rich to lean and is followed by combustion in the final lean stage. Figure 2-1 shows Concept 1A with the premix tube at the top of the figure, followed by the convectively cooled rich stage, quench

zone, and lean stage. The elongated holes in the converging section of the quench zone provide for entrance of secondary air to be rapidly mixed with the rich-stage products while accelerating through the necked-down section between rich and lean stages. Rich-stage liner cooling is accomplished by convection cooling of the outside of the liner. A thermal barrier coating was applied to the inside of the rich stage to minimize heat transfer from combustion gases to the liner wall.

Nominal rich-stage equivalence ratios of 1.4 to 2.0 were tested, with a lean-stage equivalence ratio of 0.54. The test combustor is 20 cm (8 in.) in diameter with an overall length of approximately 137 cm (54 in.) including the premix tube and downstream dilution section.

Rich/Lean Combustor with Multiple-Nozzle Dome, Concept 2

This combustor was designed to have the same rich and lean stage equivalence ratios as Concept 1A, but to have multiple fuel nozzles and swirlers to prepare the rich-stage fuel/air mixture. Figure 2-1 shows combustor Concept 2 with eight fuel nozzles and swirl cups in the head end of the rich stage. Following the rich stage is the necked-down quench zone followed by the lean stage. In addition to the multiple nozzle head-end, this combustor differs from Concept 1A in that the rich stage was shorter and the holes for admission of mixing air to the products leaving the rich stage are in the smaller diameter quench zone. Note in Figure 2-1 that the rich stage is again not cooled by air penetrating the rich stage through liner cooling holes, but rather by backside convection cooling and the application of a thermal barrier coating to the inside surface of the rich stage. The test combustor is 20 cm (8 in.) in diameter with an overall length of 127 cm (50 in.).

Rich/Lean Combustor, Concept 3

Concept 3 is a rich/lean combustor with multiple fuel nozzles and swirl cups. Following the rich stage is a narrow-passage mixing stage, where secondary and dilution air is introduced and mixed with the products of combustion from the rich stage in minimum time so as to produce minimum additional thermal NO_x . This combustor has the same multinozzle fuel injector/air swirler head-end and rich- and lean-stage equivalence ratios as for Concept 2. It differs in the design of the annular narrow quench passage between rich and lean stages.

As for combustor Concepts 1 and 2, the rich-stage liner is convectively cooled on the backside and sprayed with thermal barrier coating on the inside. The major feature of Concept 3 that enhances low NO_x performance is the narrow passage quench zone. This minimizes the distance required for penetration of the rich-stage gases by the quench-jet air (rapid transition from rich to lean stoichiometry). This feature was responsible for the excellent thermal NO_x performance discussed in Section 2.4, and is the basis for recommendation for Concept 3 as the proposed Phase II conceptual design.

2.3.2 Lean/Lean Combustors

Three lean/lean combustors were fabricated and tested, and are shown at the right of Figure 2-1. Lean/lean combustors burn lean in both stages to avoid high

flame temperature, and thus avoid generation of thermal NO_x . Two stages of combustion are employed. At low engine power conditions when the total fuel-flow rates are low, only the pilot stage of the combustor is fueled. At higher power conditions when the engine fuel-flow rate is adequate to fuel both stages of the combustor, fuel is introduced into the main-stage dome and the pilot dome fuel flow is reduced. As the engine power and fuel-flow rates are increased, the fuel/air ratio in the main stage is increased and generally reaches an equivalence ratio of approximately 0.6 at max power.

Basic problems associated with lean/lean two-stage combustors include high fuel/air ratios and consequent smoke from the pilot stage before the main stage is in operation, and CO generation when the main stage is initially fueled.

Series-Staged Lean/Lean Combustor, Concept 4

This series-staged lean-burning combustor is shown in Figure 2-1. The combustor has a pilot stage utilizing a single air-atomizing fuel injector and a two-stage counterrotating swirl cup at the forward end. This pilot burner is used for light-off and operation up to approximately 70% of peak engine power rating. Combustion air is introduced into the pilot dome through the swirler and through a band of eight dilution holes located approximately one dome height aft of the fuel nozzle tip.

The main stage employs eight single-stage swirlers and air-atomizing fuel injectors. For this combustor, the objective is to obtain rapid mixing of the fuel and air in the main dome. No attempt is made to generate a strong, flame-stabilizing recirculation zone in the main stage. This is to avoid long gas residence times associated with recirculating zones that generate thermal NO_x . Instead, ignition of the main stage gases is provided by the hot gases from the pilot dome, which is used at all engine operating conditions. The overall length of this combustor is 63.5 cm (25 in.), the pilot-dome diameter is 15 cm (6 in.) and the aft liner diameter is 20 cm (8 in.).

Series-Staged Lean/Lean Combustor with Premixed Main Stage, Concept 5

This combustor is shown in Figure 2-1 and has a pilot stage with six dual counterrotating swirlers arranged in an annulus around the main stage premixing duct. The main-stage fuel is introduced into the forward duct and mixed with the air prior to entering the combustion zone through twelve axial slots at the aft end of the premixing duct. Air-atomizing fuel nozzles are employed for both the pilot and main stage of this combustor.

Parallel-Staged Lean/Lean Combustor, Concept 6

This combustor is shown in Figure 2-1. This concept has a low-velocity pilot stage with a single swirl cup and air-atomizing fuel injector at the dome end. The pilot dome is designed for ease of ignition and efficient combustion at low power conditions. The main stage has an annular high-velocity dome with six swirl cups and fuel injectors in a concentric arrangement around the discharge end of the pilot stage. The high dome velocities and lean fuel/air ratios employed in the main stage result in low gas temperatures and short residence times for minimized thermal NO_x emissions. The combustor is 53 cm (21 in.) in overall length, the pilot dome is 15 cm (6 in.) in diameter, and the diameter at the main-stage dome is 23 cm (9 in.).

2.3.3 Catalytic Combustor Concept

A lean-reaction catalytic combustor concept was fabricated to demonstrate ultralow thermal NO_x performance for the combustion of low-nitrogen fuels. The combustor will be tested on liquid distillate fuel and low and intermediate BTU coal gases during the on-going Phase IA test program. Figure 2-2 shows the catalytic combustor test hardware with the multiple-nozzle fuel preparation section at the top, followed by the catalytic reactor holder and the downstream pilot stage employed for ignition and operation to part load prior to catalytic reactor lightoff.

2.4 COMBUSTION TEST RESULTS

Six advanced combustor concepts were tested, including the three rich/lean and three lean/lean staged combustors. The lean catalytic combustor Concept 8 will be tested in the Phase IA effort. Initial screening tests were used to evaluate the potential of each concept, followed by selection of multiple-nozzle rich/lean Concept 2 and lean/lean Concept 4 as most promising. Modifications were made and testing was continued to develop these concepts to meet the program dry low NO_x goals. The two-stage rich/lean concept was expected to have the highest potential for low conversion of fuel nitrogen to NO_x and this was indeed confirmed.

Twenty-centimeter (eight-inch) diameter combustors were tested over a range of operating conditions characteristic of the General Electric MS7001E heavy-duty gas turbine used in utility power generation applications. The MS7001E turbine has a baseload rating of 72.9 MWe at a turbine inlet temperature of 1358 K (1985 °F), pressure ratio of 11.7, and airflow of approximately 250 kg/s (550 lb/s). The standard procedure was to evaluate the combustor over the load range for the MS7001E engine and to conduct additional tests as appropriate. Other test variables were also adjusted during the tests. For example, fuel/air ratios above and below design levels were tested for diagnostic purposes. Also, the fuel flow split between the pilot and main stage for combustors with two fuel stages was varied to determine the optimum operating conditions.

Table 2-2 presents an overall summary of the key combustor test results and their evaluation. Data are presented for tests of the last concept version tested, e.g., Concept 2-5 is the fifth development modification of Concept 2.

2.4.1 Rich/Learn Combustor Tests

Initial tests with Concept 1A, the single-nozzle rich/lean combustor with a premix tube ahead of the rich stage, resulted in high NO_x emissions caused by asymmetric fuel distribution attributed to nozzle misalignment. The rich-stage equivalence ratio was increased to take advantage of the observed rapid decrease in NO_x emissions with increasing rich-stage equivalence ratio, and retests of this combustor as Concept 1A-1 showed improved performance as shown in Table 2-2, although above program NO_x goals. A significant concern with this concept is overall combustor length which may be excessive for other than application to General Electric heavy-duty turbines. Based on the concern for liner length in Concept 1A and the improved mixing associated with the multiple-nozzle domes of rich/lean combustors 2 and 3, Concept 1A is not considered a prime candidate for development to prototype status

Table 2-2
PERFORMANCE SUMMARY
RICH/LEAN AND LEAN/LEAN COMBUSTOR CONCEPTS

Program Goals	Combustion Efficiency at Baseload					Exhaust Profile	Liner Temperature K (°F)	Comments and Evaluation
	NO _x Emissions (g NO _x /kg fuel)		Yield* (%)	Smoke† (SAE No.)	Pressure Drop (%)			
	ERBS 0.0054 wt % FBN	Residual 0.23 wt % FBN						
1. Concept 1A-1 <ul style="list-style-type: none">• Premix tube with single fuel nozzle• Cylindrical quench zone, quench holes in converging line	7.0	10.7	10.2	20	<6	<0.25	production combustor levels	<ul style="list-style-type: none">• Upstream-facing quench holes resulted in excessive thermal NO_x and higher than desired CO and smoke• Overall combustor length may be excessive for applications other than GE machines• Not recommended for Phase II; multinozzle combustors 2-5 and 3-1 provide good fuel/air mixing with shorter liner length
2. Concept 2-5 <ul style="list-style-type: none">• Multiple-nozzle dome• Cylindrical quench zone, quench holes in cylindrical zone	8.5	10.7	11.8	3	>99	7-8	met goal	<ul style="list-style-type: none">• Within 10%—15% of NO_x goals for all fuels• Smoke higher than goal, but improvement potential identified• Liner temperature excessive in test hardware
3. Concept 3-1 <ul style="list-style-type: none">• Multiple-nozzle dome• Narrow passage quench zone	7.8**	10.6**	12.7**	20 (at 100 psia)	>99	6	met goal	<ul style="list-style-type: none">• Thermal NO_x performance superior to Concept 2-5, due to excellent rich-to-lean transition accomplished by narrow quench zone• Yield equivalent to Concept 2-5• Liner pressure drop less than Concept 2-5, less ΔP required for rich-to-lean jet penetration because of narrow passage quench• Liner temperatures excessive in test hardware, improvements identified in Phase II conceptual design based on Concept 3-1• Recommended for prototype development in Phase II for COLS and LBTU/IBTU coal-derived gases with NH₃

FOLDOUT FRAME

• Narrow passage
quench zone

not to be used for narrow passage

- Yield equivalent to Concept 2-5 by narrow quench zone
- Liner pressure drop less than Concept 2-5, less ΔP required for rich-to-lean jet penetration because of narrow passage quench
- Liner temperatures excessive in test hardware, improvements identified in Phase II conceptual design based on Concept 3-1
- Recommended for prototype development in Phase II for CGLs and LBTU/IBTU coal-derived gases with NH_3 contamination

Lean/Lean Concepts

4. Concept 4-1	4.5	10.5	19.0	50	10	>99	5-6	met goal	~860 K (1100 °F) on air fuels	<ul style="list-style-type: none">• Meets NO_x goals on fuels with ≤ 0.25 wt % FBN• High CO at low loads and near pilot/main stage crossover — Phase II conceptual design should resolve these problems• High NO_x yield (50%) precludes application to high FBN fuels (SRC-II CDI)• Recommended for ultralow NO_x applications with clean liquid fuels, may be considered for low NO_x application with LBTU/IBTU gas without NH_3• Conceptual design provided for potential Phase II development
• Series staged										
5. Concept 5	5.0	9.0†	15.0†	35	20 @ Baseload 60 @ 50% load	96.5	See comments	See comments	See comments	<ul style="list-style-type: none">• Ultralow NO_x performance on clean fuel• Premix tube gutters burned out, residues† and SRC-II fuel data uncertain• High CO and low combustion efficiency require further development• High smoke at part loads• Not recommended for further consideration in Phase II
• Premixed main stage										
6. Concept 6	8.0	11.0	14.0	25††	22 (SRC-II) 10 (resid)	poor, high CO emissions	4-5	met goal	~1060 K (1450 °F) (ERBS and resid)	<ul style="list-style-type: none">• NO_x exceeds goals for fuels with FBN > 0.25%• Low-pressure drop can be utilized to improve thermal NO_x performance, expected to be similar to Concept 4-1• High CO and low combustion efficiency require development• Conceptual design provided for LM2500 application
• Parallel staged										

Notes:

- Yield of NO_x from organic nitrogen at 0.87 wt % organic nitrogen content (SRC-II)
- † Measured with SRC-II and residual fuels, i.e., low hydrogen content
- ‡ ERBS doped with pyridine to FBN levels approximating residual and SRC-II fuels
- Estimated from NO_x and yield data taken at 100 psia, using measured pressure correlation
- †† Unexpectedly low for lean combustion, further tests required to confirm

ORIGINAL PAGE IS
OF POOR QUALITY.

FOLDOUT FRAME

in Phase II. Concepts 2 and 3 (discussed next) embody the same basic rich/lean attributes of Concept 1A, with improved rich-stage fuel/air mixing from the multinozzle dome, and are the basis for the conceptual design of the rich/lean combustor recommended for Phase II development.

Multiple-nozzle rich/lean Concept 2 showed early promise for low NO_x emissions with acceptable operational performance (exhaust profiles, efficiency, pressure drop, etc.). The concept was developed through five series of modifications and retests, and Table 2-2 presents the best test performance with Concept 2-5. Table 2-2 shows that NO_x performance was within 10%–15% of program goals for all fuels, including the 0.87 weight percent nitrogen SRC-II fuel, with an organic NO_x yield of approximately 15%–20%. Smoke, although higher than the program goal, was reduced by a factor of 2 by a minor air swirler modification made in producing Concept 2-5. Further improvement can be expected in Phase II. Liner temperature for the backside-cooled, thermal barrier coated rich stage of the screening test hardware was excessive. In order to concentrate program resources on development of aerodynamic features for best NO_x performance, no attempt was made to refine the rich-stage heat transfer design. Improved rich-stage heat transfer will be addressed in Phase II and is accounted for in the Phase II combustor conceptual design discussed in Section 2-5. The summary of overall results for Concept 2-5 is as follows:

Concept 2-5 Performance Summary

- NO_x performance
 - Within 10%–15% of goals for ERBS, residual, and SRC-II fuels.
 - Low FBN yield, $\sim 15\%$, at bound nitrogen contents of 1%.
- Smoke at SAE 37 exceeds goals but
 - Significant improvement was achieved with only a minor swirler modification in the last test of Concept 2-5.
 - Further mixing developments in Phase II should lead to meeting the smoke goal.
- Combustion efficiency, pattern factor, and temperature profiles met program goals.
- Pressure drop was approximately 7%-8%, approaching the program goal.
- Liner metal temperatures were approximately 1175 K (1650 °F), exceeding desired values for commercial hardware.

Multiple-nozzle rich/lean Concept 3 is characterized by a narrow-passage quench-zone design which significantly improves jet penetration and mixing, effecting a rapid and homogeneous transition from rich-to-lean combustion. In other features, it is similar to Concept 2. Table 2-2 presents the performance data summary for Concept 3-1 (modification to basic Concept 3). The data show that Concept 3-1 met or is predicted to approach NO_x goals for all program fuels, with an organic NO_x yield of 15%–20% (as for Concept 2-5). Comparing the results of Concepts 3-1 and 2-5, it

may be seen that Concept 3-1 had comparable-to-superior thermal NO_x performance, equivalent low NO_x yield, and required less pressure drop because of the superior rich-to-lean transition accomplished by the narrow-passage quench zone. The summary of overall results for Concept 3-1 is as follows:

Concept 3-1 Performance Summary

- NO_x performance
 - Approaches the ERBS goal.
 - Projected to meet the residual and SRC-II goals.
- Smoke
 - SAE 20 at 0.69 MPa (100 psia).
- Combustion efficiency, pattern factor, and temperature profiles met all program goals.
- Pressure drop was approximately 6%, improved over the 7%-8% of Concept 2-5.
- Liner metal temperatures were excessive, as for Concept 2-5, but are addressed in the Phase II conceptual combustor design.

In conclusion, Concept 3-1 has the potential for meeting program goals with high-nitrogen fuels (1 weight percent nitrogen) and with hydrogen contents as low as 9%. Concept 3-1 had thermal NO_x performance superior to that of Concept 2-5, and this is attributed to the excellent rich-to-lean transition accomplished by the narrow-passage quench zone which requires reduced quench air-jet penetration distance. Note also that Concept 3-1 had lower pressure drop than Concept 2-5 (6% versus 7-8%). This is of significance since:

- Reduced pressure drop improves cycle efficiency
- The narrow-passage quench zone enables effective rich-to-lean transition in commercial size combustors (35.6 cm diameter for the MS7001E) without requiring excessive pressure drop.

The excellent thermal NO_x performance, low yield of NO_x from FBN, and the superior rich-to-lean quench characteristics of Concept 3-1 are the basis for the conceptual design of the Phase II combustor, described in Section 10, which embodies the best feature of Concepts 3-1 and 2-5.

2.4.2 Lean/Lean Combustor Tests

Initial tests of series-staged lean/lean combustor Concept 4 showed promise for low NO_x potential with low to moderate organic nitrogen levels. Table 2-2 presents the performance data summary for Concept 4-1, modified from the initial screening test vehicle to improve fuel/air mixing. NO_x emissions were considerably below the ERBS fuel goal, met the goal for a residual fuel with 0.23 weight percent FBN, but considerably exceeded the SRC-II NO_x goal because of 50% NO_x yield from organic

nitrogen. The high NO_x yield precludes application of this concept to fuels having nitrogen content exceeding 0.25 weight percent. Smoke, liner temperatures, and combustion efficiency were acceptable at baseload turbine conditions.

This combustor concept has the potential of meeting all program goals with ERBS and possibly a residual fuel with less than 0.25 weight percent fuel nitrogen. In fact, with fuels with low nitrogen content (i.e., ERBS), this concept would meet the NO_x emissions goal with considerable margin. The two deficiencies observed, smoke at high pilot fuel/air ratios and low efficiency at lean operating conditions (low load and pilot/main stage crossover) could most likely be overcome with some development including flow-split adjustments, additional swirl cup changes, and possibly additional pressure drop. Design changes to overcome this problem are incorporated in the Phase II conceptual lean/lean combustor for consideration in Phase II applications with low-nitrogen liquid and coal-derived gas fuels. All other performance parameters including pattern factors, liner temperature, and carbon deposits were met during the testing.

The series-staged lean/lean combustor with premix, Concept 5, was tested once, and performance data are shown in Table 2-2. The test results are characterized by very low NO_x performance on ERBS fuel and high CO, low combustion efficiency. The considerable heat transfer refinement required of the premix tube nose-piece (burned off during tests), the development necessary to obtain adequate combustion efficiency, and the observed high NO_x yields preclude further consideration of this concept relative to the successful performance already shown by Concepts 2-5, 3-1, and 4-1.

The parallel-staged lean/lean combustor, Concept 6, had screening-test performance as shown in Table 2-2. Pressure drop was low and, if utilized to improve mixing as done for Concept 4-1, should result in performance very similar to Concept 4-1. The observed low NO_x yield was unexpected based on expected lean/lean combustion performance. The observed yield will likely increase if thermal NO_x performance is improved by fuel/air mixing improvements as made for Concept 4-1. The short combustor length may offer some advantage. The short length and low thermal NO_x were the bases for development of an LM2500 conceptual design based on this combustor. This concept is not recommended for further consideration in Phase II development for high nitrogen fuels.

2.5 CONCLUSIONS AND RECOMMENDATIONS

The results of the Phase I test program have demonstrated that rich/lean combustor Concepts 2-5 and 3-1 have real potential for achieving dry low NO_x emissions meeting the EPA NSPS with high nitrogen content (low hydrogen content) liquid fuels, such as SRC-II. Concept 2-5, the multinozzle rich/lean combustor, showed NO_x emissions within 10%–15% of the program goals for all liquid fuels tested. Concept 3-1 underwent considerably less testing than Concept 2-5, but showed equal if not superior potential. Concept 3-1, when compared to Concept 2-5, showed comparable-to-superior thermal NO_x performance, equivalent low organic NO_x yield and lower pressure drop. This is the result of the superior rich-to-lean transition ac-

complied by the narrow-passage quench-zone design, which requires less pressure drop due to shorter required jet penetration depth to accomplish mixing. On this basis, Concept 3-1 has been selected as the basis for the primary combustor candidate recommended for Phase II development.

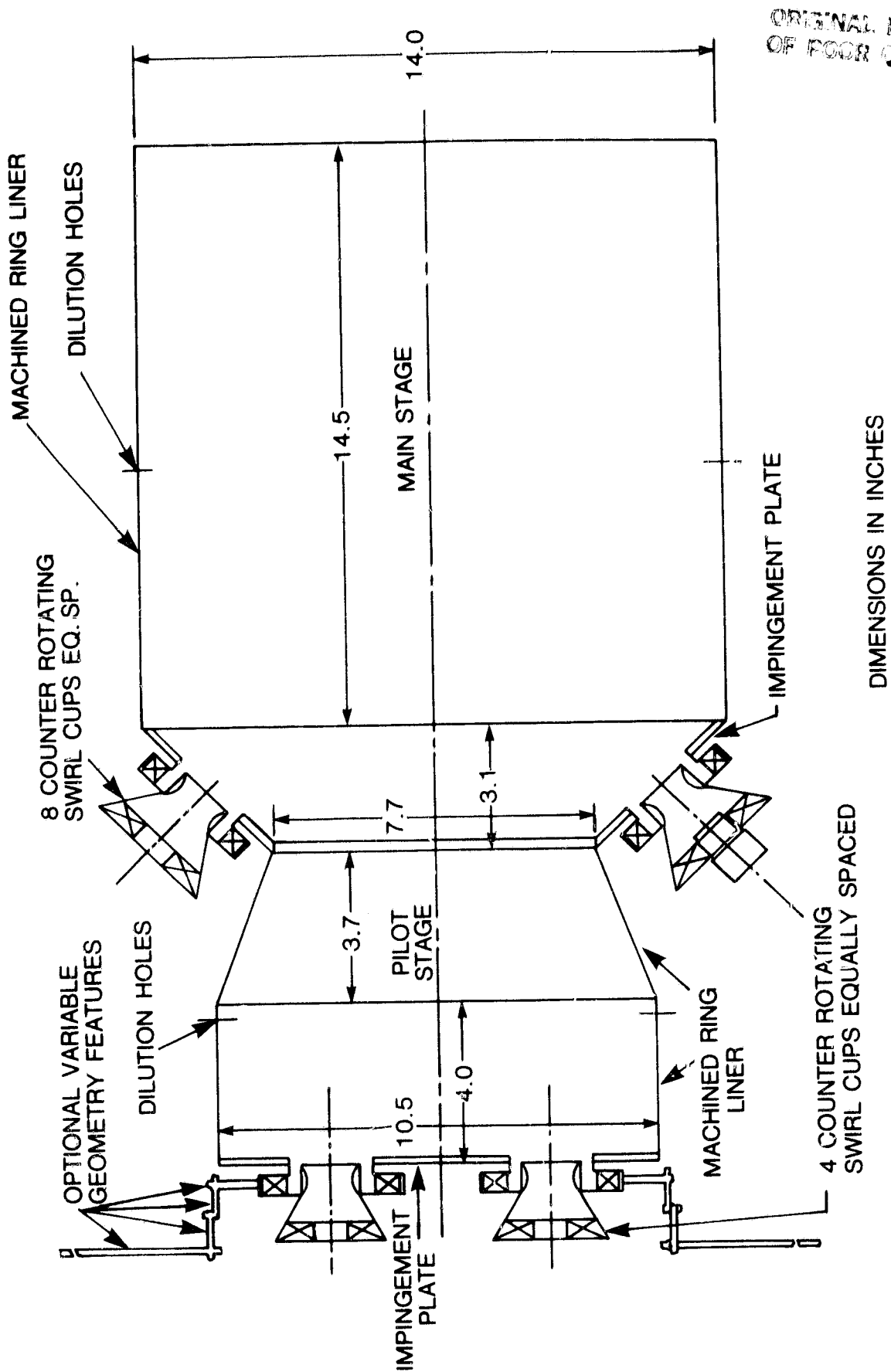
Both rich/lean concepts experience smoke emissions exceeding the program goal and higher than acceptable rich-stage liner-wall temperature. Both development areas are addressed in the proposed Phase II conceptual design based on Concept 3-1.

This rich/lean concept is also an excellent candidate for the combustion of low Btu (LBTU) and intermediate Btu (IBTU) coal-derived gases. The combination of good thermal NO_x performance and low organic NO_x yield in this rich/lean concept can accommodate the high flame temperatures associated with IBTU gases and organic nitrogen in the form of NH_3 contamination. NH_3 contamination can result from gas resaturation after low-temperature sulfur cleanup of gasifier output, and may also result from high temperature sulfur cleanup systems without gas resaturation.

The conceptual design of the combustor recommended for Phase II development with coal-derived liquids and LBTU/IBTU gases is shown in Figure 2-3, based on Phase I rich/lean Concept 3-1. Section 10.1 presents a full description of the combustor design and its features that address the smoke and liner temperature concerns experienced in the Phase I tests. The concept features a shorter rich stage than Concept 2-5 (25.4 cm versus 38.1 cm), which provides superior pressure strength. This combined with the reduced pressure drop characteristic of Concept 3-1 (because of the narrow-passage quench design) should resolve rich-stage liner strength problems. Enhanced cooling of the critical quench area is accomplished by double-wall impingement cooling with a significant portion of the rich-to-lean quench air flowing around the rich stage and through the impingement holes into the quench entrance holes. These features enhance the backside convection cooling and thermal barrier coating, which are retained in the proposed Phase II design of Figure 2-3. The Phase I test hardware was entirely convectively cooled in the rich stage.

Lean/lean Concept 4-1 did demonstrate potential for ultralow NO_x emissions on distillate fuel and capability for meeting the low NO_x goal for residual fuels with up to 0.25 weight percent nitrogen. However, it is not recommended for applications involving high-nitrogen fuels, such as SRC-II. The concept would also have potential for LBTU gas and IBTU gas with low levels of organic nitrogen. Although not recommended for high nitrogen applications, a conceptual combustor design for Phase II consideration was developed to provide a full assessment of the potential applications of the derived Phase I technology. Figure 2-4 presents the conceptual design for this lean/lean combustor, which has features provided to resolve the low combustion efficiency at low load and at pilot/main stage crossover observed in the Phase I tests.

2-15



ORIGINAL PAGE IS
OF POOR QUALITY

Figure 2-4. Conceptual design of lean/lean combustor, MS7001E cycle

Section 3

INTRODUCTION

3.1 BACKGROUND

A decline in the availability of petroleum fuels is projected to occur in the 1980s and accelerate throughout the 1990s. This is particularly true with regard to the petroleum distillate fuels currently used in many stationary power generation sources. Faced with declining supply, these are expected to be devoted to transportation and other consumer use. The availability decline will be accompanied by continued cost increases.

Fuel supplies for power generation equipment must thus move towards the utilization of petroleum products of lower cost and quality, and increasingly towards the combustion of coal-derived liquids (CDL) and gaseous fuels. Furthermore, because of the projected higher costs, increasingly stringent emissions requirements, and the uncertainty in the projected mix of fuels to be available, combustion systems for gas turbines must be efficient, environmentally acceptable, and have fuels flexibility. Lower quality petroleum residual fuels and CDLs have higher fuel nitrogen content and lower hydrogen content, which thus require significant improvements in current production combustor technology to meet emissions and operational performance requirements. Given these requirements, General Electric has completed the first phase (Phase I) of a multiphase program to develop dry low NO_x combustion technology under the sponsorship of the National Aeronautics and Space Administration (NASA). This report discusses the results of the Phase I work directed towards developing basic technology for low NO_x combustion of high-nitrogen liquid fuels. The on-going Phase IA effort will assess the subject of low NO_x combustion with coal-derived gaseous fuels.

Current planning calls for completion of a Phase II effort to develop the detailed design of a machine combustor, with Phase III to accomplish a field demonstration of a low NO_x combustion system.

3.2 PROGRAM OBJECTIVES AND SPECIFIC GOALS

The objectives of the program described in this report are to develop low NO_x combustor technology to meet current U.S. EPA NSPS emissions requirements and operational performance standards for operation of the General Electric MS7001E turbine with high-nitrogen fuels, and with fuels flexibility. A goal was established to meet these requirements dry, i.e., without the use of water injection for NO_x suppression. Dry operation leads to improved cycle efficiency to offset expected higher fuel costs and to eliminate investment and operating expenses required for water injection systems. Furthermore, water and steam injection is successful in reducing thermal NO_x but does not remove NO_x from fuel-bound nitrogen sources.

Program emissions goals are based on the EPA Standard F.R. 40 CFR Part 60 and are contained in Table 3-1. Key combustor operational performance goals are listed in Table 3-2.

Table 3-1
EMISSIONS GOALS

Pollutant	Maximum level	Operating Condition
Oxides of nitrogen	75 ppm at 15% O ₂	All
Sulfur dioxide	150 ppm at 15% O ₂	All
Smoke	S.A.E. No. = 20	All

Table 3-2
PERFORMANCE GOALS

Combustion efficiency	> 99% at all operating conditions
Total pressure loss	< 6% at baseload
Outlet temperature pattern factor	≤ 0.25 at baseload power
Combustor exit radial temperature profile	Equivalent to production combustor values

3.3 PROGRAM SCOPE AND APPROACH

Six advanced combustor concepts were tested, including three rich-lean and three lean-lean staged combustors. A lean catalytic combustor concept will be tested in the Phase IA effort. Initial screening tests were used to evaluate the potential of each concept, followed by selection of the two most promising concepts and further modification and testing to develop these concepts to meet the program dry low NO_x goals. The two-stage rich-lean concepts were expected to have the highest potential for low conversion of fuel nitrogen to NO_x, and this was indeed confirmed.

Twenty-centimeter (8-in.) diameter combustors were fabricated and tested over a range of operating conditions characteristic of the General Electric MS7001E heavy duty gas turbine used in utility power generation applications. The MS7001E turbine has a baseload rating of 72.9 MWe at a turbine inlet temperature of 1358 K (1985 °F), pressure ratio of 11.7, and airflow of approximately 250 kg/s (550 lb/s). The standard procedure was to evaluate the combustor over the load range for the MS7001E engine

and to conduct additional tests as appropriate. Other test variables were also adjusted during the tests. For example, fuel-air ratios above and below design levels were tested for diagnostic purposes. Also, the fuel flow split between the pilot and main stage for combustors with two fuel stages was varied to determine the optimum operating conditions.

SRC-II coal-derived middle distillate liquid, ERBS petroleum distillate, petroleum residual fuels, and blends of these three fuels were used for combustion tests. In addition, pyridine was added in various percentages to increase the concentration of fuel nitrogen. The ERBS fuel was a middle petroleum distillate with 12.95% hydrogen and essentially no fuel-bound nitrogen. The solvent-refined coal, SRC-II fuel, had only 9.07% hydrogen content and a high level of fuel-bound nitrogen at 0.87% by weight. The residual had a 294 K pour point and contained significant levels of vanadium and fuel-bound nitrogen. Heated storage tanks and fuel supply lines were required when using this fuel. The viscosity at 311 K was $1.345 \times 10^{-3} \text{ m}^2/\text{s}$. With the three types of fuel used, plus the blending and the pyridine doping, a very wide range of fuel properties was available for evaluating the combustor concepts.

The test rig used to evaluate the combustors during this program consisted of a 25 cm (10 in.) diameter duct divided into several spool pieces including an inlet section, a combustor housing section, and an exit instrumentation section. The spool pieces included various ports to accommodate the fuel nozzle supply lines, instrumentation rake mountings, and leadout of thermocouples mounted on the combustors. The combustion section had two spool pieces for ease of assembly and for accommodating combustors of various lengths. The test rig was mounted on a dolly used to transport the assembly between the test cell and the buildup area. The dolly also included quick disconnect fittings for the thermocouple and pressure instrumentation hookup in the test cell.

Instrumentation at the combustor exit consisted of four three-element gas sampling rakes and four three-element thermocouple rakes. The gas sampling rakes were also utilized for measuring combustor exit total pressures and for extracting the smoke samples.

The combustion tests were conducted in the General Electric facilities located in Evendale, Ohio. The test cell used in this program has an air supply capability of approximately 5.4 kg/s at temperatures up to 866 K and 2.07 MPa pressure. The air supply is heated by an indirect gas-fired preheater so that unvitiated air is supplied to the combustor test section. The fuel supply system is capable of supplying any of three types of fuels or blends of the fuels during the tests. In addition, the fuels or fuel blends could be doped with pyridine to increase the nitrogen content. The system was configured to enable changing of fuel type, blend ratios, or the amount of pyridine doping with the combustor in operation. Fuel samples were taken during the tests and analyzed to verify fuel blend ratios and pyridine content as measured by flow meters. Test cell data acquisition systems included smoke measurement and on-line gas analysis equipment. The smoke emissions were measured using a filter stain method.

3.4 REPORT CONTENTS

This report describes the results of the development test program, major conclusions, and problems requiring further development; and it presents conceptual designs of the most promising concepts (based on Phase I work) for development to prototype level in Phase II.

Section 4

TEST FUELS

Three fuel types were selected for the Low NO_x Heavy Fuels Combustor Concept Program covering a range from a light number 2 distillate (ERBS), typical of that used in hundreds of industrial gas turbines, to a high-viscosity residual fuel requiring special fuel handling and heating equipment. The third fuel was a middle distillate coal-derived liquid called SRC-II (Solvent-Refined Coal), having high fuel-bound nitrogen and low hydrogen content, and was selected to cover the expected range of fuels required in the future. By using these fuels, plus blends of the fuels, with and without doping with pyridine ($\text{C}_5\text{H}_5\text{N}$) to increase the fuel nitrogen content, a wide field of combustion-related effects were investigated during the program. Table 4-1 presents properties of the three fuels. Additional data are given in Figure 4-1, viscosity, and Figure 4-2, flame temperatures.

Table 4-1
FUEL PROPERTIES

	ERBS*	SRC II	Residual
Specific Gravity @ 298/298 K	0.8377	0.9796	0.9440
Hydrogen Content, Percent	12.95	9.07	11.52
Sulfur Content, Percent	0.085	0.20	0.49
Net Heat of Combustion, MJ/kg (Btu/lb)	42.5 (18,275)	38.1 (16,365)	41.3 (17,748)
Viscosity, M^2/S @ 311 K	1.36×10^{-6}	3.55×10^{-6}	1.345×10^{-3}
Nitrogen Content, Percent	0.0054	0.87	0.23
Surface Tension, N/m	—	—	3.29×10^{-2} @ 339 K
Surface Tension, N/m	—	—	3.06×10^{-2} @ 366 K
Pour Point, K ($^{\circ}\text{F}$)	244 (−20)	255 (−55)	294 (70)
Vanadium	—	—	26 ppm

* Experimental Referee Broad Specification petroleum distillate fuel

† Supplier's data

The primary purpose of the Low NO_x Heavy Fuels Combustor Concept Program was to evaluate the potential of various combustor concepts to burn fuels that typically have high bound nitrogen content without resulting in excessively high NO_x . EPA's New Source Performance Standards were used as a guide to establish emission limits. Additionally, the goals were to be achieved without the use of water injection.

There are certain fuel characteristics that are of concern to the combustion designer. Although not all inclusive, the hydrogen content, residual carbon, nitrogen content, viscosity, and flame temperature were of importance during the development program and are discussed below.

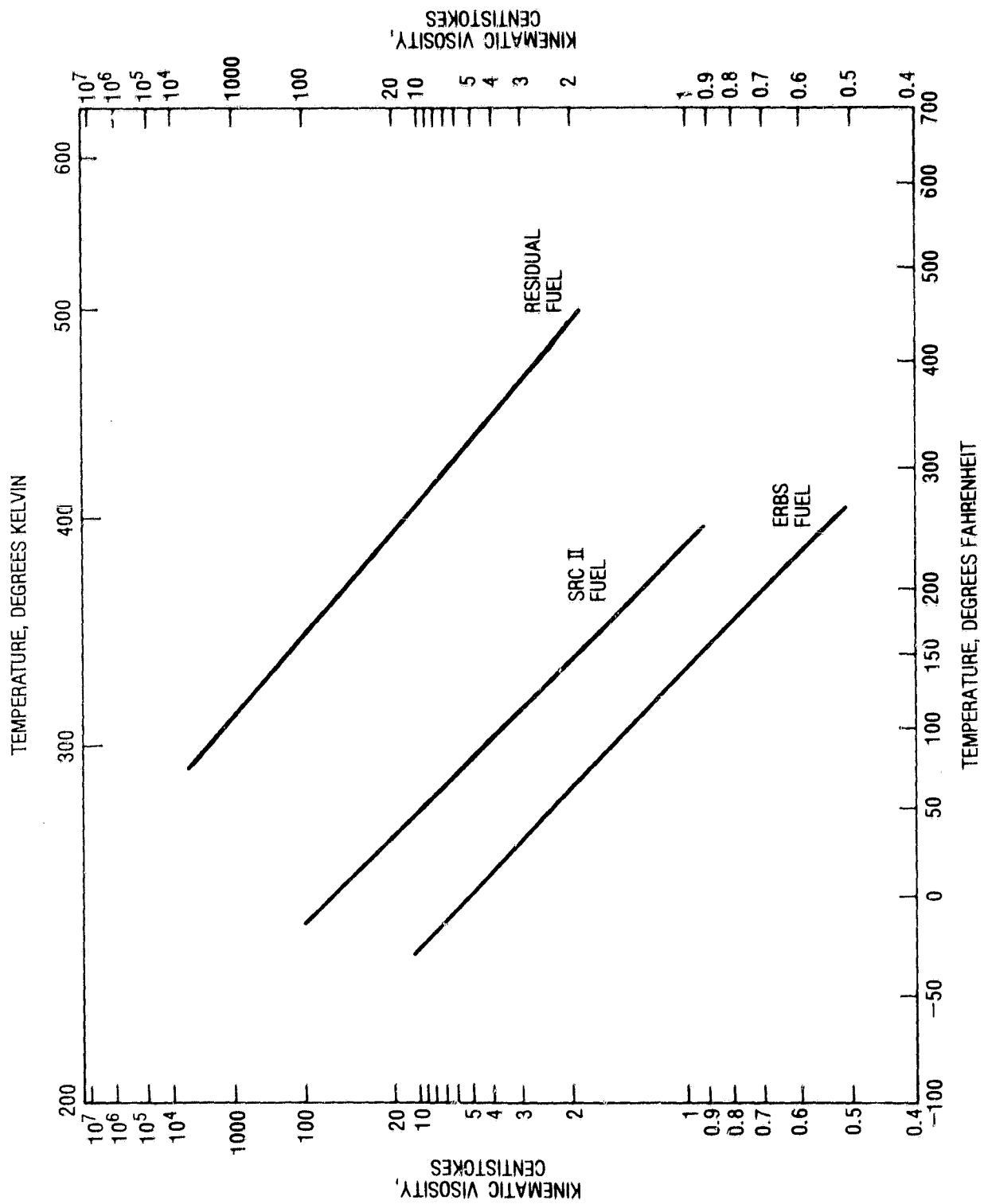


Figure 4-1. Viscosities of fuels used in Low NO_x Program

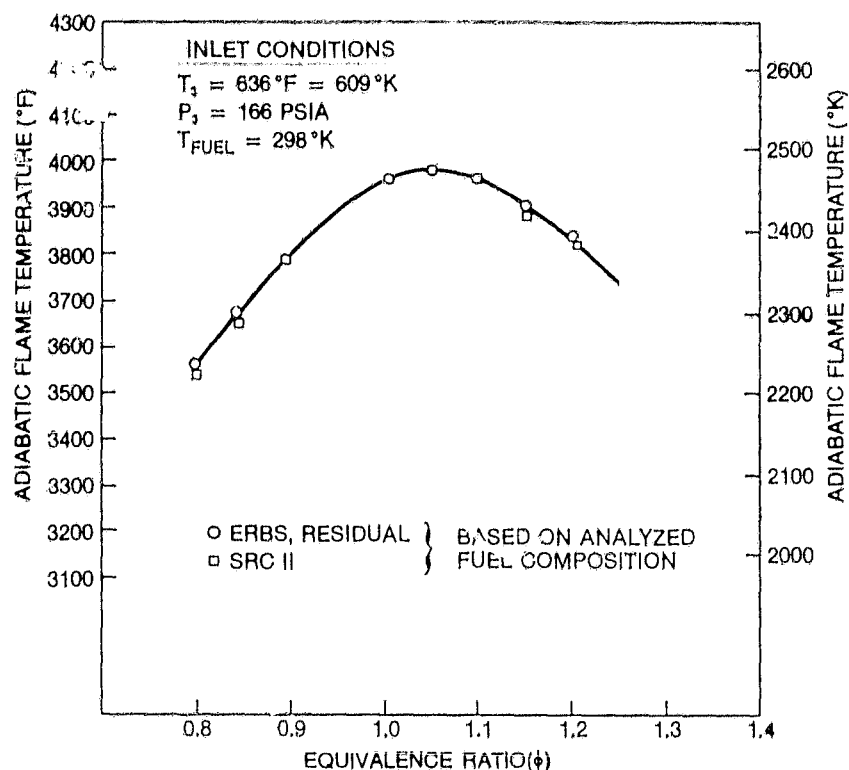


Figure 4-2. Comparative adiabatic flame temperatures for ERBS, residual, and SRC-II fuels

Flame temperature is a significant factor in NO_x production. However, the range of flame temperatures encountered in liquid fuel combustion at a given equivalence ratio is rather narrow (as shown in Figure 4-2) and is of minor significance when compared with the effects of fuel nitrogen in NO_x production although the mechanisms are different. The effect of inlet temperature is shown in Figure 4-3.

Fuel-bound nitrogen in petroleum fuels comes largely from organo-nitrogen compounds present in the original crude oil. In some distillate fuels, fuel-bound nitrogen may also come from additives such as stabilizers. Coal-derived and other synthetic fuels frequently have high nitrogen content. Chemically bound nitrogen in the fuel will contribute to the total nitrogen oxide pollutant in the exhaust gases, adding to the nitrogen oxides from the direct combination of atmospheric nitrogen and oxygen in the gas turbine combustion reaction. The particular combustion system and operating conditions will affect the total nitrogen oxide production from both atmospheric and fuel-bound nitrogen. Generally, very high conversions of fuel nitrogen to NO_x will occur in lean combustion; therefore, rich combustion techniques are better suited for the emission control of high-nitrogen liquid fuels.

The percent combined hydrogen in a hydrocarbon fuel is a critical factor in soot formation and consumption within a combustor. In general, the higher the hydrogen content in a liquid fuel, the lower the smoke level will be. As an example, paraffinic hydrocarbons with high hydrogen content (14-15%) have much less tendency to

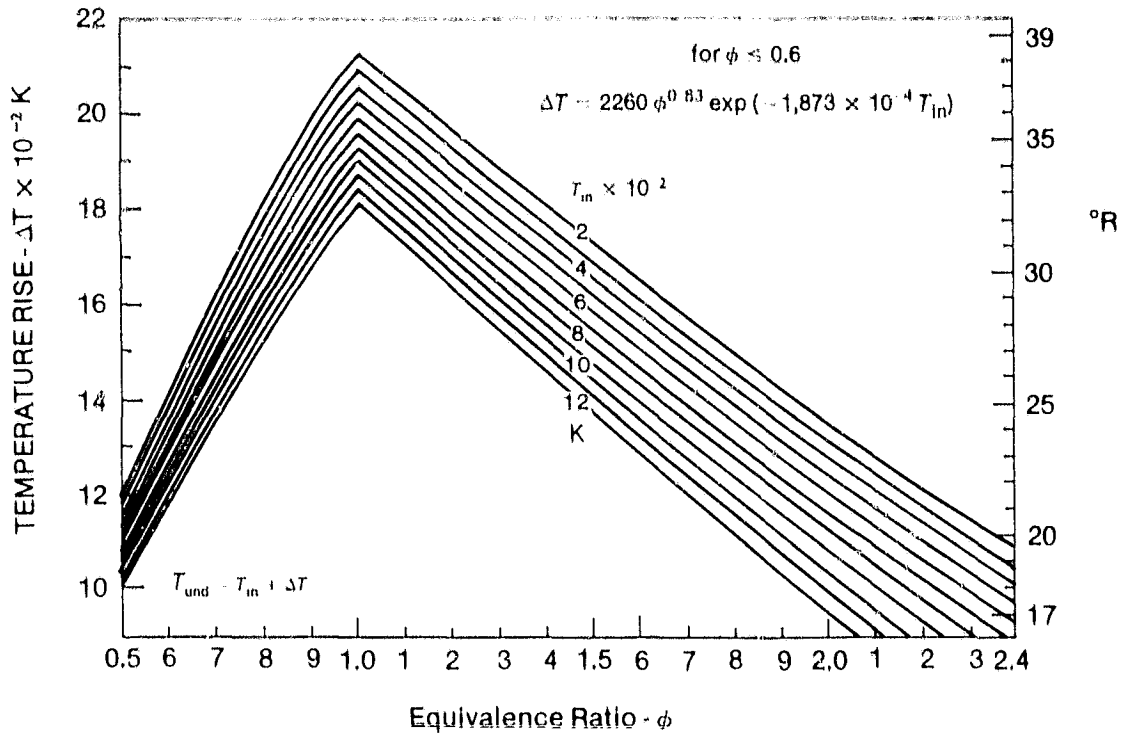


Figure 4-3. Undissociated temperature rise of hydrocarbon fuels

Reference: *The Design and Development of Gas Turbine Combustors*, Vol. I, Northern Research and Engineering Corp., Woburn, MA, 1980, p. 8.93.

smoke than do aromatic hydrocarbons which can have 10% or less hydrogen. The fuels selected for this program cover a wide range of hydrogen values, from 12.95% for the distillate fuel down to 9.07% for SRC-II. The wide range of fuel hydrogen obviously influences combustor design because a combustor with acceptable smoke performance on distillate fuel may produce heavy smoke when operating on SRC-II. The smoking tendencies of the rich-lean combustors are much more sensitive to fuel hydrogen than a lean-lean system and require special attention during the design phase. Additionally, the presence of smoke particles greatly increases radiative heat transfer from the combustion gases to the combustion hardware—another significant design problem for the rich-lean systems.

Carbon residue is measured as the residue remaining when a fuel sample is completely distilled in a standard apparatus. One effect of a high carbon residue is carbon formation near the fuel nozzle. To control this, air atomization is used in the combustion of all but the lightest of fuels. Although not a consideration in the current program, it would be necessary to ensure purging of the fuel nozzles or transferring to a lighter fuel such as distillate to prevent fuel nozzle coking during shutdown of a production-type combustion system burning a high carbon residue fuel.

The viscosity of fuel is a measure of its resistance to flow. It is important in the fuel auxiliary equipment since it determines pumping temperature, atomizing temperature, and oil pump pressure. In order to obtain proper operation of the gas turbine, the maximum viscosity at the fuel nozzles must not exceed 10 centistokes (cSt) for pressure atomizing or low-pressure-air-atomizing fuel systems, and 20 cSt for high-pressure-air-atomizing systems. When these limits are exceeded, poor ignition characteristics, smoking, unsatisfactory combustor exit temperature distribution, lowered combustion efficiency, or formation of carbon may occur. In most cases, fuel heating must be employed to ensure that these viscosity limits at the fuel nozzle are met under all ambient conditions. In all cases, the fuel at initial light-off must be at or below 10 cSt viscosity. Additionally, as viscosity directly affects fuel droplet size for a given amount of atomizing energy, it is an important parameter in prevaporization components. Surface tension of the fuel is also a determinant in atomized fuel droplet size.

Section 5

TEST FACILITIES

The combustion tests were conducted in the General Electric facilities located at Evendale, Ohio, in Cell A5. This cell has the fuel supply, air heater, high-pressure air supply, controls, and instrumentation required to conduct the combustor component tests.

Control consoles and data-recording equipment are located in the adjacent room. Some of the equipment contained in the control room and test cell is described below.

5.1 FUEL-HANDLING SYSTEM

The fuel supply system required major modification in order to handle the requirements of the program. The system was designed to supply any of the three types of program fuels, fuel blends, and fuels doped with pyridine. Figure 5-1 shows the schematic of the fuel supply system. The fuel was supplied to the cell by trailers located behind the test cell. The trailers were filled from large facility storage tanks before each test.

A special fuel storage system was designed to handle the residual fuel. Since the pour point of this fuel was 294 K and viscosity was $1.345 \times 10^{-3} \text{m}^2/\text{s}$ at 311 K, the fuel storage tanks were insulated, and a heat exchanger was provided for heating the fuel. The fuel in the trailer was heated to 340 K. Another in-line heat exchanger was also provided so that the fuel temperature could be brought up to 380 K at the fuel manifold. The lines were also steam traced.

The delivery system was configured to enable changing the fuel type, blend ratios, or the amount of pyridine doping while the test was in operation. Three-way-type research valves, located upstream of the high-pressure pump, were used to set the fuel blend ratios. Pyridine was also added upstream of the high-pressure pump. The fuel mixing, to obtain uniform mixture, was achieved through the high-pressure pump and the static mixer (provided in the line). The fuel system was capable of delivering fuel up to 6.9 MPa pressure. Turbine flow meters were used to measure the individual and combined fuel flows. Fuel samples were also taken during the tests and were analyzed to verify the addition of pyridine as measured by the flow meters. The agreement between metered and analyzed pyridine doping was quite good.

The handling of both SRC-II and pyridine was complicated by their toxic nature and nauseating odor. Special precautions were taken in order to avoid vapor inhalation or skin contact. The test area was also sealed off from unauthorized entry. Gas masks and special clothing were worn by everyone who came in contact with the vapors or the liquid. The air quality, inside the control room, was also monitored to detect the presence of excess vapor. Whenever dangerous levels were reached, the test could be shut down and the area evacuated. The area was evacuated only once during testing, due to pyridine overflow. Both SRC-II and pyridine also chemically attack the standard pump seals. Therefore, special Teflon seals were used on the pumps.

ORIGINAL PAGE IS
OF POOR QUALITY

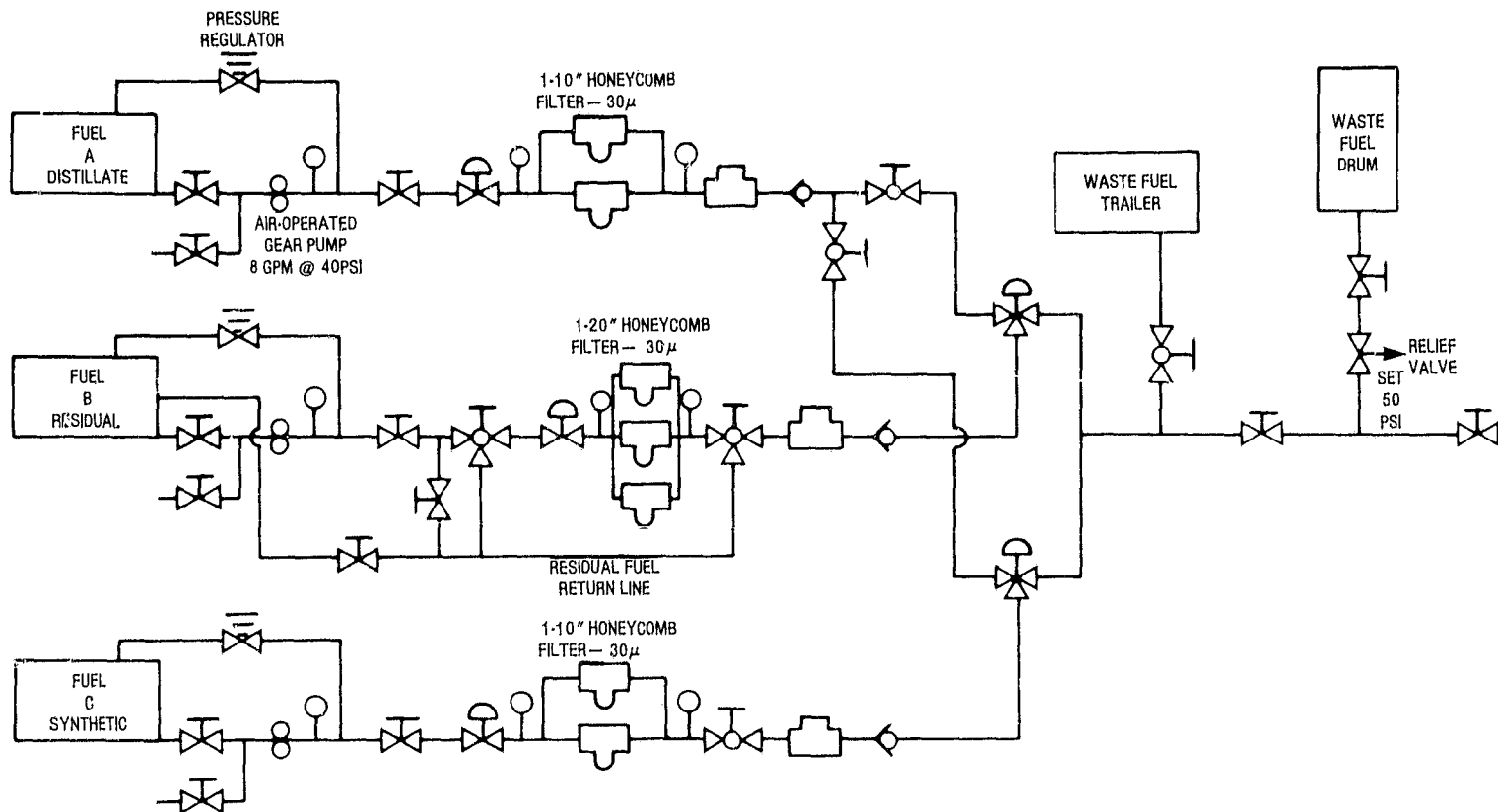
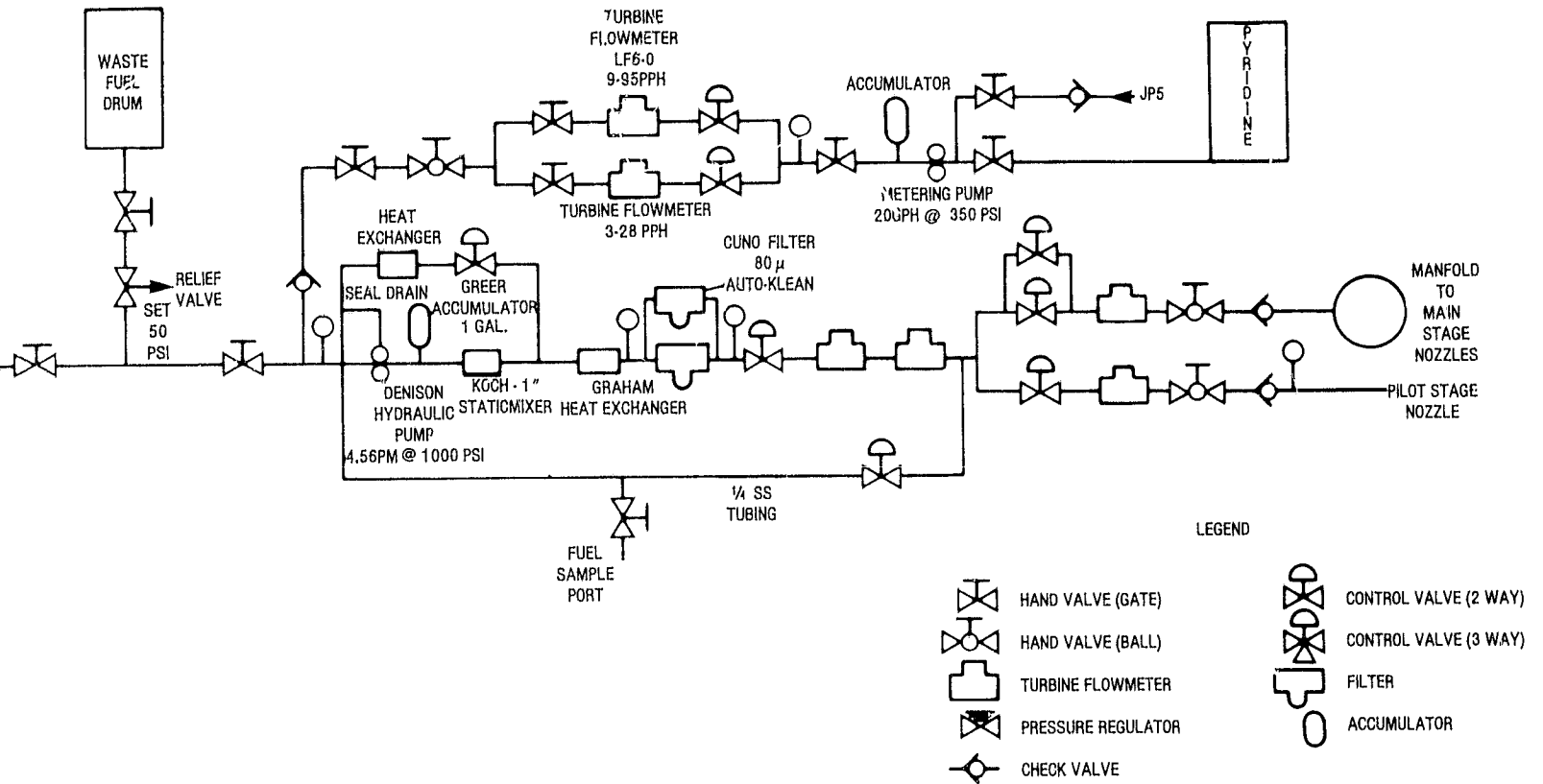


Figure 5-1. Schematic of fuel s

PRECEDING PAGE BLANK NOT FILMED

FOLDOUT FRAME

ORIGINAL PAGE IS
OF POOR QUALITY



Schematic of fuel supply system

FOLDOUT FRAME 2

5.2 AIR SUPPLY SYSTEM AND A5 TEST FACILITY

The combustor evaluations were conducted in Combustion Test Cell A5, located at the General Electric Evendale plant. The cell is supplied by air from a central air-supply system rated at 45 kg/s and 2.2 MPa. Combustor inlet air is heated to temperatures typical of actual engine operating conditions by a gas-fired, indirect air preheater nominally designed to heat 5.44 kg/s of airflow to 922 K. The exact flow/temperature limits are somewhat dependent upon the test setup and procedure.

An interior view of Cell A5, with a typical test vehicle installed, is shown in Figure 5-2. The cell piping is arranged to accommodate two test vehicles simultaneously, and even greater utilization is effected by mounting test vehicles on portable dollies with quick-change connections; buildup operations are accomplished in another area, and a vehicle occupies the cell only for the duration of actual testing. Instrumentation sensors are prewired to multiple quick-connect panels to facilitate rig installation. Table 5-1 summarizes some of the available services.

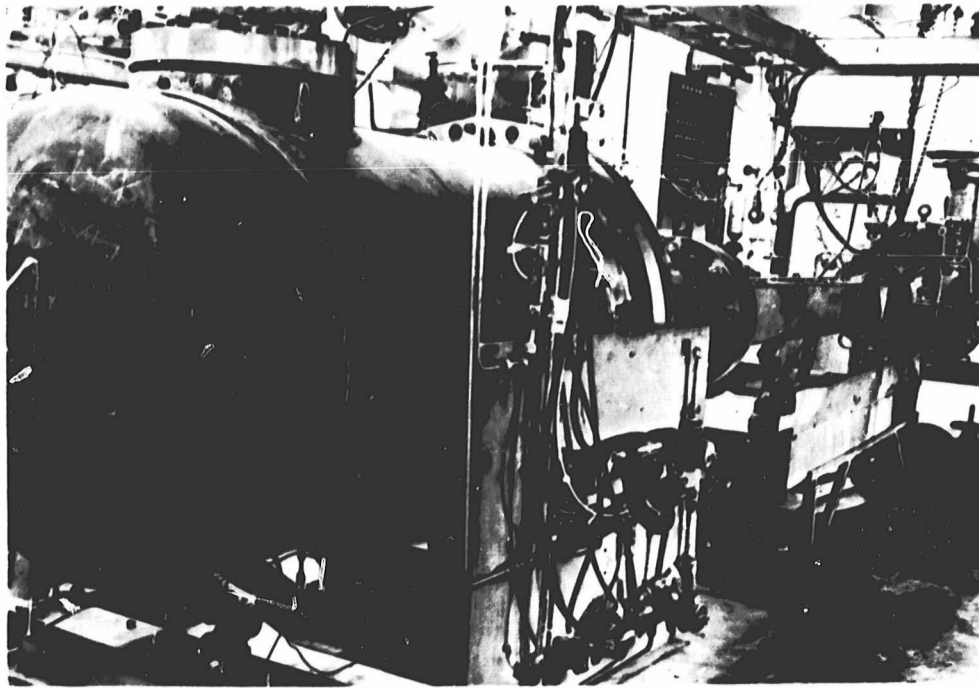


Figure 5-2. Cell A5—small combustor test facility, interior view

Airflow rates are measured by standard orifices, of appropriate sizes, conforming to the American Society of Mechanical Engineers (ASME) Measurement Code.

The control room is adjacent to the test cell. This is a soundproofed room housing the equipment for test control, monitoring, and data recording. Permanently installed equipment includes a 600 channel, digital data-acquisition system; strip-chart recorders for continuous recording; displays of pressures, temperatures, and fuel flows for use by the operators in controlling test parameters; and a small, analog computer generally programmed to compute airflows and fuel/air ratios. Portable equipment,

Table 5-1
CELL A5 SERVICES

Air	
401 Air	18 kg/s at 2 MPa
Shop Air	3 kg/s at 0.8 MPa
Cooper-Bessemer	3 kg/s at 2 MPa
Water	
Quench Capacity	10 kg/s at 2.4 MPa
Jacket Cooling	6 kg/s at 0.5 MPa
Electrical Power Circuits	
208 V, 60-cycle, 3-phase	
480 V, 60-cycle, 3-phase	
120 V, dc	
Control and Lighting: 115 V, 60-cycle, 1-phase	
Ignition: 120 V, 60-cycle, 1-phase and 24 V system	

available when needed, includes a teletype terminal for time-sharing computers. Emissions-measurement equipment is also located within the control-room complex. In addition, flame radiometers and dynamic pressure, amplitude, and frequency analyzers are available.

5.3 TEST RIG

The test rig used to evaluate the combustors during this program consisted of a 25.4 cm diameter duct divided into several spool pieces including an inlet section, a combustor housing section, and an exit instrumentation section. Figures 5-3 and 5-4 show schematics of the test rig. The spool pieces included various ports to accommodate the fuel nozzle supply lines, instrumentation rake mountings, and leadout of thermocouples mounted on the combustors. The combustion section had two spool pieces for ease of assembly and for accommodating combustors of various lengths. Figure 5-5 shows a photograph of the test spool 2 housing the head end of the test combustors. Fuel tubes are shown assembled in the spool for Concept 4. Extra ports were provided for installing fuel tubes for other concepts. Figure 5-6 shows the test rig mounted on a dolly used to transport the assembly between the test cell and the buildup area. The dolly also includes quick disconnect fittings for the thermocouple and pressure instrumentation hookup in the test cell. The inlet of the test rig is supplied with air from a settling or plenum chamber in the test facility. The discharge of the test rig is connected to a facility exhaust system with back-pressure valves.

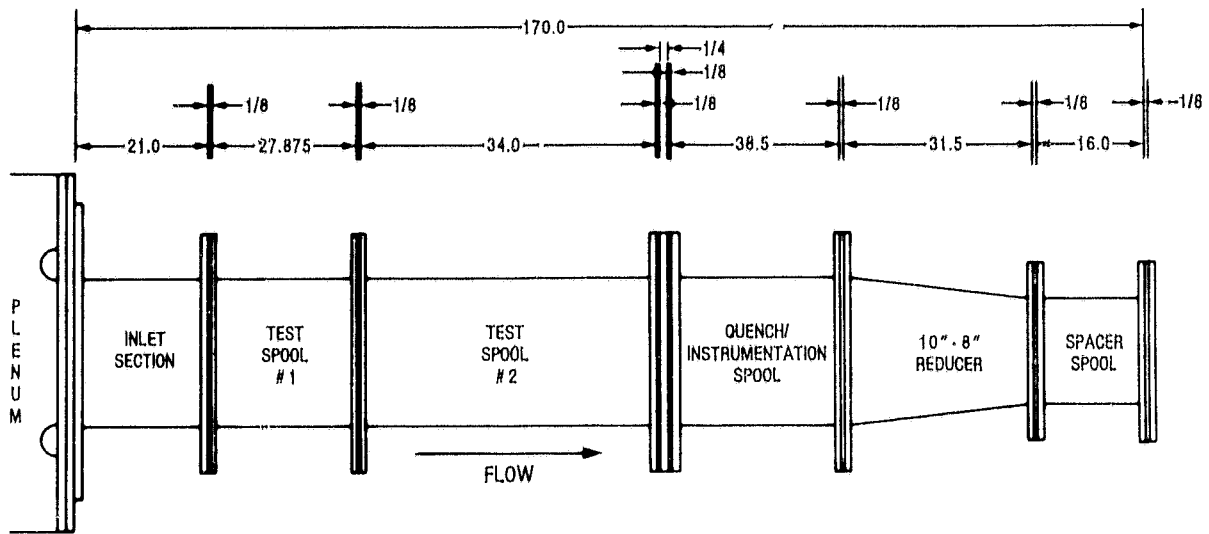


Figure 5-3. Test rig assembly

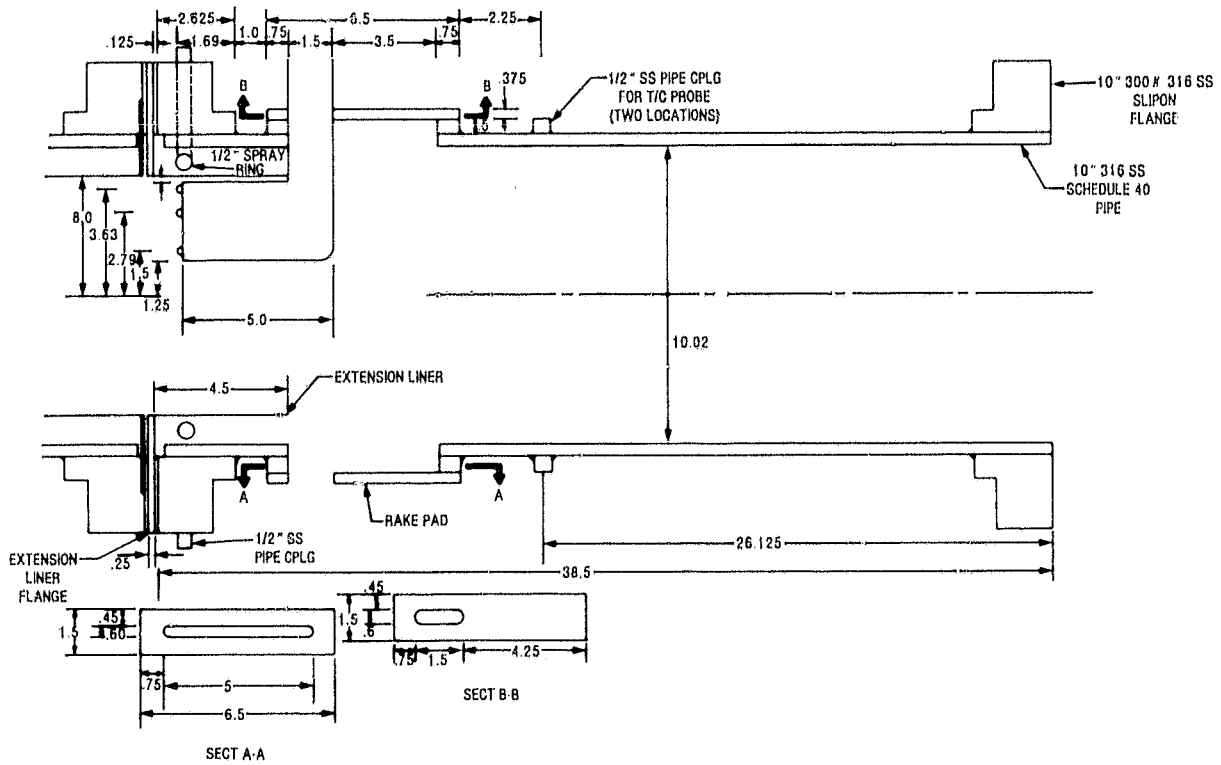


Figure 5-4. Quench/instrument spool

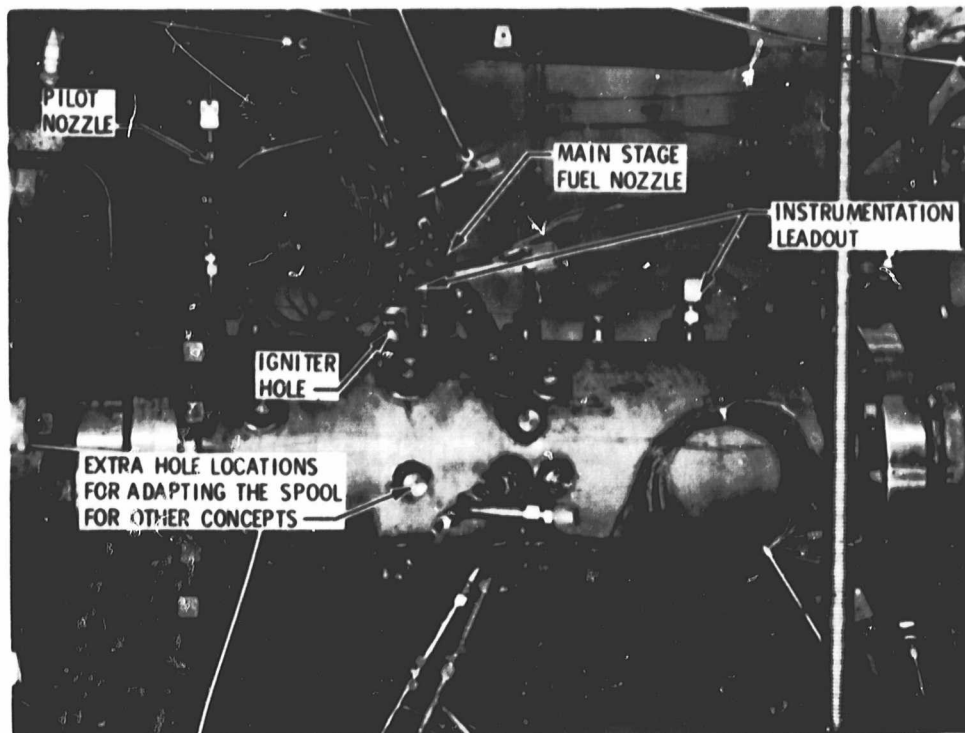


Figure 5-5. Test rig—test spool 2, showing fuel nozzles

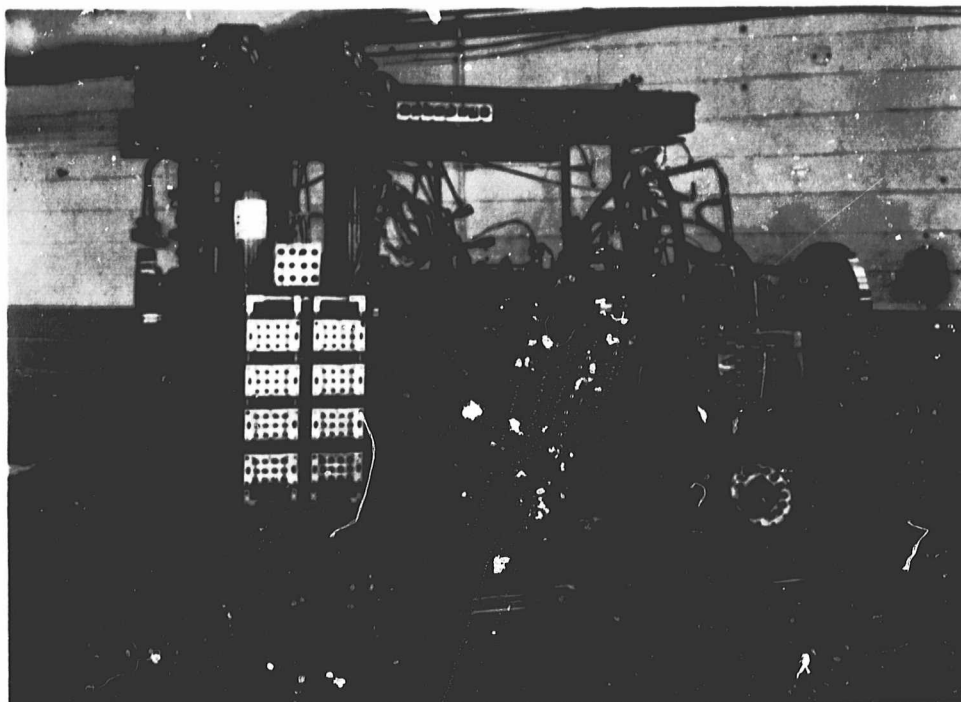


Figure 5-6. Test rig—showing test and quench spools

ORIGINAL PAGE
BLACK AND WHITE PHOTOGRAPH

5.4 INSTRUMENTATION

The combustor test rig assembly was instrumented to measure the performance and durability of the combustor. A listing of the combustor and rig instrumentation used in the test program is presented in Table 5-2.

Table 5-2
COMBUSTOR/RIG INSTRUMENTATION

Parameter	Instrumentation
Total Airflow	Standard ASME Orifice
Fuel Flows	Turbine Flow Meters
Fuel Injector Pressure Drop	Pressure Tap in Each Fuel Manifold
Fuel Temperature	Thermocouple in Fuel Manifold
Inlet Total Pressure	2 Pressure Probes
Inlet Static Pressure	4 Wall Static Taps
Inlet Total Temperature	2 Thermocouple Probes
Combustor Exit Total Temperature	4 3-Element Thermocouple Rakes
Combustor Exit Emissions/Total Pressure	4 3-Element Gas Sampling/Total Pressure Rakes
Atomizing Air Pressure Drop	Pressure Tap in Each Air Manifold
Combustor Metal Temperature	Approximately 12 Thermocouples on Dome and Liners Plus Temperature-Sensitive Paints
Inlet Air Humidity Level	Dew Point Hygrometer
Combustor Passage Static Pressure	Up to 4 Taps in the Passage
Combustor Dome Pressure Drop	Pressure Tap
Combustor Liner Pressure Drop	Up to 4 Pressure Taps

Main and verification total inlet airflow measurements were obtained using Standard ASME orifices which are an integral part of the Cell A5 facility.

Inlet total pressure and temperature were measured with two pressure and two temperature probes. Inlet static pressures were measured with four wall static taps.

Fuel flow rates were measured with turbine flow meters. Fuel flow rates were routinely corrected for fuel viscosity and specific gravity, based on fuel analysis and the measured liquid temperature. The fuel flow meters were also calibrated in the ranges for all three program fuels. A pressure tap in each fuel manifold was used in combination with internal static pressure to obtain fuel nozzle pressure drop.

Each combustor liner was instrumented with an array of metal surface thermocouples. Static pressure taps, to measure the passage and the inside pressure, were also mounted on the combustor liner. Figure 5-7 shows a typical instrumented combustor. The location of both thermocouples and pressure taps was changed as more experience was obtained. The combustors were also painted with temperature-sensitive paint.

Instrumentation at the combustor exit consisted of four three-element gas sampling rakes (shown in Figure 5-8) and four three-element thermo couple rakes (shown in Figure 5-9). The gas sampling rakes were also utilized for measuring combustor exit total pressures and for extracting the smoke samples. The three elements on each rake were mounted on centers of equal area at the combustor exit with one element of one gas sample rake located on the combustor centerline. The gas samples could be read as twelve individual samples for a detailed analysis of the gas stream profiles or manifolded together for extracting overall average gas samples. Typically, all twelve elements were manifolded together for an average reading. When read individually, the gas samples could also be used to calculate local temperatures and used along with the thermocouple readings for more detailed examination of the combustor exit temperature distribution. A sketch showing the arrangement of the rakes is shown in Figure 5-10. The probes, shown in Figures 5-11 and 5-12, were water-cooled for durability.

An extension liner was attached to the combustor exit to keep the exit area constant and also to keep the quench water from contaminating the gas sample. The quench water used to cool the exhaust gases was introduced in the exit section through a quench ring around the extension liner (see Figure 5-4). The quench water also kept the extension liner cooled. An outside view of the rig showing the rakes and the quench water manifold is shown in Figure 5-13.

5.5 EMISSIONS MEASUREMENT SYSTEM

The test cell data acquisition system included smoke measurement and on-line gas analysis equipment. A flow diagram of the emission analysis system is shown in Figure 5-14. This system has been referred to as the CAROL system, an acronym for "Contaminants Analyzed and Recorded On Line." This system contains automatic sample pressure control, automatic cold-trap regulation, and three-way valves.

The four basic instruments for measuring gaseous emissions concentrations in this on-line system are a flame ionization detector (FID) for measuring total HC concentrations, two nondispersive infrared analyzers for measuring CO and CO₂, and a heated chemiluminescent analyzer for measuring NO and NO₂. In this on-line system, flow through all of the various sampling lines to each of the basic instruments was maintained at all times. Three-way valves were used to divert each given sample stream either to an overboard manifold or into the analysis units. Each of the sample lines was maintained at 422 K up to the valve where the sample stream is divided into separate streams to each of the analysis units. The stream supplied to the FID was maintained at the same temperature all the way to the analyzer. This system con-

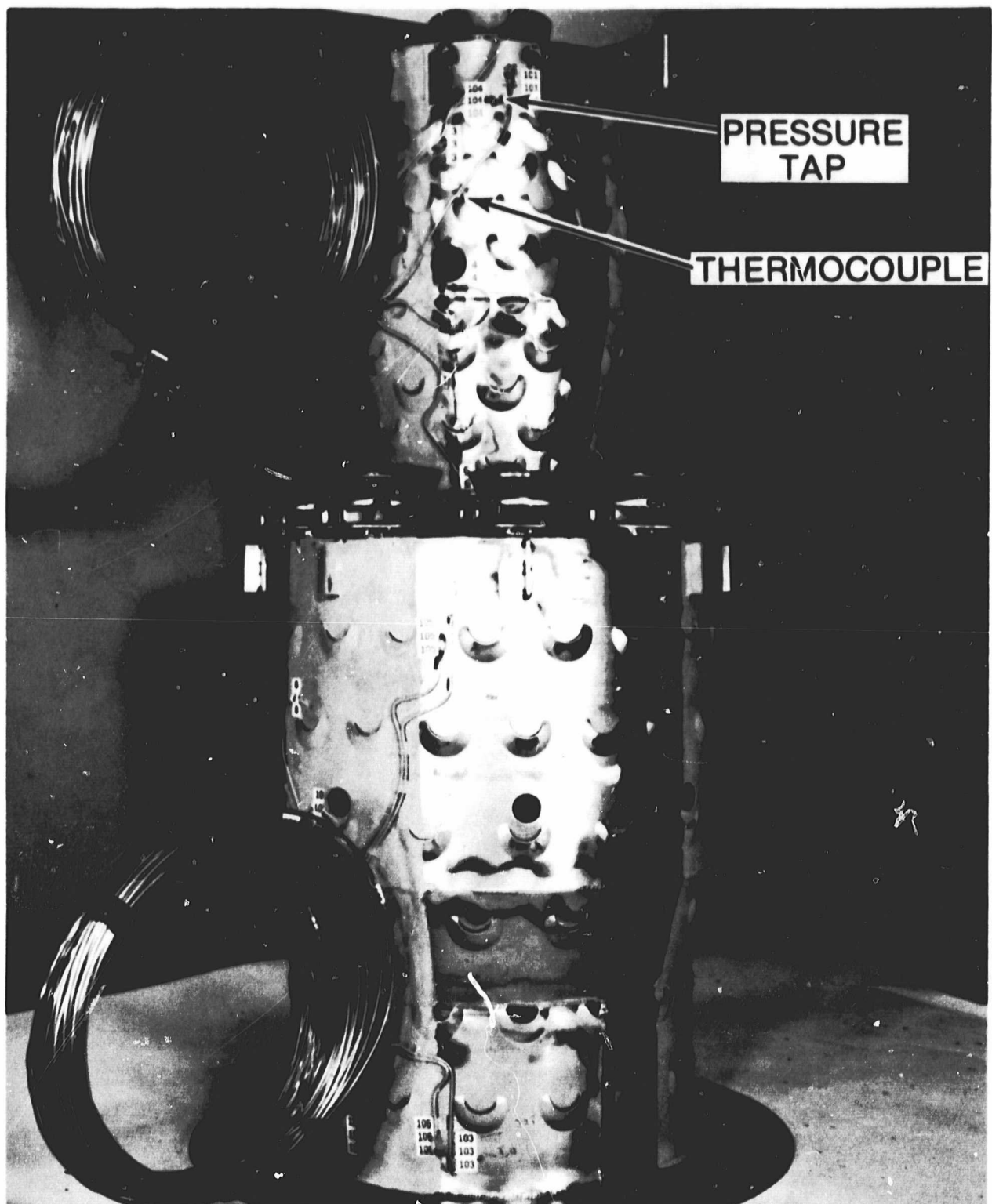


Figure 5-7. Combustor liner showing typical liner instrumentation

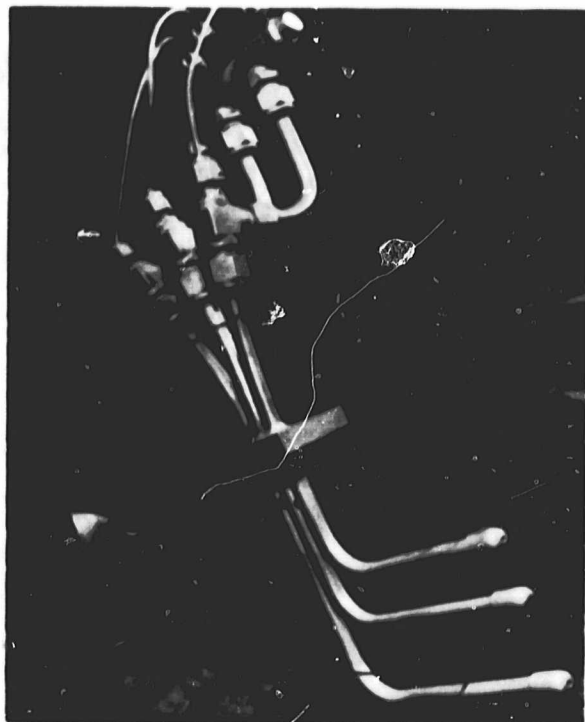


Figure 5-8. Gas sampling rakes

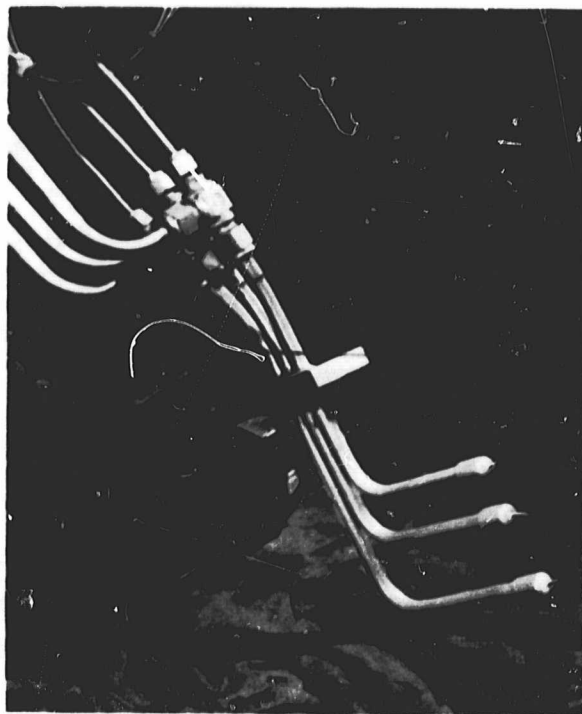


Figure 5-9. Thermocouple rake

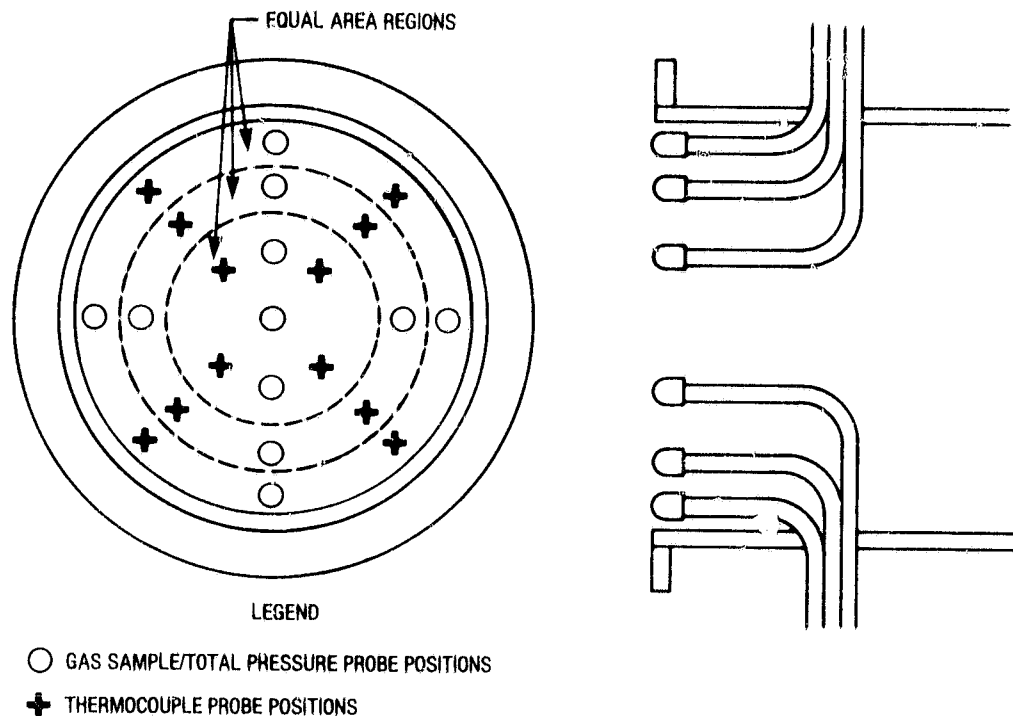


Figure 5-10. Combustor exit instrumentation rakes

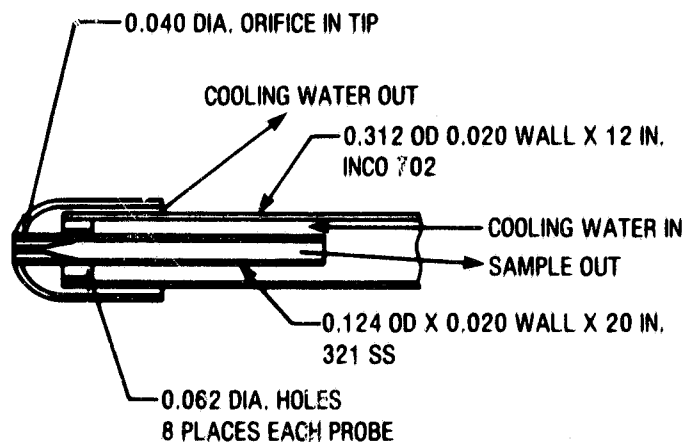


Figure 5-11. Water-cooled pressure/gas-sample probe configuration

forms fully to the specifications of SAE ARP 1256 and to the EPA requirements specified in 40 CFR Part 87. The nominal full-scale concentrations and calibration gases to be used are indicated in Table 5-3. Full calibration was conducted before each run.

Output from the CO, CO₂, HC, and NO_x analyzers of the CAROL system were manually recorded for later input to an emissions-data-reduction computer program that calculates exhaust-emission concentrations/indices, combustion efficiency, and sample fuel/air ratio.

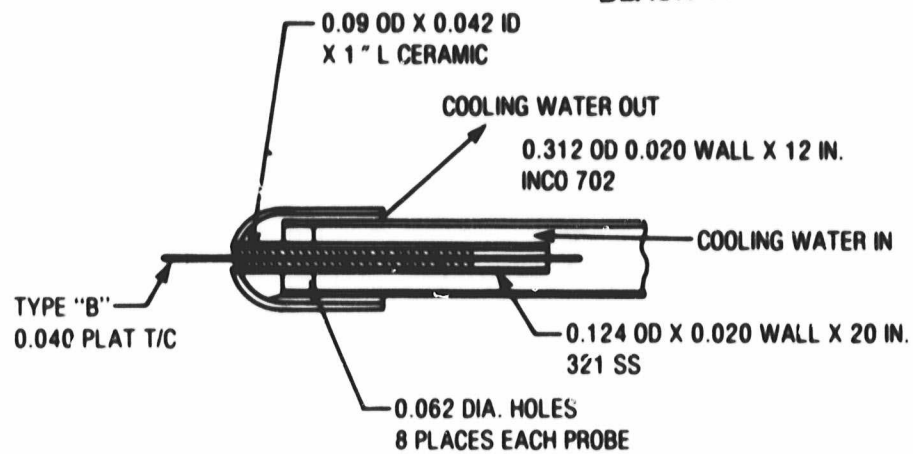


Figure 5-12. Water-cooled thermocouple rake probe configuration

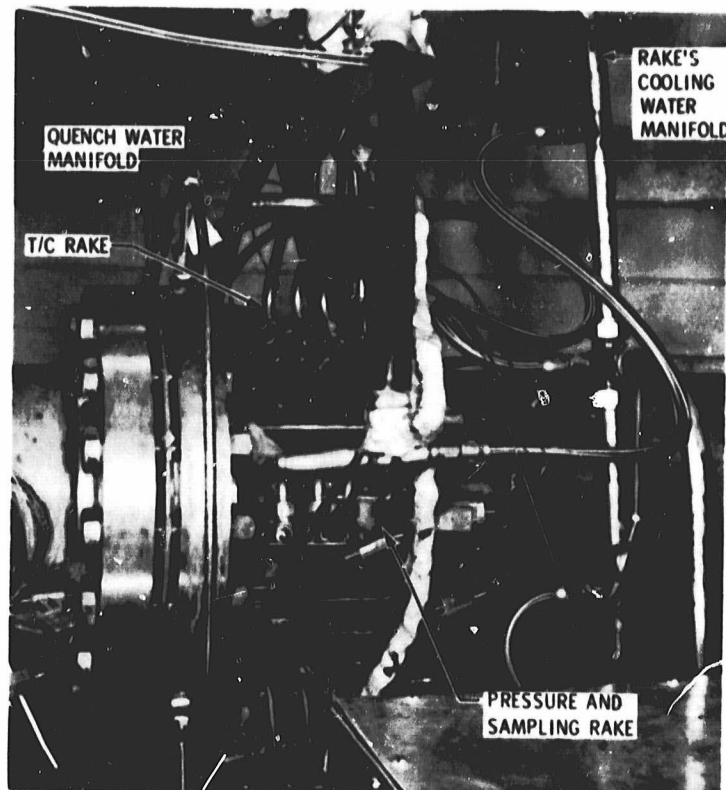


Figure 5-13. Test rig--quench spool, showing exhaust instrumentation

Table 5-3
GAS ANALYSIS SYSTEM CALIBRATION GASES

Analyzer	Range	Nominal Full-Scale Reading	Calibration Span Gases
CO	1	500 ppm	100, 225, 450, 900, and 2400 ppm
	2	1000 ppm	
	3	2500 ppm	
CO ₂	1	3%	1.25%, 2.5%, 4.0%, 6.0%, and 8.0%
	2	9%	
HC*	1	150	75, 140, 750, and 1300 ppm
	2	750	
	3	1500	
NO _x †	1	80	20, 70, 270, and 543 ppm
	2	200	

*Propane calibration gases, concentration in equivalent methane.

†NO calibration gases.

Smoke levels were measured at selected operating conditions with the standard GE smoke measurement console. This unit contains a heated filter holder and the required pump, control valves, and flow metering devices. Figure 5-15 is a photograph of the smoke measurement console, while Figure 5-16 presents a flow diagram of the smoke measurement system. This measurement system conforms completely to the requirements of the SAE (ARP 1179) and the EPA (40 CFR Part 87).

BBPR	BACK PRESSURE REGULATOR
CPG	COMPOUND PRESSURE GAGE
CV	CHECK VALVE
DT	DRYER TUBE
F	FILTER
FM	FLOWMETER
MMP	HIGH TEMPERATURE METAL BELLOW PUMP-MOUNTED IN INVERTED POSITION
NV	NEEDLE VALVE
P	PUMP
PG	PRESSURE GAGE
PR	PRESSURE REGULATOR
PPRV	PRESSURE RELIEF VALVE
SV	SOLENOID VALVE
T	TEMPERATURE INDICATOR
TV	TOGGLE VALVE

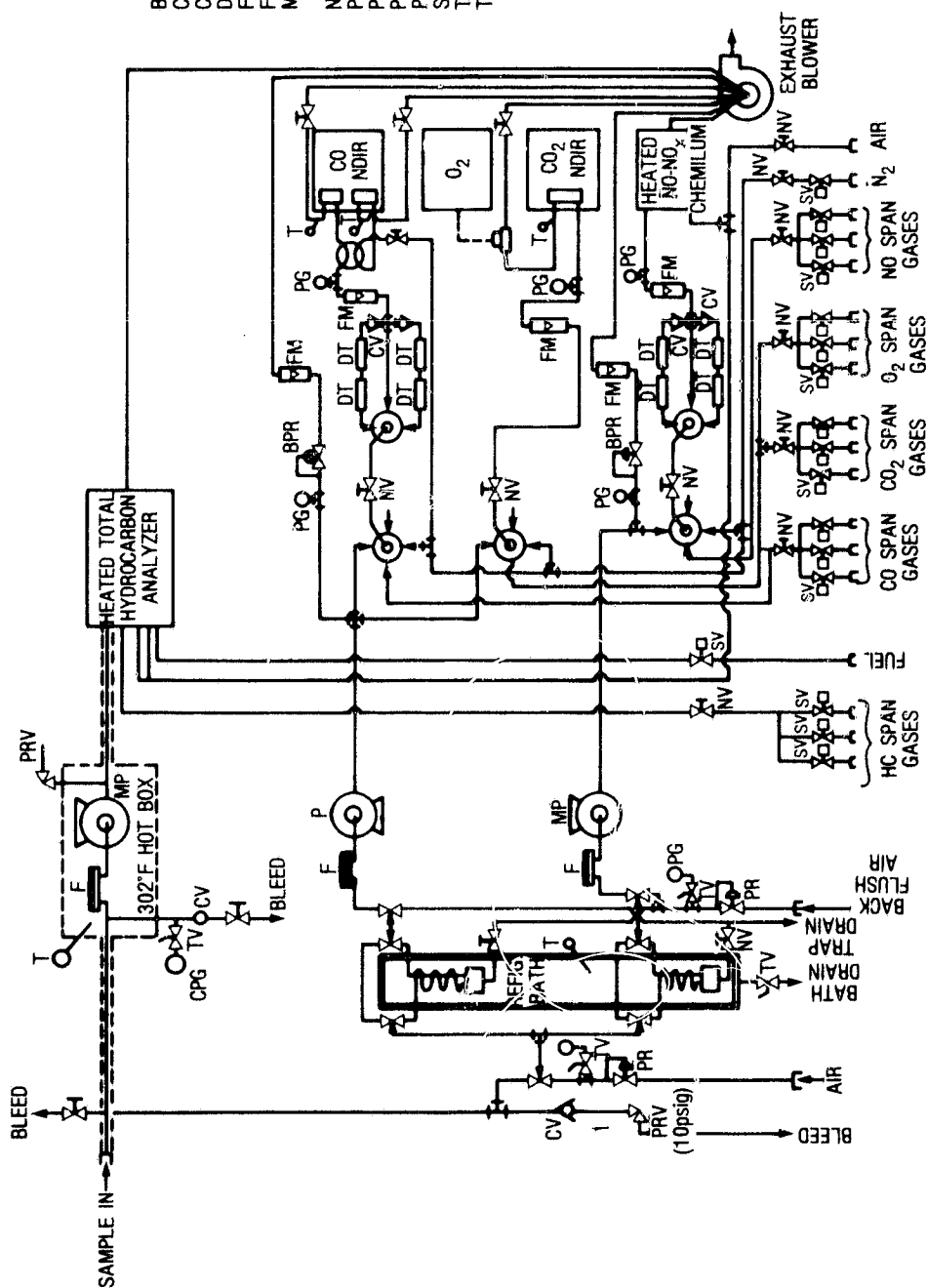


Figure 5-14. On-line exhaust emissions analysis system flow diagram

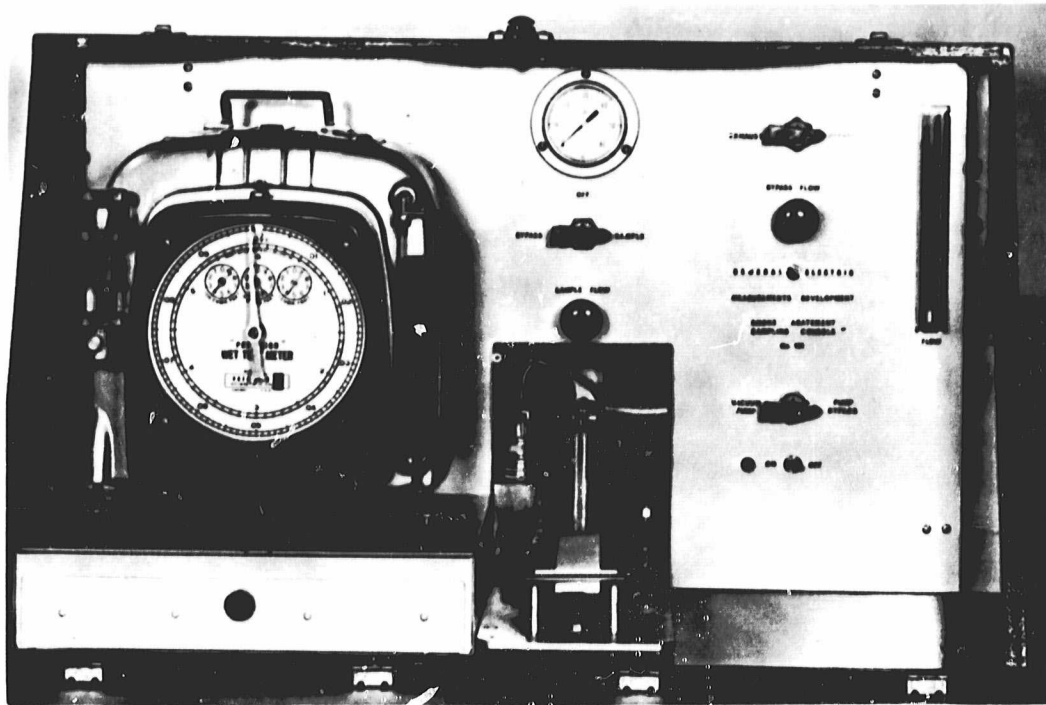


Figure 5-15. General Electric smoke measurement console

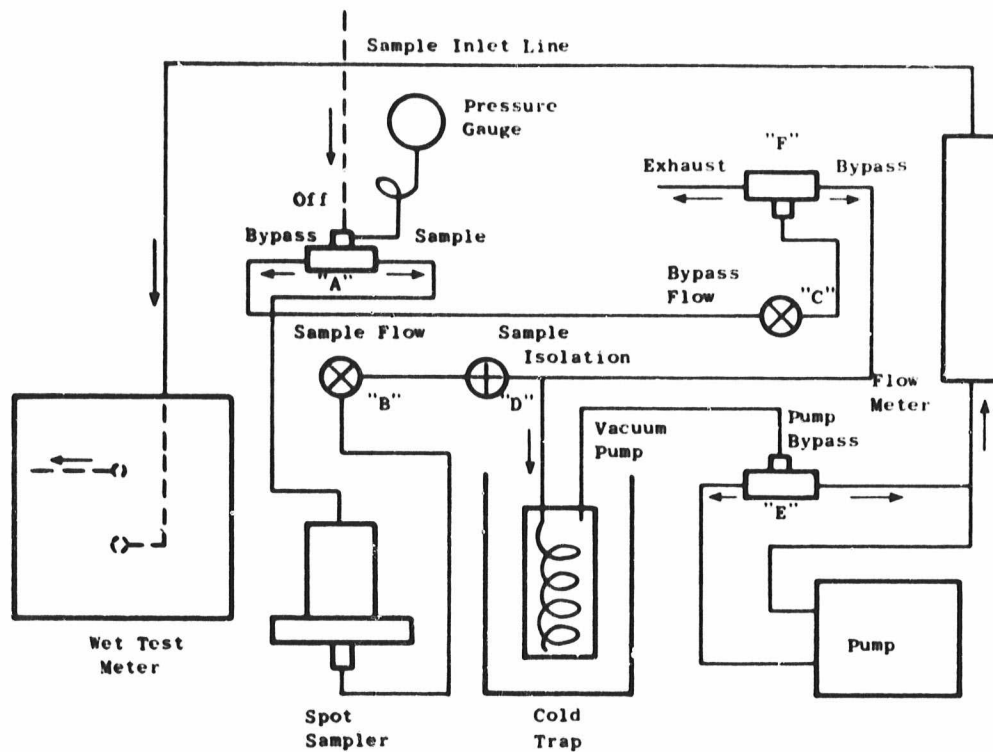


Figure 5-16. General Electric smoke measurement system flow diagram

Section 6

COMBUSTOR TEST CONDITIONS

The operating conditions used in evaluation tests of these combustors are representative of the General Electric MS7001E utility engine. The MS7001E engine has a baseload rating of 72.9 MWe at a turbine inlet temperature of 1358 K (1985 °F), pressure ratio of 11.7, and airflow of 250 kg/s (550 lb/s). The matrix of test conditions is shown in Table 6-1. The tabulated combustor airflows are scaled geometrically to the 20 cm (8 in.) test combustors of this program, conserving the mass flow per unit area. Inlet air temperature, pressure, reference velocity, and fuel/air ratio test conditions correspond precisely to MS7001E values.

The standard procedure was to evaluate the combustor over the load range for the MS7001E engine and to conduct additional tests as appropriate. Other test variables were also adjusted during the tests. For example, fuel/air ratios above and below design levels were tested for diagnostic purposes. Also, the fuel-flow split between the pilot and main stage for combustors with two fuel states was varied and had some effect on performance.

Table 6-1
COMBUSTOR TEST CONDITIONS

P_3 , Inlet Total Pressure,		T_3 , Inlet Total Temperature,		W_a , Combustor Airflow,		V_r , Reference Velocity,		W_{fT} , Total Fuel Flow,		f/a , Combustor Fuel/Air Ratio	Engine Condition
MPa	psia	K	°F	kg/s	pps	m/s	fps*	kg/hr	pph		
0.1	15.0	294	70	0.45	1.0	11.2	36.7			Ignition	
0.882	127.9	564	556	7.68	16.9	43.6	142.6	149	328	0.0054	Full Speed No Load
1.025	148.6	587	598	7.60	16.7	38.4	126.1	385	848	0.0141	50% Load
1.081	156.7	596	613	7.54	16.6	36.9	120.6	997	1094	0.0183	70% Load
1.145	166.0	606	631	7.45	16.4	35.1	114.6	630	1387	0.0235	92% Load (baseload)
1.166	169.1	609	636	7.45	16.4	34.4	112.8	679	1494	0.0253	100% Load (peak load)

*Reference Velocity Based on W_a , P_3 and $A_{Liner} = 324.3 \text{ cm}^2$ (50.27 in.²)

Section 7

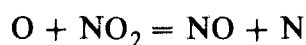
COMBUSTOR CONCEPTS

The combustors for this program were designed for reducing NO_x emissions while meeting other program goals. Oxides of nitrogen (NO_x) are present in the exhaust gases in the form of nitric oxide (NO) and a small fraction of nitrogen dioxide (NO_2).

Oxides of nitrogen in the exhaust products are formed by two mechanisms. One mechanism produces "organic NO_x ." Organic NO_x is formed during combustion by the chemical combination of CH_n radicals with nitrogen atoms which are part of the fuel molecule [the fuel-bound nitrogen (FBN)] and other chain reactions involving OH and O. The organic nitrogen-carbon bond energies of the fuel molecules are much lower than those of atmospheric molecular nitrogen, and the fuel nitrogen is more readily oxidized at lower temperatures than nitrogen in the air.

The formation of "thermal NO_x ," the second mechanism, follows from the oxidation of atmospheric nitrogen in the combustion process according to the reactions shown below:

Thermal NO Production (with Equilibrium O)



Thermal NO_x is produced mostly in regions of high temperatures in the combustor and is composed mostly of NO. Further oxidation to NO_2 is a much slower process even with high temperatures, and does not usually occur within General Electric designed gas turbines. Over long time periods and under the action of sunlight, NO in the exhaust is eventually converted to NO_2 in the atmosphere.

The curve in Figure 7-1a shows combustion temperatures of varying ratios of fuel-to-air mixtures (fuel/air) at conditions of perfectly mixed equilibrium. The highest temperatures are produced with fuel/air close to the equivalence ratio, ϕ , of 1.0, where the fuel is entirely consumed with just-sufficient oxygen.

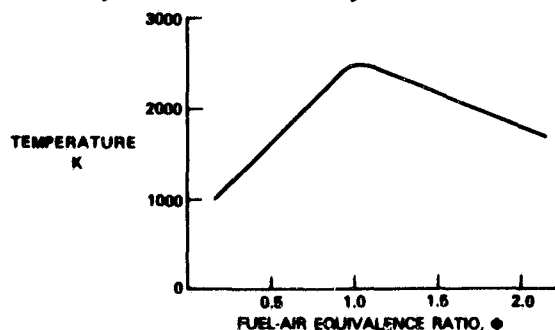


Figure 7-1a. Theoretical flame temperature

The Zeldovich relationship for the rate of thermal NO_x production in parts per million by volume per unit time (ms) is superimposed in Figure 7-1b. As can be seen from the equation of this curve at the top of the figure, the rate of NO_x production is affected by the square root of the pressure in the combustor and by the molal concentrations of nitrogen and oxygen; it is highly influenced by temperatures—a very strong exponential effect. Therefore, NO_x is produced at high rates close to stoichiometric combustion and at greatly reduced rates in rich and lean mixtures. Most gas turbine combustors have local areas in the reaction zones which burn close to stoichiometric conditions because of imperfectly homogeneous fuel-air mixtures, and most of the thermal NO_x is produced there. The final equivalence ratio leaving the combustor is very low (very lean), since excess dilution air is introduced after reaction to limit the combustor exit temperature to that desired for the turbine.

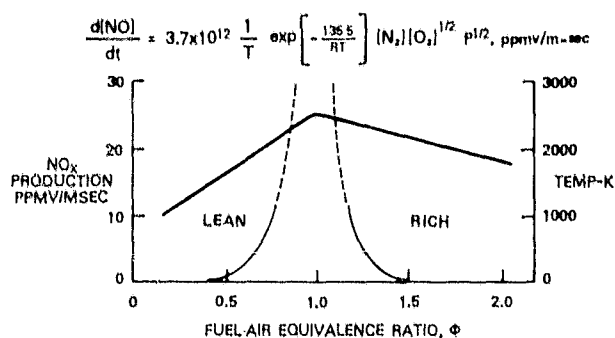


Figure 7-1b. NO_x production

The above discussion describes the rate of production of NO_x . It is clear that the total amount of NO_x is dependent upon the residence times of the fuel/air mixtures in high-temperature zones. The NO_x concentrations in real burners never approach equilibrium values; the concentrations emitted would be at least an order of magnitude greater than those observed. Nevertheless, the designer must limit residence time as much as possible, commensurate with other needs. Smaller combustors can do this, but they cannot be too small since appropriately large space rates must be maintained when using heavier fuels in order to give sufficient time to vaporize and burn these slower reacting fuels.

It is obvious that burning lean will reduce NO_x production, and this is a trend that modern combustors follow. This is particularly so because it also reduces smoke and CO emission.

At this point in the discussion, it has been indicated that lean is good, and it has been implied that perfect mixing is also beneficial. However, the combustor designer soon finds that these advantages come as mixed blessings. There is a limit to the degree of leanness that can be successfully employed in single-stage combustors because flammability limits may be exceeded. This condition is aggravated by the requirement that the combustor must operate over a very wide variation in overall fuel-to-air ratios from start to full load. When full-load conditions are lean, they become leaner by far at full speed/no load, and the flame tends to become unstable.

The tendency toward instability of excessively lean combustion inevitably brings about excessive aerodynamically induced dynamic pressure oscillations, or noise, that can wear or damage mechanical parts.

If the combustor were operated at a single design point, it would be much easier to attain more perfect mixing, and NO_x control would be enhanced. But, since the machine must start and go through changes of load, this is not feasible in the simple, single-stage combustor system. Indeed, to improve ignition characteristics it is advantageous to maintain pockets of rich fuel/air mixtures; this is counterproductive, at least in part, to the desire for well-mixed lean mixtures to minimize NO_x .

It should also be noted that the thermochemical reactions impose conditions of CO emissions when too lean and conditions of excess smoke when too rich. These modifying conditions are qualitatively indicated on the plots of temperature and NO_x production rate versus equivalence ratio in Figure 7-1c. It is seen that equivalence ratios must be between relatively narrow constraints or windows for ideal minimum emissions.

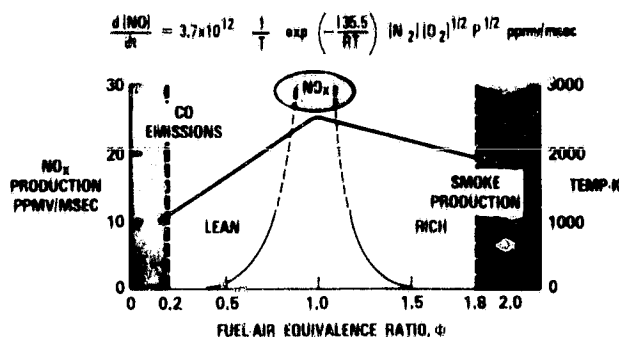


Figure 7-1c. Production of pollutants

It is apparent from the above discussion that combustors operating either very lean or very rich will have minimum thermal NO_x production. The conversion of fuel-bound nitrogen (FBN) to NO_x is best suppressed by burning in an oxygen-deficient rich zone.

This discussion suggests three fundamental approaches to reducing NO_x emissions. The first is a two-stage rich/lean combustor. This concept is operated by partially combusting the fuel in the first stage and then mixing sufficient air with the combustion products to jump from rich burning to very lean combustion. Figure 7-1c shows the equivalence ratio windows where the combustor must operate.

The lean/lean two-stage combustor allows operation over a sufficiently wide range of operating conditions to permit operation in a gas turbine. This can be accomplished by fuel or air staging and variable geometry, the former being much more desirable because of mechanical and operational simplicity.

The third approach is catalytic burning. The equivalence ratio windows shown in Figure 7-1c are widened considerably when the fuel/air mixture is burned in a catalytic section. Combining a catalytic stage and a rich first stage offers a means of reducing thermal NO_x to very low levels while simultaneously suppressing the conversion of fuel-bound nitrogen to NO_x .

Seven combustor concepts, based on these three approaches, were designed in the program. Six of the seven combustors, shown in Figure 7-2, were evaluated for NO_x emissions. The discussion of the seven designs is presented here and the test results will be discussed in a later section.

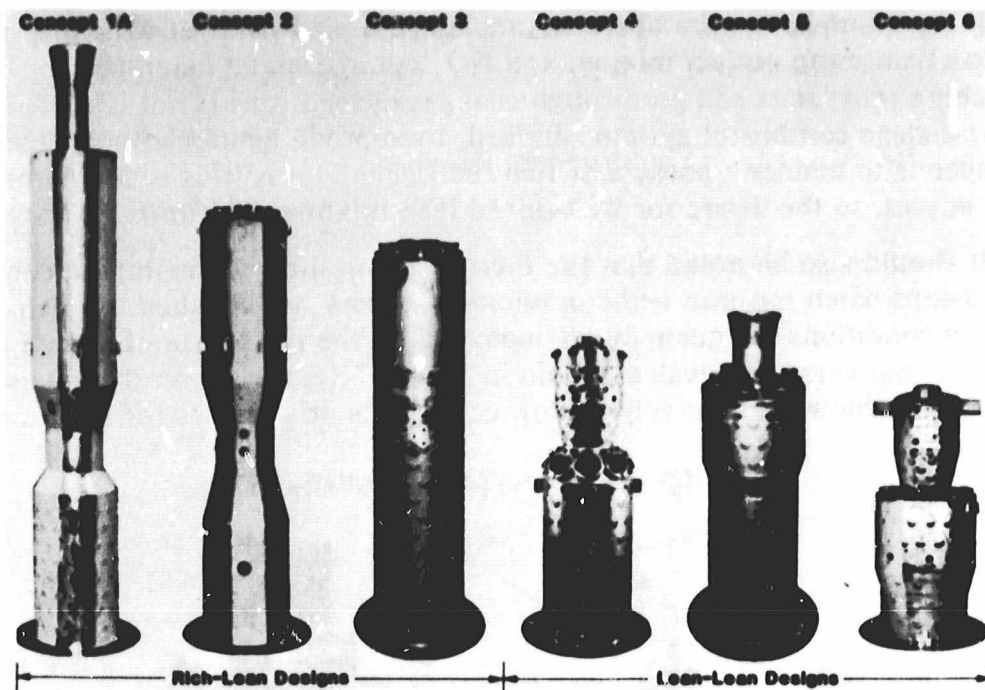


Figure 7-2. NASA/DOE low NO_x heavy fuel combustor concepts

7.1 RICH/LEAN COMBUSTOR CONCEPTS

Previous work has shown the potential of two-stage rich/lean combustion for producing low NO_x emissions with high-nitrogen fuels. The work described here is aimed at development of this concept for application to combustion systems of heavy-duty stationary gas turbines.

In this combustion mode, a rich mixture of fuel and air ($\phi \sim 1.7$) is burned in the first stage, producing incomplete combustion at low temperatures in an oxygen-deficient environment. Under these conditions, little thermal NO_x is produced while fuel nitrogen is released with minimal conversion to NO_x . This incompletely combusted mixture is then mixed with additional combustion air in a low residence time quench zone to produce a lean mixture ($\phi \sim 0.5$) with combustion completed in the lean second stage.

Two key problems are associated with the development of rich/lean combustors capable of low NO_x emissions, and are addressed in the combustor designs studied in this program. These are (a) the potential for smoke production in the rich first stage, and (b) the need for an acceptable heat transfer design of the rich stage which avoids NO_x production by eliminating a locally stoichiometric zone associated with combustion liner film cooling air. Smoke production is avoided by proper selection of rich-

stage equivalence ratio and the provision of fuel/air mixing systems to provide for mixture homogeneity. Rich-stage cooling in the test hardware was accomplished by backside convective cooling.

7.1.1 Rich/Lean Combustor with Premixing, Concept 1A

Figure 7-3 is a schematic of Concept 1A. Concept 1A contains a single fuel nozzle and axial swirl cup in a premixing tube ahead of the rich stage. This should provide uniform mixing of fuel and air and avoid smoke production. Rotational swirl is provided by a radial inflow swirler at the exit of the premixing duct. Following the rich stage is a necked-down quench zone where secondary air is introduced and mixed with the products of combustion from the rich stage in minimum time. This shifts the stoichiometry from rich to lean and is followed by combustion in the final lean stage.

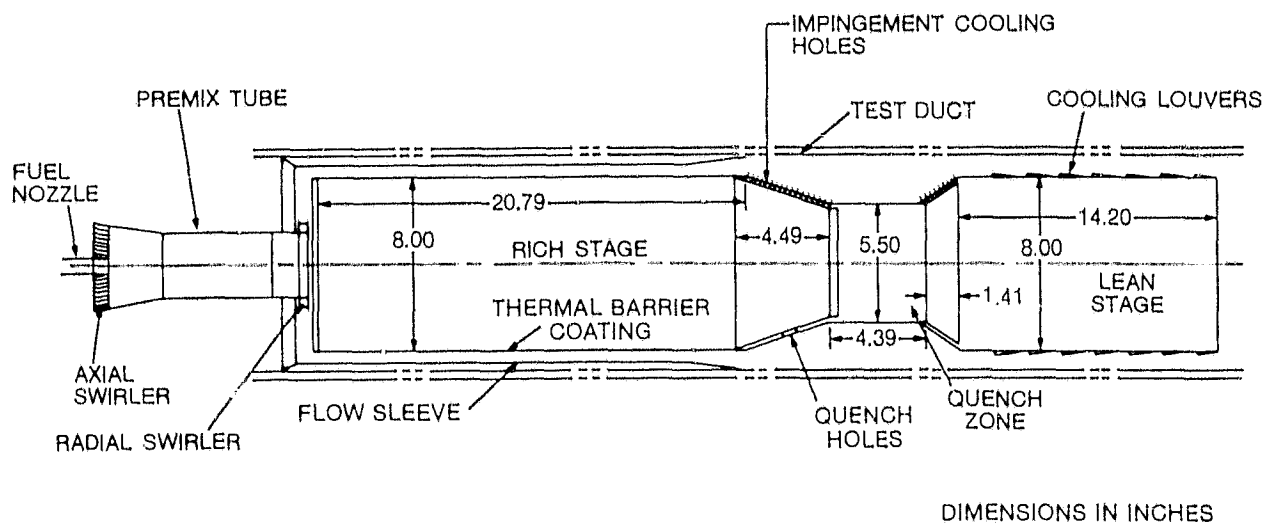


Figure 7-3. Rich/lean combustor with premixing, Concept 1A

The length of the rich stage was established by residence time requirements. Previous tests had shown that rather long residence times are required for NO formation to approach equilibrium values. The Concept 1A design has approximately 20 ms residence time based on plug flow of the gas in the rich stage. Residence time is calculated based on the adiabatic flame temperature and a rich stage length of 50 cm (20 in.). Lean-stage combustion air is injected at the end of the rich stage, and the area of the combustor is decreased to accelerate the flow to a velocity exceeding 100 m/s (300 ft/s) with a residence time of 0.9 ms. The length of the small diameter mixer is 11.2 cm (4.4 in.) and the diameter is 14.0 cm (5.5 in.). The expansion cone creates a strong vortex for flame holding in the lean stage. The downstream end of the combustor, after the dilution holes, has a length-to-diameter (L/D) ratio of unity, providing an additional 2-3 ms for complete reaction of heavier fuels.

Figure 7-4 is a photo of Concept 1A showing the premix tube at the top of the figure, followed by the convectively cooled rich stage, quench zone, and lean stage. The elongated holes in the converging section of the quench zone provide for entrance of secondary air to be rapidly mixed with the rich-stage products while accelerating through the necked-down section between rich and lean stages. Rich-stage liner cooling is accomplished by convection cooling of the outside of the liner. A thermal barrier coating was applied to the inside of the rich stage to minimize heat transfer from combustion gases to the liner wall. Louver cooling is used on the liner sleeve in the lean stage and downstream dilution zone.

Nominal rich-stage equivalence ratios of 1.4 to 1.9 have been tested, with a lean-stage equivalence ratio of 0.54. Tables 7-1 and 7-2 present the air splits and zone equivalence ratio as designed for Concept 1A. The test combustor is 20 cm in diameter with an overall length of 137 cm, including the premix tube and downstream dilution section.

7.1.2 Rich/Lean Combustor with Multiple-Nozzle Dome, Concept 2

Figure 7-5 is a schematic of Concept 2. This combustor was designed to have the same rich and lean stage equivalence ratios as Concept 1, but has multiple fuel nozzles and counterrotating swirlers to prepare the rich-stage fuel/air mixture. Figure 7-6 is a photograph showing combustor Concept 2 with eight fuel nozzles and swirl cups in the head end of the rich stage. Following the rich stage is the necked-down quench zone followed by the lean stage. In addition to the multiple nozzle head-end, this combustor differs from Concept 1A in that the rich stage was shorter (38 cm compared to 51 cm for 1A), and the holes for admission of mixing air to the products leaving the rich stage are in the smaller-diameter quench zone.

The length of the first stage was 38.1 cm (15 in.). For plug flow of the gas, the residence time is approximately 14 ms. This length was varied during Concept 2 testing to assess the effect of residence time on NO_x formation. Lean-stage combustion air is injected at the end of the rich stage, and the area of the combustor is decreased to accelerate the flow to a velocity exceeding 100 m/s (300 ft/s) with a residence time of 0.7 ms. The length of the small diameter mixer was 12.1 cm (4.78 in.), and the diameter was 14.0 cm (5.5 in.). The downstream end of the combustor, after the dilution holes, has an L/D ratio of unity, providing an additional 2-3 ms for complete reaction of heavier fuels.

The rich-stage dome is impingement cooled. This cooling air is introduced in the main stream through a gap around the swirler. This method avoids creation of a film along the liner wall, which can produce high NO_x by burning fuel at or near the stoichiometric equivalence ratio of 1. The conical and small-diameter sections of the quench zone were impingement cooled and coated on the inside surface with a thermal barrier coating.

Note in Figures 7-5 and 7-6 that the rich stage is again not cooled by air penetrating the rich-stage liner through cooling louver holes, but rather by backside convection cooling (flow sleeve inserted in test rig to increase backside cooling air velocity) and the application of a thermal barrier coating to the inside surface of the rich stage. The test combustor was 20 cm (8 in.) in diameter with an overall length of 127 cm (50 in.).

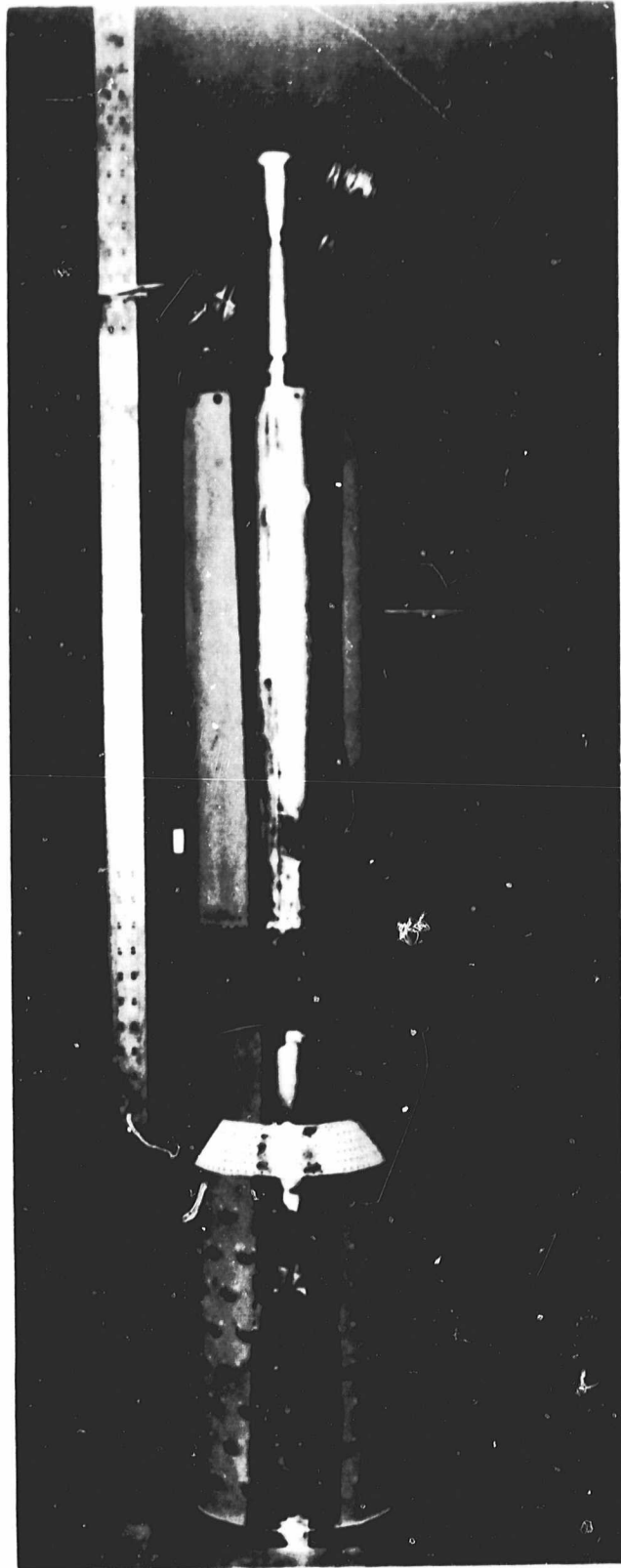


Figure 7-4. Rich/lean combustor with premixing, Concept 1A

ORIGINAL PAGE
BLACK AND WHITE PHOTOGRAPH

Table 7-1
AIRFLOW SPLITS, CONCEPT 1A

Premixer Dome Swirler	14.8%
Radial Swirler	4
Dome Cooling	<u>3.8</u>
Total Rich Stage	22.6%
Quench Flow	27.4%
Quench Cone Cooling	<u>13</u>
Total Quench Flow	40.4%
Liner Cooling	18.5%
Dilution	<u>18.5</u>
Total Cooling	37%

Table 7-2
COMBUSTOR EQUIVALENCE RATIOS, CONCEPT 1A

Load Condition	No Load	50%	70%	92%	100%
Fuel/Air Overall	0.0054	0.0141	0.0183	0.0235	0.0253
Φ Overall	0.080	0.209	0.271	0.348	0.375
Equivalence Ratios					
Rich Stage	0.354	0.925	1.20	1.54	1.66
Quench Stage	0.127	0.332	0.43	0.552	0.595

Tables 7-3 and 7-4 present the airflow splits and equivalence ratios as designed for Concept 2.

7.1.3 Rich/Lean Combustor with Narrow Passage Quench, Concept 3

Concept 3 is a rich/lean combustor with multiple fuel nozzles and swirl cups. Following the rich stage is a narrow passage mixing stage, where secondary and dilution air are introduced and mixed with the products of combustion from the rich stage in minimum time so as to produce minimum additional thermal NO_x . This combustor has the same multinozzle fuel injector/air swirler head end and rich- and lean-stage equivalence ratios as for Concept 2. It differs in the design of the mixing passage between rich and lean stages.

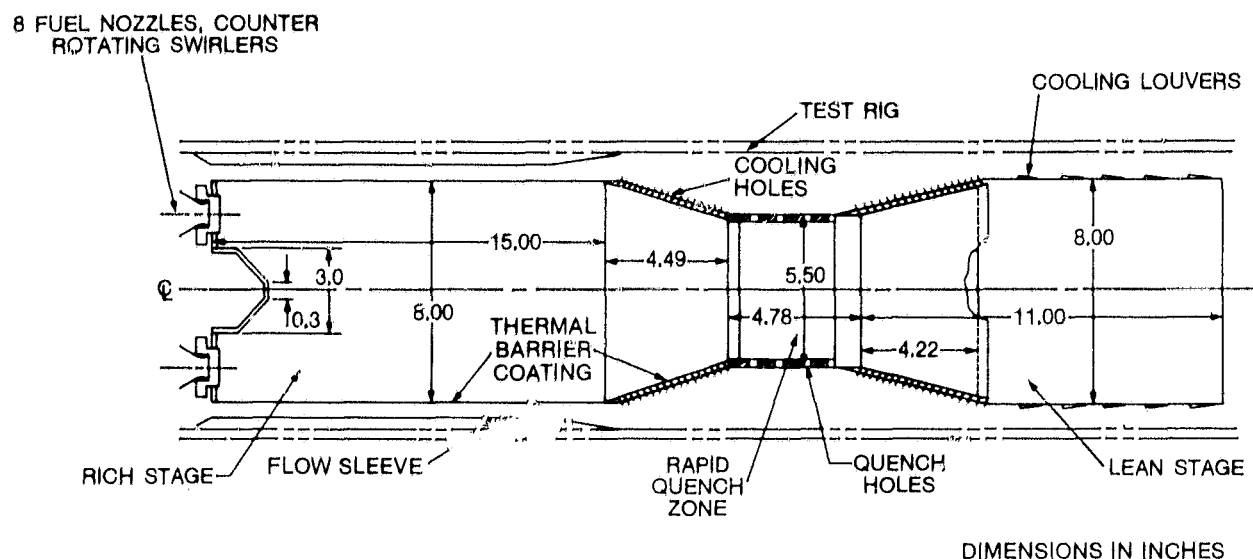


Figure 7-5. Rich/lean combustor with multiple nozzle dome, Concept 2

As for combustor Concepts 1A and 2, the rich-stage liner is convectively cooled on the backside and sprayed with thermal barrier coating on the inside.

Tables 7-5 and 7-6 present the airflow splits and zone equivalence ratios as designed for Concept 3.

7.2 LEAN/LEAN COMBUSTOR CONCEPTS

Lean/lean combustors burn lean in both stages to avoid high combustion gas temperature and thus avoid generation of thermal NO_x . In general, local average dome fuel/air ratios are maintained at less than 6/10 equivalence ratio. However, minimum local fuel/air ratios must be maintained high enough to avoid poor combustion and generation of unburned hydrocarbons and CO. In order to achieve these objectives, two stages of combustion are employed. At low engine power conditions when the total fuel-flow rates are low, only the primary or pilot stage of the combustor is fueled. At higher power conditions when the engine fuel-flow rate is adequate to fuel both stages of the combustor, fuel is introduced into the main stage dome and the pilot dome fuel flow is reduced. As the engine power and fuel-flow rates are increased, the fuel/air ratio in the main stage is increased and generally reaches an equivalence ratio of approximately 6/10 at maximum power. Therefore, by keeping equivalence ratios around 6/10, very low NO_x is generated.

Basic problems associated with lean/lean two-stage combustors include high fuel/air ratios and consequent smoke from the pilot stage before the main stage is in operation, and CO generation when the main stage is initially fueled.

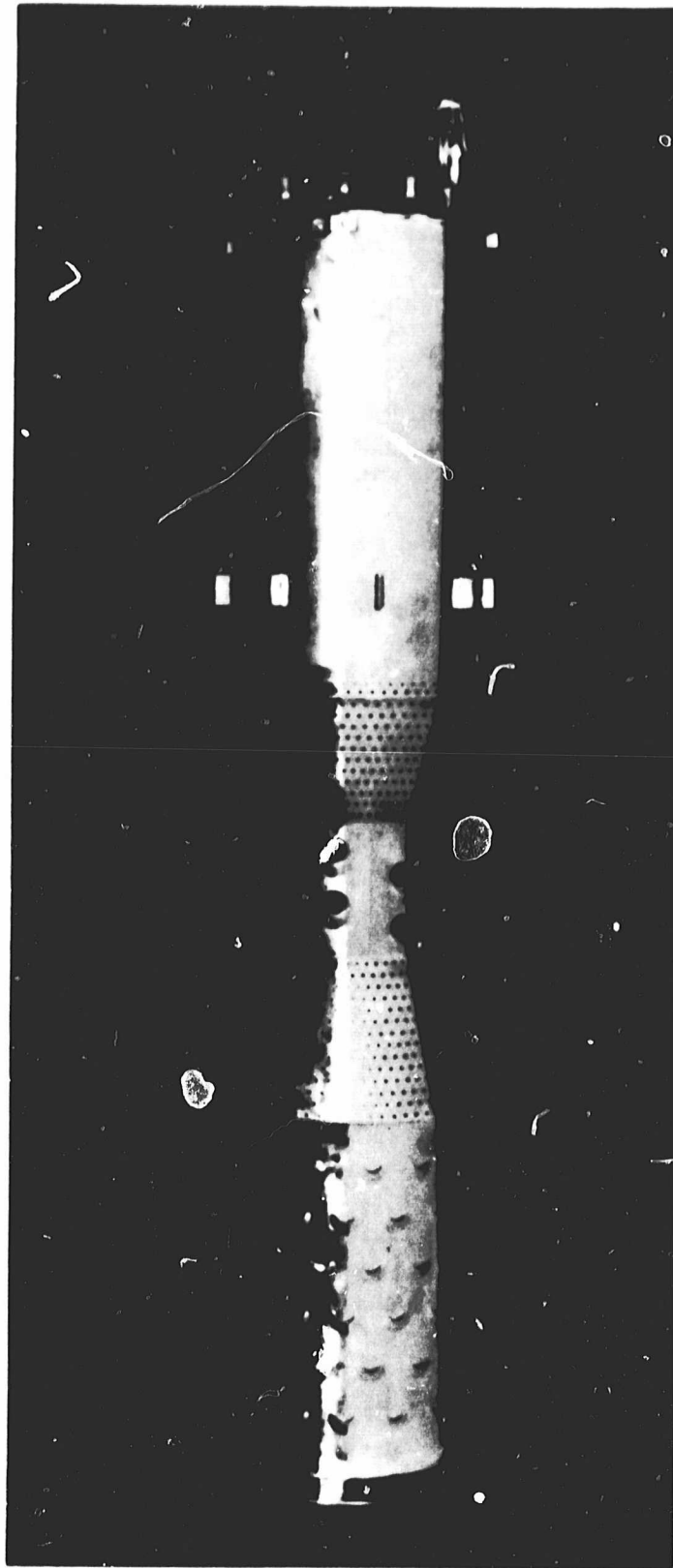


Figure 7-6. Multiple-nozzle rich/lean combustor, Concept 2

Table 7-3
AIRFLOW SPLITS, CONCEPT 2

Dome Swirler	16%
Centerbody Cooling	2.8
Dome Cooling	<u>3.8</u>
Total Rich Stage	22.6%
Quench Flow	27.8%
Quench Cone Cooling	<u>12.6</u>
Total Quench Flow	40.4%
Liner Cooling	18.5%
Dilution	<u>18.5</u>
Total Lean Stage	37%

Table 7-4
COMBUSTOR EQUIVALENCE RATIOS, CONCEPT 2

Load Condition	No Load	50%	70%	92%	100%
Fuel/Air Overall	0.0054	0.0141	0.0183	0.0235	0.0253
Φ Overall	0.080	0.209	0.271	0.348	0.375
Equivalence Ratios					
Rich Stage	0.354	0.925	1.20	1.54	1.66
Quench Stage	0.127	0.332	0.43	0.552	0.595

7.2.1 Series-Staged Lean/Lean Combustor, Concept 4

The series-staged lean-burning combustor Concept 4 is illustrated in Figures 7-7 and 7-8 and a sketch is shown in Figure 7-9. This combustor has a pilot stage utilizing a single air atomizing fuel injector and a two-stage counter-rotating swirl cup at the forward end. The first stage vanes rotate air in one direction, and the second stage vanes rotate separate air in the opposite direction. Both these airstreams mix at the exit of the pilot stage. This pilot burner is used for light-off and operation up to approximately 70% of peak engine power rating. Combustion air is introduced into the pilot dome through the swirler and through a band of eight dilution holes located approximately one dome height aft of the fuel nozzle tip.

Table 7-5
AIRFLOW SPLITS, CONCEPT 3

Dome Swirler	19.0%
Dome Cooling	<u>3.6</u>
Total Rich Stage	22.6%
Liner Cooling	9%
Mixing Section Cooling	5
Liner Quench Flow	13.2
Mixing Section Quench Flow	<u>13.2</u>
Total Quench Stage	40.4%
Liner Cooling	18.0%
Centerbody Aft Cone Cooling	6.5
Final Dilution	<u>12.5</u>
Total Lean Stage	37.0%

Table 7-6
COMBUSTOR EQUIVALENCE RATIOS, CONCEPT 3

Load Condition	No Load	50%	70%	92%	100%
Fuel/Air Overall	0.0054	0.0141	0.0183	0.0235	0.0253
Φ Overall	0.080	0.209	0.271	0.348	0.375
Equivalence Ratios					
Rich Stage	0.354	0.925	1.20	1.54	1.66
Quench Stage	0.127	0.332	0.43	0.552	0.595

The main stage employs eight single-stage swirlers and air atomizing fuel injectors. For this combustor, the objective is to obtain rapid mixing of the fuel and air in the main dome. No attempt is made to generate a strong, flame-stabilizing recirculation zone in the main stage. This is to avoid long gas residence times associated with recirculating zones that generate thermal NO_x . Instead, ignition of the main-stage gases is provided by the hot gases from the pilot dome, which is used at all engine operating conditions. For the combustor shown in Figure 7-7, 34.8% of the combustion air is used in the pilot stage and 65.2% is used in the main stage (as shown in Table 7-7). At peak load conditions, 65% of the fuel is introduced in the

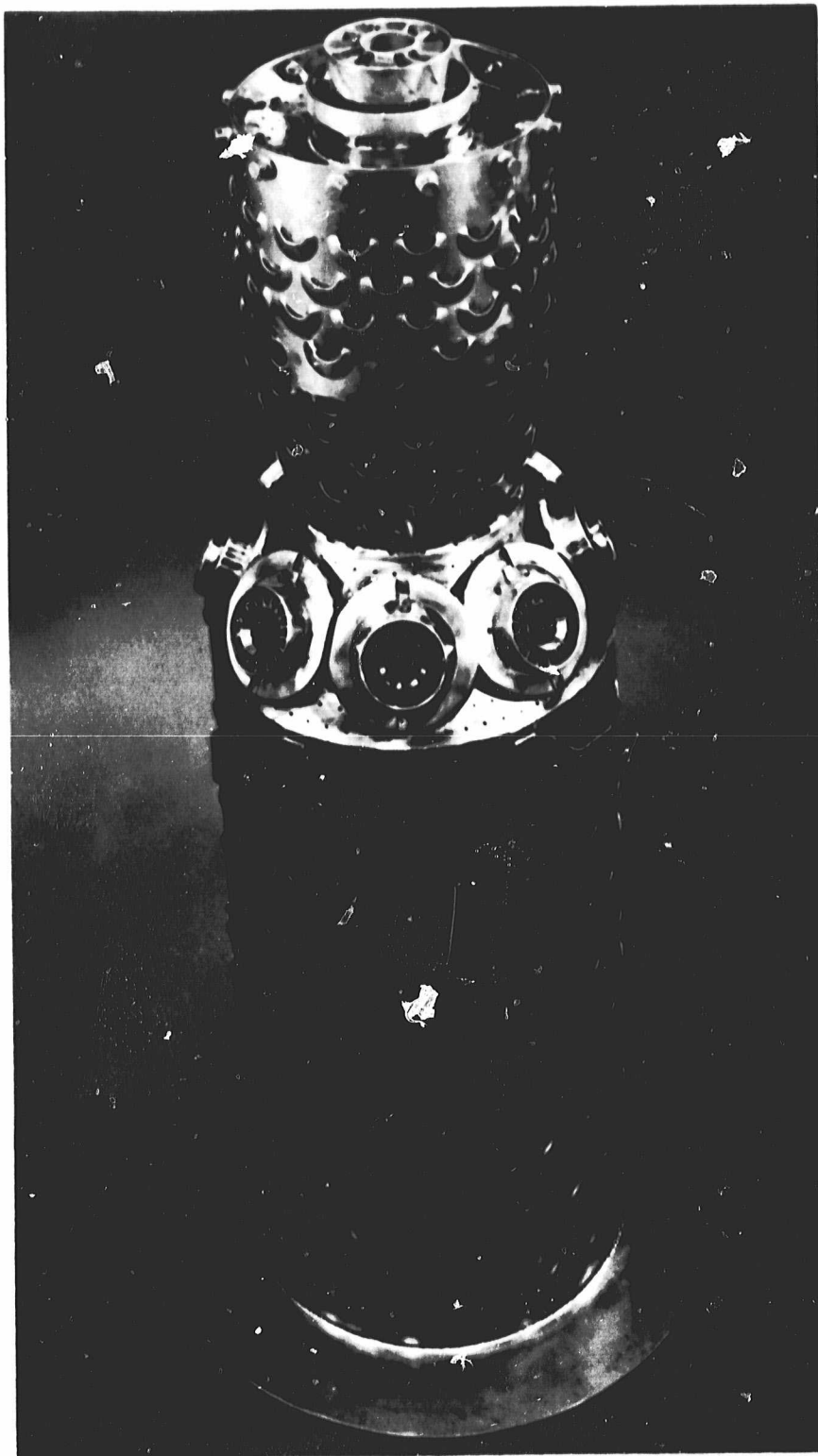


Figure 7-7. Series-staged lean/lean combustor, Concept 4

ORIGINAL PAGE
BLACK AND WHITE PHOTOGRAPH

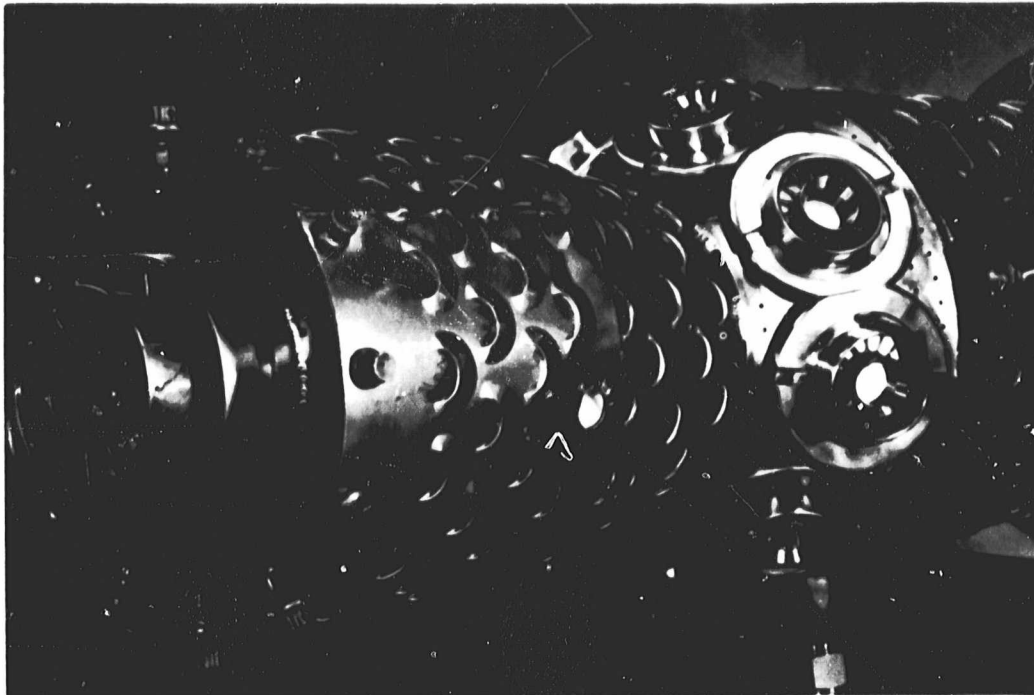


Figure 7-8. Close-up view of Concept 4

main stage, and the main-stage average equivalence ratio based on the swirler air flow is 0.63. At peak load, the pilot stage equivalence ratio based on the swirler, dome cooling, and pilot dilution air is approximately 0.59. The equivalence ratios at various load conditions is shown in Table 7-8.

The overall length of this combustor is 64.8 cm (25.5 in.), the pilot dome diameter is 15.2 cm (6.0 in.), and the aft liner diameter is 20.3 cm (8.0 in.). Approximately 24.5% of the combustor air is used for liner cooling. Cooling of the liner was achieved through punched louvers. Figure 7-9 shows the louvers schematically. The air entering the combustion zone through the slot formed by louvers forms a film on the inner surface of the combustor liner. Therefore, film cooling is achieved. Both pilot and main domes, however, were impingement cooled. Figure 7-9 also shows the impingement plate with small holes drilled in it. The air enters the combustion chamber through these holes and it then impinges on an aft plate at velocities of over 90 m/s (300 ft/s). Therefore, high-velocity jets remove the heat from the backside of the aft plates.

7.2.2 Series-Staged Lean/Lean Combustor with Premixed Main Stage, Concept 5

Figures 7-10 and 7-11 are photographs of the series-staged lean/lean design with premix tube. A schematic is also shown in Figure 7-12. This combustor has a pilot stage with six two-stage counterrotating swirlers arranged in an annulus around the main-stage premixing duct. The main-stage fuel is introduced into the forward end of the duct and mixed with the air prior to entering the combustion zone through 12 axial slots at the aft end of the premixing duct. Details of the premixing cone are

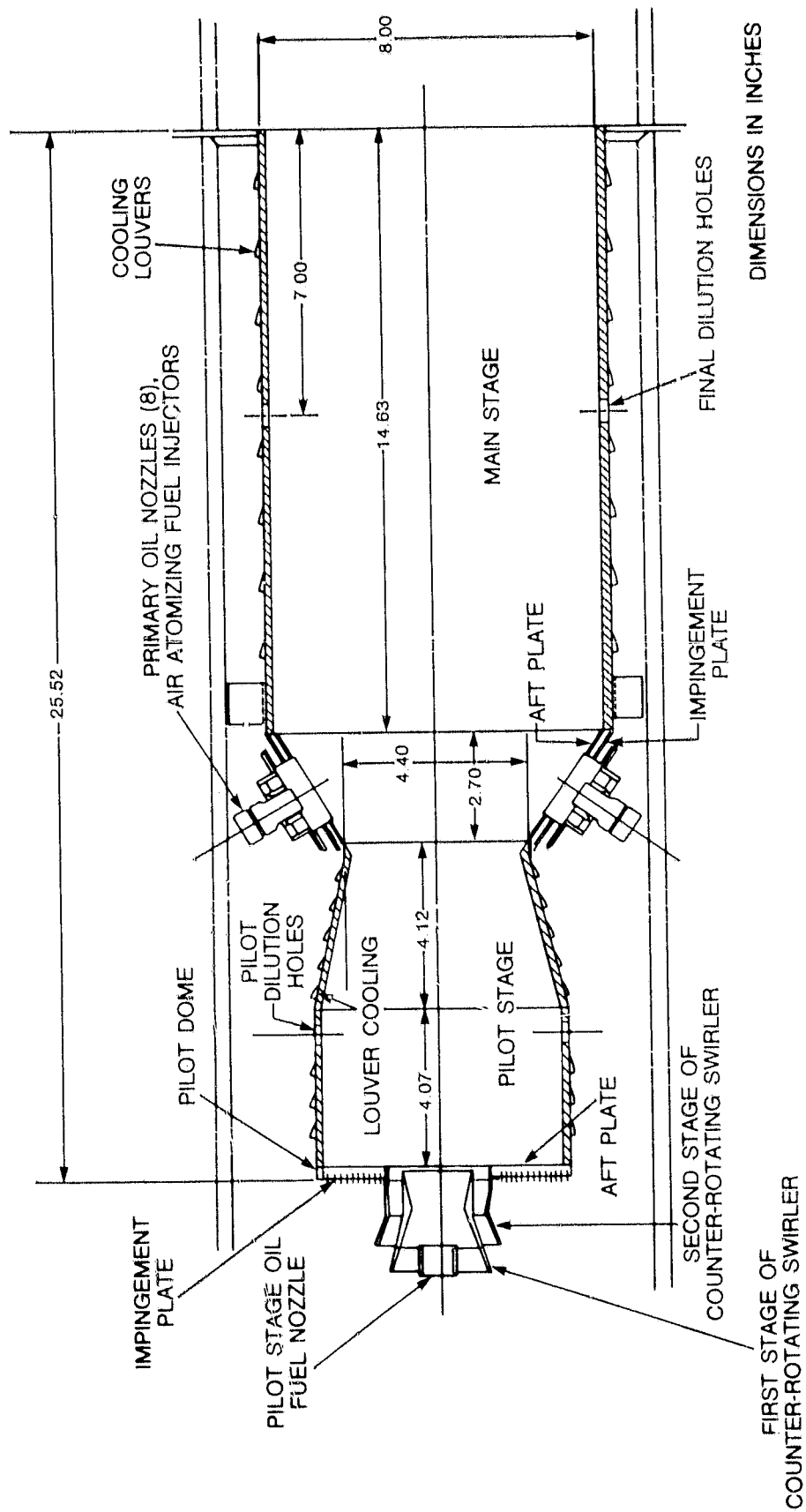


Figure 7-9. Series-staged lean/lean combustor, Concept 4

Table 7-7
CONCEPT 4 FLOW SPLITS

Pilot-Stage Dome Swirler	10.8%
Dome Cooling	4.4
Dilution	7.2
Liner Cooling	<u>12.4</u>
Total Pilot Stage	34.8%
Main-Stage Dome Swirler	32.9%
Dome Cooling	5.9
Dilution	10.4
Liner Cooling	<u>16.0</u>
Total Main Stage	65.2%

Table 7-8
CONCEPT 4 COMBUSTOR EQUIVALENCE RATIOS
(PILOT/MAIN FUEL SPLIT—35/65)

Load Condition	No Load Pilot Only	70% Pilot Only	70% Both Stages	92% Both Stages	100% Both Stages
Fuel/Air Overall	0.0054	0.0183	0.0183	0.0235	0.0253
Percent Pilot Fuel	100	100	35	35	35
Overall Equivalence Ratio	0.080	0.271	0.271	0.348	0.375
ϕ Pilot Swirl Cup	0.74	2.51	0.88	1.13	1.22
+ Dome cooling	0.53	1.78	0.62	0.80	0.86
+ Pilot Dilution	0.36	1.21	0.42	0.54	0.59
+ Pilot Liner Cooling	0.23	0.78	0.27	0.35	0.38
ϕ Main Dome	0	0	0.45	0.583	0.63
+ Main Stage Cooling	0	0	0.38	0.48	0.52
ϕ Total Combustion	0.10	0.33	0.33	0.43	0.46

shown in Figure 7-13. The hot gases from the pilot dome flow in the spaces between the slots, as shown in Figure 7-14, and mix with the main-stage mixture to provide ignition. The velocity in the premixing duct is 73.2 m/s, and the bulk-mixture residence time in the premixing duct is about 4 ms. Air-atomizing fuel nozzles are employed for both the pilot and main stage of this combustor.



Figure 7-10. Series-staged lean/lean combustor with premix, Concept 5



Figure 7-11. Series-staged lean/lean combustor with premix, Concept 5—head end and premixing duct detail

The airflow split for this combustor is similar to that of Concept 4 with 33.4% of the combustion air admitted to the pilot stage and 66.6% admitted in the main stage and aft end of the combustor. The details of the flow split are shown in Table 7-9. The equivalence ratio in the premixing duct is 0.56 at peak-load conditions. The design fuel split between pilot and main stage at peak-load conditions is 35% in the pilot and 65% in the main stage. The equivalence ratios at other load conditions are shown in Table 7-10.

The overall length of this combustor is 70.9 cm (28 in.), the pilot dome height is 6.1 cm (2.4 in.), and the premix tube diameter is 9.1 cm (3.6 in.). The louvers provided the liner cooling for this design as well. The pilot dome was again impingement cooled. The cooling of the premix tube exit nosepiece presented a design problem. Detailed finite element analysis was performed on the nosepiece. The analysis showed that with fuel air mixture flowing through the nosepiece, the maximum temperature would be approximately 1230 K (1750 °F) (aft end also coated with ceramic).

7.2.3 Parallel-Staged Lean/Lean Combustor, Concept 6

The parallel-staged lean/lean combustor is illustrated in the schematic of Figure 7-15 and the photograph in Figure 7-16. This concept has a low-velocity pilot stage with a single swirl cup and air-atomizing fuel injector at the dome end. The pilot dome is designed for ease of ignition and efficient combustion at low power condi-

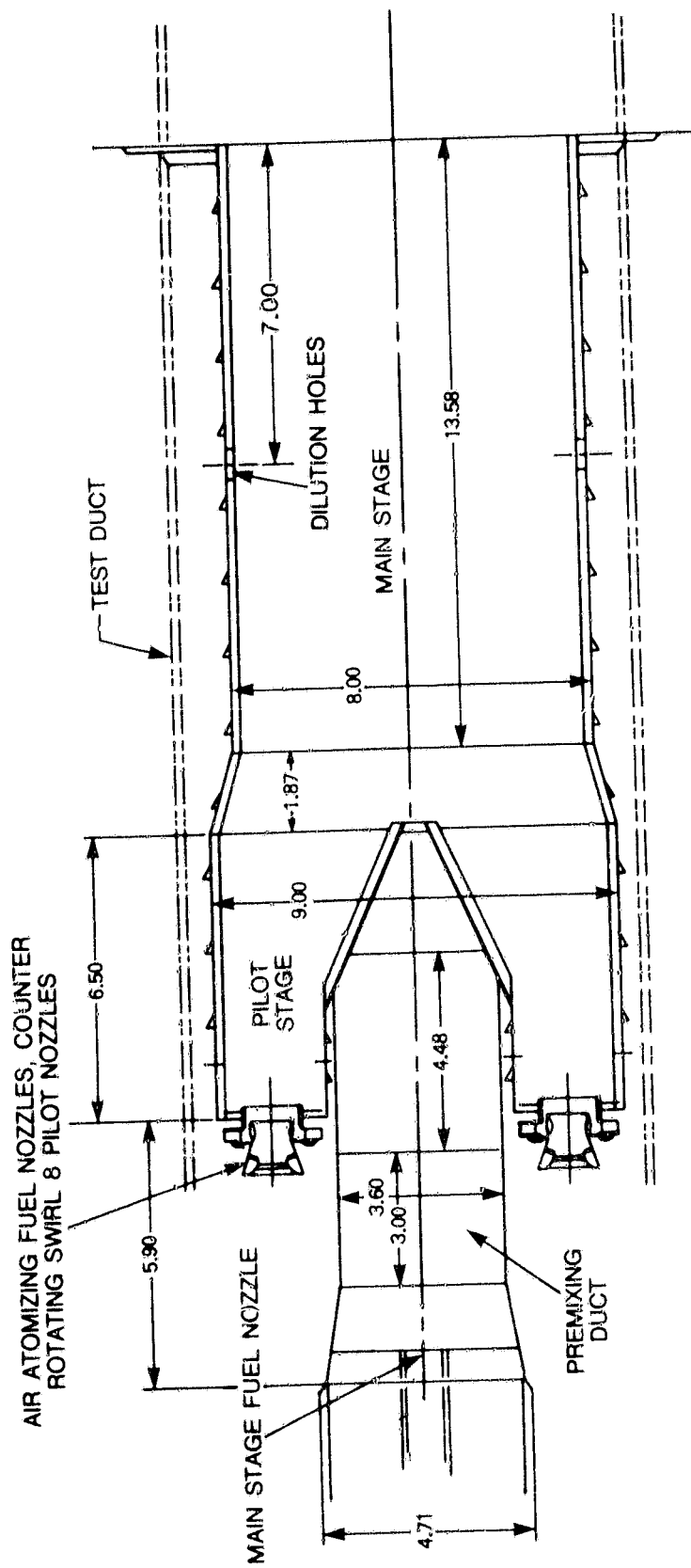


Figure 7-12. Series-staged lean/lean combustor with premix, Concept 5

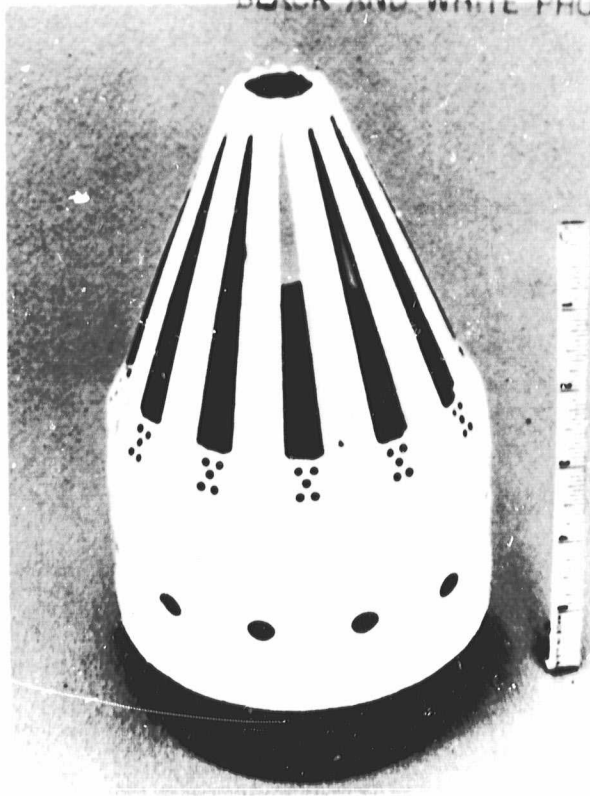


Figure 7-13. Premixing duct exit cone details, Concept 5

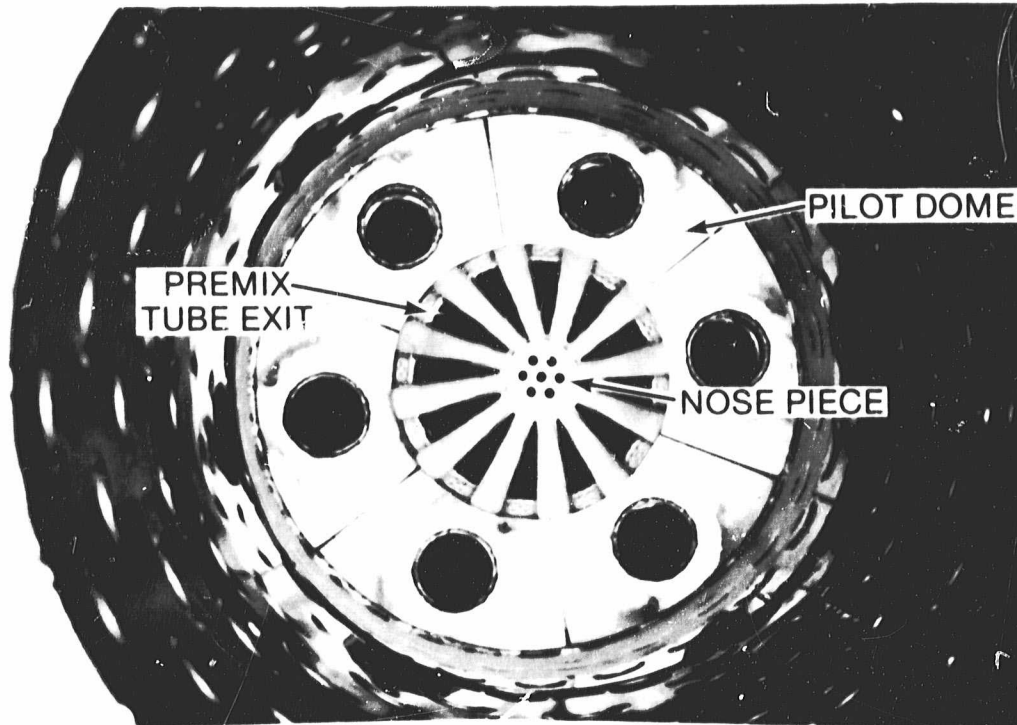


Figure 7-14. Inside view (aft looking forward) showing the exit of premix tube and the pilot dome

Table 7-9
CONCEPT 5 FLOW SPLITS

Pilot Stage Dome Swirler	11.5%
Dome Cooling	5.3
Dilution	7.2
Liner Cooling	<u>9.4</u>
Total Pilot Stage	33.4%
Main Stage Dome Swirler	43.6%
Final Dilution	9.1
Liner Cooling	12.2
Joint Cooling	<u>1.7</u>
Total Main Stage	66.6%

Table 7-10
CONCEPT 5 COMBUSTOR EQUIVALENCE RATIOS
(PILOT/MAIN FUEL SPLIT - 35/65)

Load Condition	No Load Pilot Only	70% Pilot Only	70% Both Stages	92% Both Stages	100% Both Stages
Fuel/Air Overall	0.0054	0.0183	0.0183	0.0235	0.0253
Percent Pilot fuel	100	100	35	35	35
ϕ Overall	0.080	0.271	0.271	0.348	0.375
ϕ Pilot Swirl Cup	0.70	2.36	0.82	1.06	1.14
+ Dome Cooling	0.48	1.61	0.56	0.73	0.78
+ Pilot Dilution	0.33	1.13	0.39	0.51	0.54
+ Pilot Liner Cooling	0.24	0.81	0.29	0.37	0.39
ϕ Main Dome	0	0	0.40	0.52	0.56
+ Main Stage Cooling	0	0	0.35	0.44	0.48
ϕ Total Combustion	0.10	0.32	0.32	0.41	0.44

tions with low overall engine fuel/air ratios and with low inlet pressures and temperatures. The main stage has an annular high-velocity dome with six swirl cups and fuel injectors in a concentric arrangement around the discharge end of the pilot stage. The high dome velocities and lean fuel/air ratios employed in the main stage result in low gas temperatures and short residence times for minimized thermal NO_x emissions. Although the main stage has high velocities, efficient combustion is achieved because the inlet temperature and pressure are high at high power conditions when the main

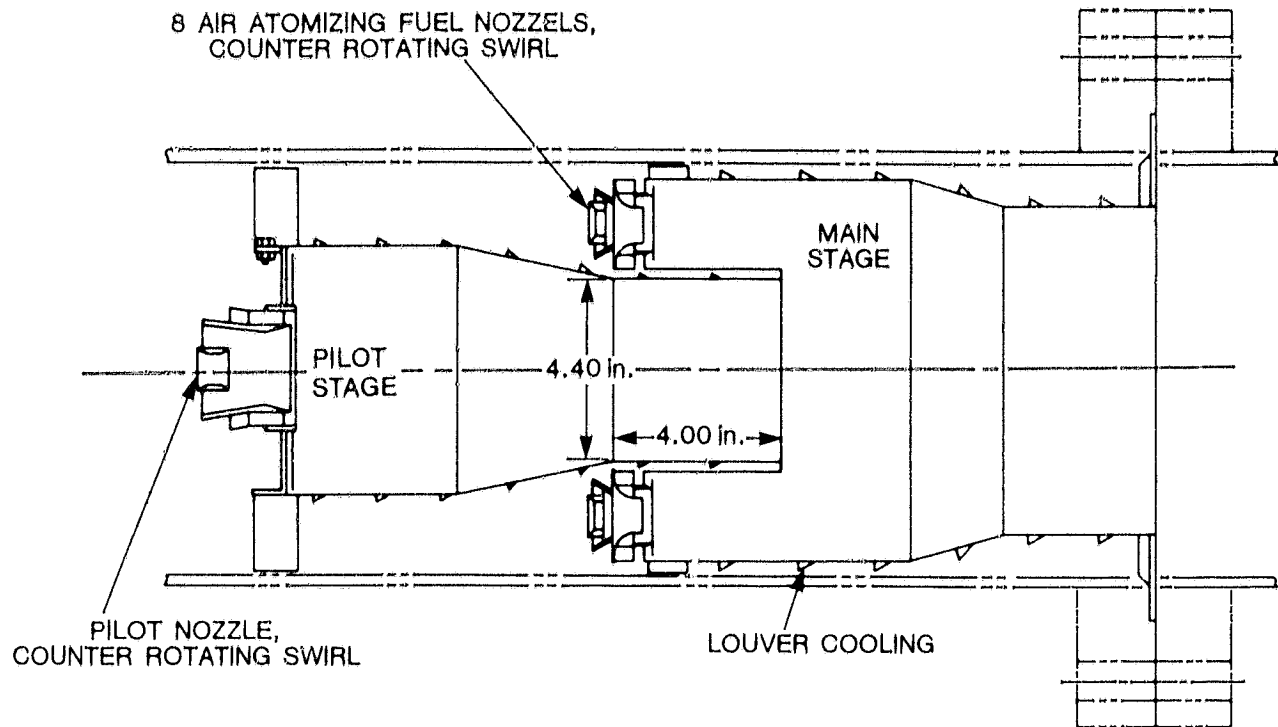


Figure 7-15. Parallel-staged lean/lean combustor, Concept 6

stage is in operation. In the parallel-staged combustor design, the main-stage dome is designed to be self-stabilized and does not require the pilot except for ignition when fuel is initially introduced in the main stage. In this concept, the pilot can be shut down after the main stage is burning.

The airflow split for Concept 6 is similar to Concepts 4 and 5 with approximately 37.6% airflow in the pilot stage and 62.4% in the main stage. The detailed airflow split is shown in Table 7-11. As in the previous two lean/lean designs, the pilot stage operates up to 70% load, and the main stage is brought on at that load. The pilot dome is similar to that of Concept 4 with equivalence ratio of about 0.58 at peak load. The main-stage equivalence ratio is about 0.67. Equivalence ratios at other load conditions is shown in Table 7-12. The combustor is 52.7 cm (21.0 in.) in overall length, the pilot dome is 15.2 cm (6.0 in.) in diameter, and the diameter at the main-stage dome is 22.9 cm. The liner is again louver cooled while the domes are impingement cooled.

7.2.4 Summary

All the lean/lean designs presented here operate with a lean mixture in both stages at most of the load conditions. Therefore, with some development, all three designs have the potential of meeting the program goals with clean fuel (ERBS). However, only limited capability for suppressing fuel-bound nitrogen is anticipated for these lean/lean combustor concepts.

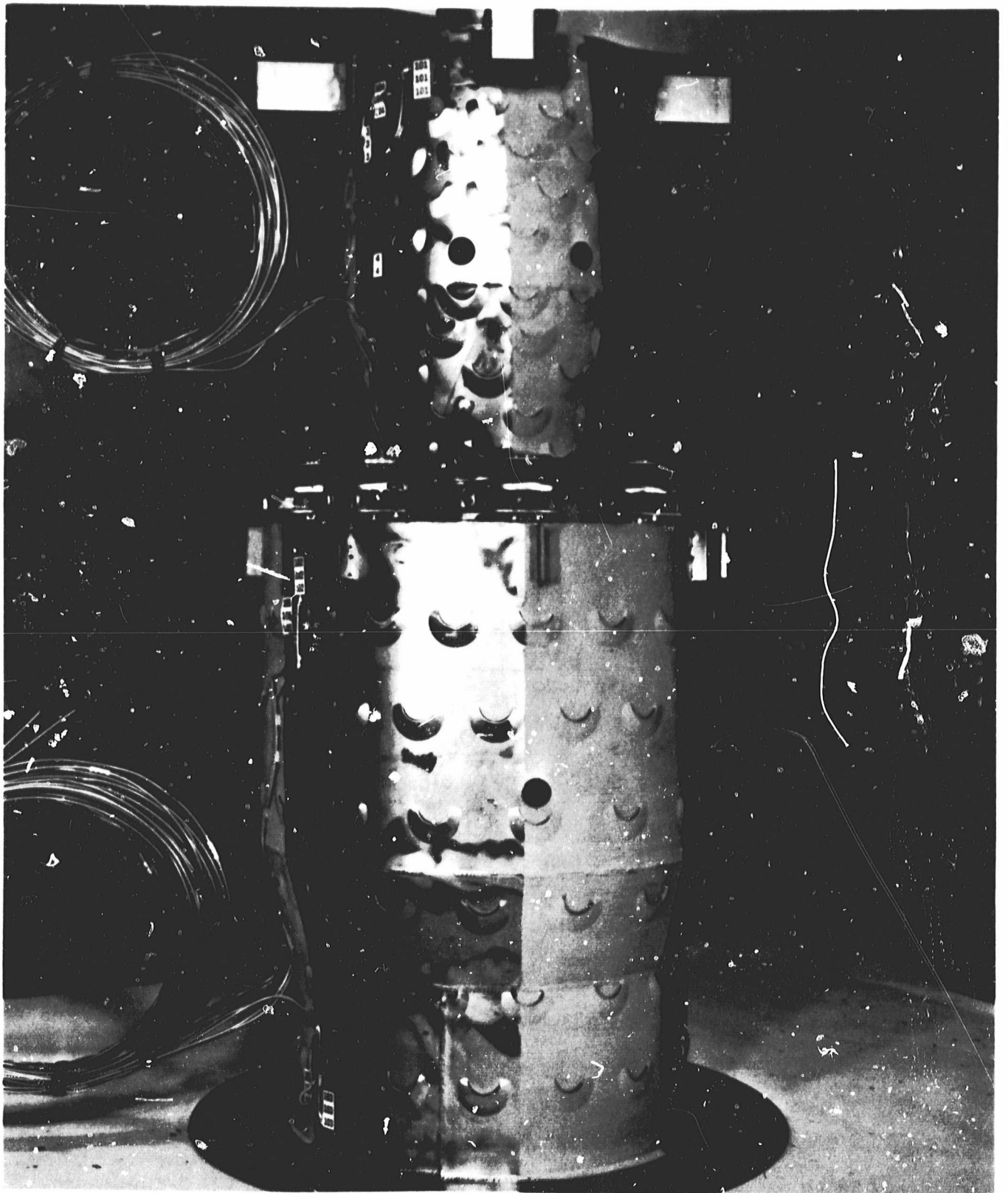


Figure 7-16. Lean/lean combustor, Concept 6

Table 7-11
CONCEPT 6 FLOW SPLITS

Pilot Stage Dome Swirler	11.28%
Dome Cooling	4.24
Dilution	7.22
Liner Cooling	<u>14.89</u>
Total Pilot Stage	37.63%
Main Stage Dome Swirler	30.69%
Dome Cooling	5.51
Dilution	7.22
Liner Cooling	16.34
Joint Cooling	<u>2.61</u>
Total Main Stage	62.37%

Table 7-12
CONCEPT 6 COMBUSTOR EQUIVALENCE RATIOS

Load Condition	No Load Pilot Only	70% Pilot Only	70% Both Stages	92% Both Stages	100% Both Stages
Fuel/Air Overall	0.0054	0.0183	0.0183	0.0235	0.0253
Percent Pilot fuel	100	100	35	35	35
ϕ Overall	0.080	0.271	0.271	0.348	0.375
ϕ Pilot Swirl Cup	0.70	2.40	0.84	1.08	1.16
+ Dome Cooling	0.51	1.75	0.61	0.78	0.85
+ Pilot Dilution	0.35	1.19	0.42	0.54	0.58
+ Pilot Liner Cooling	0.21	0.72	0.25	0.32	0.35
ϕ Main Dome	0	0	0.49	0.62	0.67

7.3 LEAN REACTION CATALYTIC COMBUSTOR CONCEPT

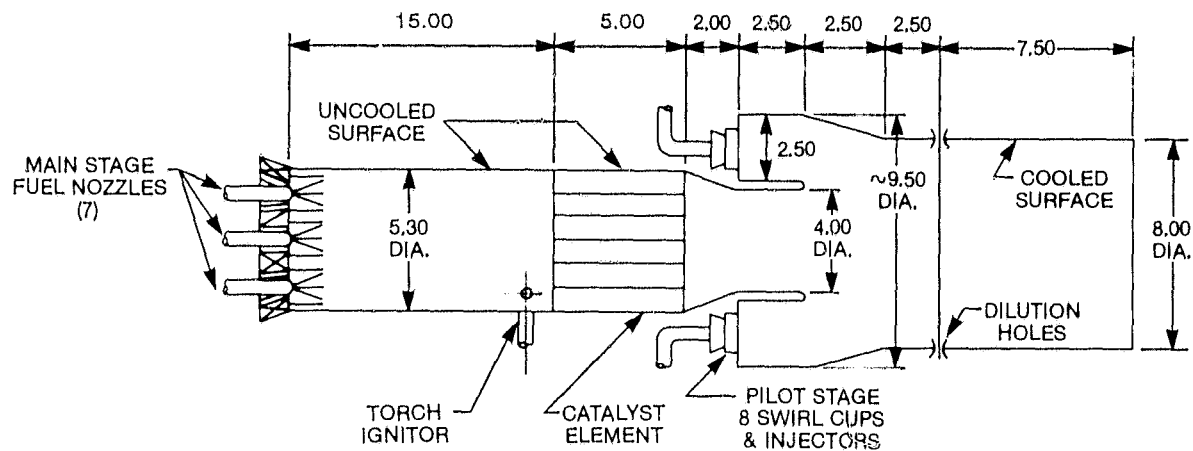
The lean reaction, parallel-staged, catalytic combustor, designed to demonstrate ultralow thermal NO_x performance for the combustion of low-nitrogen fuels, utilizes a noble metal catalyst for the combustion of the major amount of fuel at low equivalence ratios. Lean combustion, as described in the previous discussion of off-stoichiometric combustion concepts, is an effective technique for reducing NO forma-

tion by thermal fixation of combustion air nitrogen. A program for development of a catalytic combustor to meet program objectives over a wide range of load conditions would require extensive fundamental studies in the areas of fuel/air preparation (premix/prevaporization), ignition, crossover between conventional pilot and catalytic stages, and fuel staging to accomplish turndown. This was beyond the scope and available resources in this program, and so detailed design and development were directed toward the objective of minimizing emissions at the rated full-load design condition for the MS7001E. Rather than exploring the catalyst concept alone, however, General Electric designed a catalytic combustor with pilot and catalytic stages able to perform across the complete MS7001E operating range although optimized for performance and minimum emissions at the design point only. The final design and test point schedule were designed for maximum utilization of limited resources, but with large flexibility to evaluate performance at part-load conditions as well as to conduct parametric evaluation of various catalyst and combustor variables.

The incorporation of a segmented catalytic reactor was vigorously pursued to permit low NO_x performance of this combustor with high-nitrogen fuels (see Section 8.4). Sufficient experimental data were not available, nor were the results of Acurex subscale tests successful enough to permit the design and incorporation of a segmented catalytic reactor. Due to funding and time restraints, then, the catalytic combustor final design incorporated a nonsegmented catalytic reactor which is better suited for ultralow emissions performance on low-nitrogen fuels. A description of the combustor design follows.

7.3.1 Overall Arrangement and Fuel/Air Scheduling

Figure 7-17 presents the preliminary design schematic for catalytic combustor Concept 8. Figure 7-18 is a photograph of the fabricated combustor concept. A multiple-nozzle fuel preparation section precedes the catalytic reactor main stage. This section, with seven fuel nozzles, provides for thorough premixing of the fuel/air mixture and prevaporization of the liquid fuel. A 38.0 cm (15.0 in.) length is expected to provide thorough premix and prevaporization of ERBS and SRC-II fuels, and partial prevaporization of the heavy petroleum residual fuel used in this program. This section is followed by a 15 cm (6 in.) section holding the main-stage catalytic reactor, which consists of MCB-12 zirconia spinel substrate coated with a proprietary UOP noble metal catalyst. The reactor is followed by the downstream pilot-stage section, which is used for ignition, acceleration, and part-load operation to 50% load, at which point reactor light-off occurs for further load increase to full power. Catalytic reactor constraints such as maximum size, turndown ratio, and face velocity, plus the operational requirements of the MS7001E cycle, have resulted in the fuel staging portrayed in Figure 7-19. Ignition and acceleration are accomplished with fuel flow in the pilot nozzles only. They also fuel the combustor up to its crossover point when fuel is introduced to the reactor. Fuel flow is reduced and maintained at minimum flow to the pilots while the catalyst fuel flow is increased to its maximum. Any load beyond this is accomplished by increasing fuel flow to the pilots. Fixed geometry, maximum face velocity, and turndown, i.e., temperature limits, for the catalyst determine the fuel-flow range for the reactor and thus its portion of the total fuel flow at the design point.



DIMENSIONS IN INCHES

Figure 7-17. Parallel-staged lean-reaction catalytic combustor

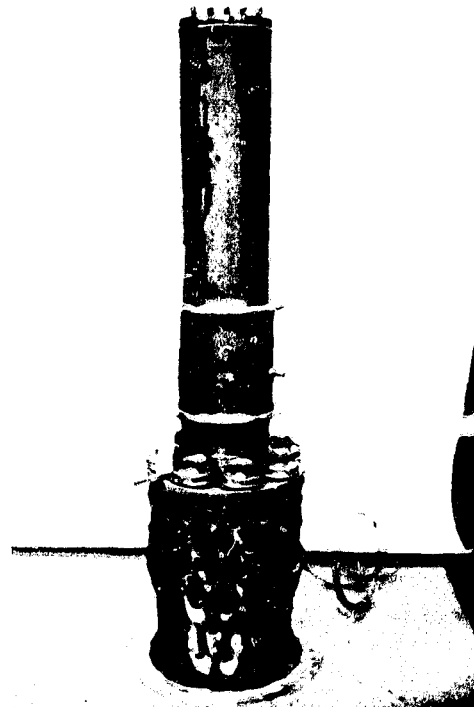


Figure 7-18. Catalytic combustor, Concept 8

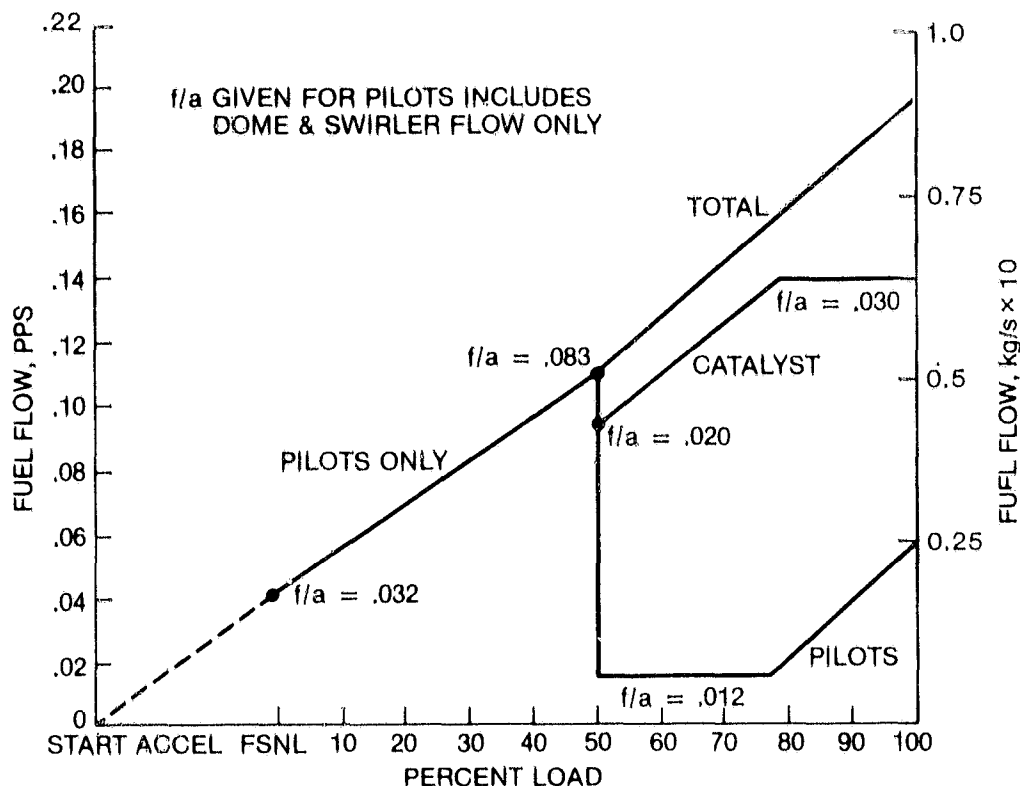


Figure 7-19. Fuel schedule, Concept 8 – MS7001E-cycle, 60/40 airflow split

Table 7-13 presents various combustor flows and equivalence ratios for different load conditions. Flow variables in this table are based on the test points described below. Catalyst pressure drop increases when fired; therefore, airflows given are what would be expected with the catalyst ignited. The crossover point occurs at 50% load when the catalyst can be fueled at a fuel/air ratio of 0.020. The pilots are continually fueled at a minimum rate above this point in order to:

1. Complete the combustion of any unburned components in the catalyst exhaust as the catalyst initially fires
2. Eliminate the need to reignite the pilots in the event of catalyst flame-out
3. Eliminate the need to reignite the pilots at high load points

The pilots burn quite rich at the 50% point before crossover, and emissions, especially CO and smoke, may be high at this point. Airflow splits at the baseload (92%) point are as follows:

Catalyst—Main Stage	60%
Pilots	
Dome Cooling	5%
Swirlers	<u>12%</u>
	17%
Liner Cooling	15%
Dilution	<u>8%</u>
	100%

Table 7-13
COMBUSTOR EQUIVALENCE RATIO FOR CATALYTIC CONCEPT 8
AIRFLOW SPLIT 60/40*

Load Condition	No Load	50%	50%†	70%	92%	100%
Overall Fuel/Air	0.0054	0.0141	0.0141	0.0183	0.0235	0.0253
Overall Fuel Flow, kg/s	0.0186	0.0477	0.105	0.135	0.172	0.185
Overall Air Flow, kg/s	3.44	3.38	3.38	3.36	3.34	3.33
Catalyst Fuel Flow, kg/s	0	0	0.0405	0.0545	0.060	0.060
Catalyst Air Flow, kg/s	2.06	2.03	2.03	2.02	2.0	2.0
Pilot Air Flow (Dome), kg/s	0.590	0.573	0.573	0.573	0.570	0.570
Pilot Fuel Flow, kg/s	0.0186	0.0478	0.0073	0.0073	0.0182	0.0245
Catalyst Fuel/Air	0	0	0.020	0.027	0.030	0.030
Pilot Fuel/Air	0.0318	0.0829	0.012	0.012	0.0324	0.0429
Pilot Fuel/Air—Overall‡	0.0135	0.0353	0.005	0.005	0.0138	0.0183
ϕ Catalyst**	0	0	0.289	0.391	0.434	0.434
ϕ Pilot (Dome)	0.460	1.200	0.179	0.179	0.468	0.621
ϕ Pilot (Dome + Cooling)	0.244	0.638	0.095	0.095	0.249	0.330
ϕ Overall‡ (Pilot)	0.195	0.510	0.076	0.076	0.199	0.264
ϕ Overall	0.078	0.204	0.204	0.265	0.340	0.366

* Airflow split based on catalyst pressure at 92% load.

† 50% load is crossover point. First case is with catalyst off; second case is with catalyst on, minimum fuel to pilots.

‡ Pilot fuel/air and ϕ overall based on the total airflow less catalyst airflow.

** $\phi = 1.0$ where fuel/air = 0.0691.

The prevaporization and catalyst sections are uncooled. The catalyst section is insulated from the combustor walls to reduce thermal gradients across the catalyst body. The pilots are similar to conventional combustors with primary zone air admission and film and convection cooling of the liner. Dilution airholes complete the mixing of air and combustion gases allowing the shaping and cooling of the combustor exhaust gases.

7.3.2 Fuel-Air Preparation

The objective of the fuel/air separation section is to present a controlled, homogeneous, prevaporized fuel/air mixture to the catalyst face and suppress autoignition tendencies upstream of the catalyst. A torch ignitor is included for initial ignition of the reactor.

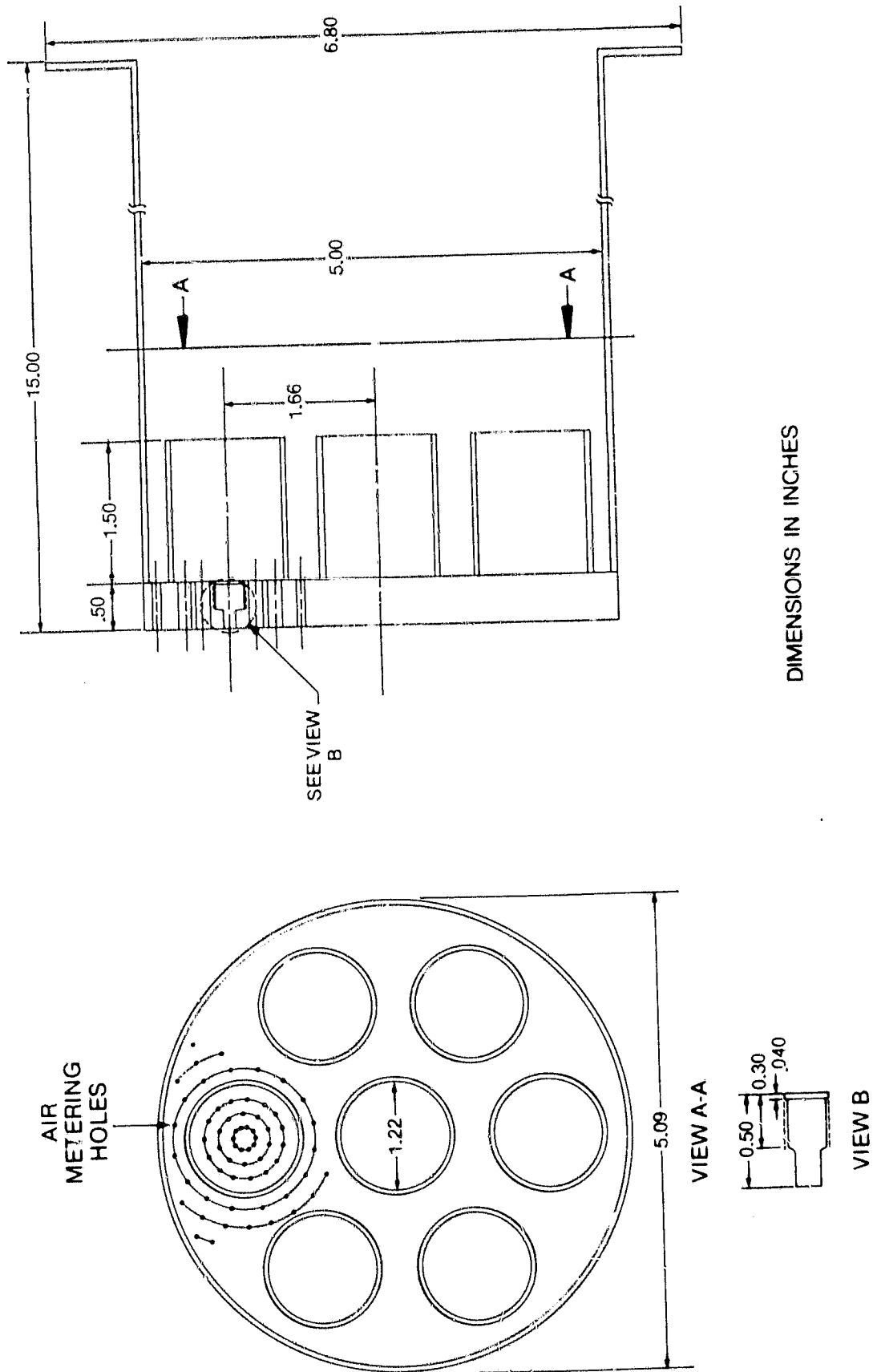
A seven fuel nozzle arrangement, analogous to the NASA multiple conical tube design of Tacina and Anderson, is used to provide superior mixing and vaporization of the liquid fuels. Cylindrical tubes are used around each fuel nozzle, for simplicity

of manufacture (considering available program resources), as opposed to the conical diffuser tubes of the NASA design. The fuel injection system uses seven pressure atomizing nozzles mounted in a perforated plate at the forward end of the premix duct. The premix duct is 38 cm (15 in.) in length. Design details of the fuel injection system are illustrated in Figure 7-20.

Features of this injection system, designed to provide uniform velocity and fuel/air ratio profiles at the catalyst face, include

1. Multiple nozzles for uniform fuel distribution.
2. High-pressure drop fuel nozzles for small fuel droplet sizes.
3. High-pressure drop ($\sim 3.6\% P_3$) across the perforated plate for high-turbulence and good mixing between the fuel and air.
4. A tube around each fuel nozzle to allow mixing of a preselected amount of air with the fuel prior to release of the mixture to the premix duct. These tubes prevent premature migration of the fuel to other parts of the premix duct.
5. Multiple air jets and long mixing lengths within each cylindrical tube allow for mixing of the air and fuel. The spaces between the individual air jets allow for spreading of the fuel.
6. Air purge to prevent recirculation of fuel into the region between the small tubes. Twenty-five percent of the premix air is used for this purpose. The air is introduced in a symmetric pattern around the tubes for uniform mixing with the fuel.
7. Adequate length aft of the small tubes to provide mixing of the fuel and air, yet short enough to avoid auto-ignition forward of the catalyst. Assuming a 7° spreading off mixing angle, the mixture from the edge of a tube would migrate to the centerline of the adjacent tube at the catalyst face.
8. Short length and no diffuser or divergent walls in the premixing duct to avoid excessive boundary layer buildup.
9. No swirlers are employed. This will avoid radial velocity gradients, recirculation, and undesirable flow directions at the catalyst face.

A full-scale model of one of the seven fuel nozzle tube assemblies (simplex nozzle inside cylindrical sleeve) was spray tested in the fuel nozzle lab at atmospheric conditions. The quality of the spray was very good (see Figure 7-21). Patternator data collected 11.4 cm (4.5 in.) downstream of the tube exit showed that very little fuel impinged on the walls of the cylindrical tube (Figure 7-22). No signs of recirculation appeared. Figure 7-23 presents results of calculations of fuel vaporization as a function of axial distance in the premix tube. It can be seen that a $50\text{ }\mu\text{m}$ droplet will vaporize only 16% in a distance of 75 cm (30 in.), which suggests that vaporization should not be used as the primary criterion for selecting premix tube length for heavy residual fuel. A 38 cm (15 in.) long premix tube is expected to provide excellent fuel/air premix and thorough prevaporization of ERBS and SRC-II fuels, with only partial prevaporization of residual fuel. Larger premix tube length (supplemented by



DIMENSIONS IN INCHES

Figure 7-20. Fuel injection system

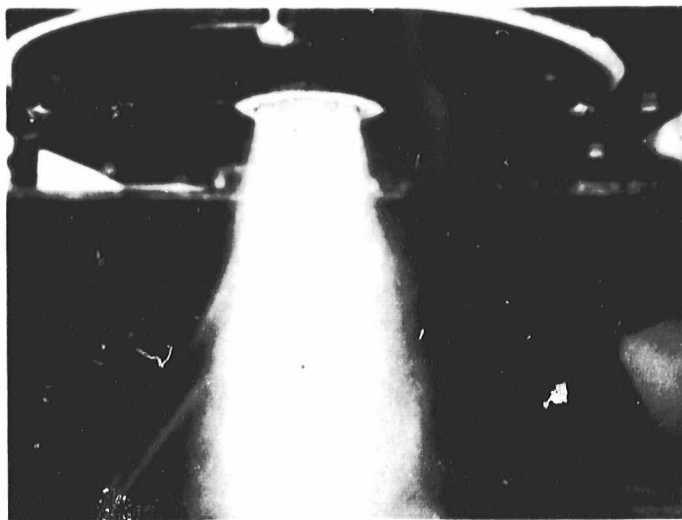


Figure 7-21. Flow visualization of fuel/air mixture at the exit of the fuel tube assembly

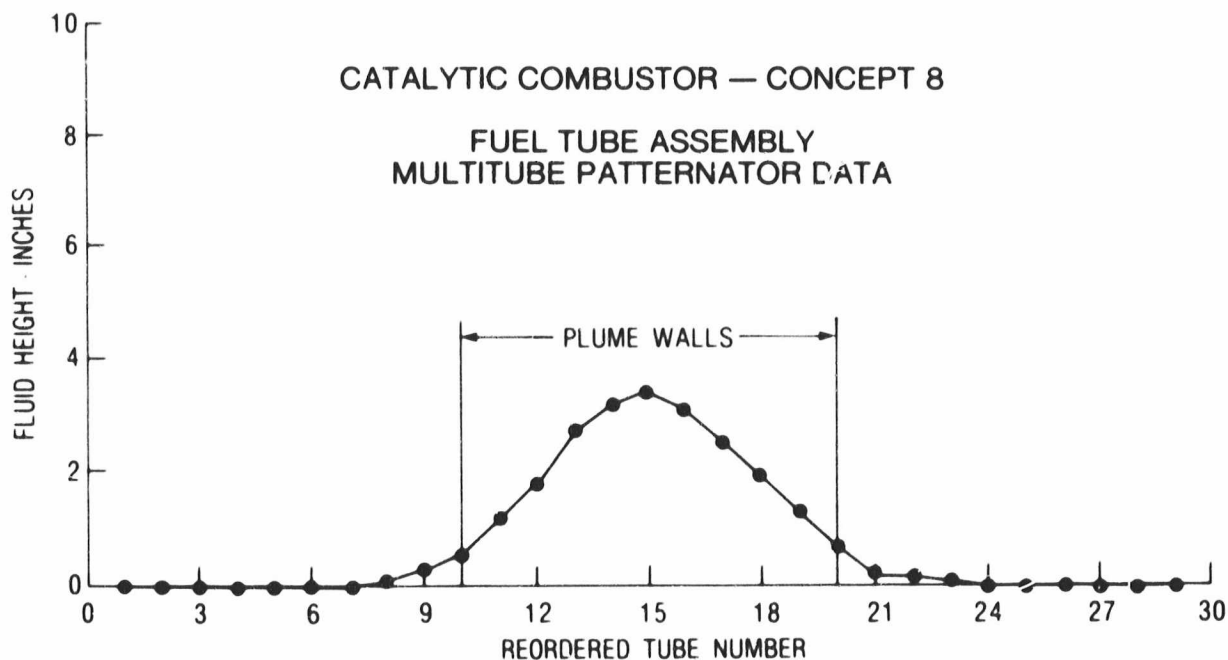
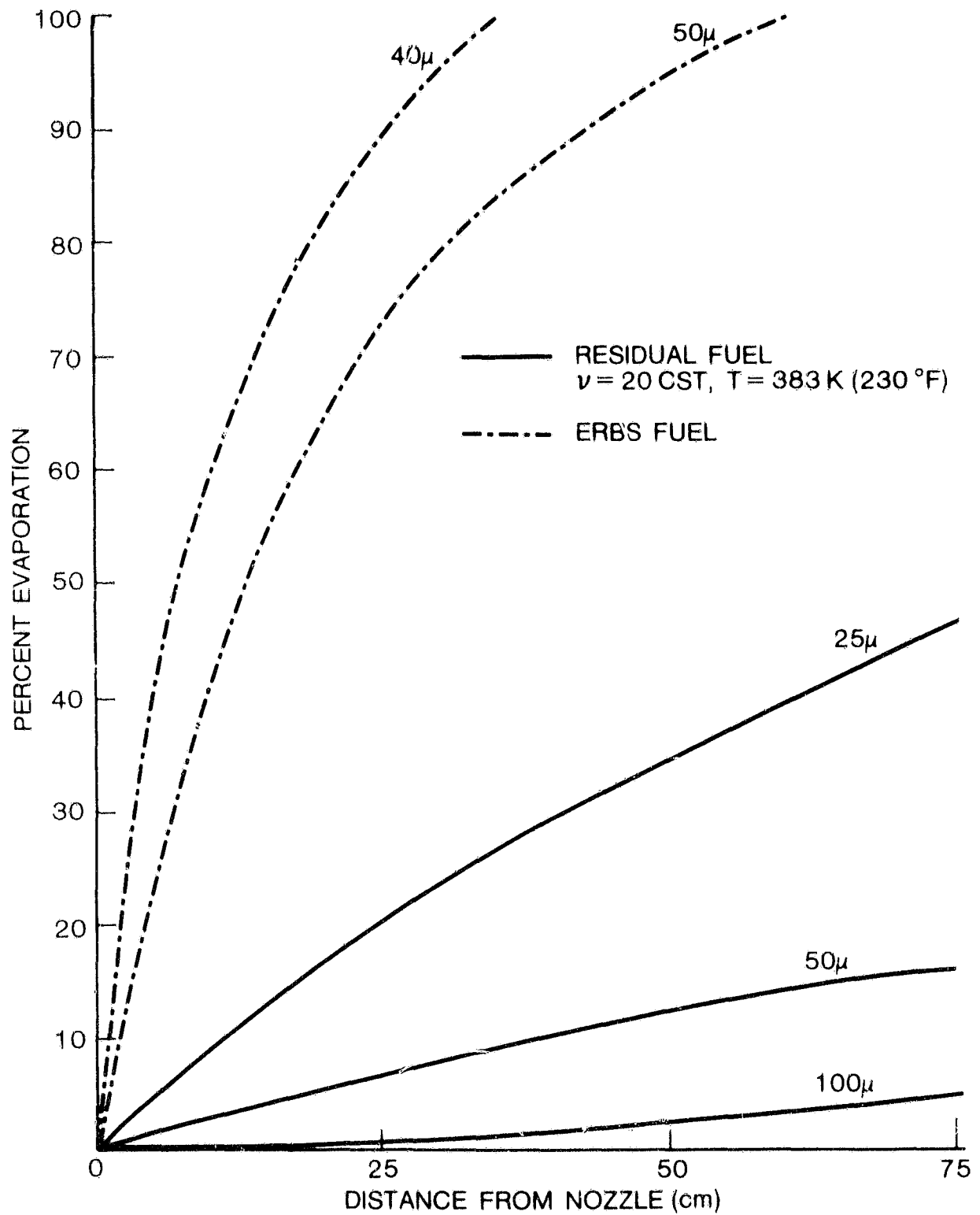


Figure 7-22. Fuel/air distribution 1.77 cm (4.5 in.) downstream of tube exit

the radiation heating of premix tube fuel and air by the catalyst face) would provide only marginal improvement in fuel vaporization, while introducing the possibility of autoignition. Although the autoignition delay time would be expected to be approximately 50 ms at the 605 K (630 °F), 11 atmosphere inlet conditions, the actual autoignition delay time will be significantly less because of radiation from the reactor bed. The 38 cm (15 in.) premix tube length provides for a nominal residence time of approximately 20 ms. This length will provide for excellent premix and thorough prevaporization of the lighter program fuels (ERBS petroleum, distillate, and the middle distillate SRC-II), while providing excellent premix and partial prevaporization of heavy petroleum residual fuel and providing margin against autoignition with this



REF: B. GAHN GE TM73-710

Figure 7-23. Fuel vaporization characteristics

heavy fuel. The fuel nozzles employed in the fuel injection system are simplex nozzles. At a residual fuel temperature of 383 K (230 °F) and a fuel pressure drop of 5.2 MPa (750 psi), these nozzles will produce 50 μm fuel droplets (40 for ERBS and SRC-II fuels).

7.3.3 Catalytic Reactor Section

The reactor, designed and supplied by Acurex Corporation, is MCB-12 zirconia spinel coated with a proprietary UOP metal coating, and is 12.7 cm (5 in.) in length and 13.5 cm (5.3 in.) in diameter. The graded cell monolith consists of entrance reactor segments with 9 cells/in.², center segments with 16 cells/in.², and exit segments with 200 cells/in.². The reactor is designed for low thermal NO_x performance at the following conditions:

Inlet Temperature	=	605 K (630 °F)
Inlet Pressure	=	11 atmospheres
Face Velocity	≤	25 m/s (80 f/s)
Minimum f/a ratio	=	0.020 (ERBS)
Maximum f/a ratio	=	0.030 (ERBS)

The catalytic reactor holder (see Figure 7-24) has been fabricated to provide for the necessary compliant mounting for the ceramic reactor, while providing for sufficient reactor insulation to approach adiabatic conditions in the reactor section. The 15.2 cm (6 in.) long holder is 14.1 cm (5.55 in.) in diameter so that a 3 mm (0.125 in.) insulation/compliant mount of Fiberfrax may be accommodated. Catalyst bed temperatures are monitored by four thermocouples embedded in the monolith.

7.3.4 Downstream Pilot Stage Section

As shown in Figure 7-25, the pilot stage section utilizes the main stage of lean/lean combustor Concept 6 previously described. Details of the necessary modifications and assembly are shown in Figure 7-26.

7.4 FUEL NOZZLE DESIGNS

Two fuel nozzle sizes were designed and fabricated for this program. The large diameter fuel nozzle is 19.6 mm (0.77 in.) OD for insertion into the 20.1 mm (0.79 in.) ID large swirler, delivers 680 kg/hr (1550 pph) liquid fuel and is used for single-nozzle combustor 1A or the single-nozzle pilot stage of Concepts 4, 5, and 6. The smaller diameter nozzle is 16.0 mm (0.63 in.) OD for insertion into the 16.5 mm (0.65 in.) ID small swirlers used in the multinozzle stages of Concepts 2, 3, 4, delivers 86 kg/hr (190 pph) liquid fuel.

ORIGINAL PAGE
BLACK AND WHITE PHOTOGRAPH

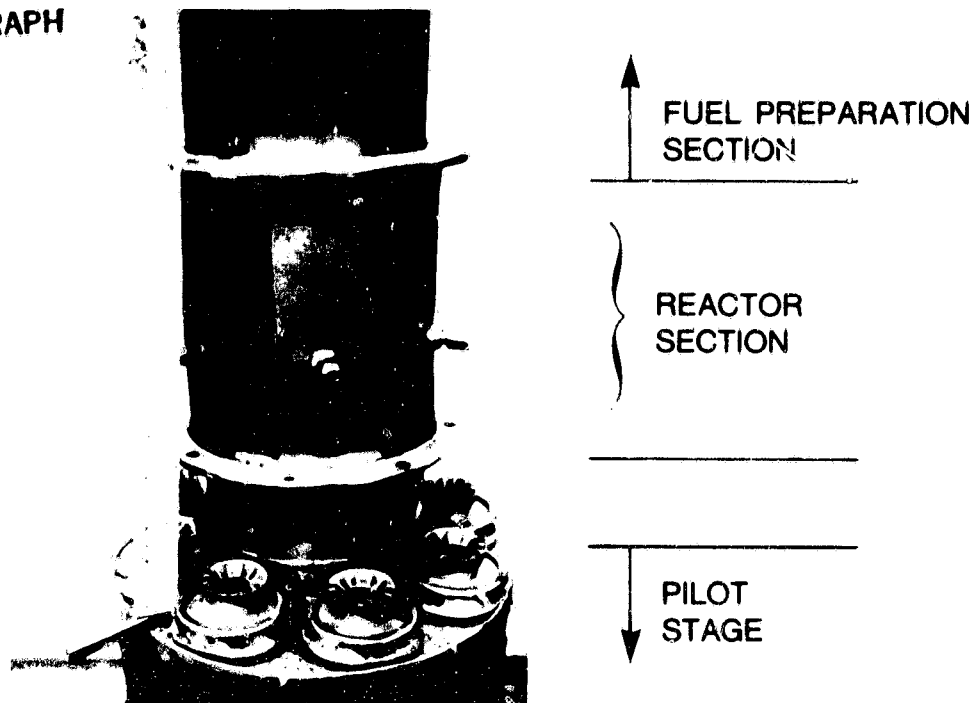


Figure 7-24. Reactor section/pilot stage

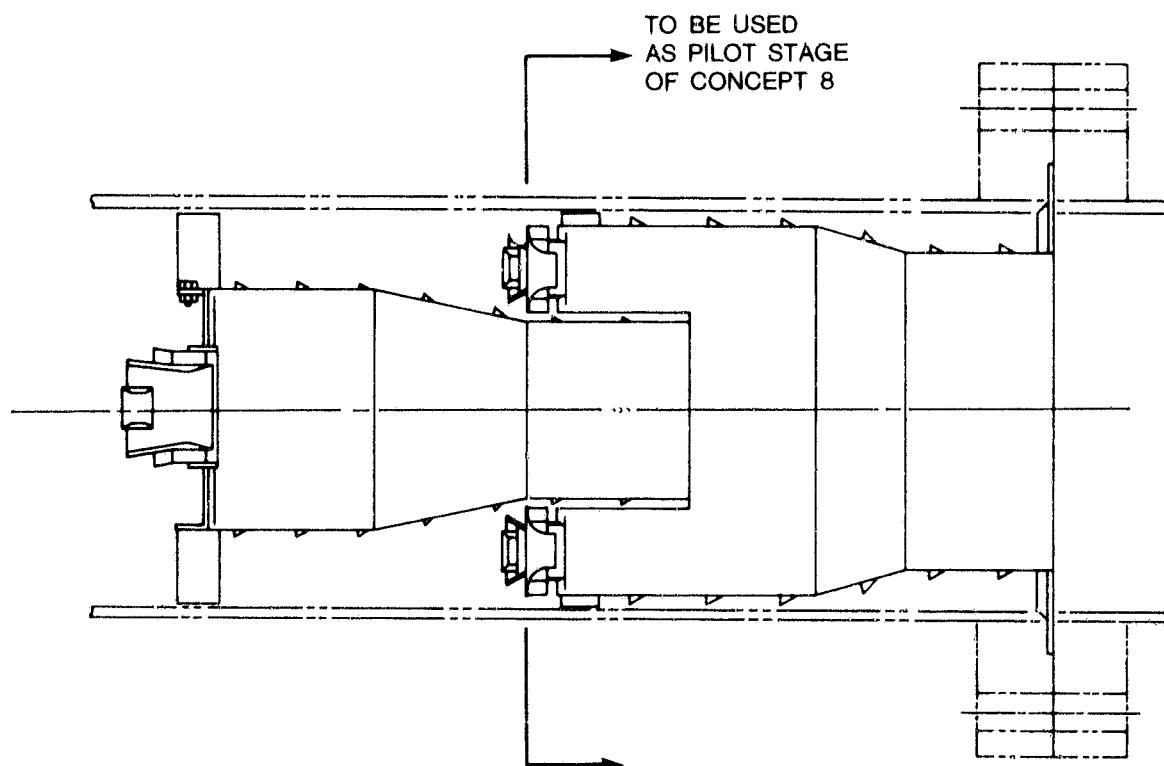
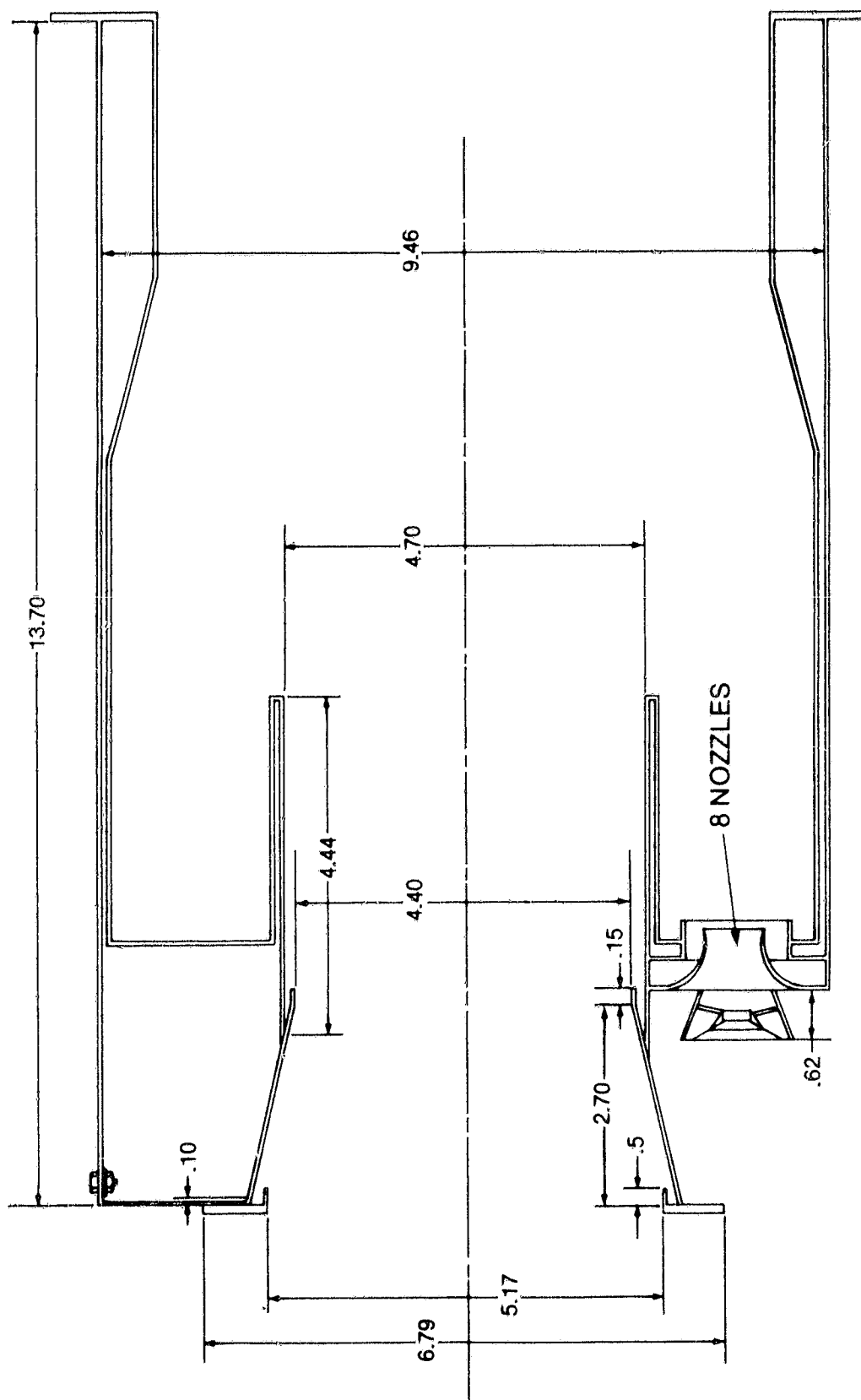


Figure 7-25. Pilot-stage section removed from Concept 6



DIMENSIONS IN INCHES

Figure 7-26. Pilot stage for combustor Concept 8

The fuel nozzle design (low-flow fuel nozzle) shown in Figures 7-27 and 7-28, is based upon current successful design practice and uses a high-velocity air stream to shear the fuel sheet into small droplets. Figure 7-29 is a photograph of the nozzle showing component parts, with the fuel and air swirl subassemblies in the right and left foreground, respectively. The fuel enters the pilot via the center of two concentric supply tubes. Spin is imparted to the fuel by angled slots machined in the conical surface, and the fuel exits from the primary orifice in a thin hollow cone. High-pressure air flows in the annulus formed by the two tubes and is swirled by vanes cut into the swirler surface. The high-velocity airstream impinges on the fuel sheet and shears the fuel droplets. The spin imparted to both the fuel and air streams is in the same rotational direction.

Based upon the results of spray tests, the design shown in Figures 7-27 and 7-28 was modified to eliminate a somewhat streaky spray pattern by the machining of additional fuel swirl channels in the fuel swirl pilot.

The fuel nozzles were calibrated for both fuel flow and atomizing air flow. The nozzle fuel flow calibrations are shown in Figures 7-30 and 7-31. The spray angle of these nozzles was also checked. The high-flow nozzles had an included angle of approximately 55° , and the low-flow nozzles had an included angle of approximately 38° . The narrow spray angles are beneficial in avoiding fuel impingement on the dome walls. These fuel nozzles were used in combustion tests of the series-staged lean-lean combustor, Concept 4, and the parallel-staged lean/lean combustor, Concept 6. These fuel nozzles are characterized by relatively low atomizing air ΔP (approximately 0.12 MPa (17 psia), or atomizing air pressure ratio of 1.1). All subsequent combustor testing was done with a modified low-flow fuel nozzle (high-flow nozzle not modified), modified to increase the atomizing air pressure ratio while conserving the desired atomizing air flow. Operation at a higher pressure ratio, for a given airflow, enhances fuel atomization (particularly for heavy fuels) and should result in improved NO_x emissions and smoke performance.

Figure 7-32 is a fuel nozzle cap sketch depicting the atomizing air cap modifications which were designed and spray tested prior to manufacture of the modified low-flow nozzles. These modifications involve the atomizing air exit orifice (diameter O) and the associated spacing length (L). The original and modified dimensions for L and O are shown on Figure 7-32. Figure 7-33 presents flow function

$\left(\frac{\dot{m} \sqrt{T}}{P} \right)$ and effective area curves versus atomizing air pressure ratio for both the

original and modified cap. With the above modifications, multinozzle combustor configurations were capable of operating at a 1.4 pressure ratio, as compared to a 1.1 pressure ratio for the original fuel nozzles, at the same airflow. For the redesign, an attempt was made to maintain the spray angle approximately constant at an included angle of 38° . The modified nozzle pieces resulted in a slightly narrower angle of approximately 30° included angle. This small change in spray angle does not significantly impact performance.

ORIGINAL PAGE IS
OF POOR QUALITY

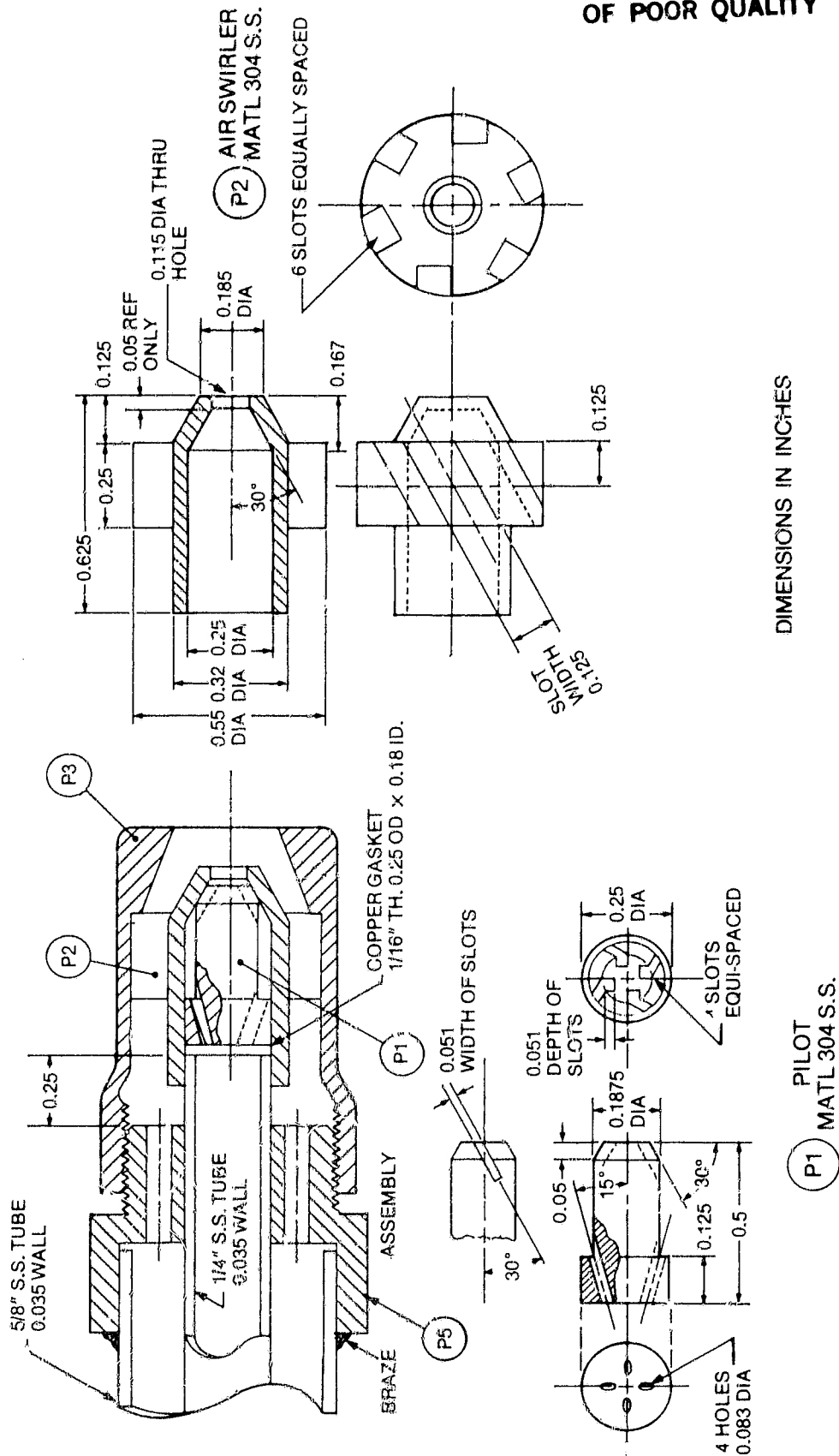
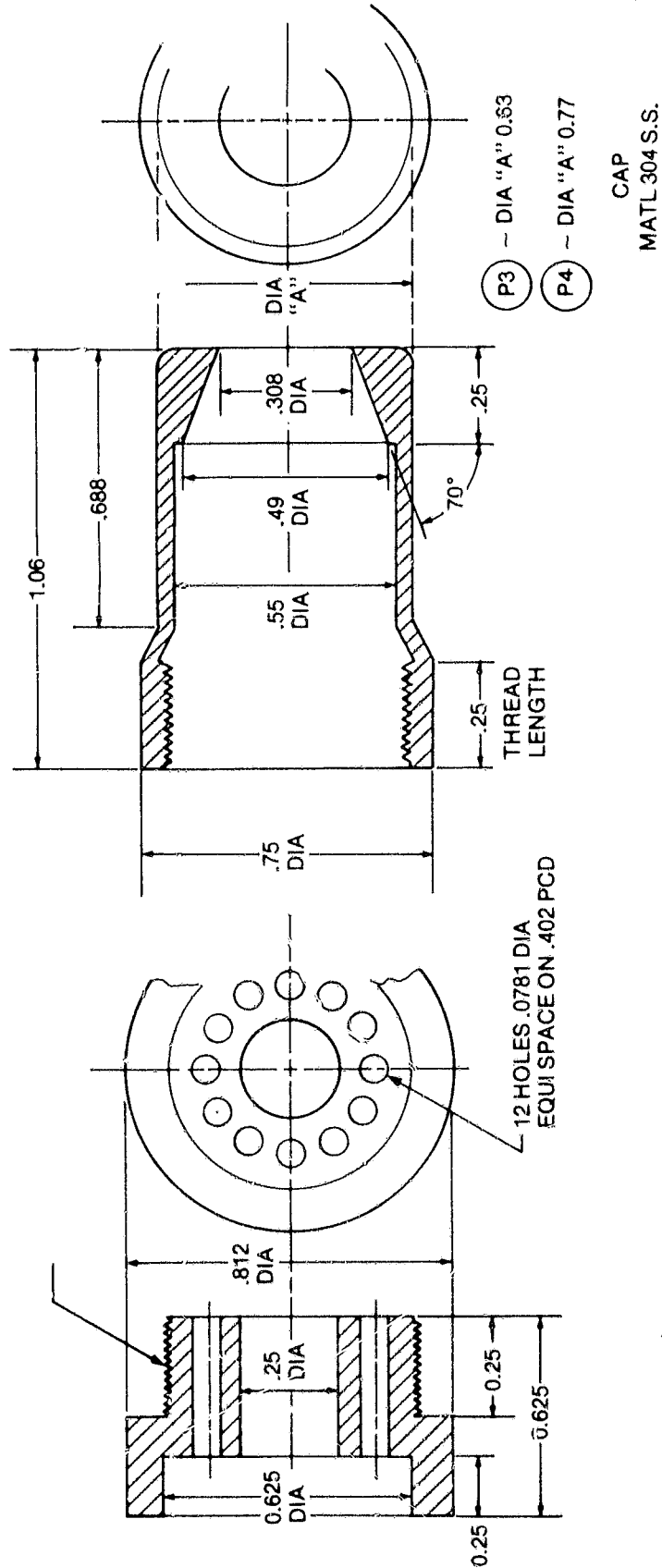


Figure 7-27. Low-flow fuel nozzle assembly

ORIGINAL PAGE IS
OF POOR QUALITY



DIMENSIONS IN INCHES

Figure 7-28. Low-flow fuel nozzle details



Figure 7-29. Fuel nozzle assembly

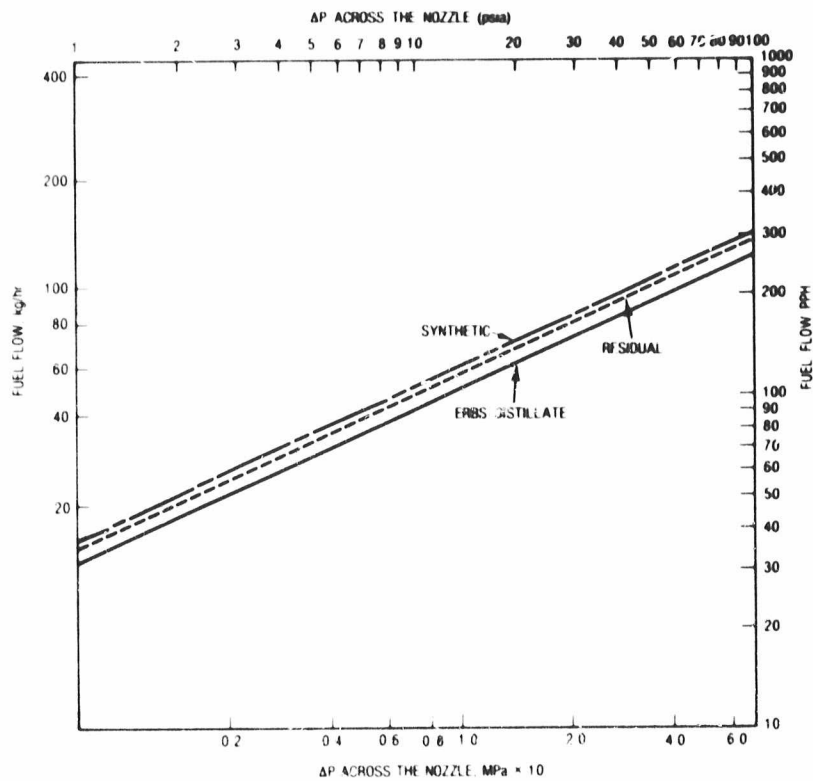


Figure 7-30. Fuel flow calibration, low-flow nozzle

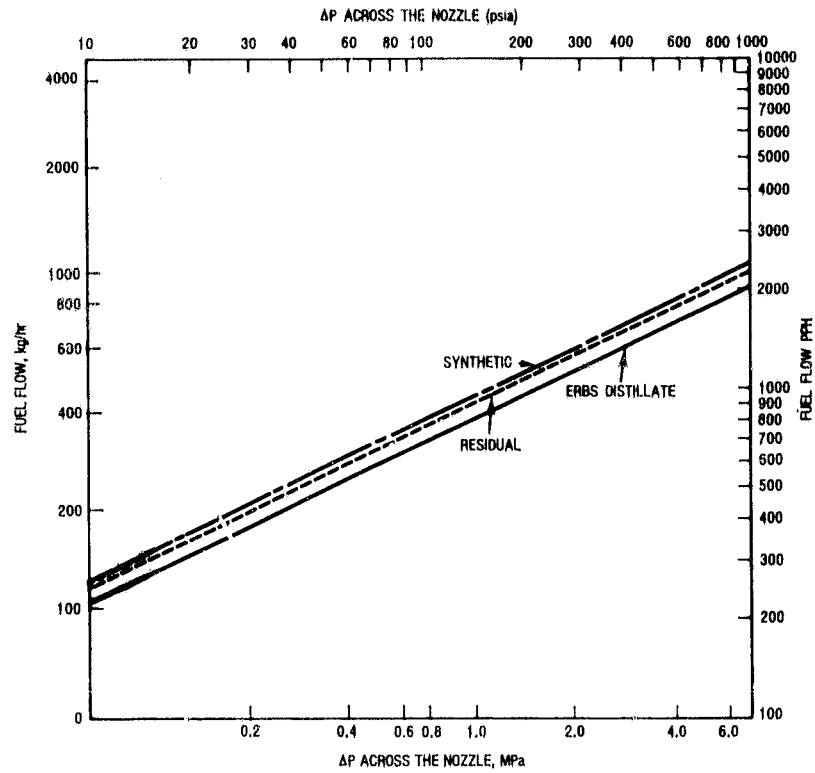


Figure 7-31. Fuel flow calibration, high-flow nozzle

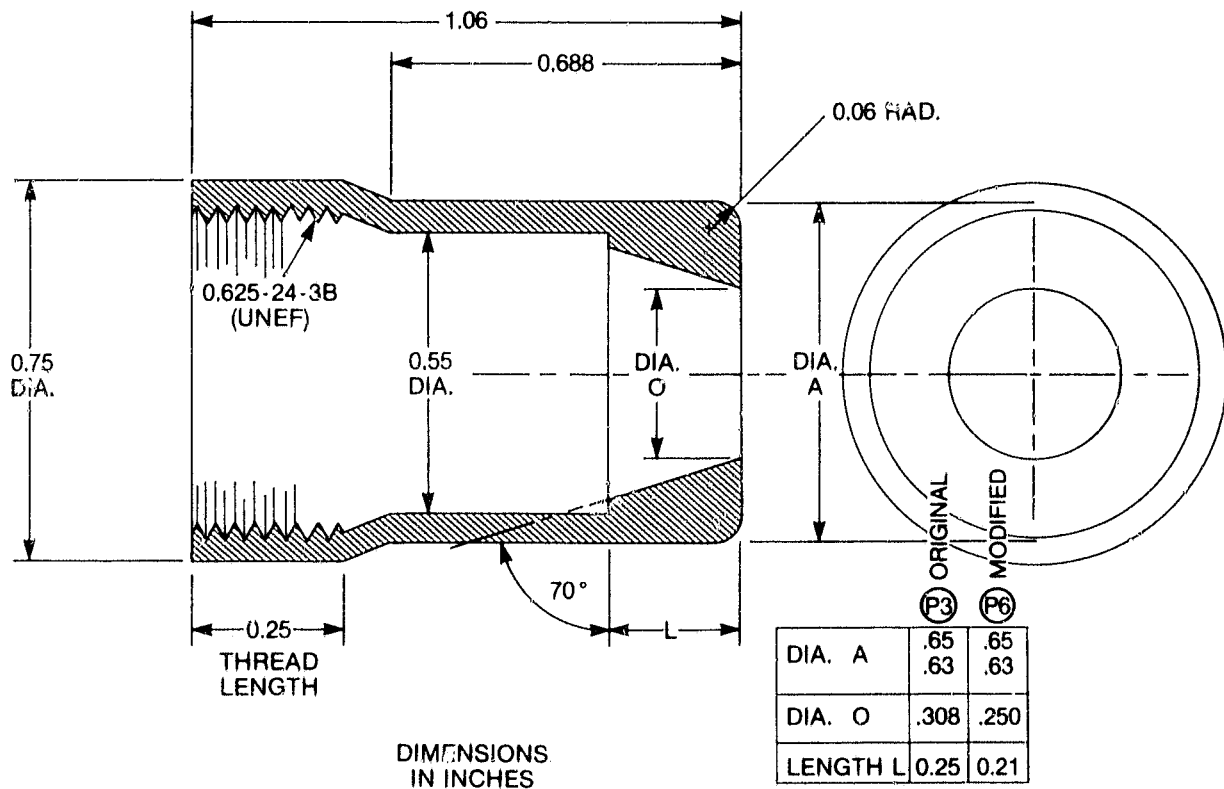


Figure 7-32. Low-flow fuel nozzle, modified for higher atomizing A in ΔP

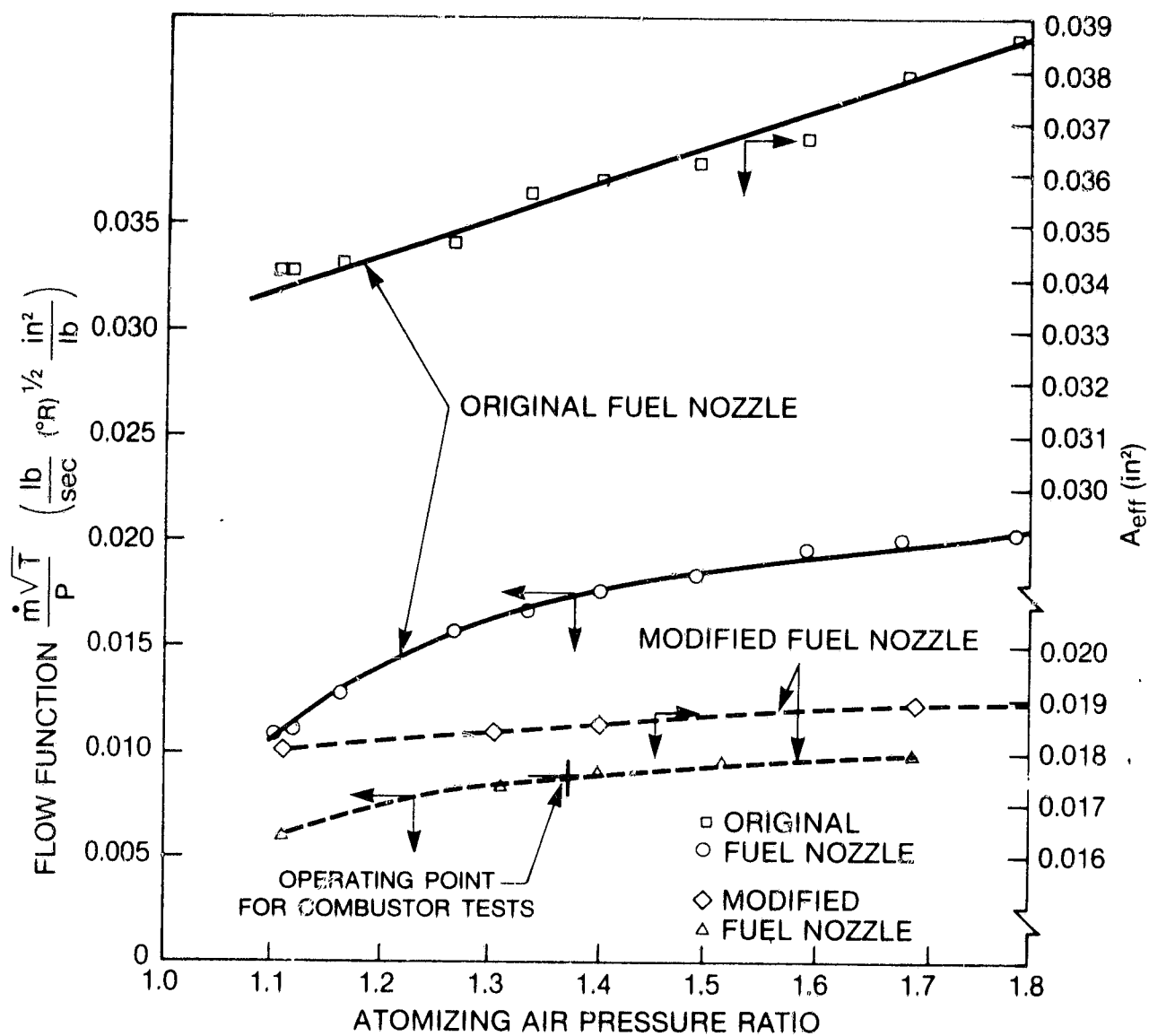


Figure 7-33. Fuel nozzle airside calibration

Section 8

COMBUSTOR TEST RESULTS

8.1 RICH/LEAN COMBUSTOR TEST RESULTS

8.1.1 Rich/Lean Combustor with Premix, Concept 1A

Initial screening tests with Concept 1A were completed with ERBS fuel. Table 8-1 presents the as-measured data for Concept 1A. The tabulated NO_x emissions indices are on an ISO humidity basis, i.e., 0.0063 grams of water vapor per gram of air, corresponding to the EPA emissions standard. Figure 8-1 presents NO_x emissions data for Concept 1A (as well as Concept 1A-1, discussed later) in Emissions Index form, i.e., grams NO_x /kg fuel at ISO humidity as a function of combustor fuel/air ratio and load for the MS7001E reference cycle. Figures 8-2 and 8-3 present CO and smoke data for Concept 1A as well as Concept 1A-1.

The initial test data from Concept 1A showed apparent off-axis fuel injection that caused a skewed exit temperature and fuel/air ratio profile measured at the combustor exit plane. Liner metal temperatures, deposits in the combustor, and visual observation of the fuel nozzle alignment also support this conclusion. The NO_x emissions were higher than expected for rich/lean combustion, which was attributed to the fuel distortion causing only a portion of the combustor to function as a rich/lean liner. Although NO_x emissions were very high, the NO_x for Concept 1A in Figure 8-1 decreased rapidly with increasing fuel/air ratio without an apparent minimum NO_x level (i.e., "bucket" in the NO_x versus fuel/air) which would be expected for a rich/lean combustor with reasonably optimized stoichiometry. This early indication of overly lean rich-stage stoichiometry was confirmed by the conclusive data of multinozzle rich/lean Concept 2, discussed in Section 8.1.2. A significant reduction in NO_x was therefore expected to be realized for Concept 1A by increasing the rich-stage fuel/air ratio, i.e., equivalence ratio.

The second test of Concept 1A (identified as Concept 1A-1, signifying the first modification) implemented a shortened fuel/air premix tube to alleviate the potential for fuel spray on the premix tube walls, and careful axial alignment of the fuel nozzle. A shorter premix tube (12.5 cm removed) is less sensitive to axial misalignment of the fuel nozzle because the shorter tube subtends a larger included angle between the nozzle injector at one end and the tube exit diameter at the other end. Also, the first-stage air-flow was decreased to set the baseload equivalence ratio at 1.9. This change was based on the rich/lean NO_x results from the initial test of Concept 2, and initial indications seen for Concept 1A. Table 8-2 summarizes the modifications made to generate Concept 1A-1.

Table 8-1

[illegible]

8-3

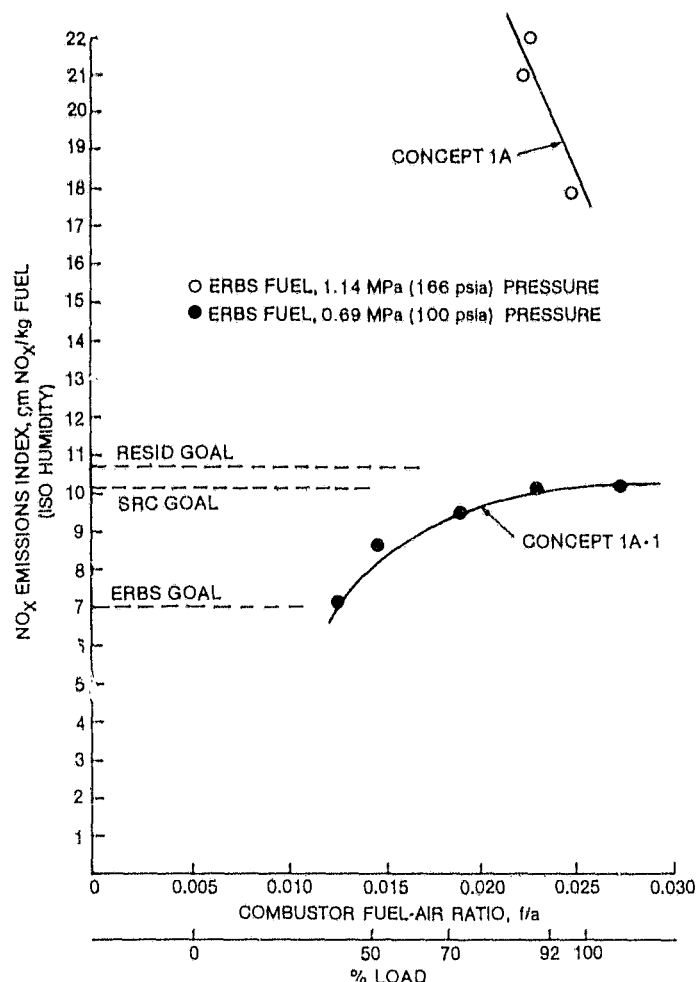


Figure 8-1. NO_x emissions vs load, Concept 1A—premixed rich/lean

Concept 1A-1 was operated at reduced pressure [0.69 MPa (100 psia) compared to a full-cycle pressure of 1.14 MPa (166 psia)], but full-cycle inlet air temperature. This change decreased the rich-stage liner heat flux, thereby allowing engineering effort to be concentrated on developing the emissions characteristics rather than expending resources on rich-stage heat-transfer modifications. Emissions data are presented in Figures 8-1 through 8-3 plotted versus the combustor fuel/air ratio. Table 8-3 presents the as-measured data for Concept 1A-1. The desired NO_x characteristic expected of rich/lean designs was not observed within the fuel/air ratio range tested even though the first-stage equivalence ratio was varied between approximately 1.0 and 2.0. Also as shown in Figures 8-2 and 8-3, the CO, UHC, and smoke emissions were higher than desired. The latter indicates thermal quenching of partially burned flame gas which may be characteristic of the secondary air-injection geometry. The NO_x behavior (Figure 8-1) is unique because it does not resemble a rich/lean combustor with a minimum or "bucket" in the NO_x curve, and because it also has a much lower slope than a lean-spray flame NO_x characteristic. Again, the mixing induced by the upstream facing quench holes probably influenced the result. The observed high level of NO_x may be due to thermal NO_x resulting from longer-than-

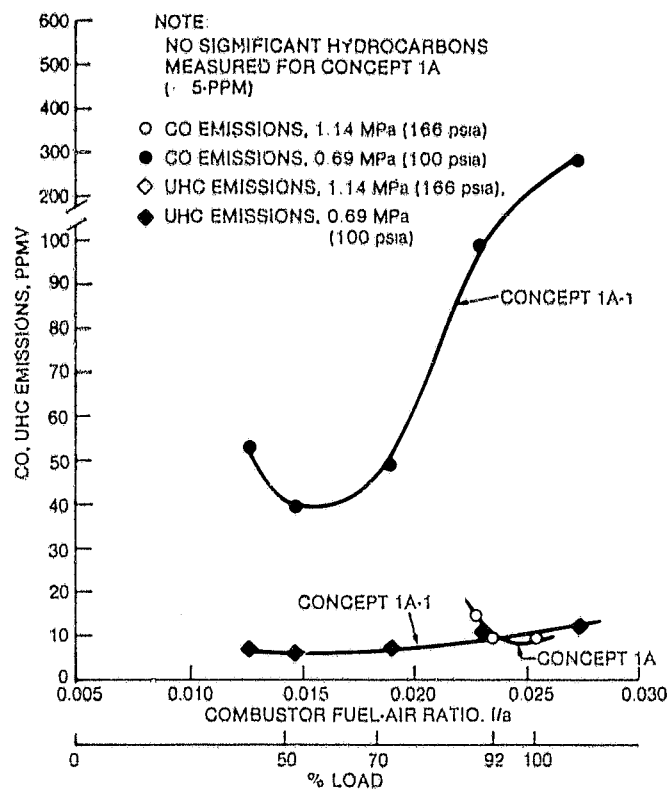


Figure 8-2. Combustible emissions vs load Concepts 1A and 1A-1—ERBS fuel

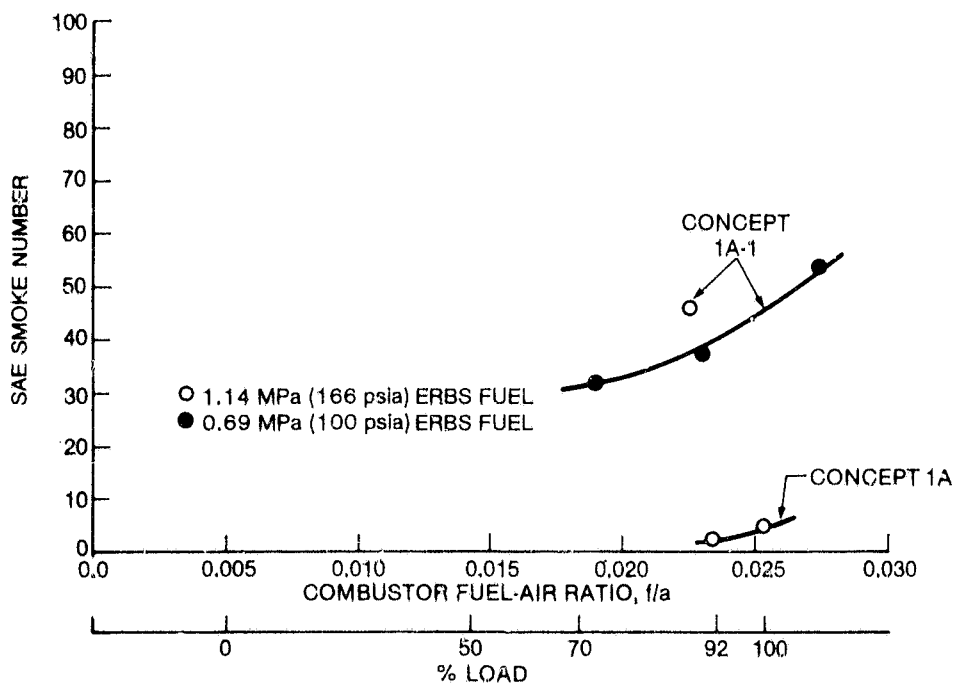


Figure 8-3. Smoke performance, Concept 1A and 1A-1—ERBS fuel

Table 8-2

TEST CONFIGURATION SUMMARY, CONCEPT 1A

CONFIGURATION	EQUIVALENCE RATIOS AT BASELOAD (92% POWER)		RICH STAGE COMBUSTION LENGTH, cm (inches)	RICH-TO-LEAN QUENCH PATTERN	OTHER COMMENTS
	Φ RICH	Φ LEAN			
1A	1.54	0.55	50.8 (20)	8 - 5.1 cm x 2.0 cm "Racetrack Slots"	
1A-1	1.74	0.55	50.8 (20)	8 - 5.1 cm x 2.0 cm "Racetrack Slots"	Modifications described in Notes 1 and 2

NOTES:

1. Shortened the premixing tube length by removing 12.7 cm (5 in.) from the straight cylindrical section of the main stage fuel/air premixing tube
2. Blocked a portion of the axial air swirler on the upstream end of the fuel/air premixer to increase rich stage equivalence ratio by decreasing air flow to rich stage

at lean stoichiometry. This likely results from the admission of quench air through the upstream facing holes in the converging cone section of the quench zone, as opposed to the shorter residence time expected from quench airholes in the narrow-diameter quench zone throat of Concept 2 (discussed later). Thus high second-stage NO_x formation could override the local minimum NO_x expected for a rich/lean burner. Since these test data are the sum of NO_x formed in the first and second stages, the lean second stage can be a major contributor to the observed result.

Concept 1A could be modified by moving the "racetrack" holes downstream into the throat section and, based on results for Concept 2 (discussed in Section 8.1.2) this modification would probably greatly improve the emissions performance. However, the construction of Concept 1A demands a long combustor to accommodate the mixing and combustion. This fact detracts from its application since existing machines have a shorter combustion casing, although the General Electric machines can be modified to accept a longer liner. A final point of interest is the possibility of exploiting the rather unexpected NO_x emissions index versus equivalence ratio curve for Concept 1A-1 (Figure 8-1). The CO and UHC emissions can probably be controlled by adjusting the lean-zone equivalence ratio through changing the hole size in the throat section. If smoke could also be reduced by similar stoichiometry changes or by improved atomization, then the observed NO_x emissions index characteristic is desirable for a low emissions design. The flat region spans a relatively wide load range which is an improvement over both lean systems and rich/lean combustors which tend to have a relatively narrow optimum operating range for low NO_x .

Table 8-3

[illegible]

Table 8-3 (Cont'd)

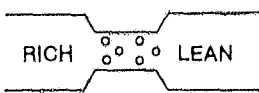
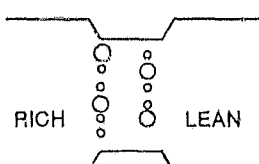
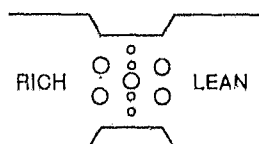
[illegible]

ORIGINAL PAGE IS
OF POOR QUALITY

8.1.2 Rich/Lean Combustor with Multiple Nozzle Dome, Concept 2

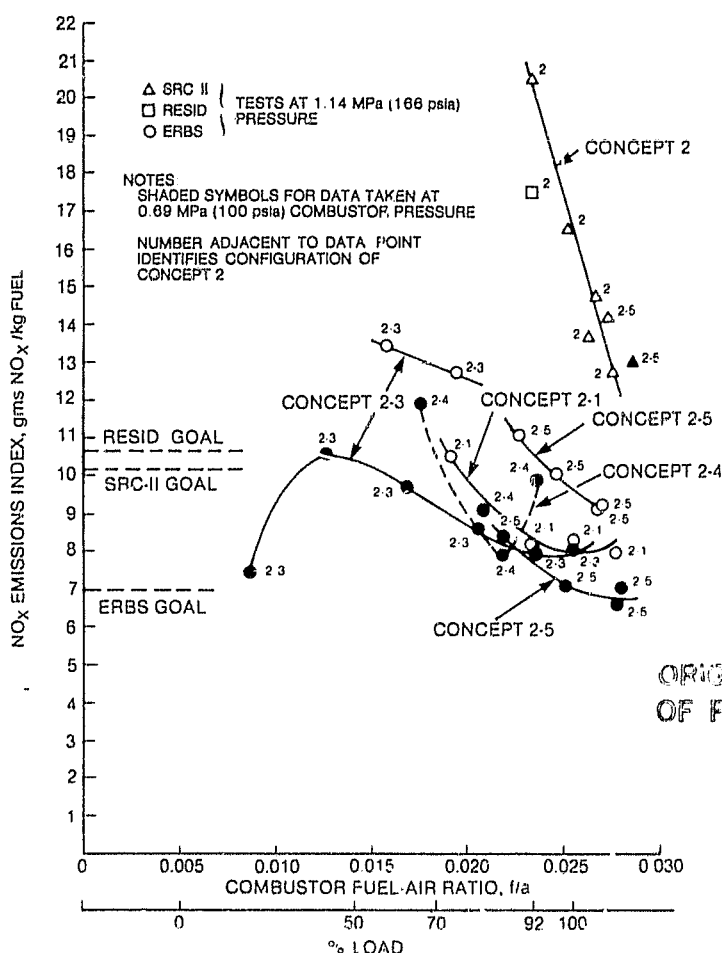
Concept 2 showed early promise for an effective rich/lean combustor design that also had the advantage of shorter overall length. Thus, the testing included the initial run and five modified versions of Concept 2 (Concepts 2-1 through 2-5). The details of the modifications made to Concept 2 are summarized in Table 8-4. Note

Table 8-4
TEST CONFIGURATION SUMMARY, CONCEPT 2

CONFIGURATION	EQUIVALENCE RATIOS AT BASELOAD (92% POWER)		RICH STAGE COMBUSTION LENGTH, cm (inches)	RICH-TO-LEAN QUENCH PATTERN	OTHER COMMENTS
	ϕ RICH	ϕ LEAN			
2	1.54	0.54	38.1 (15)	Staggered holes of uniform size, 4 rows	
2-1	1.89	0.55	38.1 (15)	Same as above with hole sizes enlarged to increase ϕ rich while holding constant ϕ lean	<ul style="list-style-type: none"> Blocked portion of rich stage swirler air to increase rich stage equivalence ratio New fuel nozzle design increased atomizing air pressure ratio with constant atomizing air mass flow.
2-2	ASSEMBLY ERROR—NO MEANINGFUL DATA				
2-3	1.89	0.55	25.4 (10)	Staggered Holes 2 Rows as Shown	
2-4	1.89	0.55	38.1 (15)	Staggered Holes 3 Rows as Shown	 <p>Added 1 mm (0.040 in.) sleeve to reduce swirler exit diameter, thus increase exit velocity</p>
2-5	1.89	0.55	38.1 (15)	Same as Original Concept 2	<ul style="list-style-type: none"> Retained sleeves on swirler Improved atomizing air side of fuel nozzles Improved fuel nozzle alignment 3 mm (0.125 in.) rich stage wall thickness

that configuration 2-2 was tested but did not produce meaningful data, and these results are omitted. Tables 8-5 through 8-9 present as-measured data and all key test parameters for Concepts 2, 2-1, 2-3, 2-4, and 2-5. Figures 8-4, 8-5, and 8-6 present the, NO_x , CO, and smoke data for all the tested combustor configurations (summarized in Table 8-4) plotted versus the combustor fuel/air ratio and MS7001E load.

Figure 8-4 presents the NO_x Emissions Index data for the tests of combustor Concept 2 and its modifications. The initial screening test is the set of data with high NO_x emissions labeled as Concept 2. The high NO_x values were due primarily to testing on SRC-II fuel which contained high fuel nitrogen (0.87% FBN). However, it may be noted that the NO_x decreased rapidly with increasing fuel/air ratio and, at the highest fuel/air ratios tested (about 0.029), the NO_x approached the EPA limit for high-nitrogen fuels. More importantly, the steep slope of the NO_x Emissions Index versus fuel/air ratio curve shown in Figure 8-4 indicates that NO_x decreased rapidly as the first-stage equivalence ratio increased. These data were run with essentially constant combustor air flowrate (scaled MS7001E conditions) and, therefore, increasing the combustor overall fuel/air ratio was accomplished by increasing fuel flow which



ORIGINAL PAGE IS
OF POOR QUALITY

Figure 8-4. NO_x emissions vs load for Concept 2 configurations

Table 8-5

[illegible]

CONCEPT 2 TEST DATA

[illegible]

Table 8-6

[illegible]

Table 8-6 (Cont'd)

[illegible]

Table 8-7
CONCEPT 2-3 TEST DATA

POINT NUMBER	READING NUMBER	HARDWARE CONFIGURATION	FUEL TYPE	FUEL % N	FUEL % H	FUEL LAY	FUEL TEMP. (°)	SIMULATED ENGINE POWER CONDITION			TINLET (°)	TINLET (PSIA)	W FUEL P (LB/HR)	W AIR P (LB/°)	W FUEL S (LB/°)	W AIR S (LB/°)	PRIMARY EQUIVALENCE RATIO	SECONDARY EQUIVALENCE RATIO	OVERALL EQUIVALENCE RATIO	PRIMARY RES. TIME (SEC.)	SECONDARY RES. TIME (SEC.)	COOLD	PRIMARY REF. VELOCITY (FT/°)	SECONDARY REF. VELOCITY (FT/°)	KIST TEMPERATURE (°)	KIST PRESSURE (PSIA)
11	1	2-3	ERBS	12.95	.0054	18275	67	15			587	101.0	308	1.79	-	8.19	.693	.202	.124	56.3	10.6	19.6	110	1010	95.7	
12	2	"	"	"	"	"	64	50			585	100.0	453	1.78	-	8.15	1.025	.298	.184	56.1	10.6	19.7	110	1226	94.5	
13	3	"	"	"	"	"	62	60			587	99.5	604	1.78	-	8.14	1.368	.398	.245	55.7	10.3	19.8	111	1430	93.7	
131	4	"	"	"	"	"	63	76			586	99.6	736	1.78	-	8.16	1.662	.484	.297	55.7	10.5	19.8	111	1657	93.7	
14	5	"	"	"	"	"	61	92			592	99.9	834	1.77	-	8.10	1.897	.552	.340	56.0	10.6	19.7	110	1788	93.9	
15	6	"	"	"	"	"	61	100			595	99.9	905	1.76	-	8.09	2.061	.600	.369	55.9	10.6	19.7	110	1893	93.9	
14	7	"	"	"	.785	"	61	92			600	100.1	809	1.76	-	8.07	1.848	.538	.321	55.6	10.5	19.9	111	1804	94.2	
14	8	"	"	"	.263	"	61	92			595	101.0	846	1.80	-	8.27	1.887	.549	.338	55.3	10.4	20.0	112	1813	94.9	
14	9	"	"	"	.796	"	61	92			599	101.0	844	1.81	-	8.30	1.876	.546	.336	54.9	10.4	20.1	112	1850	94.7	
14	10	"	ERBS /SNC	10.88	.166	17259	66	92			590	101.8	906	1.80	-	8.26	1.922	.559	.344	56.1	10.6	19.7	110	1822	95.7	
14	11	"	"	10.13	.634	16889	64	92			592	102.7	918	1.82	-	8.37	1.888	.550	.338	55.8	10.5	19.8	111	1790	96.28	
14	12	"	"	9.43	.789	16547	62	92			594	102.8	950	1.82	-	8.36	1.922	.559	.344	55.7	10.5	19.8	111	1785	96.3	
14	13	"	SNC II	9.07	.87	16368	61	92			595	102.6	936	1.83	-	8.40	1.908	.555	.341	55.3	10.4	20.0	112	1805	96.2	
13	14	"	ERBS	12.95	.0054	18275	61	50			600	159.5	954	2.98	-	13.66	1.287	.375	.230	52.6	9.9	21.0	117	1515	149.4	
131	15	"	"	"	"	"	59	70			603	166.4	1152	2.94	-	13.49	1.574	.458	.282	55.4	10.5	13.9	111	1693	-	

Table 8-7 (Cont'd)

[illegible]

Table 8-8

[illegible]

* BASED ON 6% PRESSURE DROP IN THE COMBUSTOR

Table 8-9
CONCEPT 2-5 TEST DATA

POINT NUMBER	READING NUMBER	HARDWARE CONFIGURATION	FUEL TYPE	FUEL % H	FUEL % N	FUEL LHV	FUEL TEMP (°F)	SIMULATED ENGINE POWER CONDITION			TIME (°F)	PMNT (PSIA)	W FUEL P (LB/HR)	W AIR P (LB/°)	W FUEL S (LB/°)	W AIR S (LB/°)	PRIMARY EQUIVALENCE RATIO	SECONDARY EQUIVALENCE RATIO	OVERALL EQUIVALENCE RATIO	PMNT RES. TIME (SEC.) COLD	SECONDARY RES. TIME (SEC.) COLD	PRIMARY RES. VELOCITY (FT/°)	SECONDARY RES. VELOCITY (FT/°)	EXIT TEMPERATURES (°F)	EXIT PRESSURE (PSIA)
14	1	2-5	ENBS	12.95	.0054	18275	68	100			613	59.6	889	1.80	-	8.08	1.989	.578	.362	73.9	10.3	20.5	113	1806	91.6
141	2	"	"	"	"	"	65	112			613	98.7	973	1.77	-	7.95	2.212	.643	.403	74.5	10.4	20.4	112	1999	91.5
142	3	"	"	"	"	"	67	84			614	100.2	783	1.80	-	8.11	1.945	.507	.318	74.0	10.3	20.5	113	1670	92.3
143	4	"	"	"	"	"	66	113			612	99.8	983	1.78	-	7.99	2.222	.646	.404	74.9	10.5	20.3	111	1845	92.0
14	5	"	"	"	.13	"	66	100			613	100.3	891	1.80	-	8.08	1.992	.579	.363	74.3	10.4	20.4	112	1854	92.5
14	6	"	"	"	.61	"	63	100			613	100.0	899	1.80	-	8.07	2.012	.585	.366	74.2	10.4	20.4	112	1843	92.5
14	7	"	ENBS/ SIC	10.88	.47	17259	66	100			610	100.3	958	1.80	-	8.10	2.025	.580	.369	74.4	10.4	20.4	112	1798	92.3
14	9	"	"	10.12	.64	16884	61	100			614	100.0	973	1.80	-	8.11	2.018	.587	.367	73.8	10.3	20.5	113	1798	92.2
14	10	"	"	9.44	.79	16549	60	100			611	99.8	1000	1.81	-	8.12	2.037	.592	.371	73.8	10.3	20.6	113	1785	92.1
14	11	"	SIC	9.07	.87	16368	60	102			612	99.2	1023	1.81	-	8.14	2.062	.599	.375	73.1	10.2	20.7	114	1822	91.7
142	12	"	ENBS	12.95	.0054	18275	60	87			607	165.3	1355	3.01	-	13.54	1.809	.526	.329	73.6	10.3	20.6	113	1895	153.5
14	13	"	"	"	"	"	59	96			608	165.8	1466	3.01	-	13.54	1.956	.569	.356	73.7	10.3	20.6	113	2009	153.8
143	14	"	"	"	"	"	58	108			606	165.4	1571	2.9	-	13.26	2.140	.622	.389	75.2	10.5	20.2	111	1952	152.6
14	15	"	ENBS/ SIC	10.87	.47	17254	56	96			605	166.0	1558	3.05	-	13.71	1.948	.566	.354	73.1	10.2	20.8	114	1903	153.7
14	16	"	"	10.15	.63	16900	55	96			607	166.0	1585	3.05	-	13.70	1.948	.566	.355	73.0	10.2	20.8	114	1917	153.5
14	17	"	SIC	9.07	.87	16368	55	100			607	154.8	1632	3.01	-	13.52	1.980	.576	.360	73.5	10.3	20.7	113	1879	153.0
14	20	"	ENBS	12.95	.55	18275	57	100			607	166.1	1481	2.95	-	13.25	2.019	.587	.368	75.3	10.6	20.1	110	1895	154.6
14	21	"	"	"	.22	"	58	96			609	166.1	1477	3.02	-	13.56	2.058	.572	.358	73.7	10.3	20.6	113	1801	154.6
14	22	"	"	"	.53	"	63	100			602	99.9	903	1.79	-	8.04	2.021	.588	.368	75.2	10.5	20.2	111	1866	92.8
14	23	"	"	"	.30	"	76	109			594	99.3	589	1.09	-	4.91	2.164	.629	.394	123.3	17.2	12.3	68	1843	96.7

* BASED ON 6% PRESSURE DROP IN THE COMBUSTOR

Table 8-9 (Cont'd)
CONCEPT 2-5 TEST DATA

POINT NUMBER	READING NUMBER	COMBUSTOR DELTA P (PSI)	LINER TEMPERATURE (°F)	CO (PPM)	CO ₂ (PPM)	HC (PPM)	NOX (PPM)	NOX (PPM)	NOX (PPM)	% N CONVERSION	COMBUSTION EFFICIENCY (%)	SMOKE NUMBER	PATTERN FACTOR	FAIR	COMBUSTOR AB/P (%)	FLOW VELOCITY ft^3/min	ATMOSPHERIC AIR ΔP (PSIA)	TOTAL ATOMIZING AIR FLOW (LB/HR)	PRIMARY EQUIVALENCE RATIO (INCL. ATOM. AIR)	SLIM	PERL AIR RATIO METHOD
14	1	8.0	1698	32.5	50400	7.7	122.3	95.0	-	99.95	18.8	.21	.0237		8.0	10.55	55.9	.53	1.538	7.18	.0230
141	2	7.2	1762	38.5	54000	7.7	125.5	86.9	-	99.95	22.5	.41	.0265		7.3	10.38	107.0	.75	1.555	6.59	.0278
142	3	7.9	1750	21.3	48200	4.6	131.8	112.0	-	99.17	56.2	.19	.0217		7.9	10.50	57.7	.54	1.345	8.47	.0220
143	4	7.8	1735	38.5	57100	3.8	137.5	94.1	-	99.94	17.8	.30	.0267		7.8	10.27	57.3	.53	1.712	7.15	.0280
14	5	7.7	1702	25.6	52300	2.3	156.5	115.6	15.7	99.97	14.8	.21	.0248		7.7	10.42	57.2	.53	1.540	8.70	.0250
14	6	7.5	1775	45.1	53200	1.5	215.4	161.3	20.7	99.96	27.5	.34	.0245		7.5	10.45	57.2	.54	1.590	12.35	.0253
14	7	8.0	1822	39.0	55000	0	201.6	151.5	18.8	99.96	29.5	.19	.0256		8.0	10.42	57.2	.53	1.506	11.01	.0288
14	9	7.9	1505	37.7	53200	.8	218.2	173.0	20.5	99.96	21.6	.39	.0246		7.9	10.55	57.7	.54	1.555	12.42	.0272
14	10	7.7	1729	47.3	55000	.8	244.1	190.8	20.9	99.95	30.1	.31	.0232		7.7	10.60	57.8	.53	1.575	13.53	.0280
14	11	7.5	1780	64.9	58100	.8	244.1	185.4	17.1	99.94	32.5	.31	.0265		7.6	10.78	58.3	.54	1.696	13.81	.0286
142	12	11.8	1643	22.1	49400	.8	183.8	146.4	-	99.98	34.7	.30	.0232		7.1	10.69	94.2	.38	1.451	11.13	.0237
14	13	12.0	1598	32.0	51200	0	180.9	132.8	-	99.97	35.2	.28	.0251		7.2	10.65	93.4	.88	1.516	10.10	.0246
143	14	11.8	1566	47.3	51500	.8	182.5	122.0	-	99.94	38.1	.28	.0273		7.2	10.34	93.2	.87	1.651	9.36	.0289
14	15	12.3	1800	47.3	57500	1.5	195.3	143.0	2.0	99.96	32.9	.19	.0264		7.4	10.86	93.0	.87	1.515	10.41	.0258
14	16	12.5	1871	56.0	58100	0	243.2	180.1	13.7	99.95	42.4	.12	.0265		7.5	10.87	92.8	.87	1.517	12.84	.0263
14	17	11.8	1873	64.9	59500	0	269.9	202.1	14.4	99.94	47.5	.15	.0289		7.2	10.74	92.6	.86	1.538	14.22	.0274
14	20	11.5	1441	62.7	57300	0	224.0	154.5	8.5	99.95	35.0	.21	.0268		6.9	10.15	91.1	.87	1.580	11.89	.0254
14	21	11.6	1426	67.1	54500	0	195.6	141.8	8.7	99.94	43.9	.34	.0255		7.0	10.64	92.4	.87	1.526	10.73	.0248
14	22	7.1	1475	185.0	58500	0	221.1	149.1	18.3	99.85	36.5	.28	.0274		7.1	10.28	56.8	.53	1.559	11.29	.0254
14	23	2.6	1880	107.7	60000	0	224.3	147.3	8.3	99.91	6.5	.18	.0281		2.7	3.86	54.0	.53	1.456	11.17	.0272

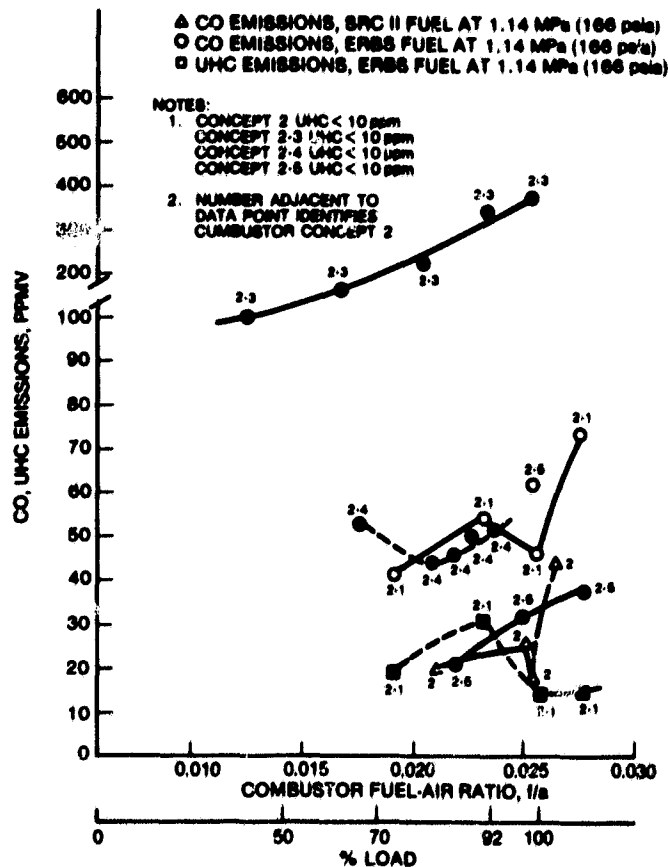


Figure 8-5. Combustible emissions vs load for Concept 2 configurations

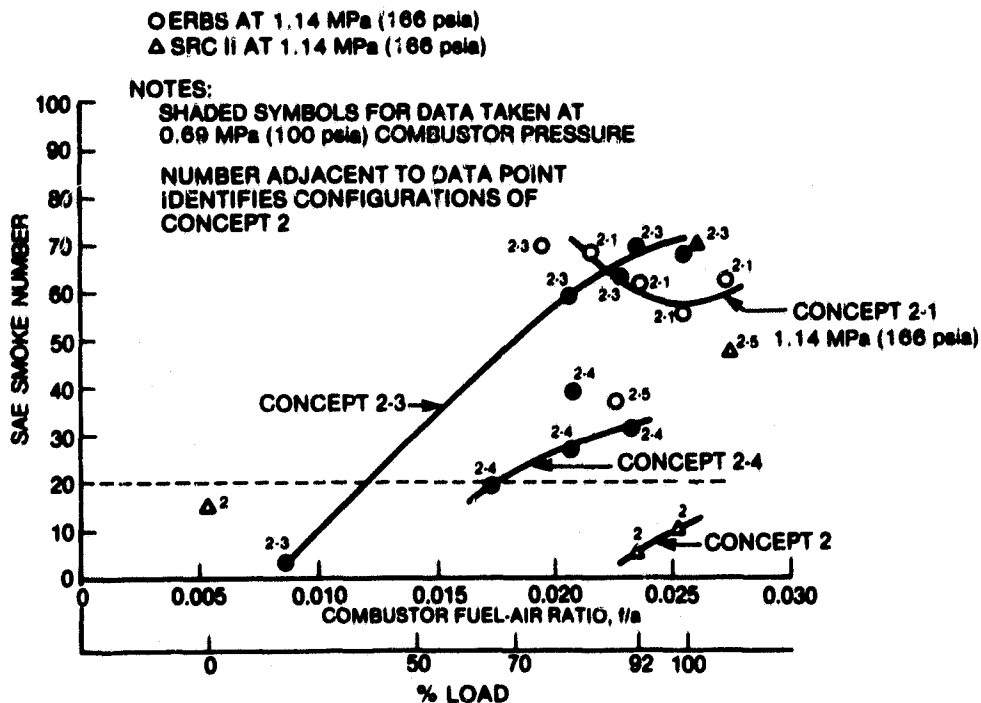


Figure 8-6. Smoke performance for Concept 2 configurations

also increases the first-stage equivalence ratio. This steep slope of the NO_x curve suggested that further reductions in NO_x could be realized by redistributing the combustor airflow to operate with a richer first stage. The NO_x emissions should pass through a local minimum at high fuel/air ratios for correct optimization of a rich/lean combustor. Also note in Figure 8-6 that smoke emissions for Concept 2 were acceptable for even the highest fuel/air ratio test conditions. Based on these data, the combustor airflows were redistributed in all three rich/lean combustors (Concepts 1A, 2, and 3) to increase the first-stage equivalence ratio to decrease NO_x emissions.

During the initial Concept 2 test, the combustor was operated on SRC-II fuel and a final point was run on residual oil. The data for the residual oil test point showed a marked decrease in combustor pressure drop, and a posttest inspection confirmed that a portion of the first-stage liner wall had overheated and failed. The failure was a local phenomenon caused by the fabrication technique used in making the rich-stage liner wall. The first stage was fabricated with several holes to provide capability for future modifications but covered with nichrome patches for the initial test run. The structure of the patch area is shown in Figure 8-7. A metal disk was inserted into the liner hole, covered with a thin nichrome sheet, and the liner inside was then flame-sprayed. Since the metal wall was discontinuous, and the nichrome patch shields this area from effective backside convection cooling, the ceramic flamespray coating was thermally stressed. The overheated regions generally started from a patched hole and extended downstream to the throat region, suggesting that the thermal barrier coating may have spalled off the surface due to excessive local thermal stress, leaving an unprotected metal liner wall. For the next tests of Concept 2, the first stage was rebuilt with a solid liner wall and a thinner 0.5 mm (0.020 in.) flame-spray coating. This failure illustrated subtle but obviously very critical construction requirements for backside convection-cooled hardware. The metal liner wall must be continuous to smoothen temperature gradients. Also a 0.5 mm (0.020 in.) thermal barrier coating was less susceptible to spalling. The thinner coating provides a lower but adequate thermal barrier, but retains the thermal barrier coating mechanical integrity required if thermal protection is to be realized.

Referring again to Figures 8-4, 8-5, and 8-6, the modifications made to generate Concept 2-1 (see Table 8-4) caused significant changes in the emissions characteristics. NO_x performance for Concept 2-1 approached the program goal of 7 g NO_x /kg fuel on ERBS fuel (Figure 8-4), but smoke emissions increased more than anticipated from the initial tests of Concept 2 (Figure 8-6). The CO emissions were

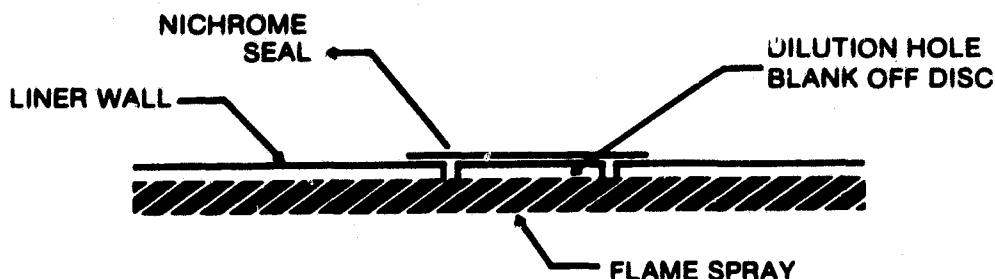


Figure 8-7. Concept 2 primary zone weld

higher than production hardware but acceptable (Figure 8-5). More importantly, the CO emissions for all the modifications of Concept 2 can be seen to increase as the overall fuel/air ratio increased, which indicates that a leaner second stage (more air) should be used for lower CO emissions.

Concept 2-1 was also tested with ERBS doped with pyridine to give levels of FBN representative of residual (0.23 weight percent FBN) and SRC-II (0.87 weight percent FBN) fuels. The NO_x versus FBN data is plotted in Figure 8-8 and indicates conversion rates of approximately 40% and 11%, respectively, at the residual and SRC-II FBN levels. These data show that the absolute levels of NO_x emissions approach the goals for ERBS, and ERBS doped with pyridine to nitrogen levels corresponding to residual and SRC-II fuels. The NO_x goals for ERBS, residual, and SRC-II are 7.0, 10.7, and 10.2 g NO_x /kg fuel, respectively.

Measured liner temperatures for Concept 2-1 are shown in Figure 8-9 for ERBS fuel tests. Temperatures approached 1200 K (1700 °F) when an ERBS/residual fuel blend were tested. Some buckling of the rich-stage liner occurred caused by pressure buckling of the liner wall at elevated temperatures. Rather than expend program resources on development of a rich-stage liner heat-transfer design, succeeding tests of Concept 2 were generally run at 0.69 MPa (100 psia) to reduce the liner pressure loading, with some test points taken at full-cycle pressure of 1.14 MPa (166 psia) to enable extrapolation of 0.69 MPa data to full-cycle conditions. The rich-stage heat-transfer design will be resolved in the Phase II effort. Figure 8-10 presents exit gas temperature profiles which met the program goals. Combustor pressure drop was approximately 6.8%, as shown in Figure 8-11.

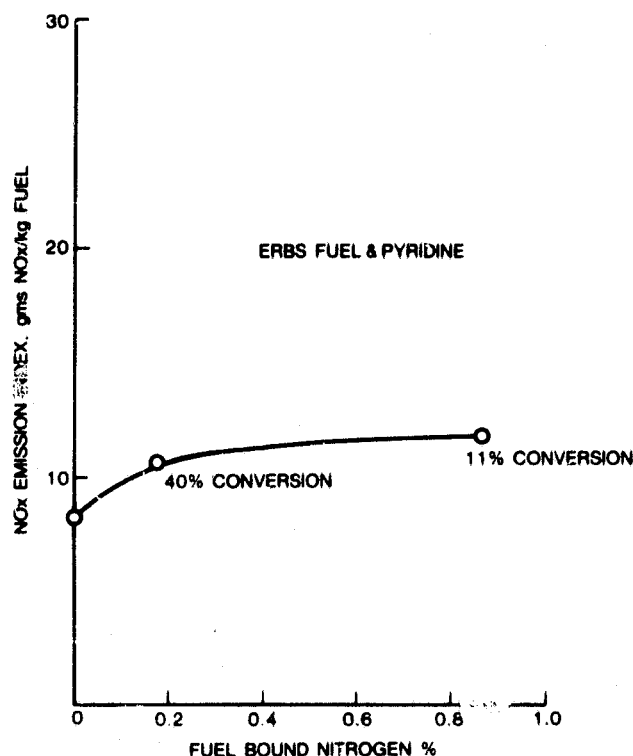


Figure 8-8. NO_x vs fuel-bound nitrogen for Concept 2-1

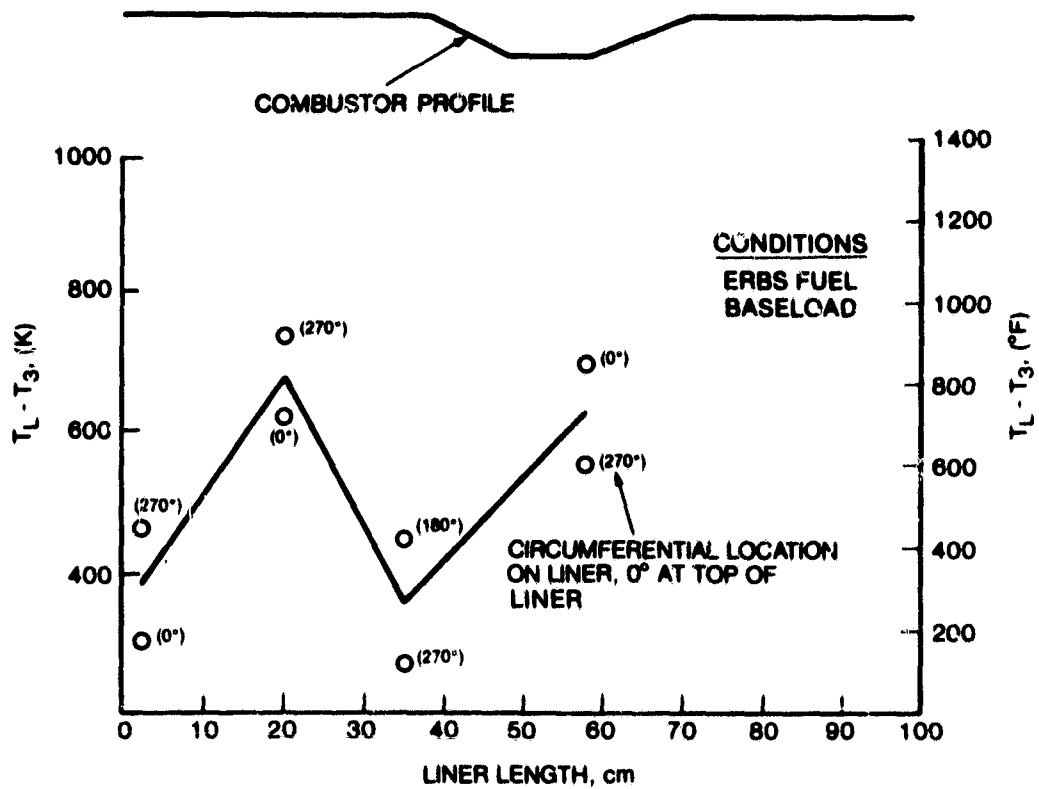


Figure 8-9. Concept 2-1 liner metal temperatures

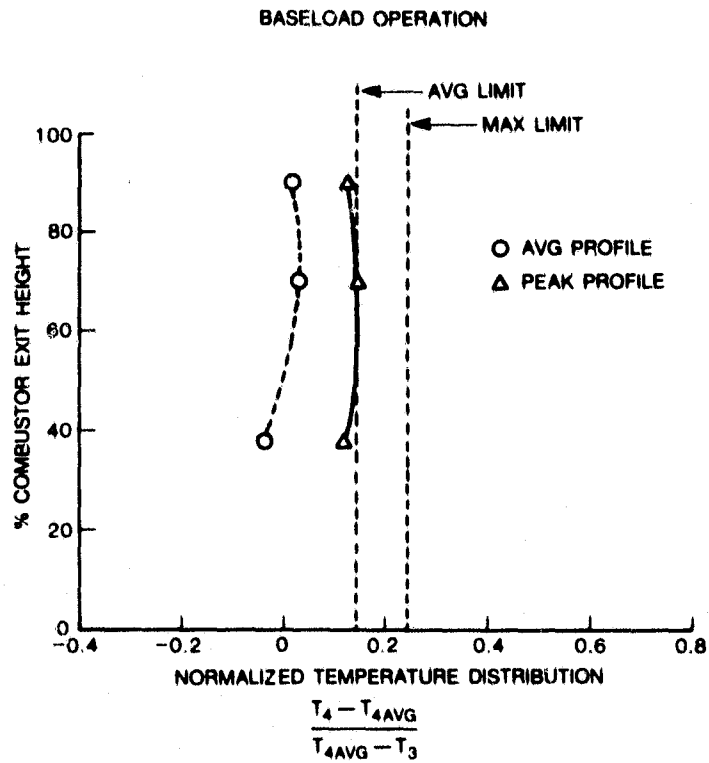


Figure 8-10. Exit temperature profiles for Concept 2-1

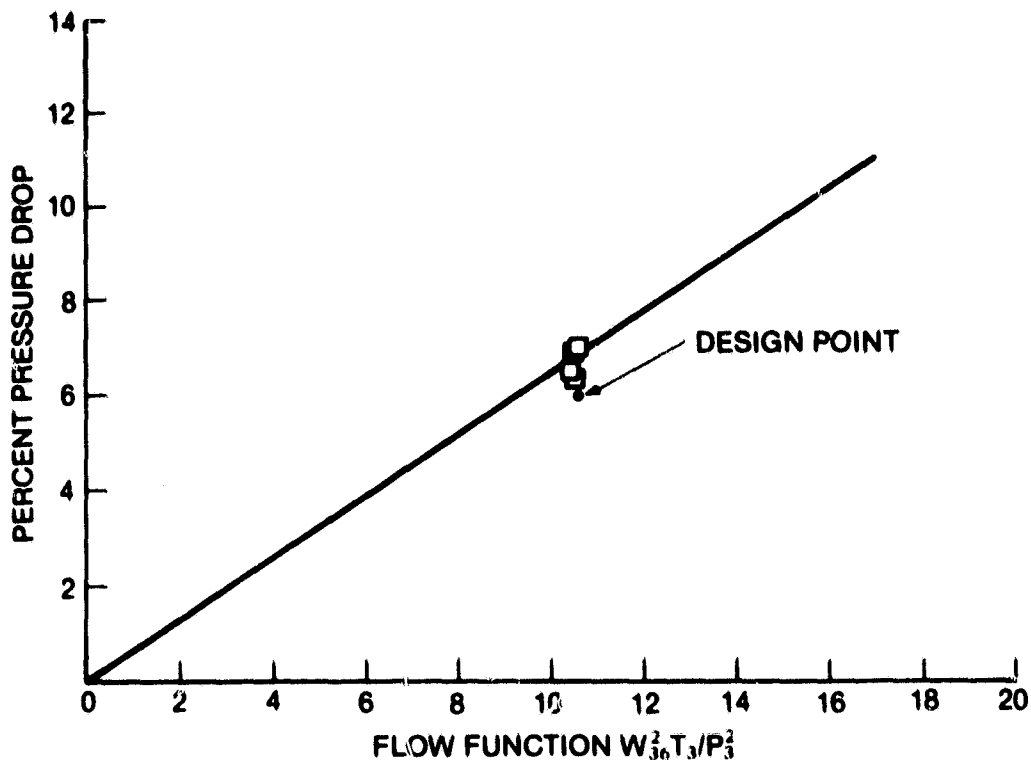


Figure 8-11. Concept 2-1 pressure drop

Configuration 2-3 used a shorter first stage (smaller rich-zone residence time) and a modified rich-to-lean quench pattern (see Table 8-4). Table 8-7 presents the measured test data for Concept 2-3. The decreased residence time would be expected to decrease the peak NO_x emissions generated by a stoichiometric first stage. This trend is shown by the comparatively moderate NO_x emissions at 0.69 MPa (100 psia) for an overall combustor fuel/air ratio of approximately 0.012 (see Figure 8-4). The baseload rich-stage equivalence ratio is 1.9 at an overall fuel/air ratio of 0.0235 and, recalling that the airflow is roughly constant over the load range, the first-stage (rich-stage) equivalence ratio is directly proportional to the overall combustor fuel/air ratio. Thus, the 0.012 overall fuel/air ratio roughly corresponds to a stoichiometric first stage. Note that projecting the NO_x emissions of other modifications (for example, Concept 2-1, 2-4, etc.) based on the test data implies significantly higher NO_x for a stoichiometric first stage.

At high load points (0.022 fuel/air and greater), Concept 2-3 had higher NO_x emissions than desired. The NO_x emissions of Concept 2-3 were about equal to those of Concept 2-1, but Concept 2-3 was tested at reduced pressure (0.69 MPa compared with 1.14 MPa). Testing Concept 2-3 at full pressure should increase the NO_x by approximately 30%, similar to that observed for testing Concept 2-5, confirmed by some 1.14 MPa (166 psia) test points (Figure 8-4). The exact cause of the higher NO_x near baseload at full-cycle conditions for Concept 2-3 compared to 2-1 is uncertain. However, the quench hole pattern impacts NO_x by controlling the rich-to-lean mixing time and the effectiveness in uniformly mixing secondary air with rich-stage gas to a uni-

formly lean equivalence ratio, avoiding stoichiometric pockets. Each parcel of rich burned gas leaving the first stage must mix with the secondary air and form a lean mixture. Since the gas is diluted from a fuel-rich to a fuel-lean condition, the mixture must pass through locally stoichiometric conditions, and the residence time at those conditions determines the amount of NO_x formed. Slow mixing increases this critical time, thereby increasing the NO_x generation. The measured exit temperature profiles for Concept 2-3 (see Figure 8-12) support the conclusion that the new quench-hole pattern for Concept 2-3 did indeed reduce the jet penetration and mixing, as seen by the profiles peaked towards the center, likely resulting in locally stoichiometric burning of some gas and the resultant high NO_x . An alternative explanation is insufficient rich-zone residence time for the kinetics to reduce the NO_x to near-thermodynamic equilibrium levels. This same effect would also impact the conversion of fuel-bound nitrogen into NO_x and will be discussed later.

The CO emissions from Concept 2-3 are shown in Figure 8-5. These emission levels were much higher than desired and were possibly affected by the rich-to-lean mixing process. The CO was almost an order of magnitude greater than the other test configurations, even though the second-stage equivalence ratio was the same as other configurations. This may indicate comparatively slow rich-to-lean mixing that decreased the effective burned gas residence time at lean mixtures. To a first approximation, a given parcel of gas moves through the combustor at an average velocity. This fixes the total combustor residence time, and the distribution of time in rich, lean, and transition zones is influenced by the mixing rates.

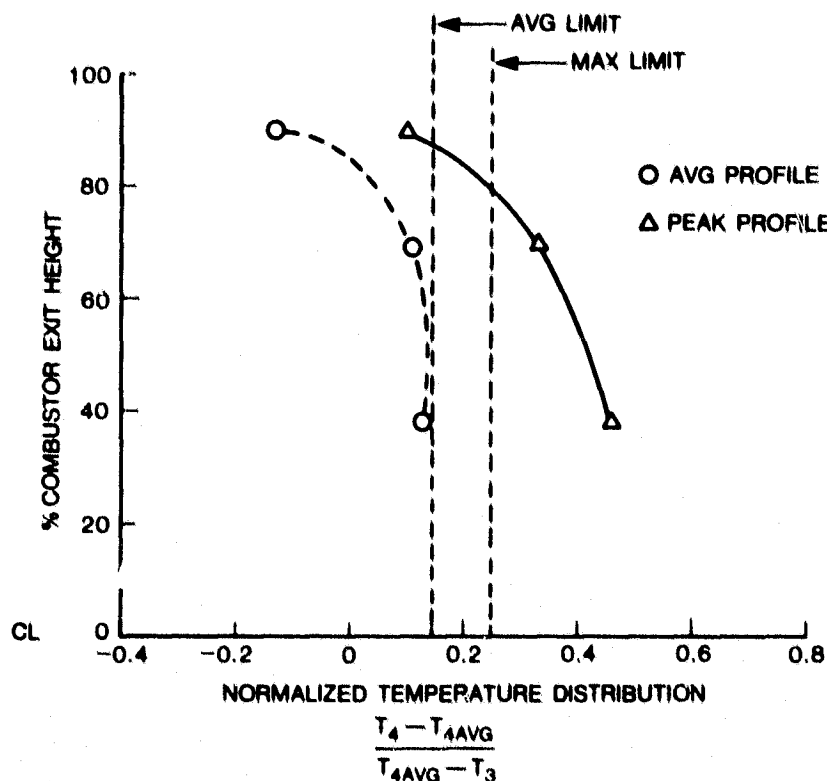


Figure 8-12. Combustor temperature profiles for Concept 2-3

A second problem with Concept 2-3 was excessive smoke emissions (Figure 8-6). These levels are particularly high considering that the test was run at decreased chamber pressure. Again, the rich-to-lean mixing process may be too slow to promote significant smoke consumption in the fuel-lean region. This would impact smoke emissions similarly to the CO, but smoke burnout in a lean region is not an effective emissions control technique because it is kinetically much slower than CO consumption. The preferred approach for smoke reduction is to minimize the fuel residence time in the very rich mixing zones in the rich stage near the fuel nozzle.

Figure 8-13 presents NO_x emissions versus FBN by tests with ERBS fuel doped with pyridine and ERBS/SRC-II blends. At FBN levels corresponding to residual and SRC-II fuels, the indicated yields are approximately 60% and 20%, respectively. Also note in Figure 8-13 that the doped ERBS and ERBS/SRC-II blend data form basically a single curve, indicating that ERBS doped with pyridine results in NO_x emissions very similar to that seen for high-nitrogen fuel blends. Figure 8-14 shows the combustor pressure drop to be approximately 6%, close to the program goal.

Concept 2-4 was developed to promote more rapid fuel/air mixing in the rich stage. A 1 mm (0.040 in.) sleeve was inserted to reduce the exit diameter of the radial inflow swirler in an attempt to increase velocity and improve mixing (see Figure 8-15). Other modifications (Table 8-4) included the original longer first stage, 38.1 cm (15 in.), and a new rich-to-lean dilution airhole pattern. The new pattern (sketched in Table 8-4) used more large holes with higher jet momentum to force the air to the combustor centerline.

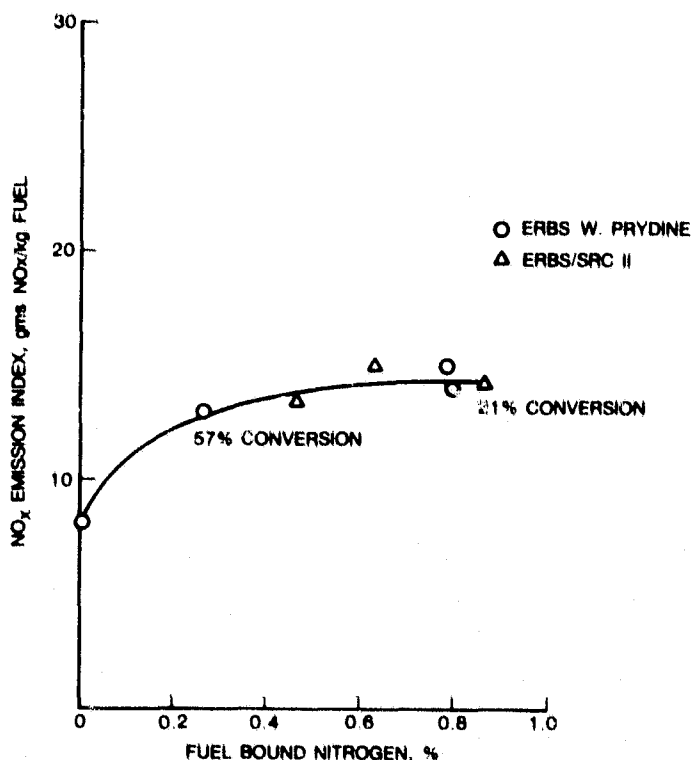


Figure 8-13. NO_x emissions vs fuel-bound nitrogen, Concept 2-3

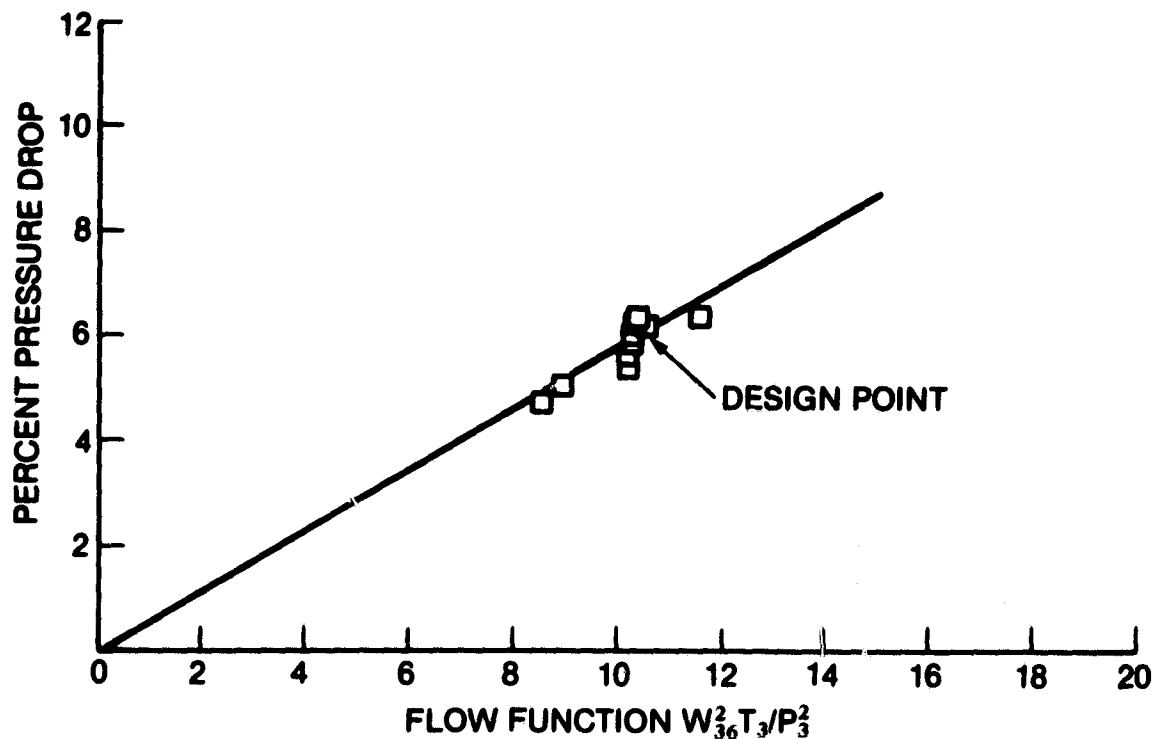


Figure 8-14. Combustor pressure drop for Concept 2-3

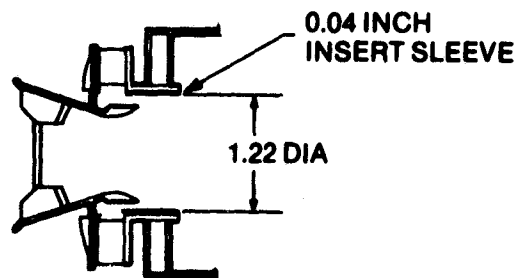


Figure 8-15. Swirl cup modification, Concept 2-4

Table 8-8 presents the Concept 2-4 test data. The measured emissions levels of combustor Concept 2-4 were improved (see Figures 8-4 through 8-6); notably, the smoke was reduced substantially compared with Concepts 2-1 and 2-3 (Figure 8-6), and the improved rich-to-lean mixing decreased the CO to acceptable levels (Figure 8-5). The NO_x emissions were not changed appreciably from previous results. In fact, if the NO_x emissions were increased 20% to 30% to account for normal cycle pressure, the NO_x would be higher than in the previous test of Concept 2-1 which ran at normal cycle pressure. The higher NO_x level can be attributed at least in part to the following. Posttest inspection of the liner revealed a small burned spot on the front end of the rich-stage converging cone, which allowed part of the liner cooling air

to leak into the rich stage. The burn spot probably deteriorated during the test, allowing the rich-stage to operate leaner than designed, resulting in increased NO_x emissions. The FBN conversion rate (Figure 8-16) was lower than for Concept 2-3, as expected with the longer rich-stage length. The high nitrogen point was obtained by addition of pyridine.

The high liner temperatures (Figure 8-17) observed at the aft end of the rich stage (during the latter part of the test) are attributed to the air leak described above, while the high temperature observed in the midsection was caused by fuel impinging on the wall. Posttest inspection of the rich stage revealed carbon deposit on the rich-stage wall as shown in Figure 8-18. One of the locations of the carbon deposit was under the thermocouple which was reading high, and all three locations of carbon deposits were in line with the swirl cups. The primary swirlers, within which the fuel nozzle sits, may have been off center towards the outer wall, resulting in fuel spray on the rich-stage liner wall. Careful alignment of fuel nozzles/swirlers eliminated this problem for Concept 2-5, described next.

Figure 8-19 shows the exit temperature profile was within goal (but not yet as flat as achieved for Concept 2-1), and the liner pressure drop was about 7%.

Although the exhaust temperature profile for Concept 2-4 was much improved over Concept 2-3, indicating better jet penetration and mixing in the quench zone, further modifications were made for Concept 2-5, returning to the quench hole pattern previously used for Concept 2-1.

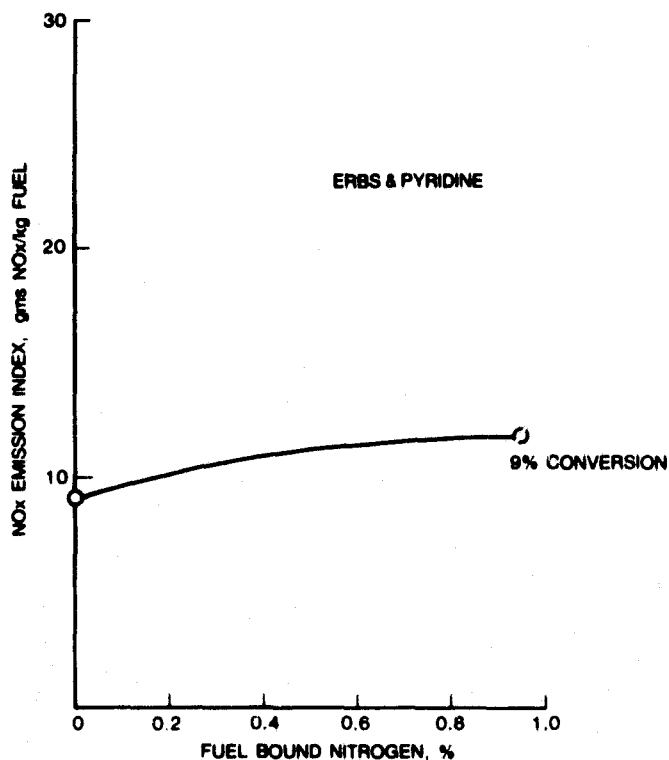


Figure 8-16. NO_x emissions vs fuel-bound nitrogen, Concept 2-4

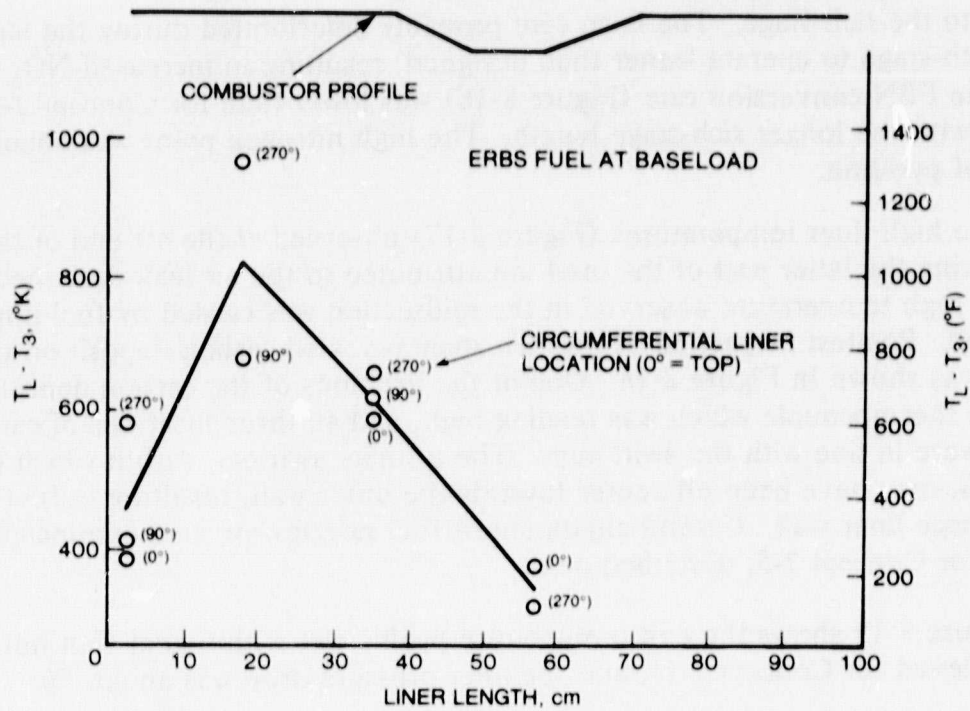


Figure 8-17. Liner temperatures, Concept 2-4



Figure 8-18. Rich-stage liner posttest inspection showing carbon deposit

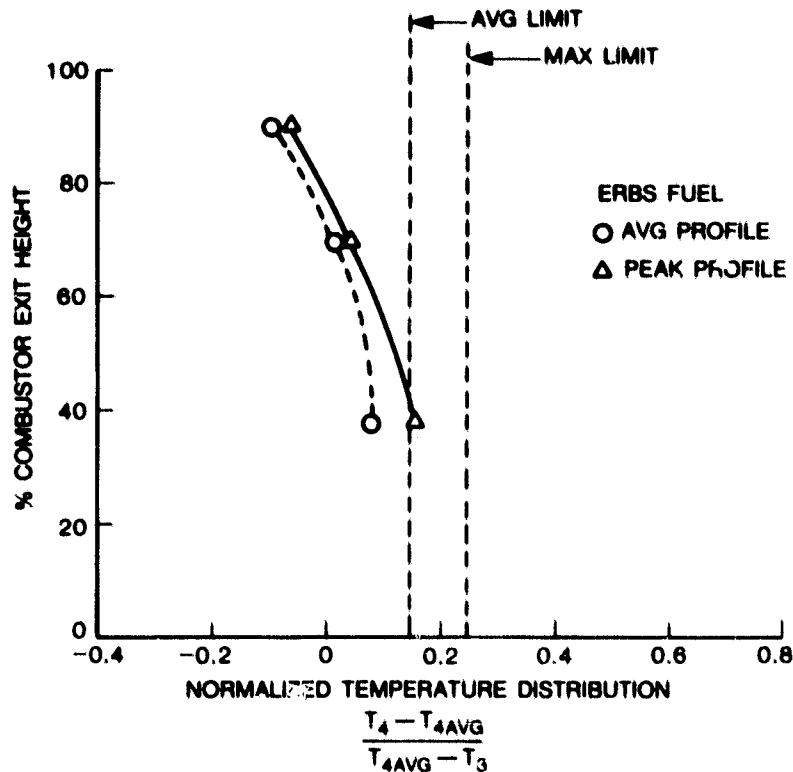


Figure 8-19. Exhaust temperature profiles, Concept 2-4

The final modification of Concept 2 (Concept 2-5) incorporated the best features from previous tests:

1. The sleeve inserts were retained on the air swirlers (modification for Concept 2-4).
2. Revert to the original rich-to-lean air mixing pattern.

Table 8-9 presents the measured data for Concept 2-5. The emissions results are summarized in Figures 8-4 through 8-6. The NO_x emissions were lower than Concepts 2-4 and 2-3, but the full-pressure NO_x emissions were about 15% higher than Concept 2-1. The mixing hole pattern with large holes creating large jets penetrating the rich flame products may promote faster mixing and hence lower NO_x than the other designs using an array of large and small holes. The CO emissions were acceptable and much less than the Concept 2-3 data; however, the trend of increasing CO with an increasing combustor fuel/air ratio again suggests a leaner second stage would decrease these emissions. The smoke emissions were above program goals but substantially below the levels of Concepts 2-1 and 2-3.

Figures 8-20 and 8-21 show the NO_x emissions as a function of fuel-bound nitrogen at 0.69 MPa (100 psia) and 1.14 MPa (166 psia), respectively. Fuel-bound nitrogen was varied by the addition of pyridine to ERBS at 0.69 MPa (100 psia). Data with ERBS/SRC-II blends were also collected at both pressures. As shown by previ-

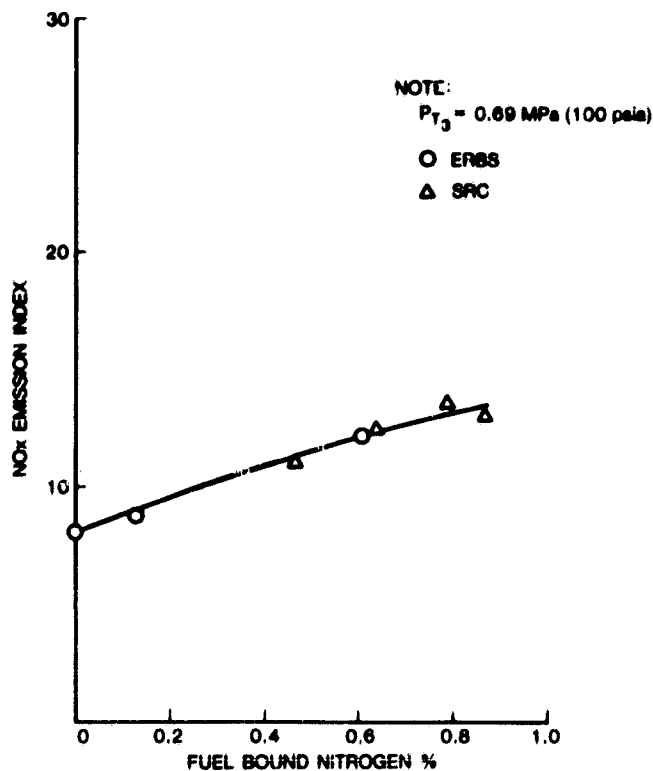


Figure 8-20. NO_x emissions vs fuel-bound nitrogen, Concept 2-5, 0.69 MPa (100 psia)

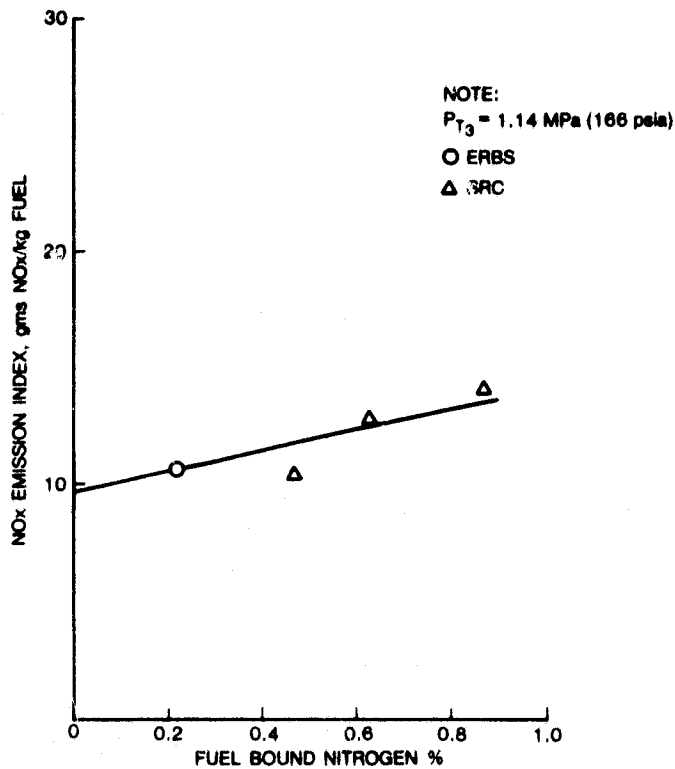


Figure 8-21. NO_x emissions vs fuel-bound nitrogen, Concept 2-5, 1.14 MPa (166 psia)

ous test data, the NO_x generated with the blends was in reasonable agreement with NO_x generated by the addition of pyridine. The conversion rates were about 15% to 20% at 0.69 MPa (100 psia) and were about 15% at 1.14 MPa (166 psia).

Combustor pressure drop (Figure 8-22) was approximately 7.8%, higher than for earlier testing and not explained at this time. Figure 8-23 shows the exhaust profiles are flat and within program goals.

8.1.3 Rich/Lean Combustor with Narrow Passage Quench Zone, Concept 3

Concept 3 was tested initially with ERBS fuel, and during this run, the liner metal temperatures in the rich-to-lean quench zone reached 1150 K (1600 °F). In an effort to preserve the test hardware and obtain NO_x emissions trends, the inlet temperature was reduced and the combustor was operated over a range of fuel/air ratios. Reducing the inlet temperature with a constant fuel/air ratio produces a double impact in liner metal temperatures. The local flame temperature decreases, which lowers the hot-side heat-transfer driving force, and a lower inlet temperature provides a lower temperature coolant, which increases the cold-side heat transfer. A 440 K (300 °F) reduction in the combustor inlet temperature reduced the liner metal temperatures, allowing the test to continue; however, excessive carbon formation increased the pressure drop, forcing early termination of the test.

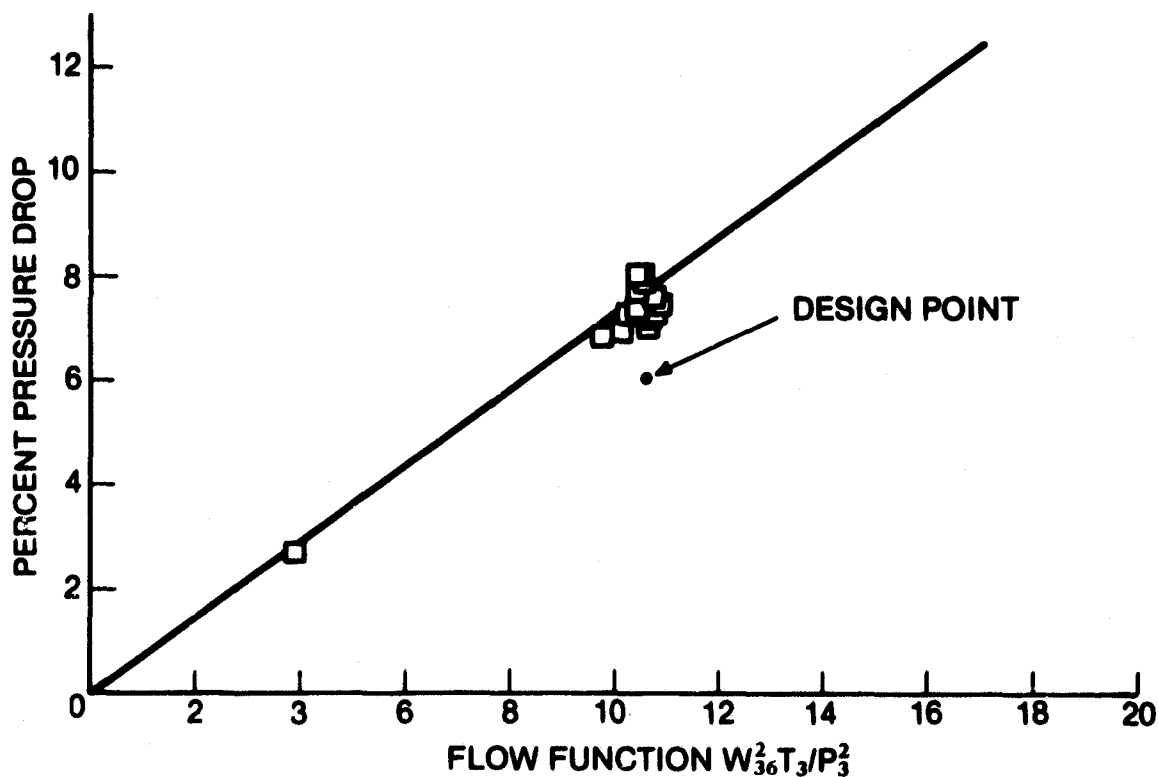


Figure 8-22. Combustor pressure drop for Concept 2-5

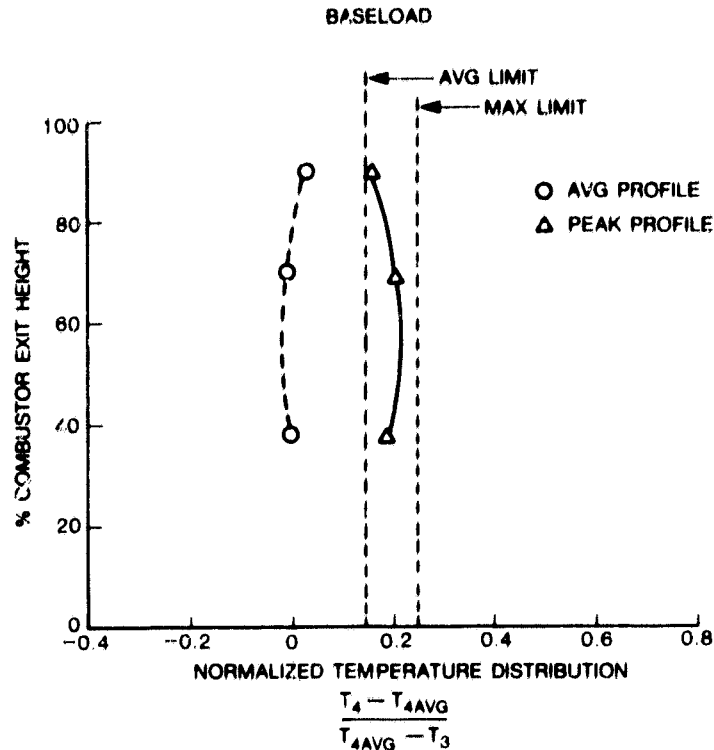


Figure 8-23. Combustor temperature profiles for Concept 2-5

The limited data (see Table 8-10 for Concept 3 test data) showed very encouraging emissions results. Figure 8-24 presents the NO_x emissions data for both Concept 3 and the modified version, Concept 3-1, and Table 8-11 summarizes the design parameters for the two versions of Concept 3. Note in Table 8-11 the rich-stage equivalence ratio at baseload (92% maximum, or fuel/air ratio of 0.0235 on ERBS) was about 1.5 and, because the cycle airflow is approximately constant over the load range, the Concept 3 test was run near a stoichiometric first stage. The NO_x Emissions Index of about 6 g NO_x /kg fuel at full inlet air temperature is a relatively low value even considering the reduced pressure testing. Recall that the condition of a stoichiometric first stage produces a maximum in the NO_x emissions index versus fuel/air ratio, and these data indicate very promising performance. This level was probably the result of the shorter Concept 3 first stage (25.4 cm as opposed to 38.1 cm used in much of Concept 2), decreasing stoichiometric residence time, and an effective rich-to-lean mixing geometry. The latter impacts the peak NO_x emissions by limiting the time for thermal quenching of the NO_x formation mechanism. Compared with Concept 2-3, which also used a short rich stage and demonstrated the lower midload NO_x peak, Concept 3 apparently provides faster mixing in the rich-to-lean stage. In Concept 2-3, the quench air had to penetrate to the combustor centerline (about 70 mm) to quench the first-stage stoichiometric flame gases, but in Concept 3, the centerbody and the liner wall form a 25.4 mm high annulus of first-stage gas, so that the jet penetration required is only 12.7 mm. This geometry is probably the major influence that lowered the peak emissions from about 10.5 g/kg in Concept 2-3 to about 8 g NO_x /kg for Concept 3.

ORIGINAL PAGE IS
OF POOR QUALITY

Table 8-10 (Cont'd)

[illegible]

ORIGINAL PAGE 70
OF POOR QUALITY

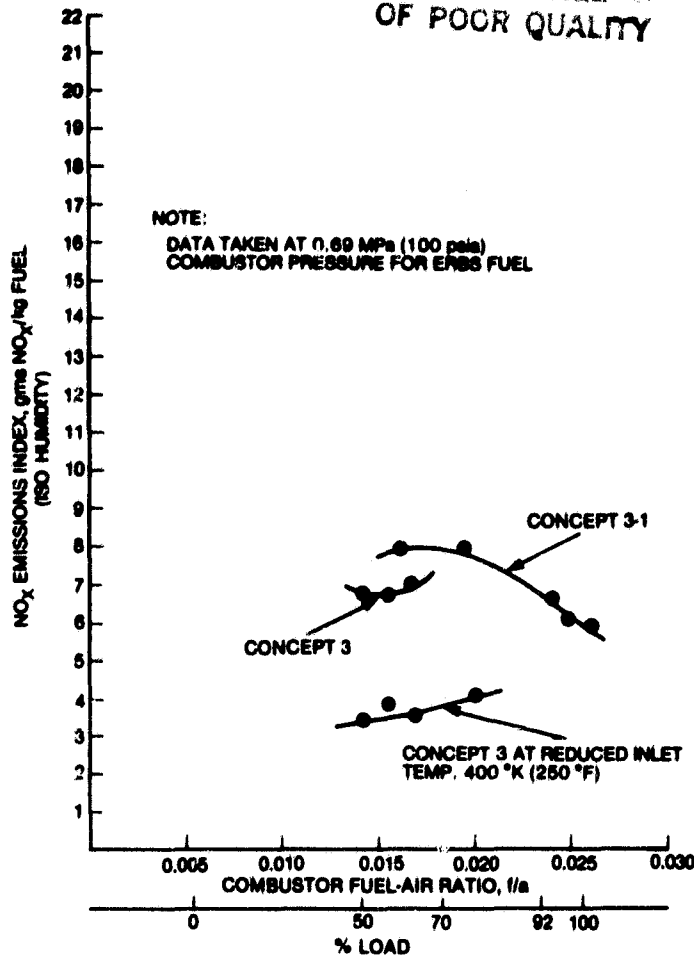


Figure 8-24. NO_x emissions vs load, Concept 3

Figure 8-25 presents the CO and UHC emissions for the two versions of Concept 3 plotted versus the overall combustor fuel/air ratio. The series of four points labeled "Concept 3 with inlet temperature reduced by 440 K (300 °F)" are the data from the low inlet air temperature portion of the run and, as expected, these data are higher than the corresponding data at full inlet air temperature. For a constant overall fuel/air ratio, the fuel flow was fixed, and the higher local flame temperatures associated with the hotter inlet air increased the burning rate.

The smoke emissions, plotted in Figure 8-26 versus overall fuel/air ratio, follow the above trends. Smoke emissions were much higher with the low inlet air temperature, which is consistent with the observed carbon buildup that forced termination of the test.

Concept 3 was modified by placing flow shields around the areas of observed high metal temperature to produce Concept 3-1. These shields increase the local backside velocity in these areas to increase the convective heat-transfer coefficient, thereby providing additional liner cooling. The combustor airhole distribution was not changed, but the addition of these shields probably had a minor influence in the flows

Table 8-11
TEST CONFIGURATION SUMMARY, CONCEPT 3

CONFIGURATION	EQUIVALENCE RATIOS AT BASELOAD (92% POWER)		RICH STAGE COMBUSTION LENGTH, cm (inches)	RICH-TO-LEAN * QUENCH PATTERN	OTHER COMMENTS
	Φ RICH	Φ LEAN			
3	1.82	0.55	25.4 (10)	Rich-to-lean quench air fed from each side of a narrow passage mixing section. Mini- mum quench air pene- tration distance of the three rich-lean concepts.	Improved cooling by enhanced backside air velocity in the rich to lean quench areas.
3-1	1.82	0.55	25.4 (10)		

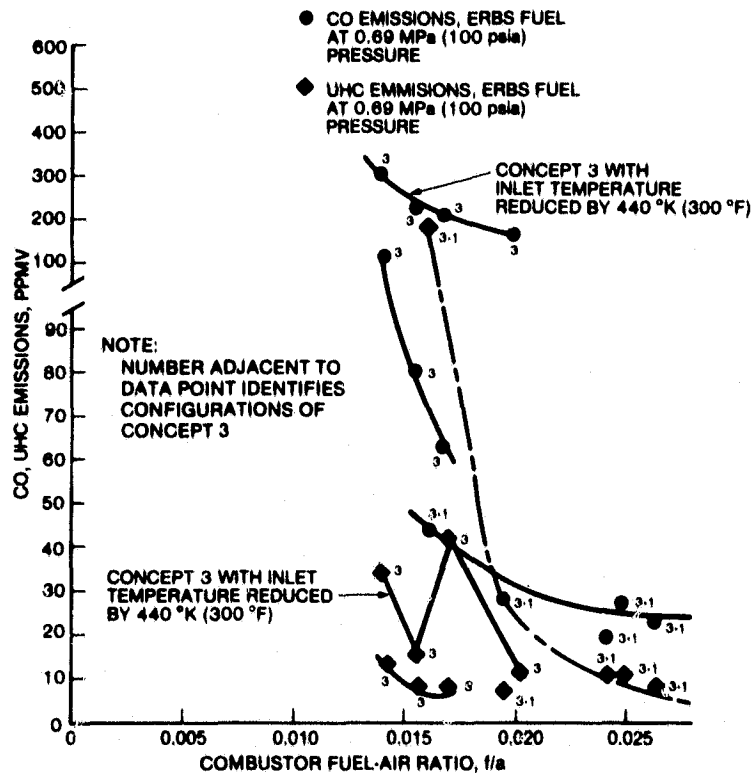


Figure 8-25. Combustible emissions, Concept 3—ERBS fuel

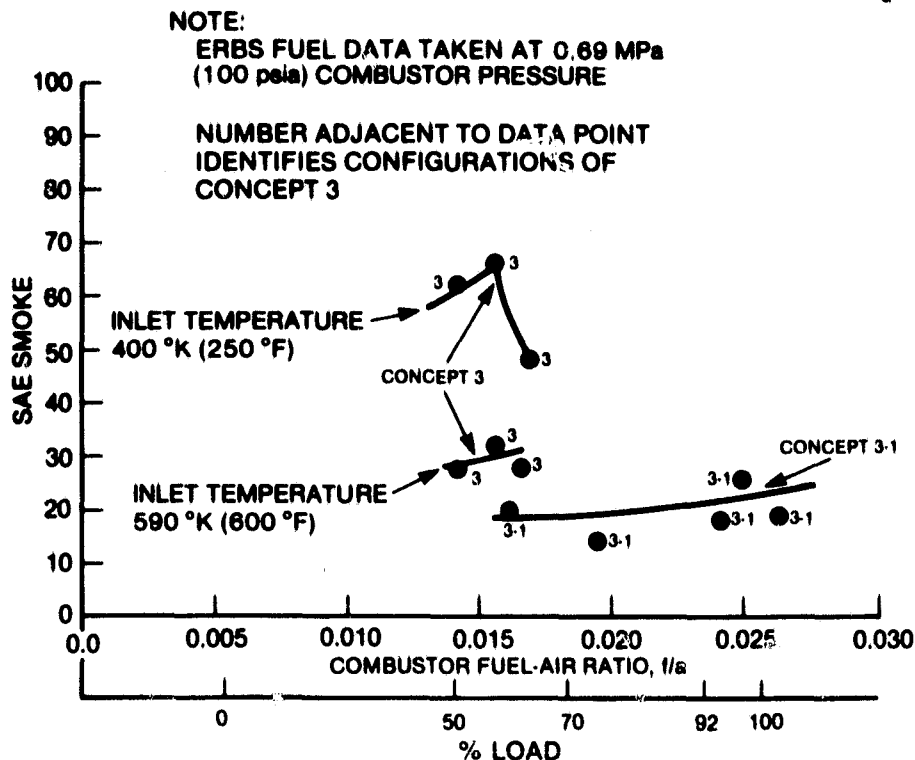


Figure 8-26. Smoke performance, Concept 3

through changing the pressure drop characteristics of the secondary and dilution zone air. Possibly, the first-stage equivalence ratio was decreased by this modification, but the decrease should have been small.

Table 8-12 presents the test data for Concept 3-1. The NO_x emissions (Figure 8-24) for the midload peak were similar to those observed in the initial test. With a near-stoichiometric first stage (f/a overall about 0.015), the NO_x emissions were about 8 g NO_x /kg fuel and decreased with an increasing fuel/air ratio. However, the Emissions Index never reached a local minimum for high rich-stage equivalence ratios, which suggests that additional emissions reductions are possible by redistributing the air to increase the first-stage equivalence ratio. Comparing the variations of Concept 2 (2-3 or 2-5) with Concept 3-1 shows about a 15% NO_x reduction with Concept 3-1. This performance could be due to the liner geometry and superior rich-to-lean mixing configuration.

The CO emissions (Figure 8-25) were acceptable, with most measurements less than 50 ppm. Unburned hydrocarbons were generally less than 10 ppm, but one midload measurement greater than 100 ppm was observed. This reading is unlike other data and previous experience because at this point, the UHC emissions are higher than CO. Usually the UHC emissions are less than CO, which follows chemical explanations that hydrocarbons are easier to oxidize than CO. Further testing would be required to clarify this point.

Table 8-12

[illegible]

8-41

Figure 8-26 presents the smoke emissions versus the overall combustor fuel/air ratio. This configuration also showed low smoke for all points run. Also, the rich stage fuel/air mixing could be improved by installing a converging collar on the rich-stage air swirler to improve fuel/air mixing, similar to that used in Concept 4-1 (discussed later). This modification should decrease the smoke formation.

After testing on ERBS fuel, Concept 3-1 was run on a blend of ERBS and SRC-II. This fuel change increased the liner heat flux, which caused a failure of the enlarged portion of the centerbody. Thus, Concept 3-1 demonstrated a desirable rich-to-lean mixing scheme, but the liner cooling and liner geometry must be improved. The annular rich stage minimizes the required jet penetration distance for rich-to-lean transition, thereby improving the mixing, but the centerbody approach to achieving this geometry needs improvement. Figure 8-27 presents NO_x emissions for ERBS and an ERBS/SRC-II blend, with yield of about 30% at 0.45% FBN.

Figures 8-28 and 8-29 present exhaust-temperature profiles, and pressure-drop data met program goals.

8.2 LEAN/LEAN COMBUSTOR TEST RESULTS

Screening tests were conducted on lean/lean combustor Concepts 4, 5, and 6. Each of the three lean/lean designs showed potential for achieving ultralow NO_x levels with ERBS fuel. Due to the inability of the lean/lean designs to meet NO_x goals

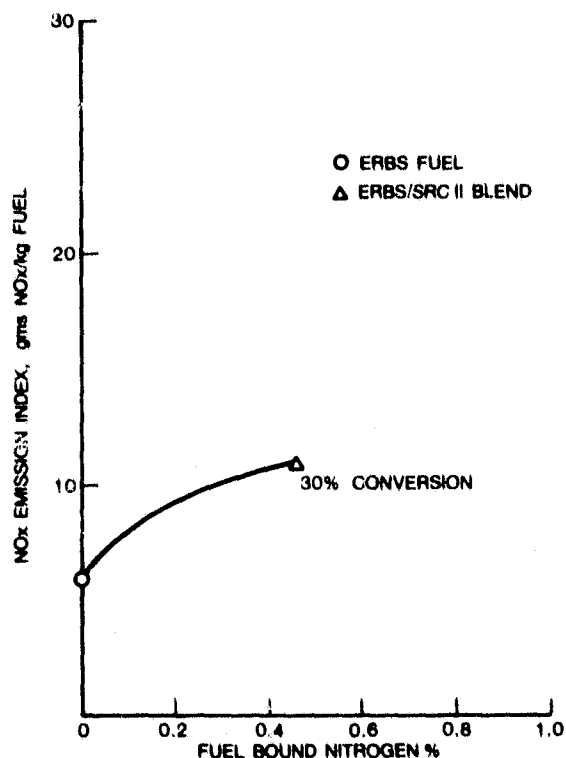


Figure 8-27. NO_x emissions vs fuel-bound nitrogen, Concept 3-1

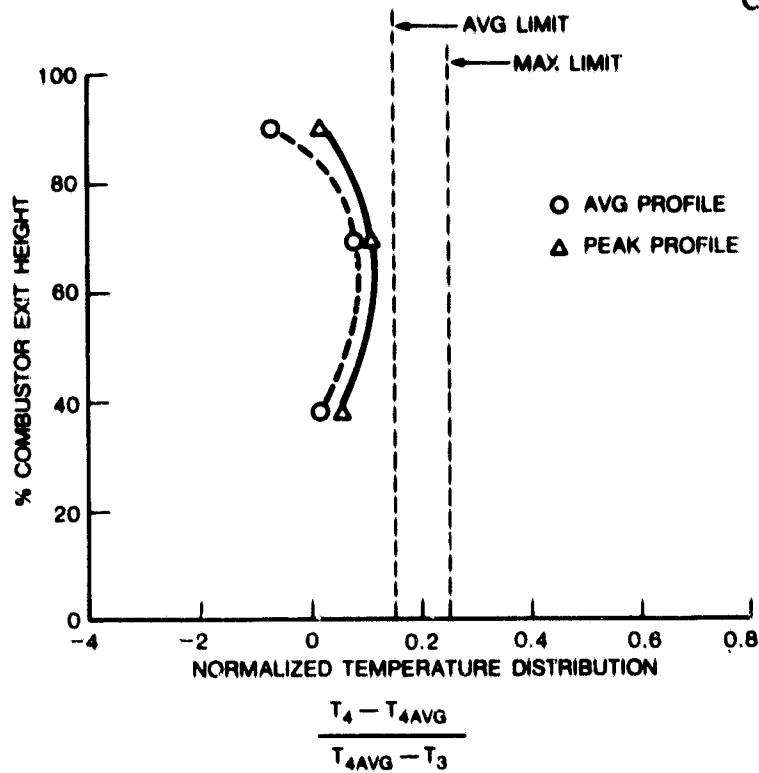


Figure 8-28. Combustor temperature profiles for Concept 3-1

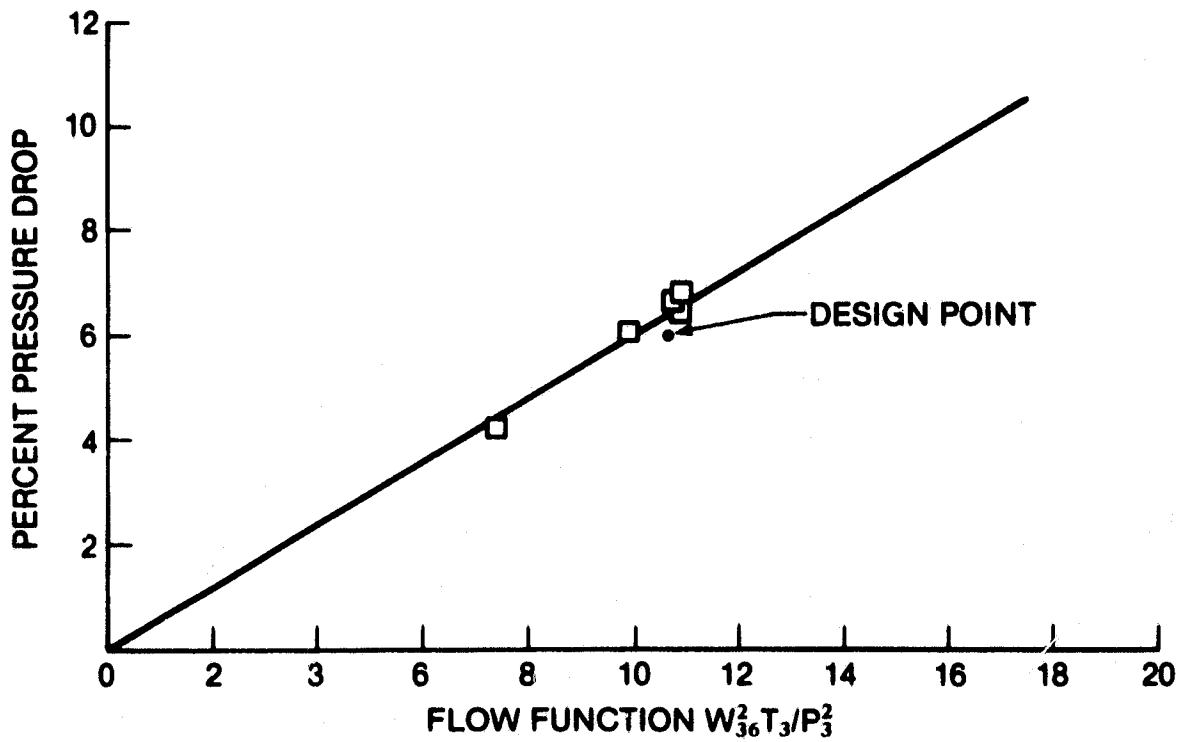


Figure 8-29. Combustion pressure drop for Concept 3-1

with SRC-II fuels, only one modification was made to these designs. Concept 4 was selected for modification and reevaluated as Concept 4-1. The results obtained with these four tests are presented below.

8.2.1 Series-Staged Lean/Lean Combustor, Concept 4

The initial screening test of combustor Concept 4 was completed by measuring a total of 20 data points and burning both ERBS and residual fuel. The combustor liner met the program clean-fuel NO_x emissions goal (95 ppmv at 15% O_2 or 7.1 g NO_x/kg fuel) over a portion of the load range, but exceeded the goals in the 70%-100% load range. When burning residual fuel, the conversion of fuel nitrogen to NO_x increased the NO_x substantially. The CO, UHC, and smoke emissions were low and within program goals for both fuels.

Table 8-13 presents the as-measured data taken for Concept 4 with both ERBS distillate and petroleum residual fuels. The tabulated NO_x emissions indices are on an ISO humidity basis, i.e., 0.0063 grams of water vapor per gram of dry air, corresponding to the EPA emissions standards.

Figure 8-30 presents the NO_x emissions data for combustor Concept 4. The data measured when burning both ERBS and residual fuels were plotted in Figure 8-30 as NO_x emissions index, EI (g NO_x/kg fuel or ppmv at 15% O_2) versus MS7000 load and combustion fuel/air ratios.

The ERBS fuel test points spanned the MS7000 load range. For less than 70% load, the fuel was injected into only the pilot stage. Above 70% load, fuel was injected into both stages with 65% of the total fuel flow in the second stage. The discontinuity at 70% load is caused by the change in fuel injection from pilot-only to dual-stage operation. As shown at the 70% load point, dual-stage operation decreased the NO_x emissions compared with single-stage values, and the combustor NO_x emissions only slightly exceeded the EPA limit at full load.

Figures 8-31 and 8-32 show the liner for Concept 4 during posttest inspection. Figure 8-31 shows the liner in excellent condition and free of deposits. Figure 8-32 is a view of the interior of the liner looking upstream towards the pilot dome end. Some minor carbon deposition exists on the pilot-stage swirler.

Figure 8-30 also presents the NO_x emissions data measured while burning residual fuel at a fuel-flow split of 35% in the pilot stage and 65% in the main stage. Comparison of the residual oil NO_x data with that measured for ERBS fuel indicates a relatively consistent increase in NO_x of approximately 4.1 g NO_x/kg fuel when burning residual oil. The higher NO_x was due to organic nitrogen species in the residual oil. If the ERBS data are used as a nitrogen-free fuel baseline and the difference in NO_x emissions is attributed to fuel-bound nitrogen only, then the FBN conversion with residual oil is about 52% at MS7000 baseload condition. Tests conducted later in the program (note comments made in Section 8.1) showed that this assumption is valid and that residual and SRC-II fuels can be simulated by addition of pyridine to ERBS distillate.

Table 8-13
CONCEPT 4 TEST RESULTS

POINT NUMBER	READING NUMBER	HARDWARE CONFIGURATION	FUEL TYPE	FUEL % H	FUEL % N	FUEL LAY	FUEL TEMP (°F)	SIMULATED ENGINE POWER CONDITION				TINLET (°F)	TINLET (PSIA)	W FUEL P (LB/HR)	W AIR P (LB/HR)	W FUEL S (LB/HR)	W AIR S (LB/HR)	PRIMARY EQUIVALENC RATIO	SECONDARY EQUIVALENC RATIO	OVERALL EQUIVALENC RATIO	PRIMARY RES. TIME (SEC.) COLD	SECONDARY RES. TIME (SEC.) COLD	PRIMARY REF. VELOCITY (FT/S)	SECONDARY REF. VELOCITY (FT/S)	EXIT TEMPERATURE (°F)	EXIT PRESSURE (PSIA)
1.1	3	4	ERBS	12.95	.0054	18275	101	0				544	127.0	316	5.95	0	11.15	.213	0	.075	10.0	7.0	50	144	871	118.0
1.2	4	"	"	"	"	"	79	50				588	148.9	813	5.81	0	10.89	.563	0	.196	11.5	8.1	43	125	1465	140.7
1.31	5B	"	"	"	"	"	74	70				606	156.4	1072	5.78	0	10.82	.746	0	.260	12.0	8.4	42	120	1672	148.7
1.3	6	"	"	"	"	"	73	70				607	156.9	376	5.78	711	10.82	.262	.444	.263	12.0	8.4	42	120	1686	149.1
1.5	7	"	"	"	"	"	68	100				635	168.8	516	5.64	980	10.56	.368	.627	.371	13.0	9.1	39	111	2108	161.4
1.3	8	"	RESID	11.52	.23	17748	214	70				603	156.6	379	5.78	705	10.82	.257	.429	.256	12.0	8.4	42	120	1721	148.8
1.44	9	"	"	"	"	"	214	92				627	167.9	481	5.78	893	10.82	.326	.543	.324	12.7	8.8	40	114	1944	160.1
1.3	1	4	ERBS	12.95	.0054	18275	48	70				569	156.5	360	5.81	703	10.85	.249	.436	.256	11.9	8.3	42	121	1648	148.6
1.41	2	"	"	"	"	"	48	92				630	166.2	335	5.81	1021	10.89	.232	.633	.326	12.4	8.7	40	116	1931	158.7
1.42	3	"	"	"	"	"	49	92				624	166.2	626	5.85	766	10.95	.430	.472	.333	12.4	8.7	40	116	1926	158.5
2.3	4	"	"	"	"	"	52	--				600	150.4	430	5.88	495	11.02	.294	.303	.220	11.4	8.0	44	126	1517	142.1
2.4	5	"	"	"	"	"	53	--				605	149.4	425	5.88	792	11.02	.291	.486	.289	11.3	7.9	45	128	1777	141.6
2.5	6	"	"	"	"	"	54	--				596	150.5	427	5.78	1097	10.82	.297	.685	.369	11.6	8.1	43	124	2020	142.5
1.4	7	"	"	"	"	"	54	92				622	156.0	490	5.74	905	10.76	.342	.568	.340	12.7	8.8	40	114	1964	158.7
1.4	8	"	RESID	11.52	.22	17748	214	92				627	165.5	501	5.67	892	10.63	.246	.553	.335	12.7	8.8	40	114	1436	158.5
1.43	9	"	"	"	"	"	214	92				631	166.1	500	5.71	886	10.69	.342	.547	.332	12.7	8.8	40	114	1245	159.0
1.5	10	"	"	"	"	"	212	100				633	168.6	524	5.74	974	10.76	.358	.596	.356	12.8	8.9	39	113	1325	161.3
2.4	12	"	"	"	"	"	224	--				600	149.7	422	5.87	783	10.95	.282	.469	.280	11.4	7.9	44	127	1277	141.4
2.7	14	"	"	"	"	"	216	--				602	149.6	564	7.02	936	13.14	.281	.469	.280	9.5	6.6	53	152	1203	137.7
2.6	15	"	"	"	"	"	225	--				601	149.5	346	4.66	620	8.74	.293	.467	.283	14.3	10.0	35	101	1436	144.4

Table 8-13 (Cont'd)
CONCEPT 4 TEST RESULTS

POINT NUMBER	READING NUMBER	COMBUSTOR DELTA P (PSI)	LINER TEMPERATURE (°F)	CO (PPM)	CO ₂ (PPM)	HC (PPM)	NOX (PPM)	NOX (PPMD)	% N CONVERSION	COMBUSTION EFFICIENCY (%)	SMOKE NUMBER	PATTERN FACTOR	FAIR			COMBUSTOR A/P/P (%)	FLOW FUNCTION W 32.17/P ³	ATOMIZING AIR DP (PSIA)	TOTAL ATOMIZING AIR FLOW (LBM/S)	ELIMOX	WEL AIR NATO RETURNED
1.1	3	9.0	815	253.3	11000	51.2	15.3	56.4	-	98.47	5.4	.52	.0054			7.1	18.17	18.6	.33	4.09	.0051
1.2	4	8.2	1355	45.5	29700	9.3	79.4	106.2	-	99.89	22.2	.54	.0140			5.5	13.18	10.95	.35	8.04	.0135
1.31	5B	7.7	1372	136.1	39300	9.3	123.4	124.4	-	99.81	30.3	.68	.0186			4.9	12.02	12.3	.36	9.41	.0178
1.3	6	7.8	1171	288.6	39300	9.3	71.5	71.7	-	99.63	4.7	.21	.0187			5.0	11.91	13.0	.35	5.43	.0180
1.5	7	7.4	1453	26.5	57000	2.3	143.5	99.9	-	99.97	.7	.20	.0266			4.4	10.0	12.3	.36	7.58	.0257
1.3	8	7.8	1150	260.3	42100	8.5	138.0	133.9	-	99.68	15.2	.16	.0196			5.0	11.84	13.7	.36	9.94	.0182
1.44	9	7.8	1633	144.6	50900	8.5	183.4	147.4	-	99.84	9.7	.20	.0236			4.6	10.61	49.6	.73	10.95	.023
1.3	1	7.7	1156	286.2	38800	10.9	50.9	53.8	-	99.62	5.0	.20	.0183			4.9	12.13	12.5	.35	4.08	.018
1.41	2	7.6	1423	91.4	49103	3.1	114.8	96.3	-	99.9	5.0	.13	.0230			4.6	10.96	13.6	.37	7.31	.025
1.42	3	7.7	1242	62.2	49800	1.5	119.4	95.9	-	99.94	2.7	.32	.0233			4.6	11.01	13.5	.37	7.25	.023
2.3	4	8.3	1087	846.3	32400	60.6	38.9	47.3	-	98.6	9.3	.33	.0157			5.5	13.36	14.3	.35	3.52	.0152
2.4	5	7.8	1200	149.9	43700	6.2	91.0	82.7	-	99.82	5.7	.25	.0206			5.2	13.28	12.4	.33	6.25	.020
2.5	6	8.1	1305	56.0	55300	.8	134.0	95.7	-	99.95	.3	.18	.0259			5.4	12.85	11.7	.32	7.24	.0255
1.4	7	7.3	2292	43.2	50600	0.0	129.1	100.1	-	99.96	4.7	.21	.0237			4.4	10.7	13.6	.36	7.62	.0235
1.4	8	7.0	1430	47.6	53900	.8	206.6	155.8	-	99.95	9.3	.20	.0249			4.3	10.5	12.4	.36	11.63	.0237
1.43	9	7.1	1345	124.6	51800	.4	190.3	149.6	-	99.88	5.0	.21	.024			4.2	10.6	28.5	.53	11.13	.0235
1.5	10	7.3	1325	38.8	58100	0.0	226.7	158.6	-	99.97	5.0	.22	.0268			4.3	10.44	13.5	.36	11.84	.0252
2.4	12	8.3	1277	271.6	45300	7.8	118.0	106.4	-	99.69	10.3	.20	.0211			5.5	13.46	14.7	.36	7.87	.020
2.7	14	11.9	1203	379.8	45300	24.1	109.6	98.2	-	99.53	14.8	.21	.0212			7.9	19.3	17.6	.40	7.29	.020
2.6	15	5.1	1438	188.4	43900	7.8	122.3	113.5	-	99.77	10.0	.20	.0204			3.4	8.5	11.6	.35	8.42	.020

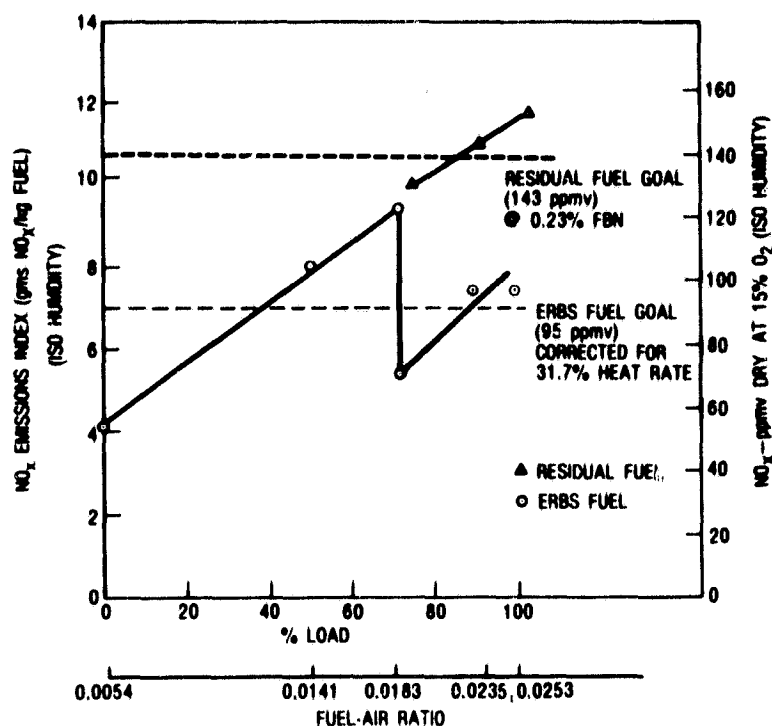


Figure 8-30. NO_x performance for Concept 4—series-staged lean-lean

Figure 8-33 presents the CO and unburned hydrocarbon emissions data corresponding to the NO_x data shown in Figure 8-30. The CO emissions were high at the no-load condition and, similar to conventional production combustors, CO decreased with increasing load. The increase in CO between 50% and 70% load was possibly caused by incomplete mixing of the pilot flame products with the main-stage air. The high pattern factor observed for the 70% load pilot-only operation supports this explanation. When the combustor was switched to two-stage operation, the CO increased because of the relatively fuel-lean flames in both the first and second stages. This emissions characteristic is similar to single pilot stage operation at very low loads with lean flames. Overall, the CO emissions were acceptable considering that the production MS7000 combustor can be longer than the test vehicle, thereby increasing the residence time available for CO burnout. The unburned hydrocarbon emissions were low over the entire load range except for the no-load point and at transition to two-stage operation. At this load, low fuel/air ratios provide insufficient temperature rise. Two methods are presented later in this report to remedy this problem.

Figure 8-34 presents the smoke emissions data. On ERBS fuel, the only unacceptable point was the 70% load pilot-only condition. The high pilot-stage equivalence ratio promoted smoke formation. Burning residual fuel, the smoke emissions met the program goals. Increasing load decreased the smoke even though the flame equivalence ratio increased. At first glance, this behavior appears erroneous; however, similar results have been noted for MS7000 production combustors. Residual fuel spray flames usually form some smoke in locally fuel-rich regions, but the final smoke emissions depend on whether or not the smoke is consumed in the postflame

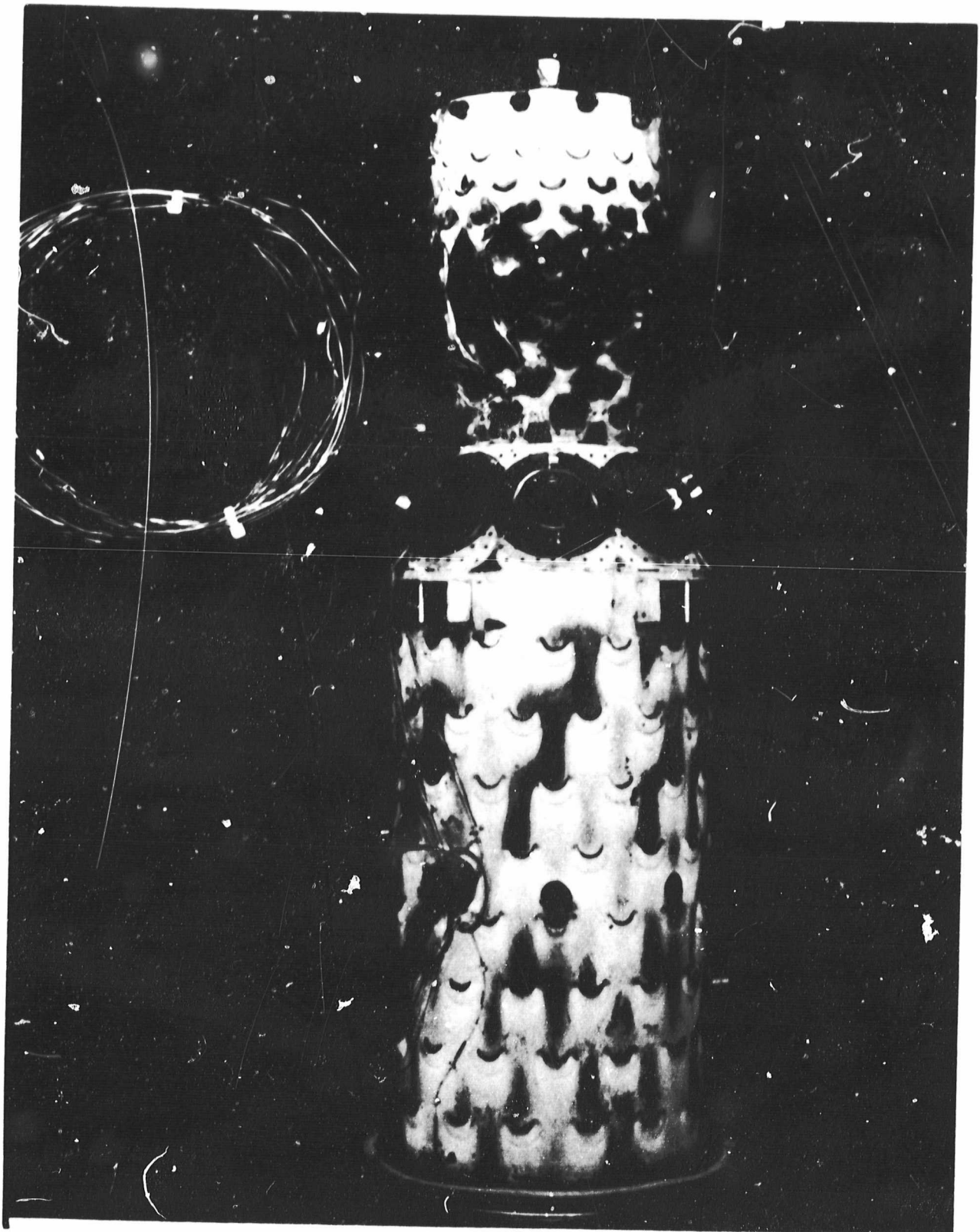


Figure 8-31. Posttest view, combustor Concept 4

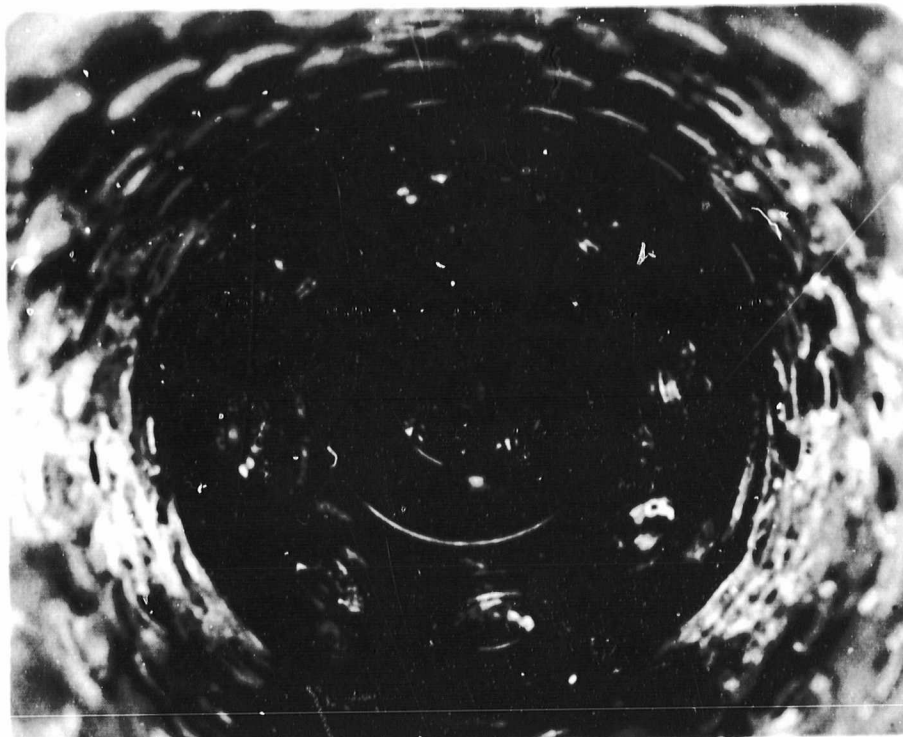


Figure 8-32. Posttest view of pilot dome, combustor Concept 4

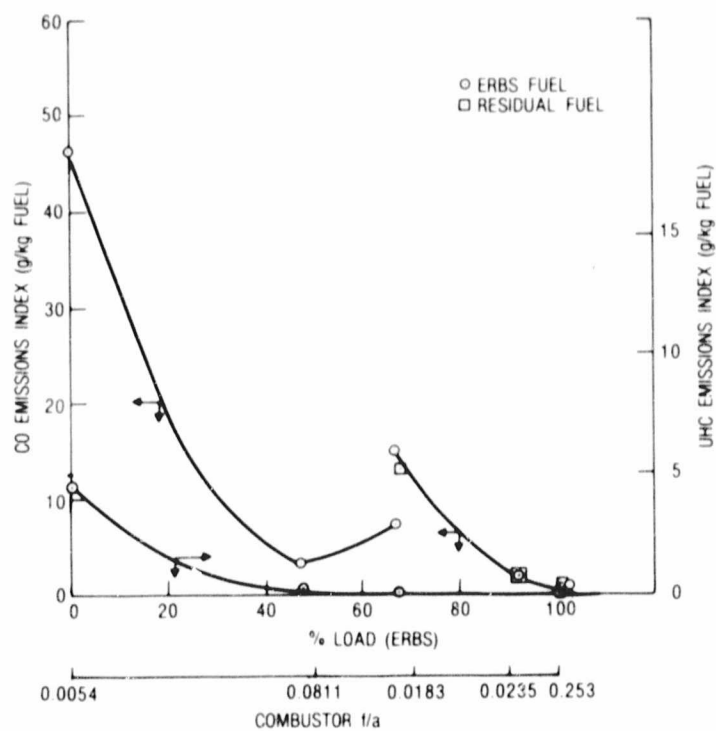


Figure 8-33. CO and UHC emissions, Concept 4

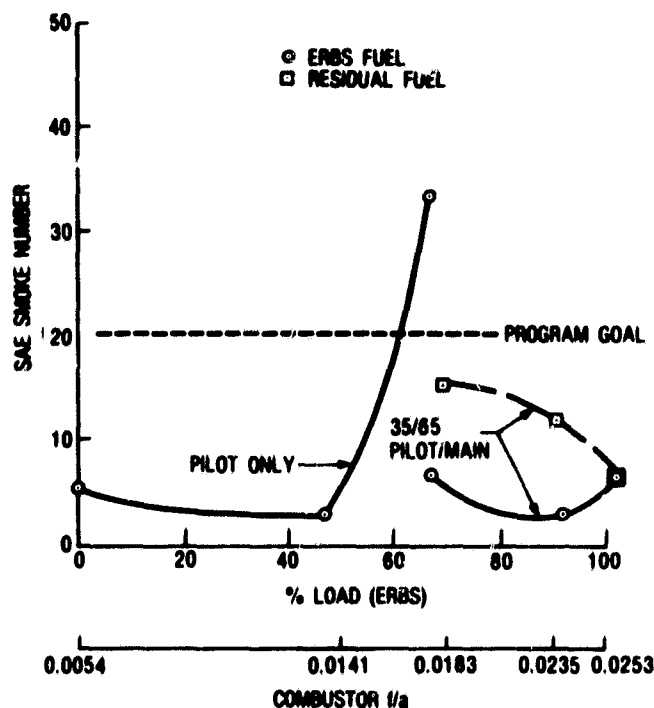


Figure 8-34. Smoke emissions, Concept 4

region. In that region smoke burnout can be thermally quenched, similar to CO. As shown in the current data, increasing the flame equivalence ratio (increasing load) probably causes higher smoke formation locally in the flame, but the hotter postflame region promotes smoke burnout. Undoubtedly, further increase in the flame equivalence ratio will generate a condition where smoke formation will overpower smoke consumption. Although the point was not run, the 70% load on pilot-only operation burning residual fuel would probably generate excessive smoke. The transfer point for switching to two-stage operation may have to be changed to a lower load to alleviate the potential for smoke emissions.

The combustor exhaust temperature pattern factor and profile factor are defined as

$$\text{Profile factor} = \frac{T_C - T_{avg}}{T_{avg} - T_{in}}$$

where

- T_{max} = maximum reading of 12 combustor exit thermocouples
- T_C = circumferential average temperature at a constant radial location
- T_{avg} = average of 12 combustor exit thermocouples
- $T_{avg} - T_{in}$ = combustor temperature rise

As defined, the profile factor represents the average radial variation in temperature, hence the term profile; the pattern factor identifies the worst local hot spot. When operating on only the pilot stage, the exhaust gas temperatures are peaked near the centerline, resulting in high pattern and profile factors. However, the actual temperature levels are low because the overall fuel/air ratio is low during pilot-only operation. In two-stage operation, the values are reasonable and would be improved in an actual engine because of increased mixing time in the transition duct between the combustor and the first-stage turbine nozzle. The detailed average and peak profiles (the *max* value of each profile is profile factor and pattern factor, respectively) are presented in Figure 8-35. Figures 8-36 and 8-37 present liner temperatures along the liner length for ERBS and residual fuel, respectively. Although somewhat higher for the more radiant flame of the residual fuel, liner temperatures are well within acceptable values.

Figure 8-38 presents the overall combustor pressure drop versus flow function. The figure also shows that pressure drop was below the design goal. This pressure drop margin was used in subsequent testing to improve fuel/air mixing. Figure 8-39 shows the liner pressure drop at various liner lengths for peak load conditions. The figure shows good agreement between the predicted liner ΔP and measured liner ΔP . The difference basically comes from overall lower pressure drop.

The analysis of data has shown that the NO_x emissions were a strong function of secondary stage equivalence ratio. Spray tests of the main-stage swirlers were subsequently conducted and indicated insufficient mixing of fuel and air. The local rich regions in the main stage prevented reaching the potential NO_x emissions levels of

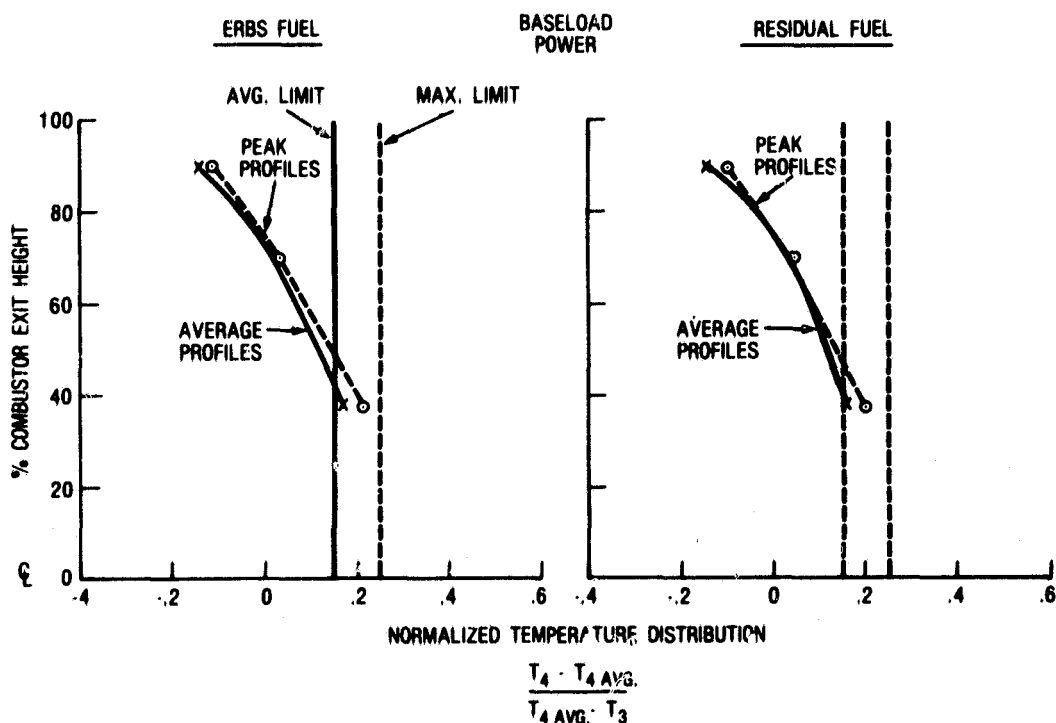


Figure 8-35. Exit temperature distributions at baseload, Concept 4

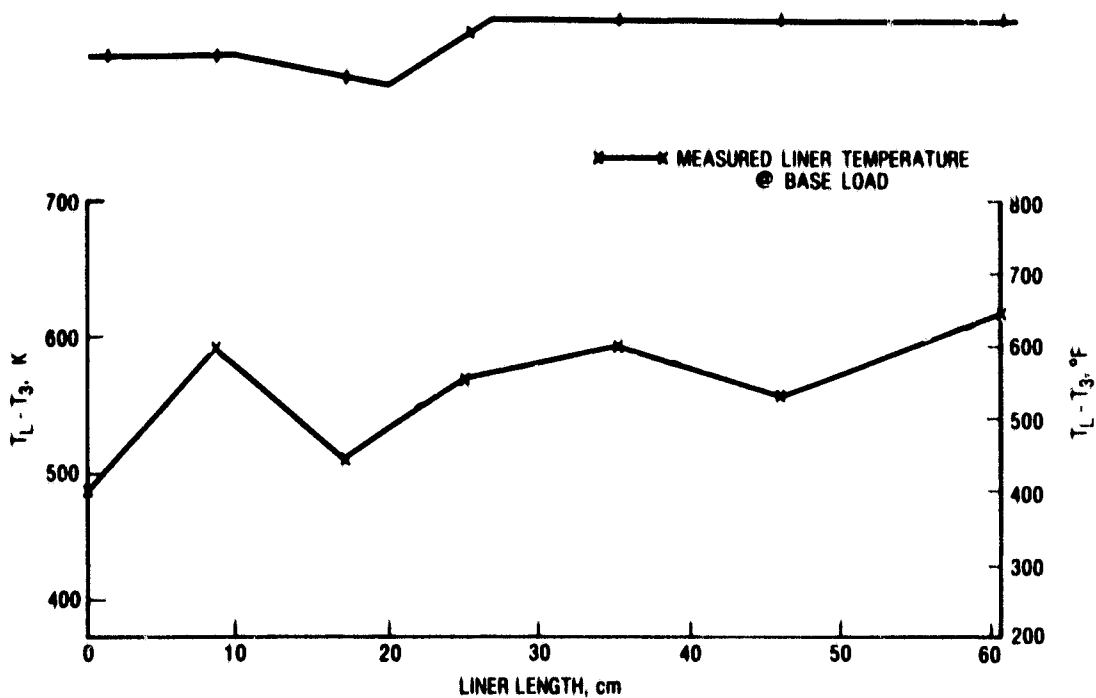


Figure 8-36. Liner metal temperatures, Concept 4--ERBS fuel

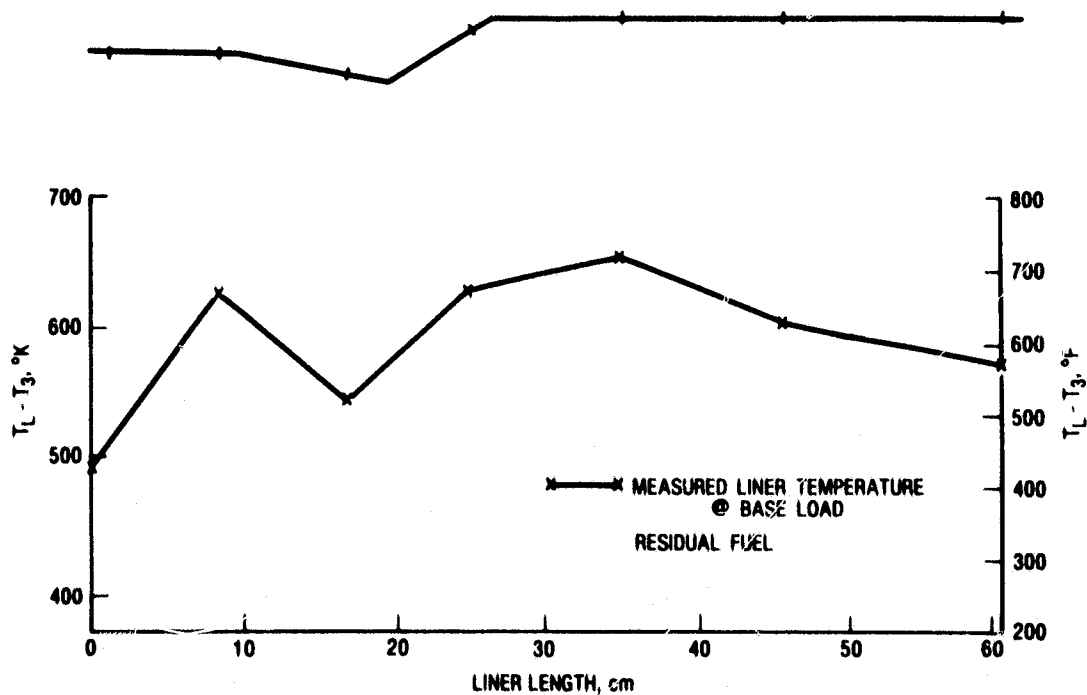


Figure 8-37. Liner metal temperatures, Concept 4--residual fuel

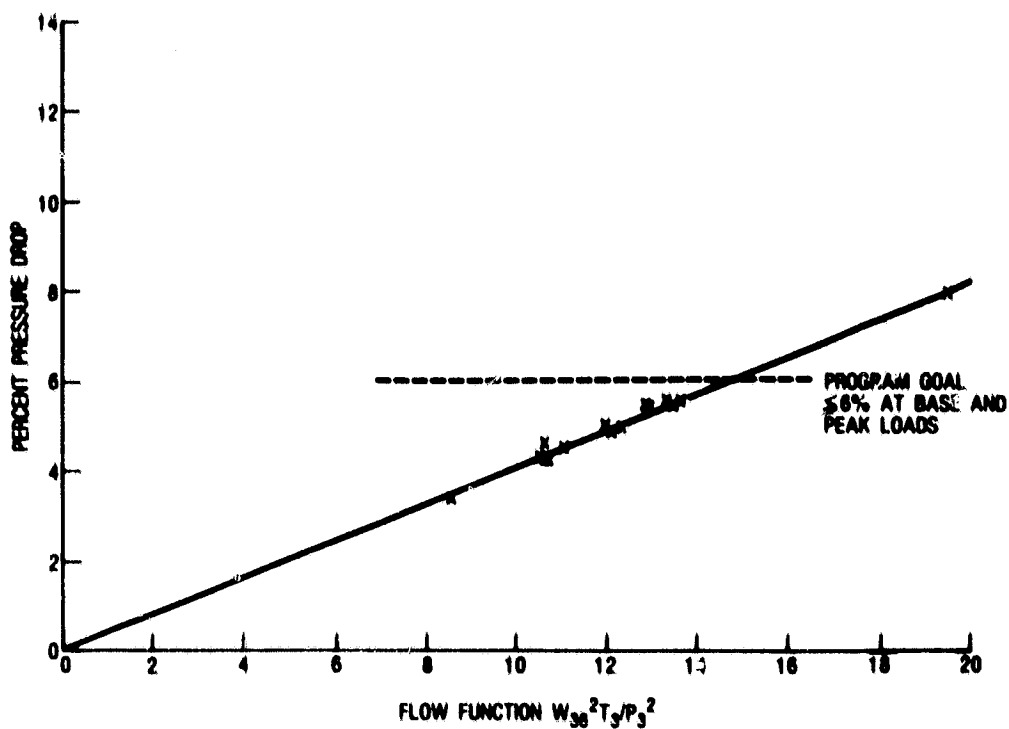


Figure 8-38. Pressure drop vs flow, Concept 4

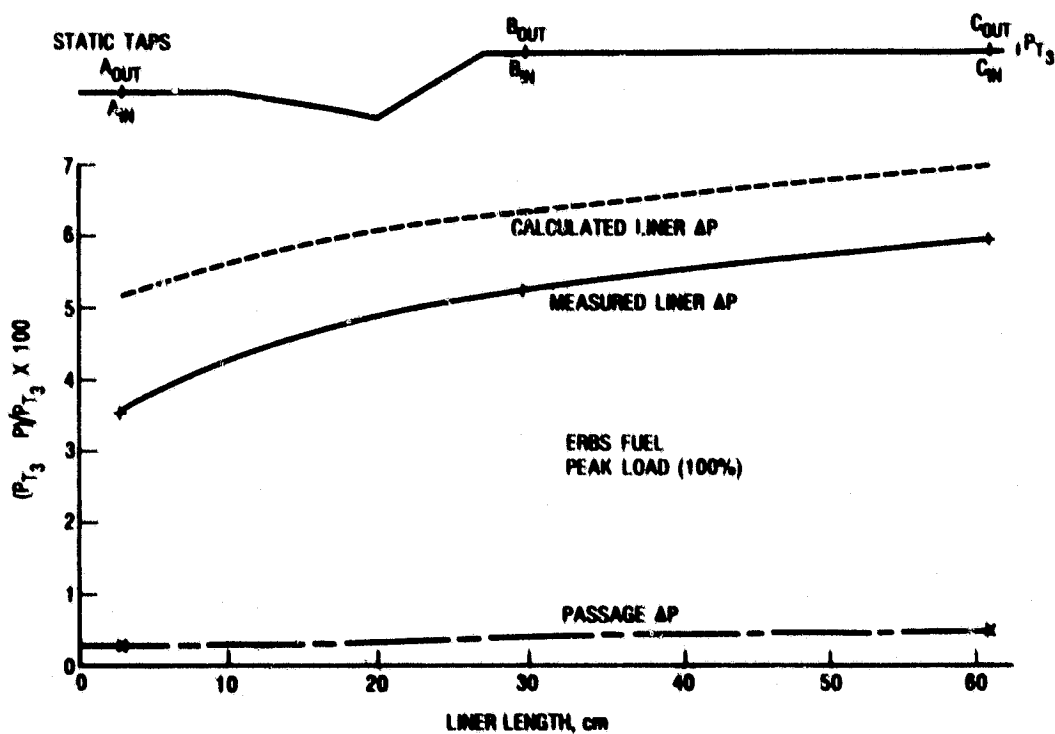


Figure 8-39. Liner ΔP vs length, Concept 4

this design. Figure 8-40 illustrates the initial spray pattern and the spray pattern obtained after a flow guide sleeve was added to the swirler. Because of the encouraging results obtained in the nozzle spray test, the swirler modification was planned for the subsequent test of Concept 4-1 (modification of Concept 4).

As mentioned previously, some carbon deposit was observed on the pilot swirler (see Figure 8-32). It was speculated that the carbon deposit was due to nichrome patches installed on selected swirler vanes to reduce swirler flow. The NO_x emissions generated in the pilot stage were also excessive at 50% and 70% loads. At these loads, the pilot exit equivalence ratio is high enough to generate excessive NO_x . The mixing in the main stage was enhanced as described previously. However, the mixing in the pilot stage could also be enhanced by increasing the pressure drop since pressure drop margin is available (4.5% measured as opposed to a 6% program limit). The liner metal temperatures were well within safe limits indicating that a portion of the cooling air could be diverted to the flame zone.

Based on the above observations, the following modifications were made to Concept 4 to generate the next test vehicle, Concept 4-1:

1. The cooling louver slots were closed to about 0.63 mm height to increase the pressure drop (approximately a 25% decrease in area).
2. The nichrome patches were removed from the pilot-stage air swirler to reduce carbon deposition. The pilot-stage dilution airflow was reduced to maintain a constant pilot stage airflow.
3. A conical venturi section was added to the main-stage swirlers to converge the swirling airflow into the fuel spray.

These modifications are summarized on Figure 8-41.

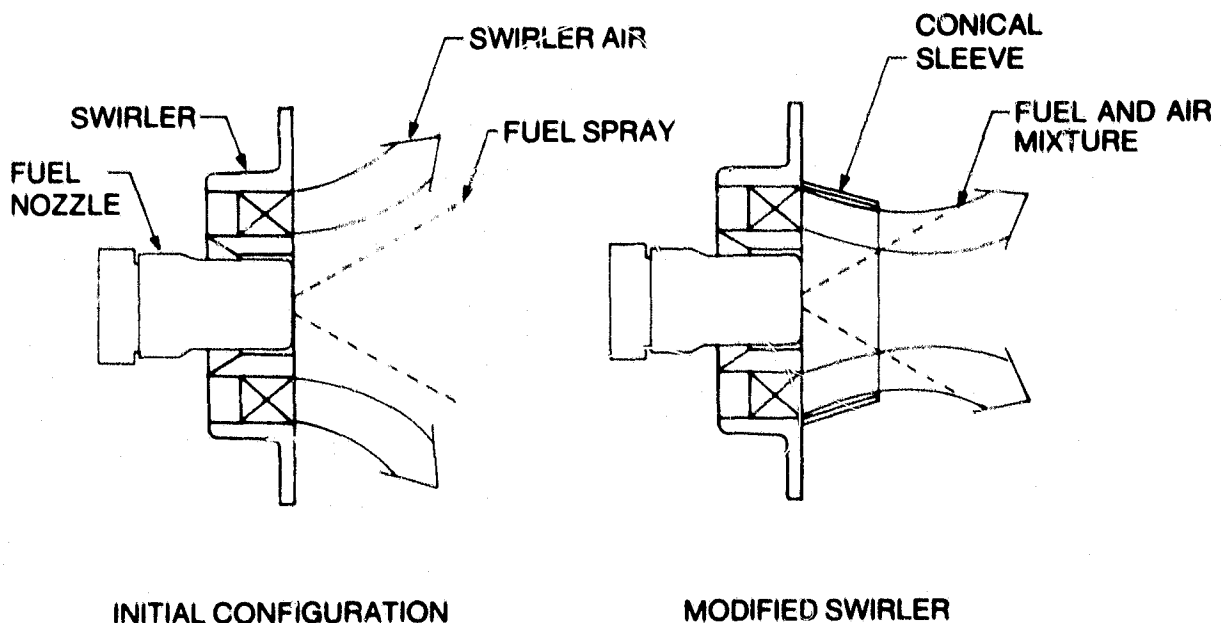
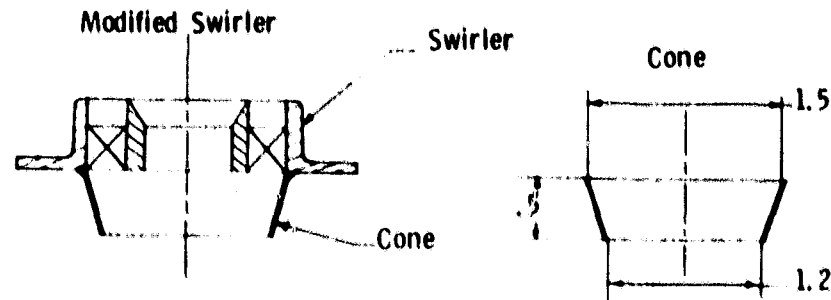


Figure 8-40. Fuel nozzle/swirl cup spray pattern

1. MAIN STAGE SWIRLERS MODIFIED TO ENHANCE FUEL-AIR MIXING



2. REDUCED LOUVER GAP TO INCREASE LINER PRESSURE DROP

3. REMOVED NICHROME FROM PILOT SWIRLER TO REDUCE CARBON

REDUCED PILOT DILUTION AREA TO KEEP SAME PILOT FLOW

Figure 8-41. Modifications to Concept 4 (Concept 4-1)

Table 8-14 summarizes the measured flow splits for Concept 4-1 and Concept 4.

With the foregoing changes, the NO_x level with ERBS fuel was well below the program goal at the baseload condition, as shown in Figure 8-42. Table 8-15 presents the data for Concept 4-1 with all three program fuels. Comparing the NO_x results from Concept 4 (Figure 8-30) to the results presented in Figure 8-42, one can see that substantial improvement was made at almost all load conditions. On pilot-only operation at the 70% load condition, the NO_x levels slightly exceeded the limit. With residual fuel, the goals were also met at the baseload condition, but were above the limit at peak load and at the transition point. With the SRC-II fuel with higher nitrogen content, the NO_x emission levels were significantly above the limits, owing to relatively high rates of conversion of the fuel nitrogen. The NO_x data as a function of fuel bound nitrogen are plotted in Figure 8-43. For residual fuel the yield was 80% at baseload, and for SRC-II fuel the yield was 51%. Pyridine was added to residual fuel to simulate other nitrogen levels. The increased mixing in the domes resulted in higher yields (80% compared to 52% for Concept 4). This explains the decrease in yield with SRC-II fuel.

Figure 8-42 also shows that as the fuel-bound nitrogen is increased in going from ERBS to residual to SRC-II, the NO_x curve slope increases (both stages fueled). This suggests that the conversion is lower at low loads and higher at high loads. For constant conversion, the NO_x curves with residual and SRC-II fuel should be parallel to the curve with ERBS fuel. When both stages are fueled, both stages are operating

Table 8-14
MEASURED FLOW SPLITS FOR CONCEPTS 4, 4-1

Concept 4 (Basic Series-Staged Lean/Lean)		
Pilot-Stage	Dome Swirler	10.8%
	Dome Cooling	4.4
	Dilution	7.2
	Liner Cooling	12.4
	Total Pilot Stage	34.8%
Main-Stage	Dome Swirler	32.9%
	Dome Cooling	5.9
	Liner Cooling	16.0
	Total Main Stage	54.8%
Dilution Air		10.4%
Total Combustor		100%
Concept 4-1 (Modified Series-Staged Lean/Lean)		
Pilot Swirler		14%
	Cap Impingement Cooling	5
	Pilot Dilution	4
	Cooling Louvers	14
	Total Pilot Stage	37%
Main-Stage Swirlers		32%
	Impingement Cooling	6
	Cooling Louvers	13
	Total Main Stage	51%
Dilution Air		12%
Total Combustor		100%

with lean fuel mixtures. Gerhold et al.* have shown that FBN conversion to NO_x increases with the equivalence ratio until $\phi = 0.85$, and then conversion decreases. Since the equivalence ratio in both stages increases with load, the conversion increases and the curves are therefore steeper.

The CO and UHC are plotted versus load in Figures 8-44 and 8-45. As shown in these figures, these emissions for Concept 4-1 were highest at low-load pilot-only

* Gerhold, Fenimore, and Dederick, *Two-Stage Combustion of Plain and N Doped Oil*, Reprint 8599, General Electric Company, Corporate Research and Development, Schenectady, NY.

Table 8-15
CONCEPT 4-1 TEST DATA

POINT NUMBER	READING NUMBER	HARDWARE CONFIGURATION	FUEL TYPE	FUEL % N	FUEL % N	FUEL LHV	FUEL TEMP (°F)	SIMULATED ENGINE POWER CONDITION				TIMING (°)	PMINT (PSIA)	W FUEL P (LB/HR)	W AIR P (LB/HR)	W AIR S (LB/S)	PRIMARY EQUIVALENCE RATIO	SECONDARY EQUIVALENCE RATIO	OVERALL EQUIVALENCE RATIO	PRIMARY RES. TIME (SEC.)	SECONDARY RES. TIME (SEC.)	PRIMARY REF. VELOCITY (FT/S)	SECONDARY REF. VELOCITY (FT/S)	EXIT TEMPERATURE (°F)	EXIT PRESSURE (PSIA)	
1.31	2	4-1	EBBS	12.95	.0054	18275	50	70				608	157.3	1071	6.15	0	10.48	.700	0	.259	10.5	8.4	44.4	120	1593	148.4
1.32	3	"	"	"	"	"	51					604	153.0	374	6.25	706	10.64	.241	.442	.257	10.1	8.1	45.9	124	1465	143.8
1.4	4	"	"	"	"	"	52	92				635	167.6	473	6.14	891	10.45	.310	.568	.331	10.9	8.8	42.6	115	1806	158.6
1.3	5	"	"	"	"	"	51	70				610	157.0	372	6.17	709	10.50	.242	.450	.261	10.5	8.4	44.4	120	1496	148.3
1.1	6	"	"	"	"	"	58	0				548	127.0	317	6.19	0	10.54	.206	0	.076	8.9	7.1	52.2	141	843	118.0
1.1	7	"	RESID	11.52	.23	17748	218	"				530	128.5	347	6.31	0	10.75	.215	0	.080	8.9	7.1	52.5	142	831	119.1
1.2	8	"	"	"	"	"	231	50				594	148.2	843	6.14	0	10.46	.538	0	.199	10.1	8.1	46.3	125	1382	139.6
1.31	9	"	"	"	"	"	232	70				618	157.7	1101	6.26	0	10.66	.689	0	.255	10.2	8.2	45.5	123	1602	149.0
1.3	10	"	"	"	"	"	213	"				616	158.4	362	6.14	767	10.45	.231	.477	.267	10.5	8.4	44.4	120	1574	150.0
1.4	11	"	"	"	"	"	219	92				624	166.5	469	6.11	920	10.41	.301	.574	.329	11.0	8.8	42.2	114	1832	158.9
1.40	13	"	"	"	"	"	222	"				634	166.8	219	6.13	1170	10.44	.140	.728	.328	10.9	8.8	42.6	115	1812	159.0
1.41	14	"	"	"	"	"	226	"				626	167.5	358	6.10	1035	10.39	.230	.647	.331	11.1	8.9	41.8	113	1825	159.3
1.42	15	"	"	"	"	"	219	"				628	166.5	635	6.05	754	10.31	.411	.475	.333	11.1	8.9	41.8	113	1854	158.5
1.5	16	"	"	"	"	"	220	100				638	169.9	539	6.11	967	10.40	.346	.604	.357	11.1	8.9	41.8	113	1938	162.0
1.4	17	"	"	"	.56	"	221	92				636	166.8	500	6.10	897	10.38	.321	.561	.332	10.9	8.8	42.6	115	1871	158.8
1.4	18	"	"	"	.48	"	219	"				627	166.8	501	6.06	897	10.32	.324	.565	.334	11.1	8.9	41.8	113	1852	158.8
1.4	19	"	SRC II	9.07	.87	16365	45	"				663	166.9	487	6.07	890	10.34	.293	.521	.306	11.0	8.8	42.2	114	1731	159.1
1.5	20	"	"	"	"	"	44	100				642	169.4	525	6.06	960	10.32	.316	.563	.331	11.1	8.9	41.8	113	1812	161.7
1.32	21	"	"	"	"	"	44	70				618	155.5	371	6.17	707	10.51	.219	.407	.236	10.2	8.2	45.5	123	1234	148.2

Table 8-15 (Cont'd)

CONCEPT 4-1 TEST DATA

[illegible]

Table 8-15 (Cont'd)
CONCEPT 4-1 TEST DATA

POINT NUMBER	READING NUMBER	COMBUSTOR DELTA P (PSI)	LINER TEMPERATURE (°F)	CO (PPM)	CO ₂ (PPM)	H ₂ (PPM)	NO _x (PPM)	NO _x (PPM)	% N CONVERSION	COMBUSTION EFFICIENCY (%)	SMOKE NUMBER	PATTERN FACTOR	PAWR	COMBUSTOR AIR/F (%)	FLOW FUNCTION $\frac{W}{36.1 \cdot P^{.5}}$	ATOMIZING AIR ΔP (PSIA)	TOTAL ATOMIZING AIR FLOW (LBS)	ELONG	FUEL AIR RATIO MEASURED
1.31	2	8.9	1322	69.4	36800	0	95.3	102.3	-	99.81	21.5	.49	.0174	5.66	11.9	64.8	.81	7.75	.0179
1.32	3	9.2	943	3175.1	30900	1297.3	28.4	33.5	-	91.96	6.7	.25	.0167	6.06	12.9	63.0	.78	2.40	.0178
1.4	4	9.0	1144	713.0	46000	60.2	71.2	60.2	-	99.14	1.7	.16	.0221	5.36	10.7	64.7	.83	4.53	.0228
1.3	5	8.7	967	3037.8	31500	1111.9	32.9	38.9	-	92.73	5.9	.22	.0169	5.59	12.0	65.0	.82	2.77	.018
1.1	6	9.0	761	402.5	11400	142.9	17.0	56.8	-	97.18	4.1	.44	.0057	7.14	17.4	60.0	.73	4.28	.0053
1.1	7	9.4	750	476.8	11700	108.7	30.6	106.8	43	97.19	23.7	.72	.0058	7.32	17.8	68.0	.76	7.80	.0057
1.2	8	8.6	1299	83.9	30500	10.1	114.4	153.7	60*	99.83	19.0	.45	.0142	5.77	13.2	65.8	.79	11.41	.0141
1.31	9	8.7	1428	91.6	39300	7.8	160.4	167.3	60	99.86	27.3	.49	.0183	5.55	12.4	59.3	.80	12.41	.0181
1.3	10	8.4	923	2259.3	36800	365.0	97.0	104.0	64	96.22	37.4	.24	.0183	5.32	11.6	60.9	.79	7.49	.0189
1.4	11	7.6	1025	755.0	47900	46.6	166.7	141.1	80	99.14	9.9	.24	.0226	4.55	10.7	62.1	.81	10.43	.0234
1.40	13	7.8	1186	2223.2	44000	540.5	144.6	130.2	-	96.46	55.3	.12	.0217	4.65	10.8	59.9	.80	9.42	.0233
1.41	14	8.2	1050	891.3	47900	77.7	161.0	135.7	-	96.93	12.6	.18	.0226	4.89	10.5	61.5	.79	10.04	.0225
1.42	15	8.0	1129	708.8	48400	45.0	172.5	143.6	-	99.19	7.4	.23	.0228	4.74	10.5	62.6	.80	10.61	.0236
1.5	16	7.9	1120	393.0	52600	19.4	198.3	152.6	60*	99.60	4.8	.18	.0245	4.64	10.4	57.0	.81	11.31	.0234
1.4	17	8.0	1053	669.6	48400	37.3	261.6	217.2	64	99.25	7.0	.17	.0227	4.75	10.7	59.7	.80	16.11	.0235
1.4	18	8.0	1087	697.5	48100	40.4	239.2	200.0	66	99.21	6.3	.18	.0226	4.84	10.5	61.5	.81	14.81	.0237
1.4	19	7.8	1100	1013.7	44600	70.7	265.1	274.2	51	98.68	3.7	.22	.0207	4.69	10.6	59.6	.82	19.08	.0233
1.5	20	7.7	1158	455.2	51400	22.5	310.4	275.0	42*	99.50	4.5	.20	.0235	4.54	10.3	67.0	.83	19.35	.0252
1.32	21	7.3	859	1955.8	26000	3165.9	129.1	211.4	39	86.45	37.9	.32	.0142	4.67	12.4	69.7	.83	12.88	.0179

* The Conversion for SMC II is based on the assumption that the conversion with Residual fuel is 60% at the same conditions.

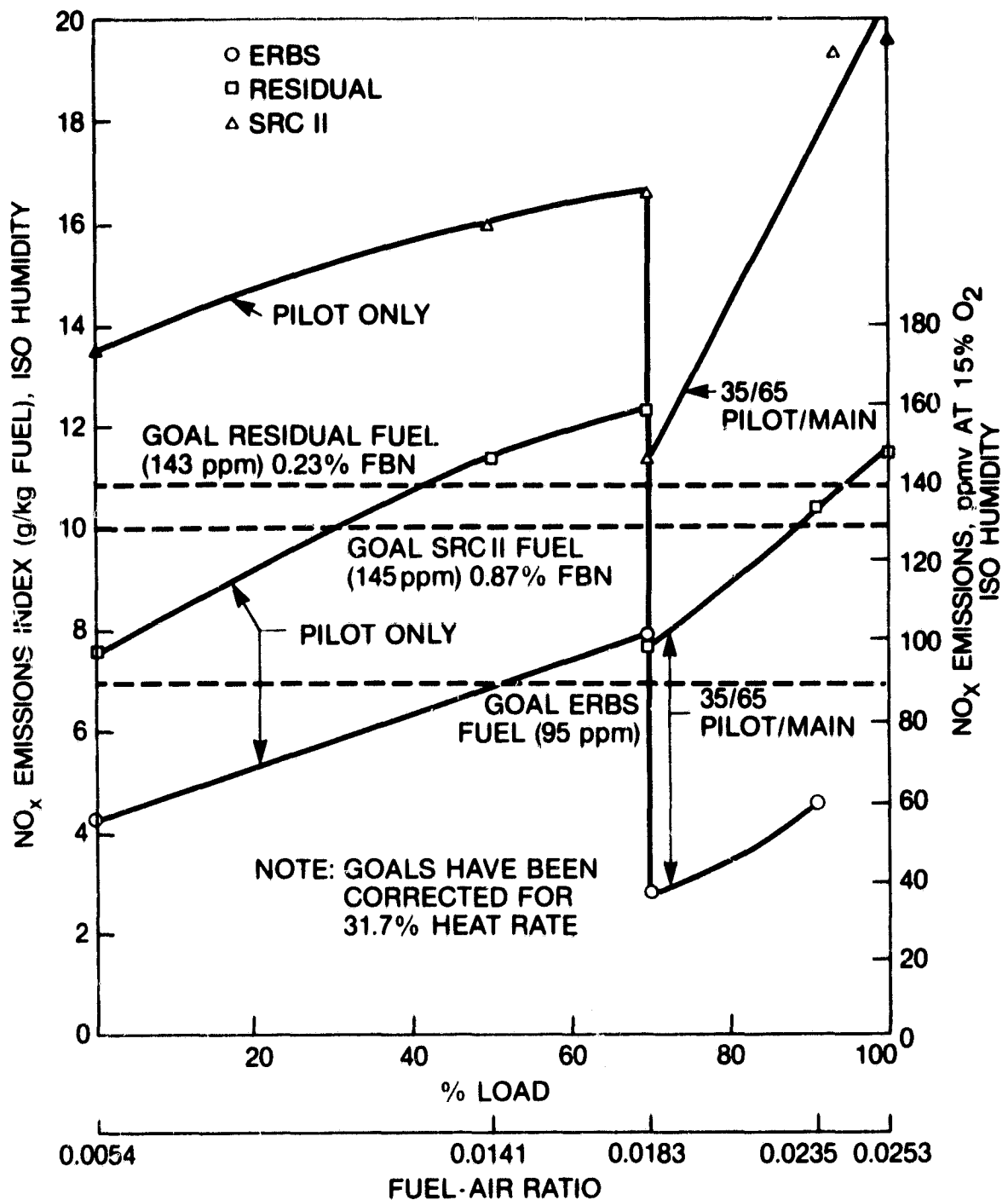


Figure 8-42. NO_x performance vs load, Concept 4-1

operation and the midload changeover to two-stage operation. Low fuel/air ratios at both these conditions provide insufficient temperature rise. Alternate methods to alleviate this problem are presented in a later section.

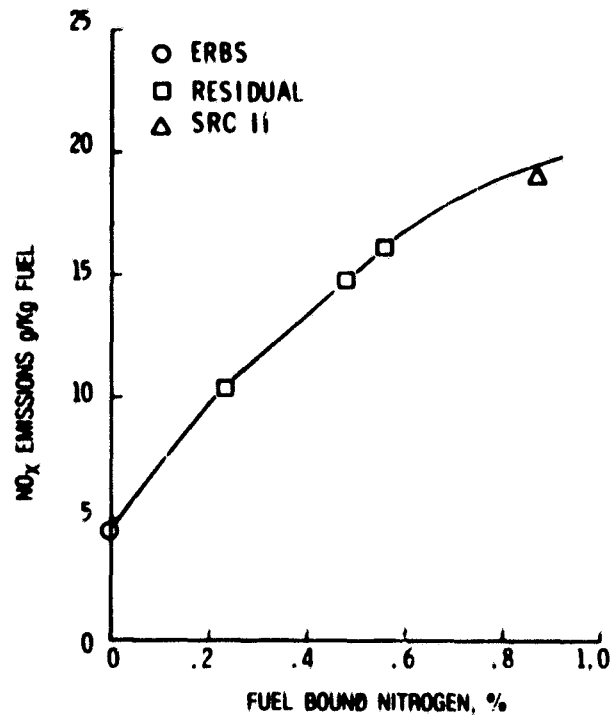


Figure 8-43. NO_x vs fuel-bound nitrogen, Concept 4-1

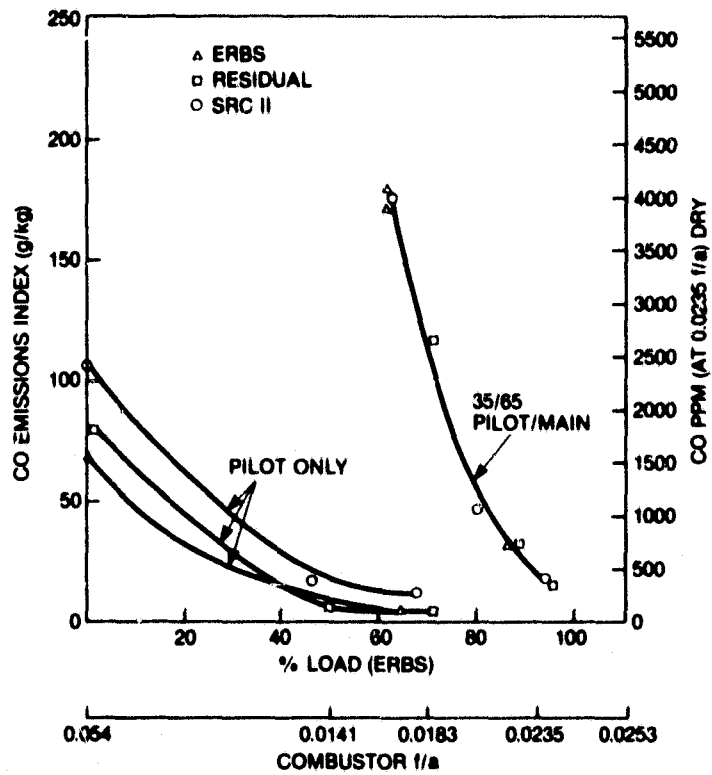


Figure 8-44. CO emissions vs load, Concept 4-1

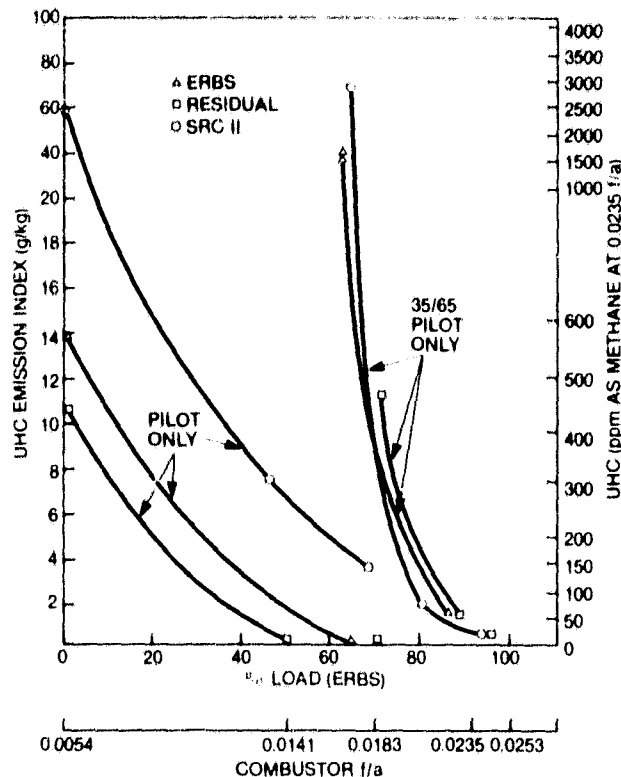


Figure 8-45. Unburned hydrocarbons vs load, Concept 4-1

Additional emissions measurements using both individual and ganged emissions probes were performed on Concept 4-1 to verify agreement between individual and ganged rake elements and to provide details of the emissions profiles across the combustor. It should also be noted that one sampling probe was moved to the combustor axial centerline location to obtain emissions samples from the core gases, which are at potentially the highest temperature (highest NO_x) region. Results of comparisons between individual and ganged elements are shown in Figure 8-46. In addition to the good agreement between the average of individual readings and ganged readings, a noteworthy point is that the maximum (center core) emissions did not deviate greatly from the radial averages. This contour is indicative of fairly uniform exhaust profiles. The temperature profiles measured at the exit also indicate this and are presented in Figure 8-47 for all three fuels. Both the pattern factor and the profile meet the goals with all three fuels.

Smoke performance of Concept 4-1 is shown in Figure 8-48. Smoke performance is well within the program goal of SAE 20 across the load range for all three fuels, except at the transfer point to dual-stage operation (70% load). Heavy fuels are particularly poor on smoke at this transfer point.

Figure 8-49 presents liner pressure drop versus flow function data for Concept 4-1. A comparison of these data to Figure 8-38 indicates the magnitude of the increase in liner pressure drop (and thus mixing) attained with Concept 4-1 by virtue of the modifications made. The pressure drop at baseload conditions increased to about 5.5% from 4.5%.

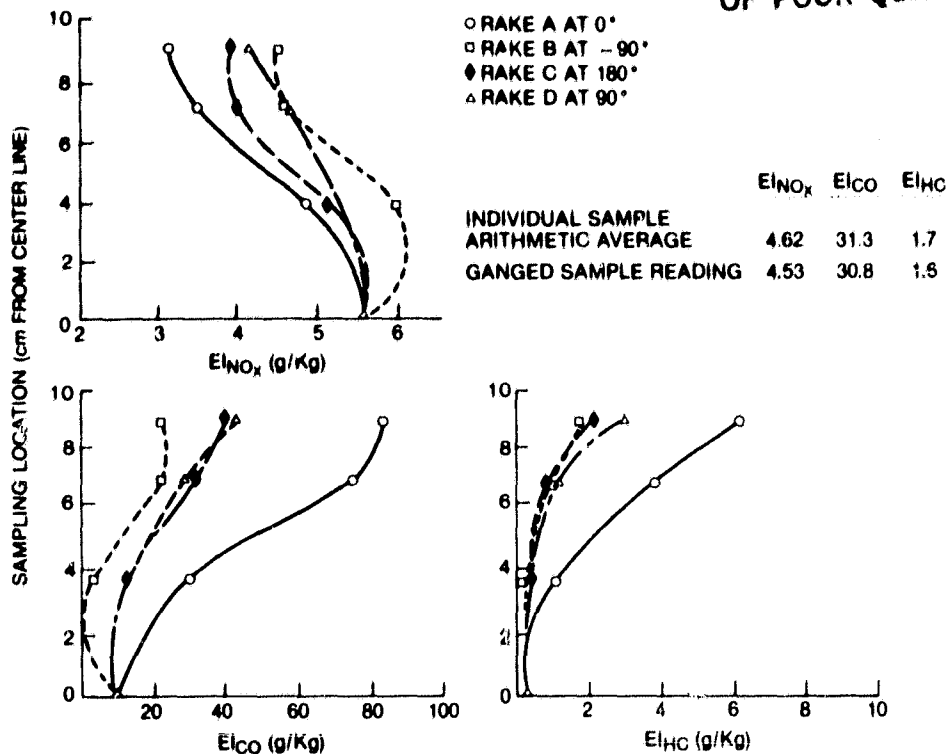


Figure 8-46. Individual vs ganged sample data, Concept 4-1—ERBS fuel at 9.2 percent

The liner temperatures were also well below the metal limit (Figure 8-50). These temperature measurements were made with the cooling flow reduced to 27% of the combustor airflow.

Carbon deposits presented no problem with this combustor design. There were some very light deposits in both the pilot- and main-stage swirlers and on the dome of the main stage; see Figure 8-51. These deposits are believed to have reached a stabilized thickness as the combustor accumulated approximately 16 test hours, with 7 on the residual fuel during the last test run.

Combustion efficiencies were greater than 99% at most conditions with all three fuels except at full-speed no load, where the efficiency was 97%, and at the pilot/main stage crossover point, where the efficiency was 92% after transfer to the main stage.

It appears that this combustor concept has the potential for meeting all program goals with ERBS and possibly a residual fuel with less than 0.25 weight percent fuel nitrogen. In fact, with fuels with low nitrogen content (i.e., ERBS), this concept would meet the NO_x emission level with considerable margin. The two minor deficiencies observed, smoke at high pilot fuel/air ratios and low efficiency at lean operating conditions could most likely be overcome with some development including flow split adjustments, additional swirl cup changes, and possibly additional pressure drop. All other performance parameters including pattern factors, liner temperature, and carbon deposits were met on the initial testing. This combustor concept does not appear to have the potential for meeting NO_x emission goals with fuels with nitrogen contents much in excess of 0.25%.

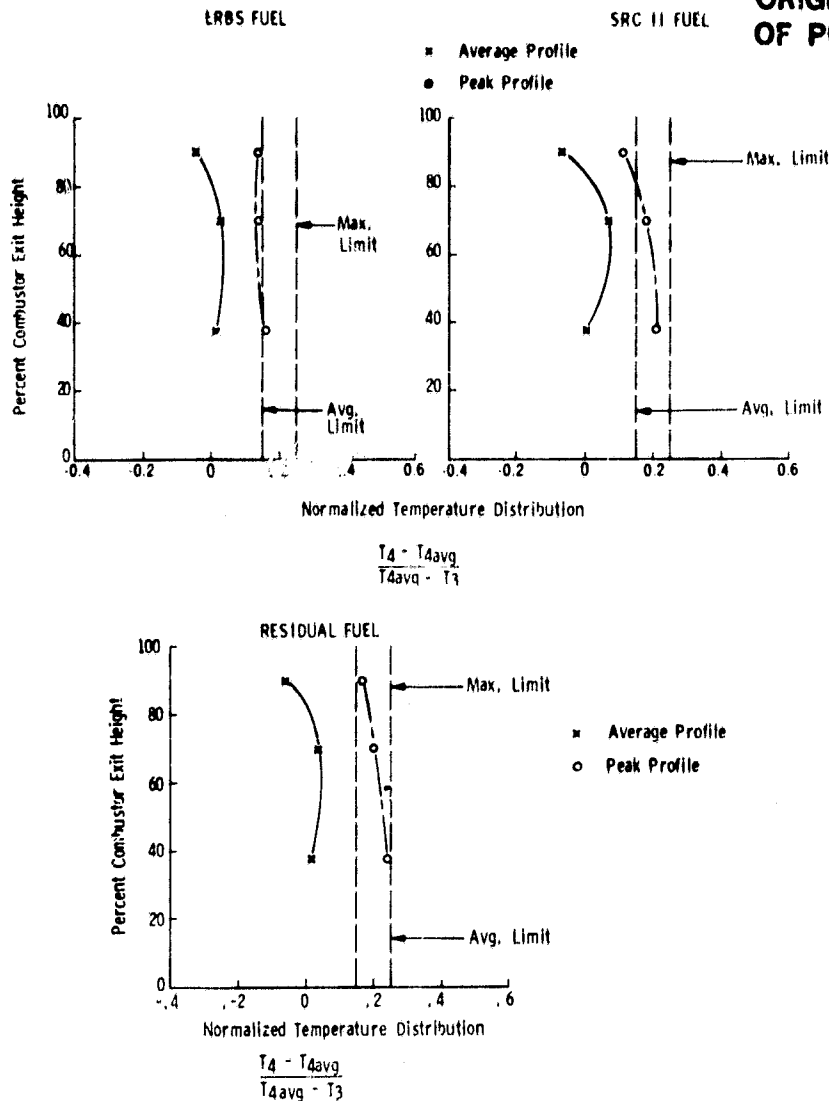


Figure 8-47. Exit temperature distribution at baseload, Concept 4-1

8.2.2 Series-Staged Lean/Low Combustor with Premixed Main Stage, Concept 5

The series-staged lean/lean design with a premix tube was tested with ERBS distillate and coal-derived SRC-II fuels. The combustor liner met the program clean-fuel NO_x emission goal over most of the load range. It only exceeded the goals at 70% pilot-only operation. When burning SRC-II fuel, the conversion of fuel-bound nitrogen into NO_x increased the emissions above goals. High CO and UHC were, however, a major problem.

Table 8-16 presents the data measured for this design with ERBS distillate and SRC-II fuel. During these tests, blends of ERBS and SRC-II were also tested. The NO_x data are shown in Figure 8-52. The combustion efficiency is also noted for each point. At full-speed no load condition, the low combustion efficiency (high CO and UHC) was probably due to flame quenching by the air from the premix tube. A

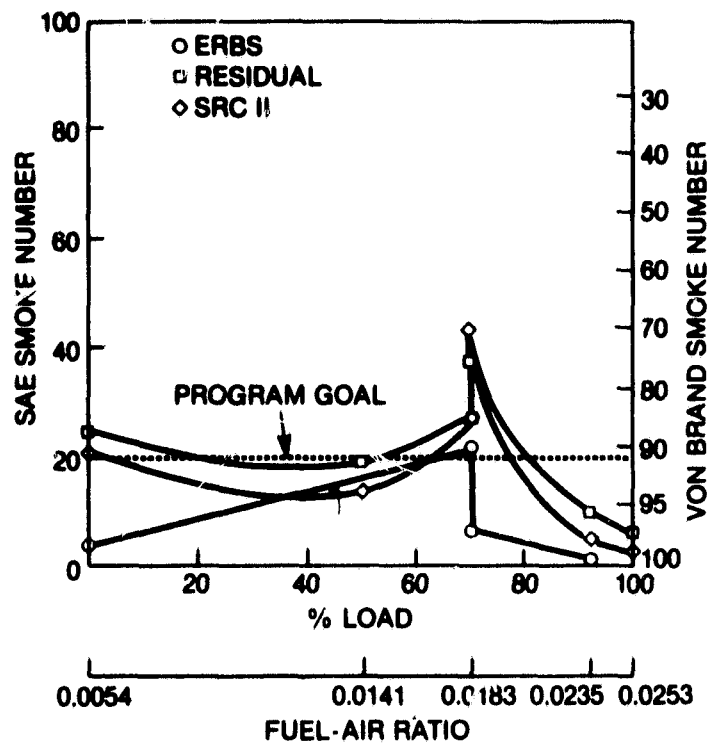


Figure 8-48. Smoke data, Concept 4-1

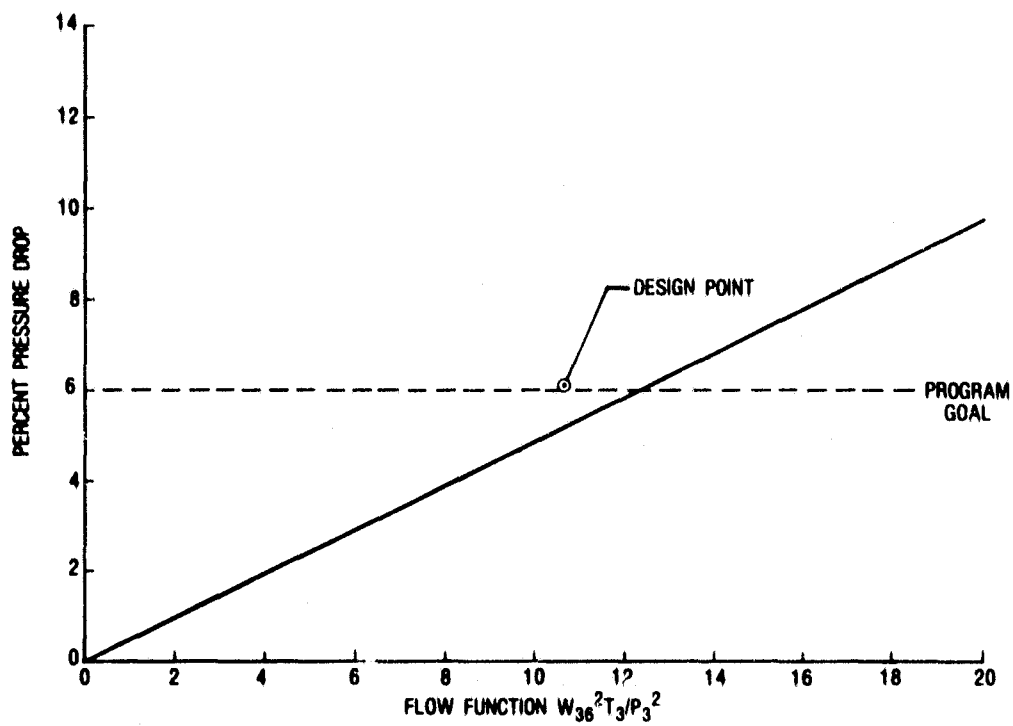


Figure 8-49. Liner pressure drop, Concept 4-1

ORIGINAL PAGE
BLACK AND WHITE PHOTOGRAPH

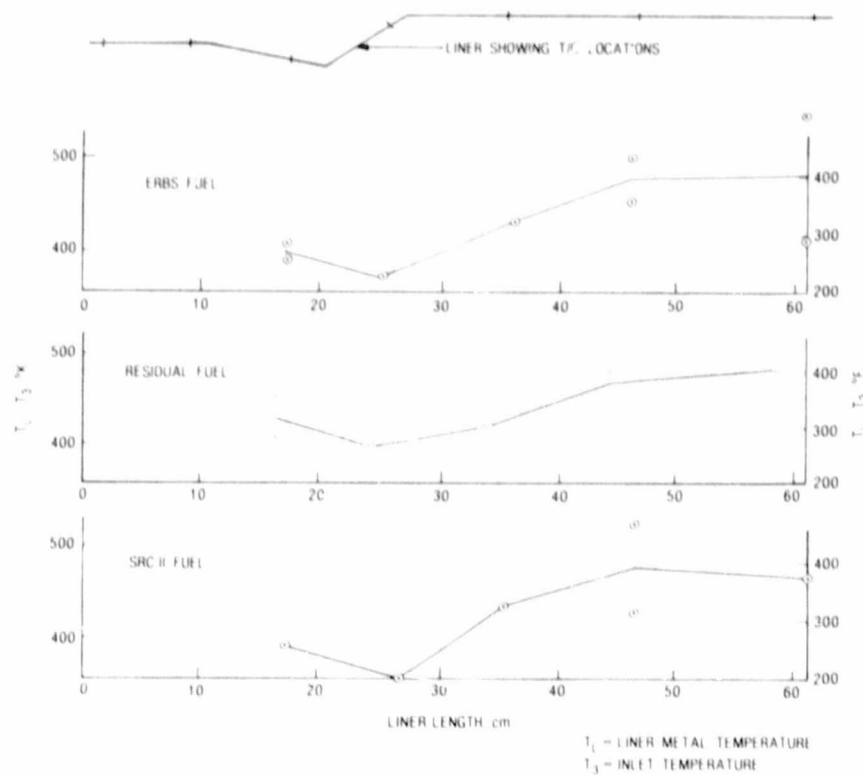


Figure 8-50. Liner temperature distributions, Concept 4-1 at baseload

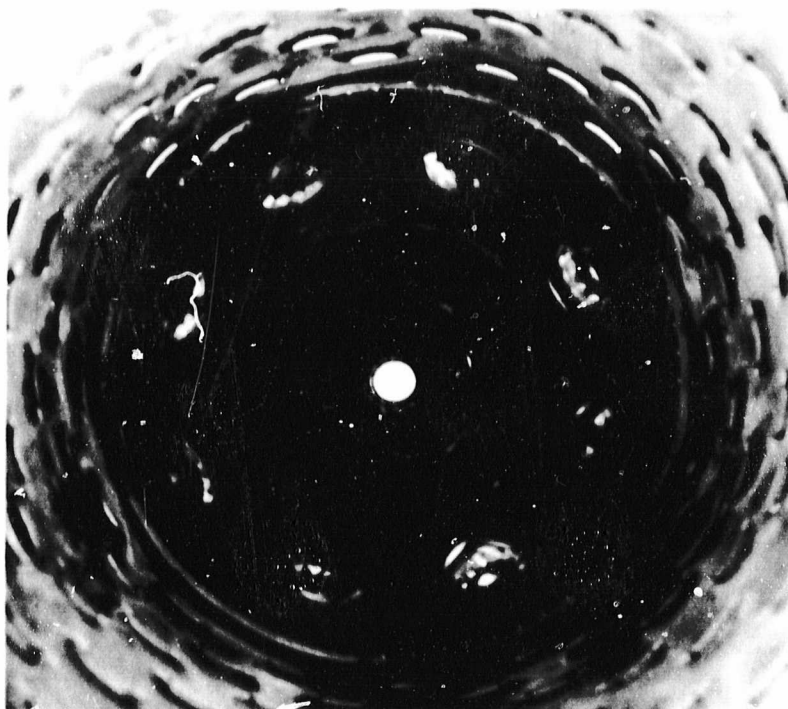


Figure 8-51. Posttest view of pilot dome, Concept 4-1

Table 8-16
CONCEPT 5 TEST RESULTS

POINT NUMBER	READING NUMBER	HARDWARE CONFIGURATION	FUEL TYPE	FUEL % H	FUEL % H	FUEL LHV	FUEL TEMP (°F)	SIMULATED ENGINE POWER CONDITION			TIME (°F)	INLET (PSIA)	W FUEL P (LB/HR)	W AIR P (LB/HR)	W FUEL S (LB/HR)	W AIR S (LB/HR)	PRIMARY EQUIVALENCE RATIO	SECONDARY EQUIVALENCE RATIO	OVERALL EQUIVALENCE RATIO	PRIMARY RES. TIME (SEC.)	SECONDARY RES. TIME (SEC.)	PRIMARY RES. VELOCITY (FT/SEC)	SECONDARY RES. VELOCITY (FT/SEC)	VELOCITY (FT/SEC)	KEET TEMPERATURE (°F)	KEET MEASURE (PSIA)
11	1	5	ERBS	12.95	.0054	18275	78	0			523	128.2	329	5.74	0	11.44	.231	.00	.077	8.0	3.1	46.6	140	767	114.4	
12	2	5	"	"	"	"	77	50			578	149.5	849	5.56	0	11.09	.614	.00	.205	9.1	3.6	40.9	123	1421	135.0	
131	3	5	"	"	"	"	78	70			618	156.5	1095	5.52	0	11.00	.798	.00	.266	9.2	3.6	40.2	121	1644	148.8	
13	4	5	"	"	"	"	78	70			615	156.7	380	5.71	683	11.39	.268	.368	.250	8.9	3.5	41.5	124	1227	149.4	
14	5	5	"	"	"	"	83	92			631	166.8	492	5.47	878	10.92	.361	.493	.336	9.7	3.8	38.1	114	1802	159.5	
141	6	5	"	"	"	"	86	92			633	165.7	359	5.39	1004	10.74	.268	.574	.340	9.9	3.9	37.7	113	1692	159.4	
142	7	5	"	"	"	"	85	92			635	165.0	615	5.40	736	10.76	.458	.420	.336	9.8	3.9	38.0	114	1791	158.7	
143	8	5	"	"	"	"	86	92			633	167.8	659	5.61	663	11.19	.494	.364	.324	9.6	3.8	38.7	116	1760	160.8	
146	10	5	"	"	"	"	87	100			634	165.1	617	5.39	874	10.75	.460	.499	.371	9.8	3.9	37.9	113	1898	158.8	
147	11	5	"	"	"	"	92	70			634	167.3	623	5.45	487	10.88	.460	.275	.273	9.8	3.9	37.8	113	1544	160.9	
14	12	5	"	"	.2357	"	97	92			643	167.9	619	5.51	722	10.98	.452	.403	.327	9.7	3.8	38.4	115	1772	161.2	
14	13	5	"	"	.8158	"	95	92			638	167.2	647	5.31	742	10.98	.472	.415	.339	9.7	3.8	38.3	115	1783	160.6	
15	14	5	"	"	.0054	"	97	100			639	167.7	703	5.51	732	11.00	.513	.409	.349	9.7	3.8	38.3	115	1783	161.5	
14	15	5	ERBS	10.92	.457	17278	89	100			637	167.4	747	5.52	868	11.01	.518	.461	.374	9.7	3.8	38.4	115	1847	160.6	
14	16	5	ERBS /SNC	10.12	.637	16883	50	100			637	167.3	749	5.54	880	11.04	.507	.457	.369	9.7	3.8	38.4	115	1867	160.6	
14	17	5	SNC II	9.07	.87	16365	87	92			642	166.7	677	5.55	829	11.06	.446	.419	.331	9.6	3.8	38.9	116	1701	160.2	

8-69

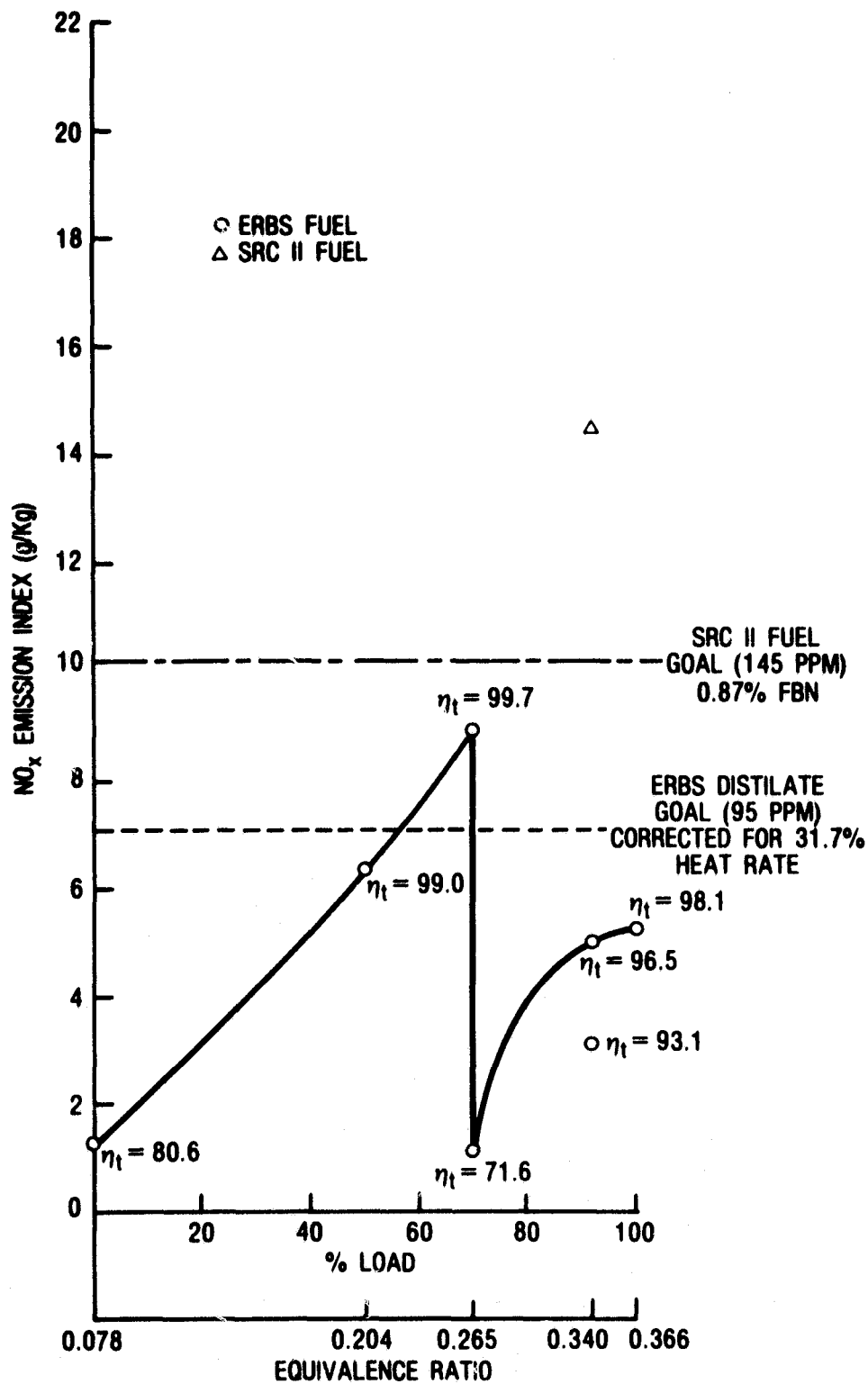


Figure 8-52. NO_x performance vs load, Concept 5

ORIGINAL PAGE
BLACK AND WHITE PHOTOGRAPH

longer pilot stage should eliminate this problem. High NO_x at the 70% pilot-only point (before transition to dual-stage operation) can be reduced by enhancing fuel/air mixing through increase in pressure drop and through airflow adjustment.

One of the problems associated with this design was discussed earlier in Section 7.2.2, i.e., the durability of the premix duct-exit nosepiece. When the main stage was fueled, combustor liner pressure drop decreased by 12% (5.2% to 4.6%). It is believed that the nosepiece was overtemperated at that time. Posttest inspection revealed gutters missing from the nosepiece; see Figure 8-53. When the nosepiece gutters burned away, airflow increased in the premix tube. This caused low efficiencies when both stages were fueled. By increasing the fuel flow in the pilot stage, therefore causing a hotter pilot flame, the combustion efficiency was increased. Figure 8-54 presents the NO_x and combustion efficiency as a function of pilot-to-main fuel split. The richer flame increased the NO_x as expected.

This series-staged design was tested with ERBS doped with pyridine and also with blends of ERBS and SRC-II. The NO_x data, at baseload condition, versus fuel-bound nitrogen are shown in Figure 8-55. The conversion rates for FBN ranged from 32% to 45%. These rates are lower than typical lean/lean designs. Since the pilot stage is operating with a fuel-rich mixture, the conversion is low in that stage. The NO_x levels with the blends of SRC-II and ERBS form a single curve with the NO_x levels from ERBS doped with pyridine, confirming the suitability of pyridine doping as a substitute for SRC-II in testing for NO_x emissions. These data also suggests that hydrogen content had little effect on NO_x formation.

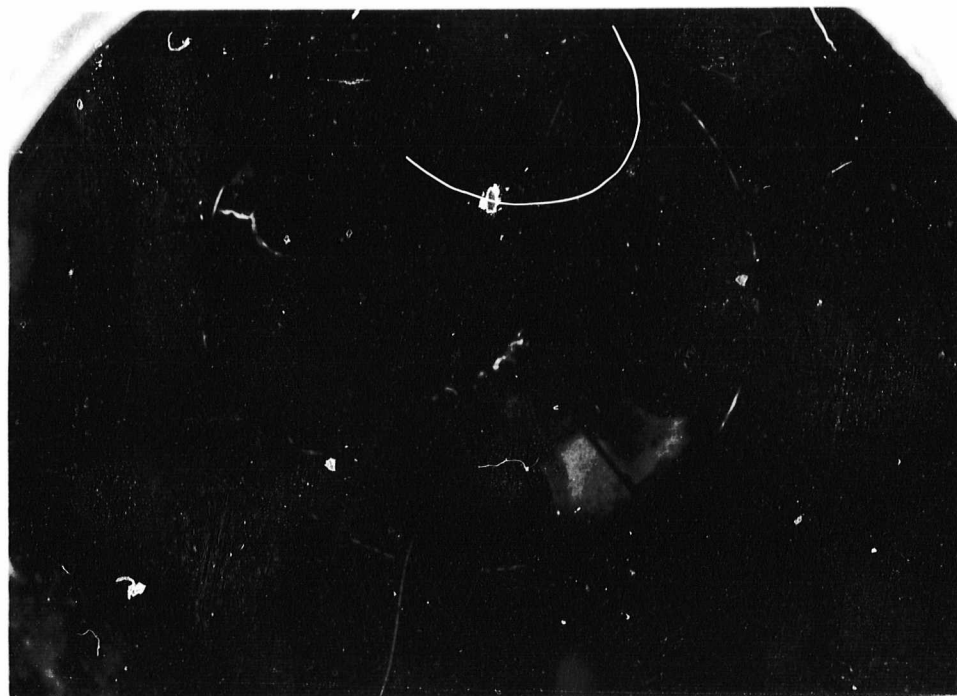


Figure 8-53. Posttest inside view (aft looking forward), Concept 5

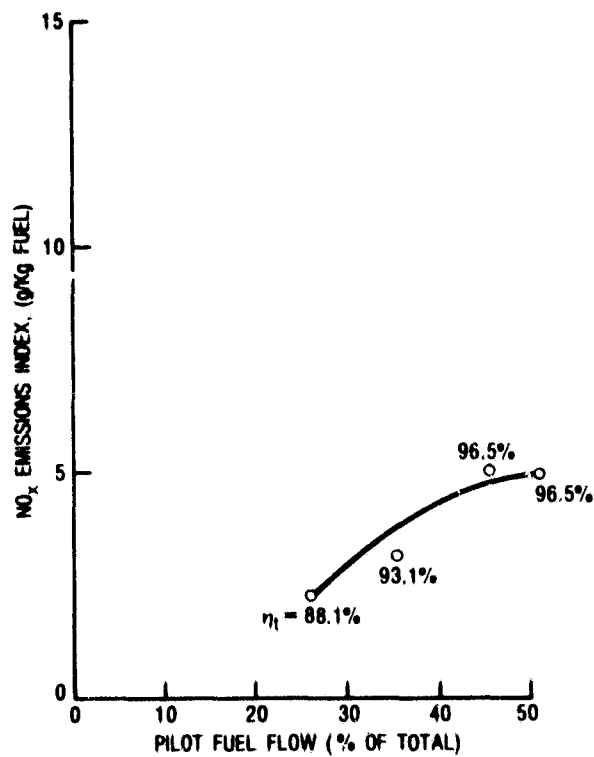


Figure 8-54. NO_x vs pilot fuel flow with ERES fuel at baseload, Concept 5

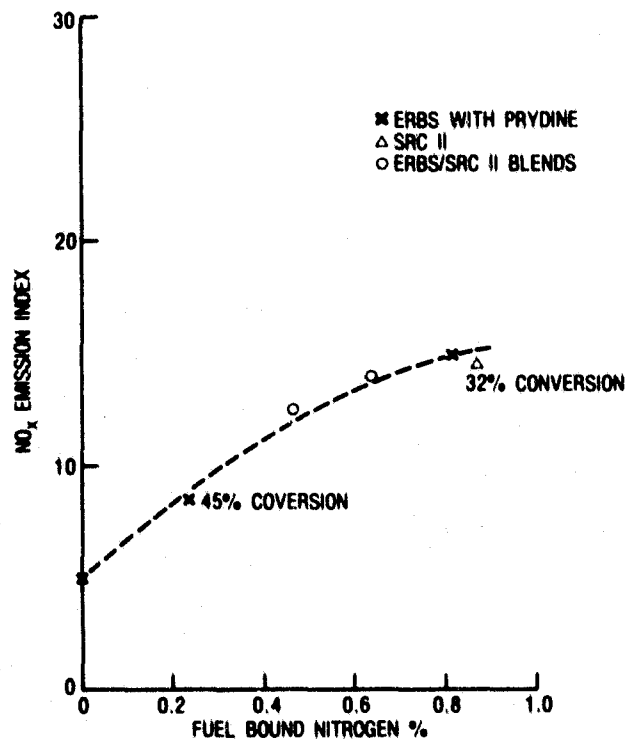


Figure 8-55. NO_x vs fuel-bound nitrogen, Concept 5

The smoke data are presented in Figure 8-56. The smoke is very high and is generated in the fuel-rich pilot stage. The pressure drop as a function of flow function is shown in Figure 8-57. At baseload conditions, the combustor liner overall pressure drop is lower than the design limit. Therefore, this margin can be utilized in enhancing fuel/air mixing in the pilot stage and should result in reduced smoke. The exit temperature profile is shown in Figure 8-58. Since the nosepiece gutter was missing, the combustion gases concentrated toward the middle and caused center-peaked profiles.

This combustor liner also has potential for meeting ultralow NO_x emissions goals with high combustion efficiency. Both increased pressure drop and improved premix duct exit piece should produce low NO_x , high combustion efficiency, and low smoke. With development, this design should also meet NO_x goals with fuels with up to 0.25% fuel bound nitrogen by weight. With reduced NO_x , the conversion of FBN will likely increase. However, combustion efficiency at FSNL can also be increased by increasing the pilot-stage length and by adjusting the flow splits.

8.2.3 Parallel-Staged Lean/Lean Combustor, Concept 6

Combustor Concept 6 was tested primarily on residual fuel, with baseload data points also taken for both ERBS and SRC-II fuels. The emissions were similar to those measured for Concept 4. Several test points were run with pyridine added to the fuels. The data from this design are presented in Table 8-17.

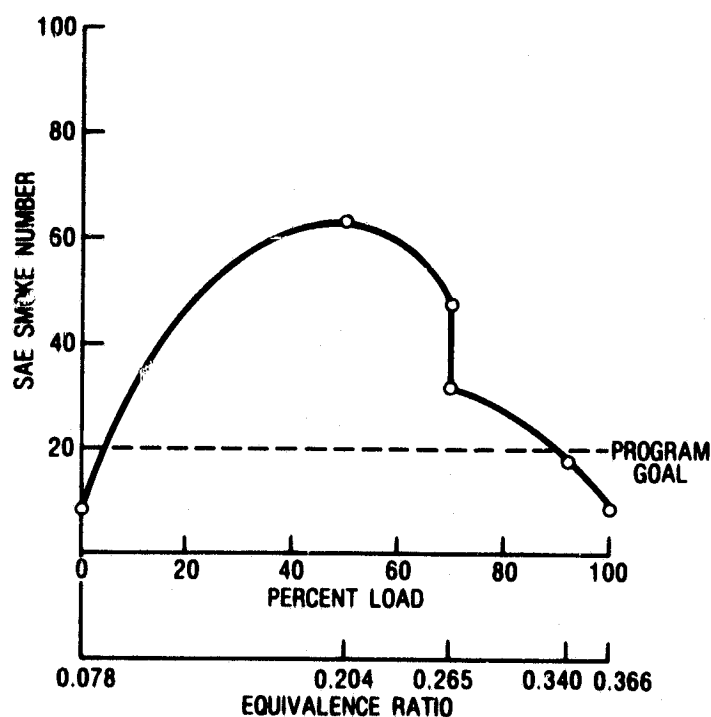


Figure 8-56. Smoke performance with ERBS fuel, Concept 5

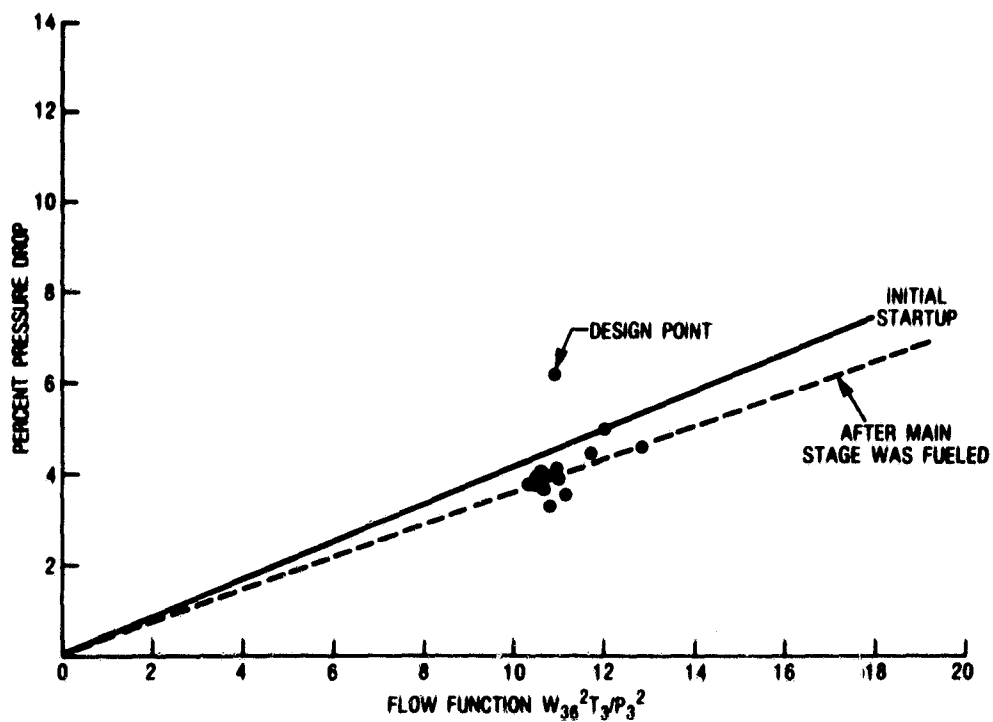


Figure 8-57. Liner pressure drop, Concept 5

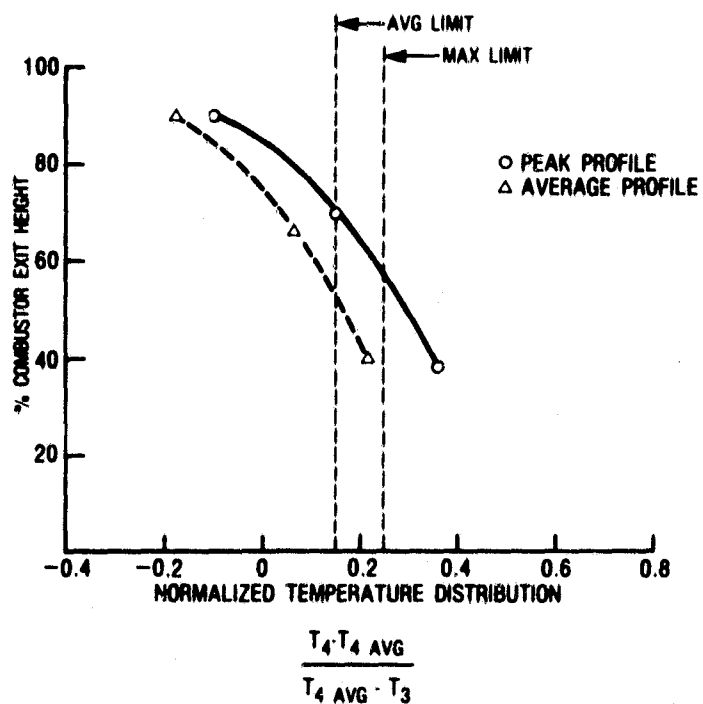


Figure 8-58. Exit temperature distribution with ERBS fuel at baseload, Concept 5

8-75

Table 8-17 (Cont'd)

POINT NUMBER	READING NUMBER	COMBUSTION GASES (°F)	LINEAR TEMPERATURE (°F)	CO (PPM)	CO ₂ (PPM)	HC (PPM)	NO _x (PPM)	NO _x (PPM)	% N CONVERSION	COMBUSTION EFFICIENCY (%)	SMOKE NUMBER	PATTERN FACTOR	FAIR				COMBUSTION A/R/P (%)	FLOW FUNCTION $\frac{W}{36.1/P_2}$	ATOMIZING AIR ΔP (PSIA)	TOTAL ATOMIZING AIR FLOW (LB/H)	ELIMOX	FUEL AIR RATIO RETURNED
1.41	2	6.7	1330	281.9	45700	46.5	111.5	96.6	-	99.80	1.6	.25	.0216				4.0	11.4	13.7	.36	7.32	.0220
1.4	3	6.5	1271	308.1	45400	31.8	120.8	104.9	-	99.80	3.9	.12	.0214				3.9	10.7	12.4	.35	7.98	.0232
1.40	4	6.5	1493	341.1	49200	54.3	140.1	112.5	-	99.56	5.8	.31	.0232				3.9	10.6	10.8	.32	8.30	.0235
1.4	6	6.4	1245	384.1	47700	37.2	135.2	128.7	14.0	99.54	13.1	.14	.0225				3.8	10.6	11.0	.35	9.71	.0235
1.4	7	6.5	1305	373.7	48500	31.8	232.4	204.9	23.1	99.57	9.0	.13	.0229				3.9	10.6	10.2	.32	15.52	.0236
1.1	8	7.8	949	346.5	11500	54.3	37.7	135.9	-	98.10	22.1	1.08	.0056				6.0	17.5	12.0	.31	9.72	.0080
1.2	9	7.0	1701	139.5	26500	7.0	114.3	177.6	-	99.71	23.6	1.13	.0124				4.7	13.4	9.8	.32	13.11	.0140
1.3	10	6.7	1112	984.1	37400	142.0	122.9	133.2	-	98.36	32.1	.14	.0179				4.2	11.7	13.0	.32	9.75	.0192
1.4	11	6.3	1276	474.4	47800	45.8	172.9	147.6	40.0	99.42	10.4	.13	.0224				3.8	10.4	12.0	.35	10.93	.0242
1.4	12	6.2	1247	496.0	46800	36.5	182.7	158.6	22.4	99.40	19.0	.15	.0219				3.8	10.6	13.4	.36	11.78	.0235
1.4	14	6.2	1318	487.4	45200	31.0	254.4	229.2	44.0	99.40	11.8	.13	.0212				3.7	10.5	10.7	.33	16.98	.0232
1.45	15	6.0	1670	762.6	42700	87.7	111.5	106.0	-	98.93	24.6	.16	.0202				3.6	10.6	11.4	.35	7.82	.0230
1.46	16	6.0	1466	1268.5	34400	232.0	107.2	125.0	-	97.59	41.1	.32	.0167				3.6	10.9	12.2	.36	9.12	.0181
1.47	17	6.5	1722	117.7	61100	7.8	254.1	170.4	-	99.84	17.1	.13	.0282				3.9	10.4	10.7	.35	12.66	.0290
1.4	18	5.8	1580	472.8	49500	34.9	223.0	199.3	20.0	99.40	24.6	.09	.0226				5.5	10.6	12.5	.35	13.98	.0243

Figure 8-59 presents the NO_x emissions levels obtained with ERBS and residual fuels. The NO_x emissions levels were close to the program goals at baseload conditions with ERBS fuel (exceeded goal by 12%) and residual fuel (exceeded goal by 2%). However, they were considerably above the goals with SRC-II fuel (37% above goal). Comparing these data with those obtained with Concept 4 (refer to Figure 8-30), the NO_x levels with both fuels were essentially the same with both designs. Combustor liner pressure drop, shown in Figure 8-60, was similar to Concept 4 pressure drop. Good mixing of the fuel and air is very important to avoid local rich regions. Therefore, it is likely that this combustor concept would respond to pressure drop increases and swirl cup improvements as did series-staged combustor Concept 4 (both designs had similar pilot dome design). Therefore, this Concept should also have the potential for very low NO_x levels with fuels having moderate levels of fuel-bound nitrogen.

Figure 8-61 presents the CO and unburned hydrocarbon (UHC) emissions indices versus machine load. As shown, the CO was high across the entire load range tested, and the unburned hydrocarbons were also high, except for the 50% load point. Additional residence time in the secondary zone would improve the combustible emissions, and additional secondary zone length would be available for an MS7001 combustor based on this design. The combustion efficiencies were, however, above the goals at most loads.

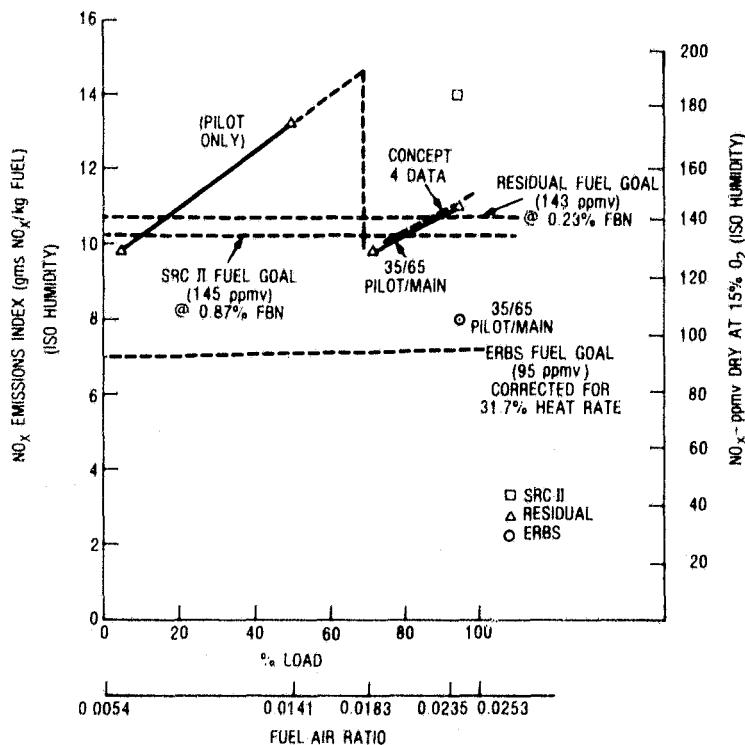


Figure 8-59. NO_x performance, Concept 6

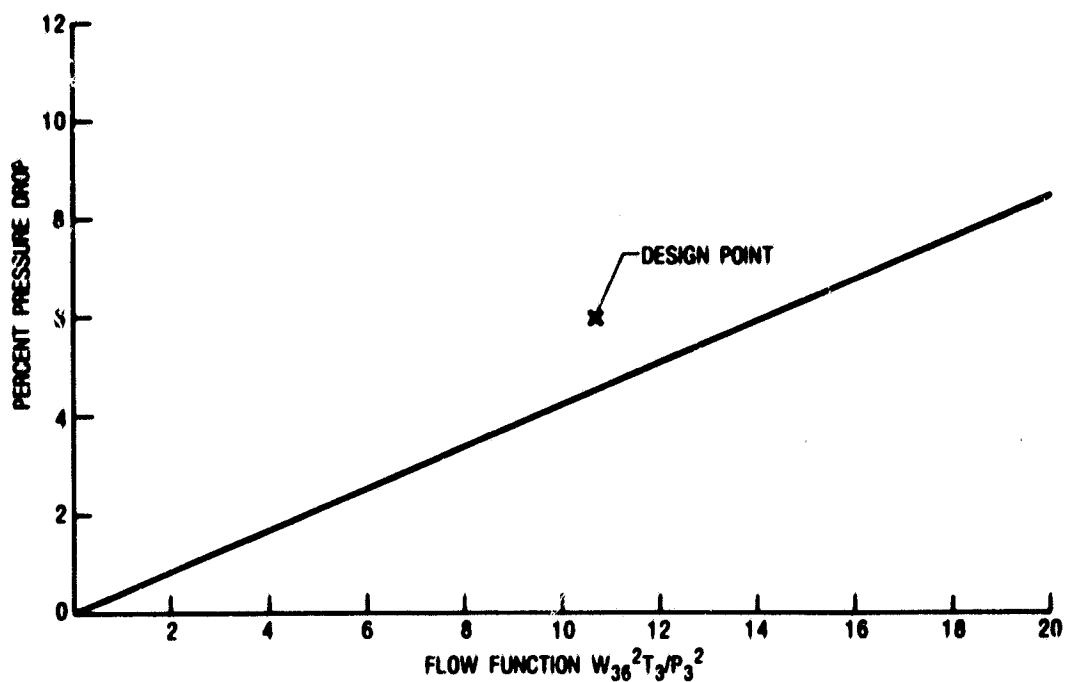


Figure 8-60. Combustor liner pressure drop, Concept 6

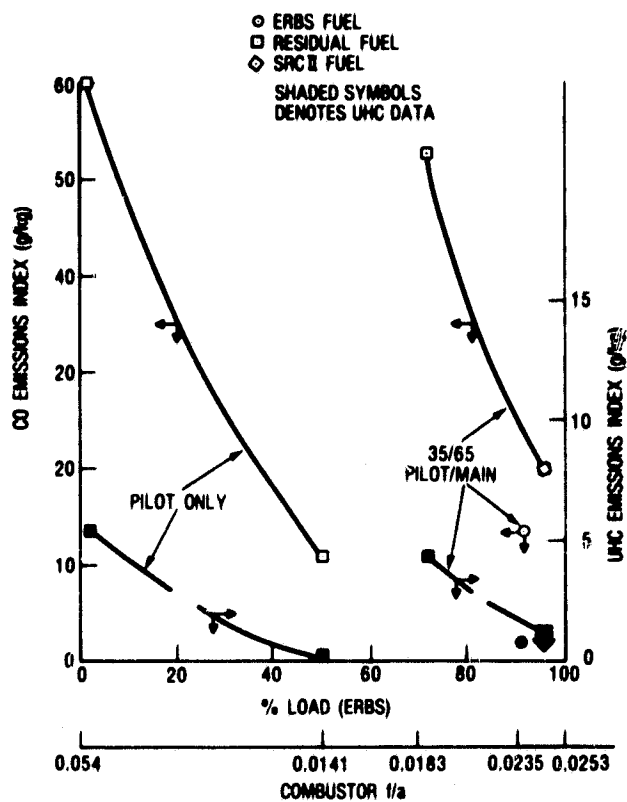


Figure 8-61. CO and UHC emissions, Concept 6

It may be noted that the NO_x emissions for Concept 6 were lower at 4.5% pressure drop than for Concept 4 at 5.5% pressure drop with SRC-II fuel. This NO_x level represents an unexpectedly low level of conversion of fuel-bound nitrogen for a lean-burning combustor. NO_x levels were also low with ERBS fuel doped with pyridine to 1% fuel nitrogen as shown in Figure 8-62. Conversion rates were also low with residual fuel doped with pyridine. The conversion rates varied from 36% at low FBN to about 22% at high FBN. The low fuel-bound conversion rates may be explained by incomplete mixing. It was noted in Concept 4 that when mixing was improved, the conversion rates increased. It is expected that when improvements are made to reduce NO_x with ERBS fuel, this advantage will be lost, and this concept should also behave like a typical lean/lean. Conversion rates for Concept 6 are discussed, along with other combustors tested, in Section 8.3.

Figure 8-63 presents smoke data for Concept 6. At baseload conditions, smoke level was very low even with the residual fuel. (Although smoke data were not taken at the transition point (pilot only), it is suspected that the smoke level would be above the program limits, and that some development would be required.

The peak liner temperatures for Concept 6 were approximately 700 K above the inlet temperature (see Figures 8-64 and 8-65). The maximum measured temperatures were located in the main-stage liner wall. The increase in liner temperature relative to Concept 4 is attributed to the more confined main-stage dome and consequent close proximity of the combustion process to the liner walls; see Figure 8-66. The liner temperature levels do not present a significant problem. However, additional cooling would be required for high pressure ratio engines or regenerative systems with combustor inlet temperatures in excess of 700 K.

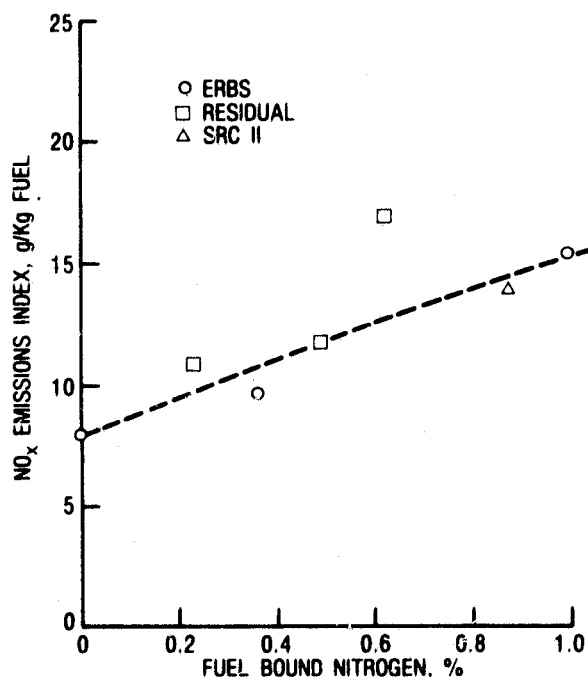


Figure 8-62. Effect of FBN on NO_x Concept 6

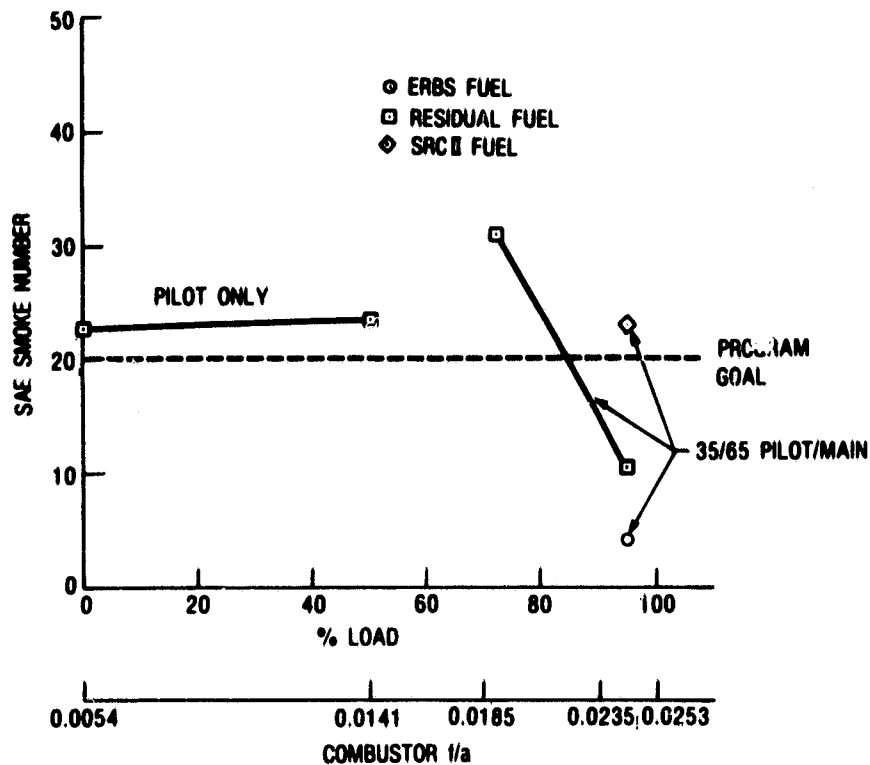


Figure 8-63. Smoke emissions, Concept 6

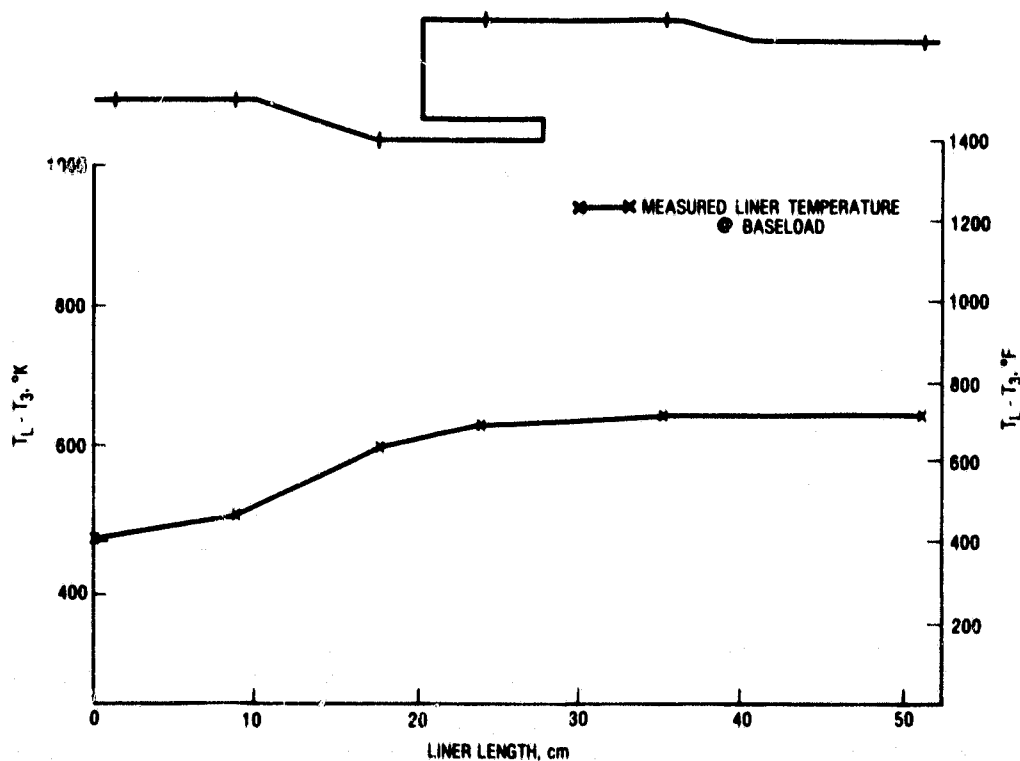


Figure 8-64. Liner metal temperatures, Concept 6—ERBS fuel

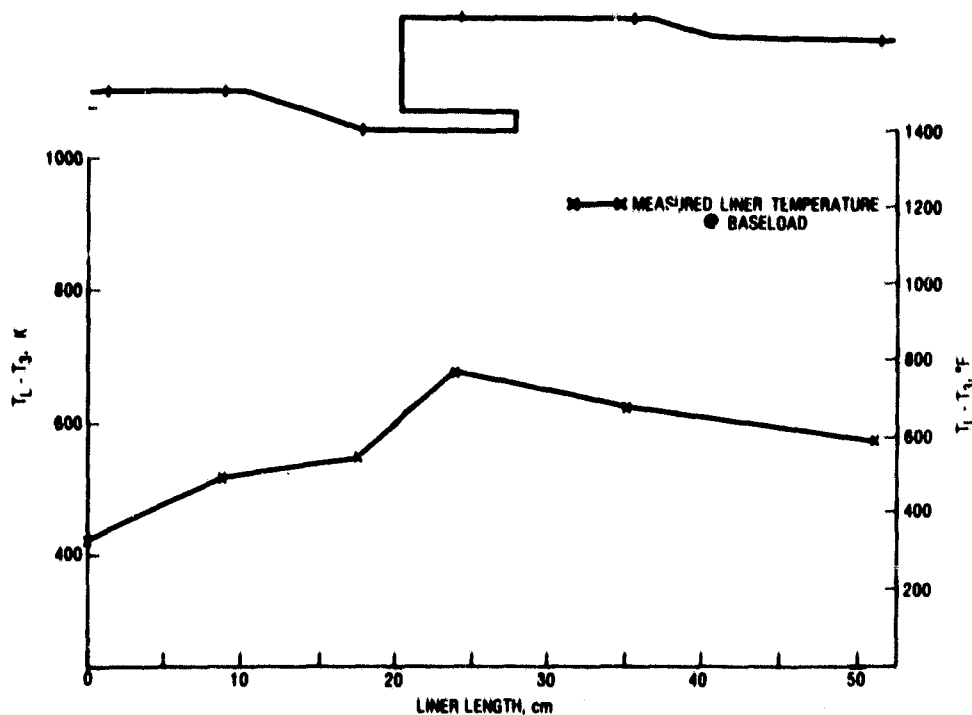


Figure 8-65. Liner metal temperatures, Concept 6—residual fuel

The measured pattern factor and temperature profiles were excellent for this configuration. As shown in Figure 8-67, the pattern factor was less than the goal of 0.25 with all fuels tested. Carbon deposits, as shown in Figure 8-68, were very light and occurred only in the swirl-cup region. Testing duration was approximately 20 h with 10 h of these conducted with residual fuel. Thus the carbon deposits had probably reached a stabilized thickness. Slight modification may be required in the swirl cup to eliminate the deposits.

Some parametric tests were also conducted with this design. These data were used in correlating the NO_x emissions with the inlet parameters. This analysis is presented later in this report.

This design also has high potential for meeting ultralow NO_x levels with clean fuels and also has potential for meeting NO_x goals with fuels with moderate fuel-bound nitrogen (<0.25%). Smoke and combustion efficiency goals can also be met with some modification. Increasing the pressure drop should solve most of these problems.

8.3 NO_x YIELD FROM FUEL NITROGEN

The residual oil and SRC-II fuels contain organically bound nitrogen at levels of 0.23 and 0.87 weight percent, respectively. The characteristic defining this species is a single nitrogen atom chemically bound to the carbon and hydrogen in the fuel. This

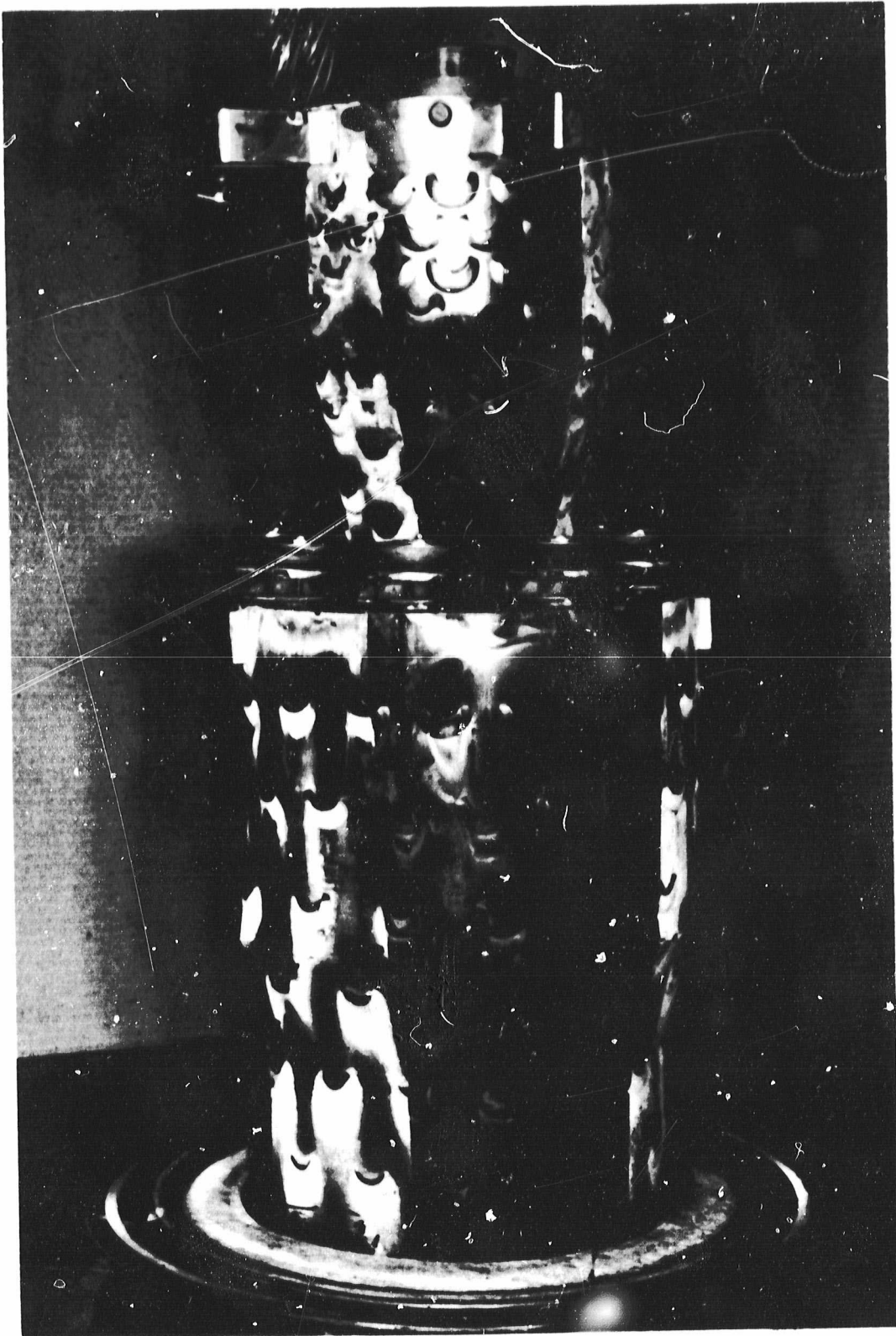


Figure 8-66. Posttest view, Concept 6

ORIGINAL PAGE
BLACK AND WHITE PHOTOGRAPH

ORIGINAL PAGE
BLACK AND WHITE PHOTOGRAPH

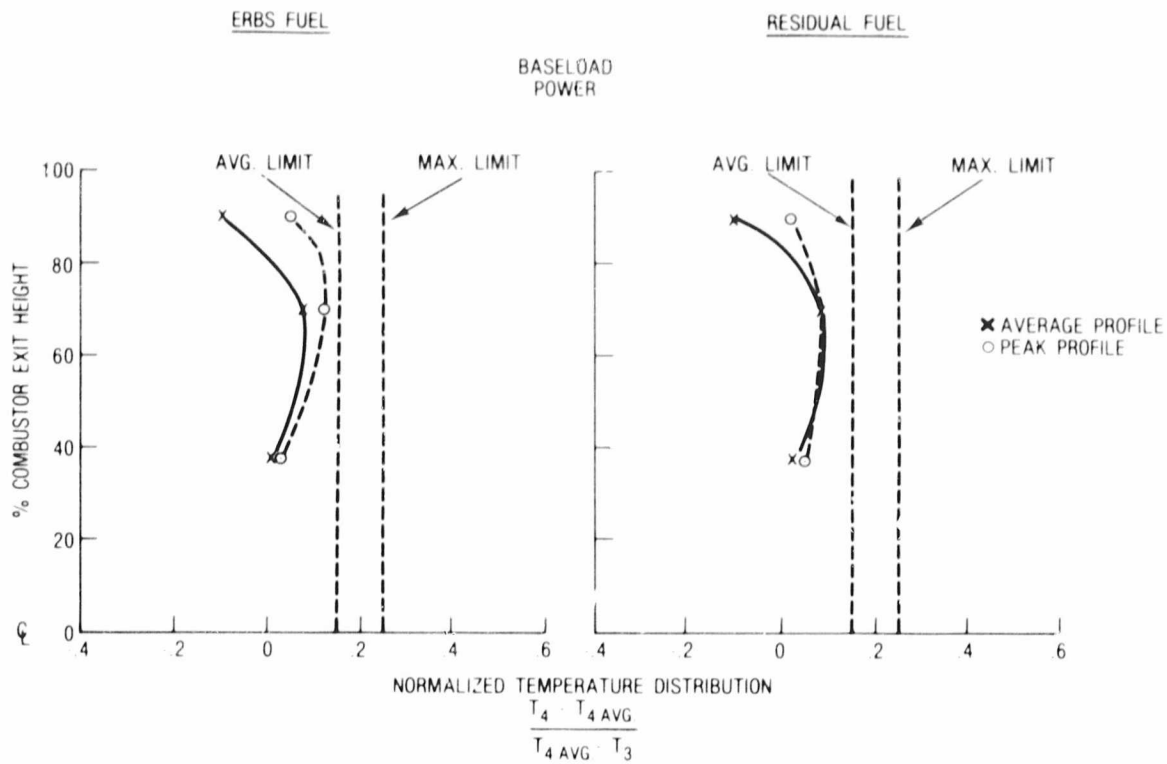


Figure 8-67. Exit temperature distributions, Concept 6 at baseload

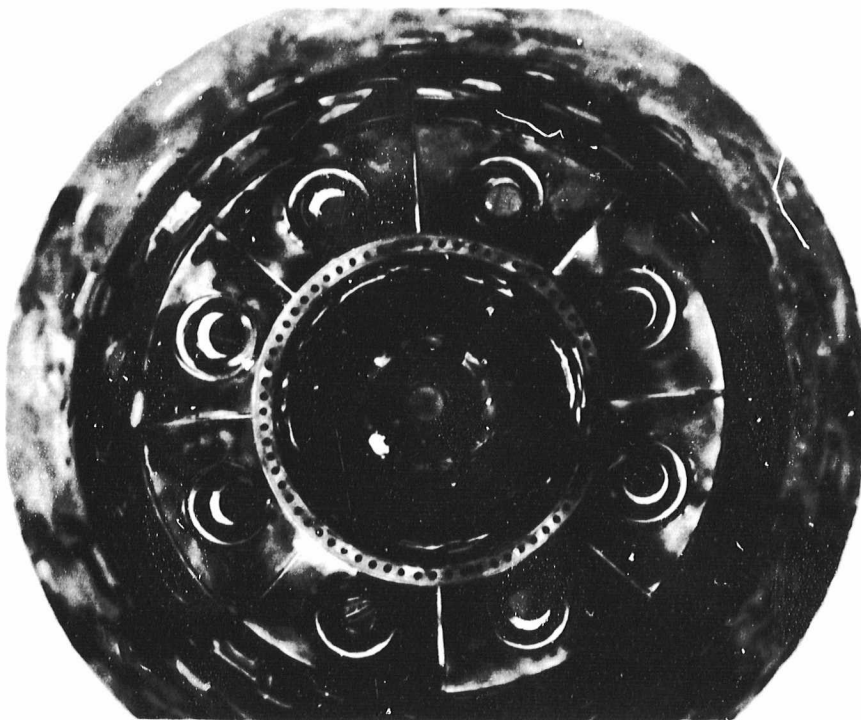


Figure 8-68. Posttest dome view, Concept 6

is distinct from N_2 in the air because with N_2 the nitrogen atoms are bound only to other nitrogen atoms. The chemical structural difference manifests itself in a flame. Conceptually, burning a fuel nitrogen species converts the carbon into CO_2 and the hydrogen into H_2O leaving free N atoms which, in an oxidizing atmosphere, readily oxidize into NO. On the other hand, N_2 in the air requires dissociation of the two N atoms prior to the oxidation, and this dissociation requires significantly higher energy (usually provided by locally high flame temperatures) to liberate the N from N_2 than burning a fuel-nitrogen compound.

The effect on NO_x emissions of fuel N is to increase the emissions above the normal thermal NO_x formed from N_2 in the air. The magnitude of the increase is a function of both the amount of N in the fuel and the fractional conversion of this into NO_x . The latter quantity is called the yield of NO_x from fuel N and is a useful parameter for comparing combustor designs to evaluate their sensitivity to fuel N. The yield, (Y), is defined from the measurement procedure as

$$Y = \frac{(\text{NO}_x) \text{ with FBN} - (\text{NO}_x) \text{ without FBN}}{(\text{NO}_x) \text{ all FBN converted into } NO_x}$$

Determining the yield requires two NO_x measurements, and one must be a clean fuel for the determination of baseline (NO_x) without FBN. Other definitions for measurements of the yield can be based on the differential NO_x observed when nitrogen compounds are added to a fuel to increase the fuel N. In this instance yield can be computed from the following,

$$Y = \frac{(\text{NO}_x) \text{ High FBN} - (\text{NO}_x) \text{ original}}{\text{NO}_x \text{ increase if all added FBN were converted to } NO_x}$$

Most data from this program were taken and analyzed using the first definition and used ERBS fuel as a zero FBN reference condition. For some tests, this is an exact determination because ERBS fuel was doped with pyridine (C_5H_5N) to increase the fuel-nitrogen content. The other fuels (SRC-II and the residual oil) have an inherent fuel-nitrogen level, and this cannot be removed to establish a nitrogen-free baseline for these fuels. Cleaning fuel N generally requires extensive hydrogenation, which changes other fuel properties and still would not provide a baseline. The problem in establishing a good NO_x baseline is finding a fuel that has the same or at least very similar thermal NO_x formation characteristics, because with no fuel N, all NO_x generation is thermal. For these fuels (ERBS, SRC-II, and residual), the problem was resolved by comparing the thermal NO_x generation from each fuel by evaluating the theoretical NO_x formation based on calculated flame temperatures.

A comparison of adiabatic equilibrium flame temperatures for the three fuels (ERBS, residual, and SRC-II) is shown in Figure 8-69. These results indicate that the three fuels have virtually identical adiabatic flame temperatures over the range of equivalence ratios investigated. The above information, which was calculated using the NASA Isobaric Adiabatic Chemical Equilibrium Computer program and analyzed fuel properties, was used as input to the Zeldovitch equation to predict the theoretical

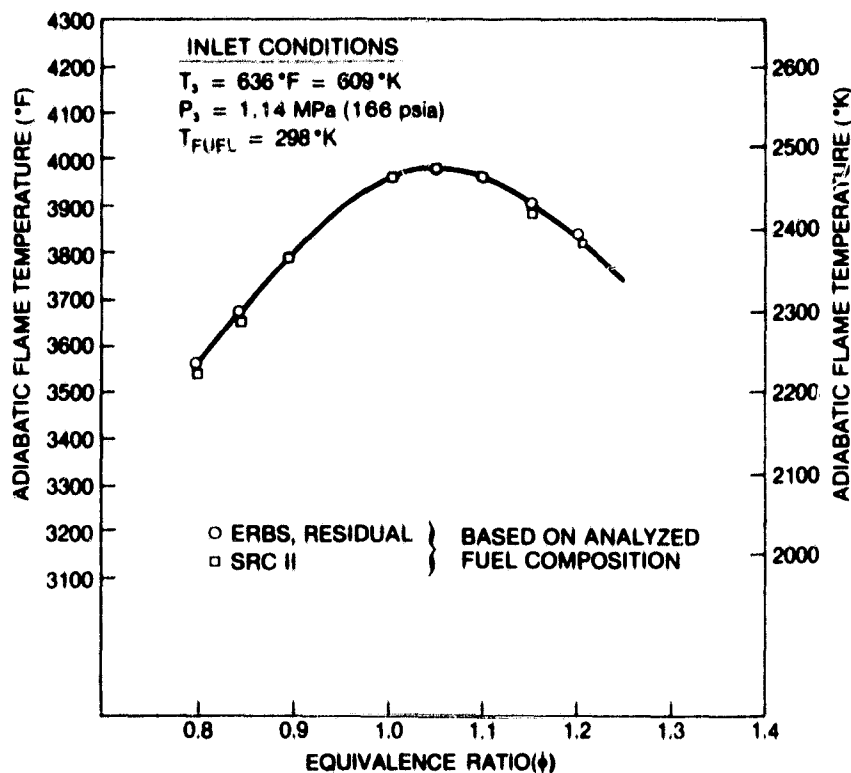
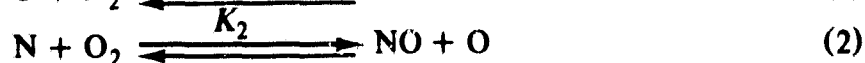
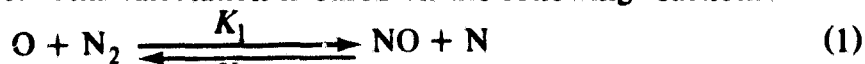


Figure 8-69. Calculated adiabatic flame temperatures for ERBS, residual, and SRC-II fuels

thermal NO formation rate. This calculation is based on the following reactions:



The following was assumed in deriving the expression for the NO_x formation rate:

1. Reverse reactions to Equations 1 and 2 were neglected (NO in flame \ll equilibrium)
2. N atom formation is steady state $\frac{d[\text{N}]}{dt} = 0$
3. O atoms are in chemical equilibrium

The following equation is the resulting expression for theoretical thermal NO formation rate:

$$\frac{d[\text{NO}]}{dt} = 2K_1[\text{N}_2][\text{O}] \quad (3)$$

where

$$K_1 = 1.84 \times 10^{14} \exp(-38374/T(\text{K})) \text{ cc/mole-s}$$

The NO formation rate was then converted to ppm/ms, because combustor residence times are on the order of milliseconds, and plotted in Figure 8-70.

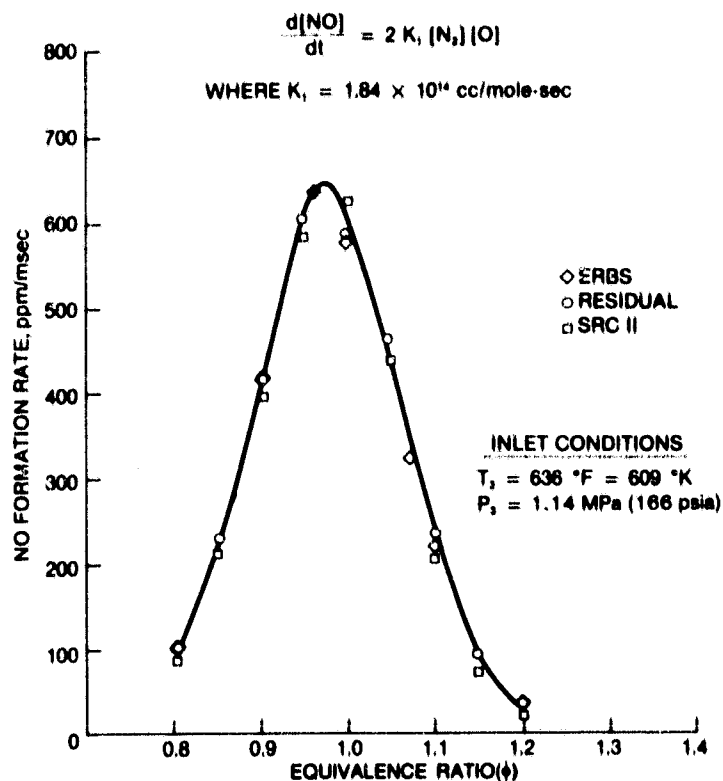


Figure 8-70. NO_x Production rate vs equivalence ratio (ϕ)

Since the calculated NO_x formation rates for the three fuels are essentially identical, the measured ERBS fuel thermal NO_x data are a reasonable baseline nitrogen-free emissions level.

The same sets of hardware were run on various fuels and, therefore, the fluid mechanics, mixing rates, and hence local equivalence ratios should be similar. Consequently, equality of thermal NO_x formation rates suggests similar thermal NO_x formation. Also the air-atomizing fuel nozzles are less sensitive to fuel properties than a pressure-atomizing system. This insensitivity to fuel properties would tend to establish similar spray flames for the three fuels. These considerations supported using the ERBS data for a nitrogen-free baseline in the yield calculations.

Much of the fuel nitrogen sensitivity testing used pyridine-doped ERBS fuel. Table 8-18 compares the nitrogen content based on metered flowrates of fuel and pyridine, and nitrogen content measured by wet chemical laboratory analyses of fuel samples drawn during the tests. The agreement between the nitrogen levels based on metered flow and the wet chemical analyses improved substantially for Concept 4-1 compared with results for the earlier-tested Concepts 1A and 6 because an accumulator was added to the pyridine flow system to damp the pump pulsations. Subsequent tests used the improved system, and the only data impacted by the pulsations were Concepts 1A and 6.

Table 8-18
NITROGEN ANALYSIS

Date	Concept	Fuel	Nitrogen Content, Percent	
			Metered	Analyzed
2-19-80	6	ERBS	0.41	0.36
		ERBS	0.76	0.99
		Residual	0.43	0.49
		Residual	0.65	0.62
2-28-80	1A	ERBS	0.42	0.30
		ERBS	0.65	0.45
3-13-80	4-1	Residual	0.42	0.48
		Residual	0.50	0.56

Figure 8-71 presents a plot of the yield of NO_x from fuel nitrogen for concepts tested in this program versus the weight percent nitrogen in the fuel. Also shown is a curve representative of MS7001 production combustor data for baseload operation. All of the current data were measured for the 92% (baseload) condition. The production liner baseline curve shows near unity yield for low nitrogen levels and decreases to an asymptote of roughly 0.3 at high fuel nitrogen levels. The less than quantitative yield is typical of a spray-flame combustor: the fuel air mixing and burning occur simultaneously, and a portion of the fuel nitrogen is reduced to N_2 in the locally fuel rich portions of the flame. The amount of fuel N reduced depends on both the local flame conditions and the residence time in the rich zone. A rich/lean design will, in general, decrease the yield below conventional levels because the initial flame is constrained to a fuel-rich condition, while in a conventional combustor excess air is always present. Similarly a very fast mixing lean spray flame enhances fuel N conversion into NO_x because the residence time in the locally rich zones decreased due to enhanced mixing. The current data illustrate these effects.

The improved mixing series-staged lean/lean design (Concept 4-1) exhibited higher yields than the rich/lean combustors. The pyridine-doped data for Concept 4-1 were taken with residual oil fuel (pyridine added to increase fuel nitrogen above the nominal 0.23 weight percent), and the yields were calculated from the incremental values of fuel N and NO_x . The yield from Concept 4-1 was also higher than typical values for the conventional production combustor because the rapid mixing in Concept 4-1 decreases the flame gas residence time in the fuel-rich region in the center of the spray. In a conventional combustor, the flame is overall fuel lean, and a less than unity yield results from a portion of the fuel N reacting in the locally fuel-rich flame zones. Therefore, decreasing the residence time in these zones by increasing the fuel/air mixing rate causes a higher yield.

nitrogen to NO_x . Thus, a catalytic combustor design producing ultralow NO_x with fuels containing negligible nitrogen would lose most of its low emission advantage when burning a high-nitrogen fuel. A segmented reactor design proposed by Acurex offered a potential solution to this dilemma. By partially combusting the fuel in a catalytic first stage, much of the fuel nitrogen would be converted into NO_x . In a gap between the catalytic first and second reactor stages, gas-phase reactions would convert this NO_x and remaining fuel nitrogen into molecular nitrogen, which would behave the same as the atmospheric nitrogen while passing through the second catalytic stage.

To incorporate this segmented catalytic reactor in the combustor design, two series of tests were conducted by Acurex Corporation and are reported in Appendices A and C. Appendix B presents an analysis of the first series of tests. Promising results from the first series of tests indicated the desirability and need for further development, which resulted in the execution of the second series of subscale tests. The second series of tests showed that the gapped reactor designs selected for testing were able to produce low N conversions only at the expense of poor combustion efficiency reflected in high concentrations of unburned hydrocarbons and carbon monoxide.

These subscale tests demonstrated that the development and inclusion of a reactor with internal gap for the catalytic concept was not feasible within the time and budget constraints of the original Phase I program. Thus a decision was made to proceed with the final design for the catalytic combustor Concept 8 as a low-nitrogen, clean-fuel burning combustor utilizing a reactor without a gap (see Section 7.3 for Concept 8 description). Additionally, the subscale tests indicated directions for further experimental work to define and develop the conditions favorable for the deNO_x process in a segmented reactor design. Finer analytical analysis of the pertinent kinetics should be supplemented by experimental work with gas sampling at various locations in the gap and downstream of various first-stage configurations.

The combustor hardware described in detail in Section 7.3 will be tested during the Phase IA extension of the Low NO_x Combustor Concept program. The planned test schedule is shown in Table 8-19.

Table 8-19

PROPOSED TEST POINT SCHEDULE CATALYTIC COMBUSTOR CONCEPT 8

Test Point	Fuel	P_3 , Inlet Total Pressure		T_3 , Inlet Total Temperature		W_a , Combustor Airflow,		W_{f1} , Total Fuel Flow		f/a , Combustor Fuel/ Air Ratio	Comments
Baseline -- Distillate Fuel		MPa	Psia	K	°F	kg/s	pps	kg/hr	pph		
1.0	No. 2	0.10	15.0	294	70	0.20	0.5	TBD	TBD	TBD	Starting, MS7000E Cycle, True Density
1.1		0.882	127.9	564	556	3.64	8.00	71	156	0.0054	No Load, MS7000E Cycle, True Density
1.2A		1.025	148.6	587	598	3.58	7.87	181	399	0.0141	50% Load, Crossover Point (Pilot only)
1.2B		1.025	148.6	587	598	3.58	7.87	181	399	0.0141	50% Load, Crossover Point (Catalyst only)
1.3		1.081	156.7	596	613	3.56	7.83	235	516	0.0183	70% Load, MS7000E Cycle, True Density
1.4		1.145	166.0	606	631	3.53	7.77	299	657	0.0235	92% Load, MS7000 Cycle, True Density
1.5		1.166	169.1	609	636	3.52	7.75	321	706	0.0253	100% Load, MS7000 Cycle, True Density
Gaseous Fuel Tests											
2.1	9.98 MJ/m ³ (268 Btu/scf)	0.882	127.9	564	556	3.64	8.00	280	616	0.021	No Load
2.2B		1.025	148.6	587	598	3.58	7.87	670	1473	0.052	50% Load
2.4		1.145	166.0	606	631	3.53	7.77	1182	2601	0.093	92% Load
2.5		1.166	169.1	609	636	3.52	7.75	1268	2790	0.100	100% Load
2.6		1.166	169.1	609	636	3.52	7.75	1268	2790	0.100	100% Load-NH ₃ Inj.*
3.1	8.56 MJ/m ³ (230 Btu/scf)	0.882	127.9	564	556	3.64	8.00	321	706	0.024	No Load
3.2B		1.025	148.6	587	598	3.58	7.87	824	1813	0.064	50% Load
3.4		1.145	166.0	606	631	3.53	7.77	1424	3133	0.112	92% Load
3.5		1.166	169.1	609	636	3.52	7.75	1636	3599	0.129	100% Load
3.6		1.166	169.1	609	636	3.52	7.75	1636	3599	0.129	100% Load-NH ₃ Inj.*
4.1	7.07 MJ/m ³ (190 Btu/scf)	0.882	127.9	564	556	3.64	8.00	431	948	0.033	No Load
4.2B		1.025	148.6	587	598	3.58	7.87	1107	2436	0.086	50% Load
4.4		1.145	166.0	606	631	3.53	7.77	1920	4224	0.151	92% Load
4.5		1.166	169.1	609	636	3.52	7.75	2118	4659	0.167	100% Load
4.6		1.166	169.1	609	636	3.52	7.75	2118	4659	0.167	100% Load - NH ₃ Inj.*

* NH₃ Injection rate will be determined prior to test—

Expected range—200-600 ppmv

ORIGINAL PAGE IS
OF POOR QUALITY

Section 9

DATA EVALUATION AND CONCLUSIONS

Section 8 presented the test data obtained during screening and development tests of the six Phase I rich/lean and lean/lean combustors. As noted in Section 8, initial screening tests of each combustor were completed. Concept 4 (series-staged lean/lean) and Concept 2 (multinozzle rich/lean) were subsequently selected for further development towards achieving the program dry low NO_x goals with clean and nitrogen-bearing fuels.

This report section addresses the following key areas of discussion:

- Summary and evaluation of the data presented in Section 8
- Identification of those concepts and aerodynamic features which led to the best NO_x performance achieved in the Phase I test program
- Conclusions and recommendations which are embodied in the conceptual designs proposed in Section 10 for consideration in Phase II development of a dry low NO_x combustor.

9.1 RICH/LEAN COMBUSTOR CONCEPTS

9.1.1 Data Correlations

The rich/lean combustor concepts were tested at a variety of conditions characteristic of the MS7001E load cycle and at some conditions representing variations of key parameters, e.g., atomizing air, residence time, rich/lean stage equivalence ratios, and cycle pressure. The NO_x data from these tests have been fit to correlation equations which include the major combustion parameters as functional dependencies. These correlation equations may be used to smoothen or reduce the effect of data scatter, allow for estimation of emissions at other than tested conditions, and enable estimation of emissions at other engine cycle conditions. It should be noted that in some cases the correlation equations are fit to a relatively small data set (e.g., for Concept 3-1).

The data obtained from these tests have been correlated in the following functional form:

$$EINO_x = K \left(\frac{P_3}{A} \right)^a \left(\frac{\Phi_p}{B} \right)^b \left(\frac{\Phi_s}{C} \right)^c \left(\frac{D}{V_r} \right)^d \exp \left(\frac{T_3 - E}{f} + \frac{6.33 - H_o}{52.63} \right) \quad (1)$$

where

- P_3 = Inlet total pressure (psia)
- T_3 = Total inlet temperature (°F)
- V_r = Secondary reference velocity (ft/sec)
- Φ_p = Primary equivalence ratio
- Φ_s = Secondary equivalence ratio
- H_o = Inlet humidity (lb/lb air)
- $EINO_x$ = NO_x emissions index (g/kg fuel)

Using the above correlation, NO_x emissions can be estimated for any cycle conditions where straight-line correlations were achieved. The constants A through E were chosen so that at MS7001E baseload conditions, $EINO_x = K$.

Concept 2 (Rich/lean combustor with multiple-nozzle dome)

This concept was tested a number of times. The modifications made for each test sequence (2-1, 2-2, 2-3, 2-4, and 2-5) are summarized in Table 8-4 of Section 8.1. The test matrix is presented in Table 9-1a. Each box in the matrix represents three variables (quench-hole pattern, swirler design, and rich-stage residence time). The results for NO_x , smoke, and FBN conversion rate are shown in Tables 9-1b, 9-1c, and 9-1d, respectively. For example, the top left-hand box in each of the four tables shows the test variables and the NO_x , smoke, and yield results for one test. A test with quench-hole pattern 1, the swirler design without sleeve insert and with 75 ms residence time in the rich stage, results in 8.2 g/kg fuel NO_x emission, 62 SAE smoke number, and 11% FBN conversion. From this table it is apparent that quench-hole pattern primarily affected NO_x , swirler design affected smoke most significantly, and rich-stage residence time affected FBN conversion rate. The best combination, therefore, is quench-hole pattern 1, the swirler design with sleeve insert and 75 ms rich-stage residence time. This set of variables was tested as combustor Concept 2-5 (See Table 8-4 of Section 8.1 for modification details). Therefore, the NO_x correlation for only this version of Concept 2 is presented below.

The constants in Equation 1 were evaluated from the data in Table 8-9 of Section 8.1. Since the rich/lean designs are fueled at the rich-stage dome end only, the factor for secondary stage equivalence ratio was deleted and replaced by atomizing air pressure ratio, which influences NO_x . The correlation equations are graphically presented in Figure 9-1. The reference atomizing air pressure ratio was taken to be 2.0.

For ERBS fuel, the correlation equation is:

$$EINO_x = 8.5 \left(\frac{P_3}{166} \right)^{0.5} \left(\frac{1.75}{\Phi_p} \right)^{0.8} \left(\frac{114}{V_r} \right) \left(\frac{2.0}{A_{pr}} \right)^{0.3} \exp \left(\frac{T_3 - 630}{350} + \frac{6.33 - H_o}{52.63} \right) \quad (2)$$

Table 9-1
MS7001 BASELOAD CONDITION, CONCEPT 2

a. Test Matrix

		Quench Hole Pattern		
		No. 1	No. 2	No. 3
S W I R L E R	Without Sleeve	75 ms	55 ms	—
	With Sleeve	75 ms	—	75 ms

b. EINO_x Data

		No. 1	No. 2	No. 3
S W I R L E R	Without Sleeve	8.2	10.5	—
	With Sleeve	8.4	—	11.8

c. Smoke Data

		No. 1	No. 2	No. 3
S W I R L E R	Without Sleeve	62	70	—
	With Sleeve	35	—	32

d. Percentage FBN Conversion Rate (for SRC II)

		No. 1	No. 2	No. 3
S W I R L E R	Without Sleeve	11	21	—
	With Sleeve	14	—	9

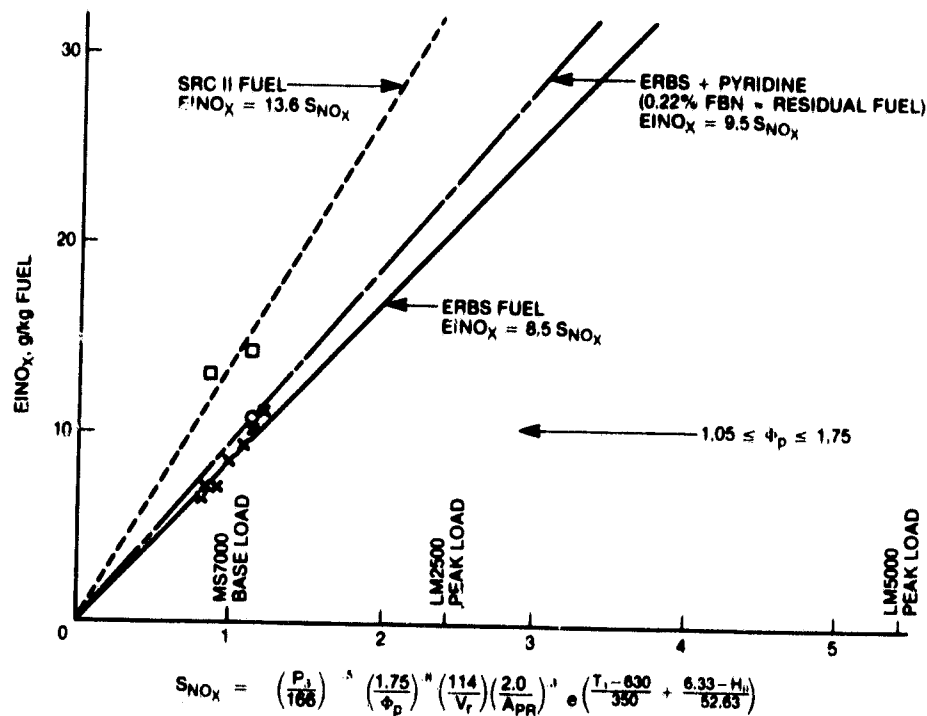


Figure 9-1. Data correlation for Concept 2-5

For residual fuel (estimated from Pyridine blends), the correlation equation is:

$$EINO_x = 9.5 \left(\frac{P_3}{166} \right)^{0.5} \left(\frac{1.75}{\Phi_p} \right)^{0.8} \left(\frac{114}{V_r} \right) \left(\frac{2.0}{A_{pr}} \right)^{0.3} \exp \left(\frac{T_3 - 630}{350} + \frac{6.33 - H_o}{52.63} \right) \quad (3)$$

For SRC-II fuel, the correlation equation is:

$$EINO_x = 13.6 \left(\frac{P_3}{166} \right)^{0.5} \left(\frac{1.75}{\Phi_p} \right)^{0.8} \left(\frac{114}{V_r} \right) \left(\frac{2.0}{A_{pr}} \right)^{0.3} \exp \left(\frac{T_3 - 630}{350} + \frac{6.33 - H_o}{52.63} \right) \quad (4)$$

where A_{pr} is the atomizing air pressure ratio.

In the above three correlations, $1.05 \leq \Phi_p \leq 1.75$ because in this range NO_x decreases as Φ_p increases. The conversion rate for fuel bound nitrogen, Y , can also be calculated using these equations.

For residual fuel (estimated with pyridine addition)

$$Y = 13.8 \left(\frac{P_3}{166} \right)^{0.5} \left(\frac{1.75}{\Phi_p} \right)^{0.8} \left(\frac{114}{V_r} \right) \left(\frac{2.0}{A_{pr}} \right)^{0.3} \exp \left(\frac{T_3 - 630}{350} + \frac{6.33 - H_o}{52.63} \right) \quad (5)$$

For SRC-II fuel:

$$Y = 17.8 \left(\frac{P_3}{166} \right)^{0.5} \left(\frac{1.75}{\Phi_p} \right)^{0.8} \left(\frac{114}{V_r} \right) \left(\frac{2.0}{A_{pr}} \right)^{0.3} \exp \left(\frac{T_3 - 630}{350} + \frac{6.33 - H_o}{52.63} \right) \quad (6)$$

For MS7001 cycle baseload conditions (92% load), Equations 5 and 6 result in 13.8% and 17.8% yield for residual and SRC-II fuels, respectively. The difference between the two values is within experimental error, and agrees with the yield values discussed in Section 8.3.

Concept 3-1 (Rich/lean combustor with narrow-passage quench)

The correlation equation used for this concept was similar to that used for Concept 2-5. For atomizing air pressure effect, the same factor was used as in Equations 2, 3, and 4. It was assumed that since the dome is similar in both designs, atomizing air pressure should affect NO_x in the same manner. Figure 9-2 shows the NO_x data and correlation fits as a function of the operating parameters. The data used in the correlation was taken from Table 8-10 of Section 8.1. The equation for ERBS fuel is:

$$FINO_x = 7.8 \left(\frac{P_3}{166} \right)^{0.5} \left(\frac{1.7}{\Phi_p} \right) \left(\frac{114}{V_r} \right) \left(\frac{2.0}{A_{pr}} \right)^{0.3} \exp \left(\frac{T_3 - 630}{350} + \frac{6.33 - H_o}{52.63} \right) \quad (7)$$

where $1.05 \leq \Phi_p \leq 1.7$

The NO_x emissions for Concept 3-1 for ERBS fuel are therefore approximately 10% less than for Concept 2-5, (compare Equations 2 and 7), and this is discussed in Section 9.1.2.

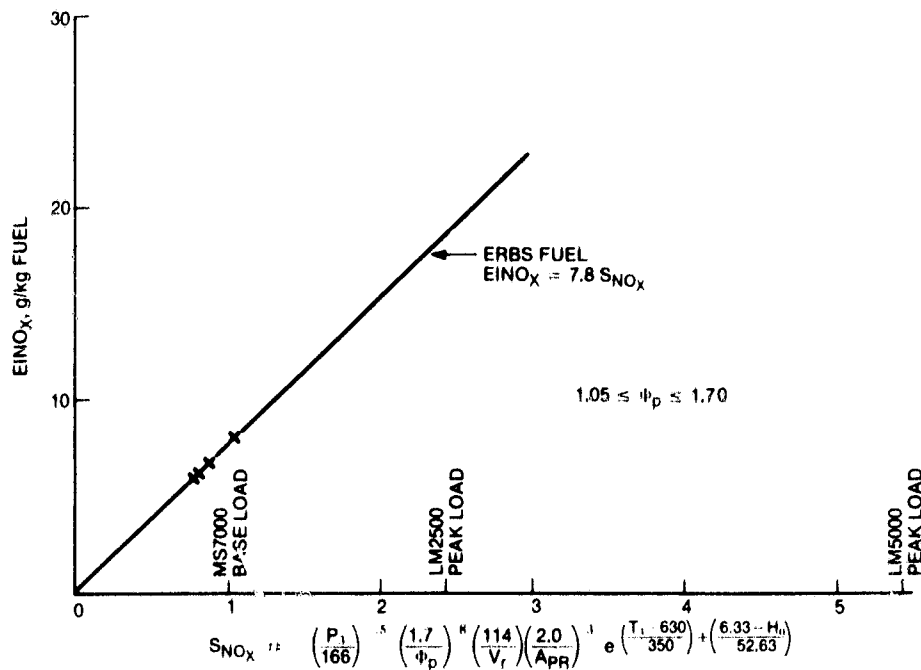


Figure 9-2. Data correlation for Concept 3-1

9.1.2 Summary and Evaluation, Rich/Lean Combustors

Concept 1A

Concept 1A (premixed rich stage) is an idealized design that enhances the benefits of rich/lean combustion but requires a long liner. The current test program evaluated the effect of upstream facing rich-to-lean quench holes, as discussed in Section 8.1.1. Table 9-2 presents overall results obtained with tests of Concept 1A-1. The NO_x emissions were unlike results achieved for the other rich/lean designs (for 1A, NO_x increased with increasing fuel/air ratio), and resembled a production combustor with an overall fuel-lean diffusion flame zone. This suggests that the upstream facing rich-to-lean quench holes caused the quench air to penetrate upstream into the rich stage providing longer-than-desired residence time at near stoichiometric conditions, acting much like a conventional liner. Other quench-hole patterns in which quench air penetrates perpendicularly into the gases exiting from the rich stage (as for Concept 2, discussed next) would probably decrease the NO_x emissions. However, overall liner length remains a problem for Concept 1A in many machine applications because of restricted available combustor length. In view of this concern for liner length in Concept 1A and the good mixing associated with the multiple-nozzle domes of rich/lean combustor concepts 2 and 3, Concept 1A is not considered the prime candidate for development to prototype status in Phase II. Concepts 2 and 3 embody the same basic rich/lean attributes of Concept 1A, with good rich-stage fuel/air mixing from the multinozzle dome, and are the basis for the conceptual design of the rich/lean combustor recommended for Phase II development.

Concept 2

The rich/lean combustor with multiple-nozzle dome, Concept 2, approached the rich-stage mixing problem by using multiple fuel nozzles, each having a counter-rotating air swirler. This distributes the fuel and air in the rich stage homogeneously and decreases the characteristic required mixing length by using smaller fuel/air introduction sites. The basic design worked well, and testing several variations during the course of development of this concept showed improvement in both smoke and NO_x .

Table 9-2 presents the key emissions results achieved with the final tested version, Concept 2-5. The tabulated data are based on the measured data discussed in Section 8.1.2, with adjustments made as described below to estimate the performance potential demonstrated by Concept 2-5. Table 9-2 shows that NO_x emissions for Concept 2-5 are within 10%–15% of the program goals for all fuels, including the 0.87 weight percent FBN SRC-II fuel. Although smoke was above the program goal of SAE 20, significant improvement was made by improved fuel/air mixing with a simple change made to the air swirlers. It is expected that the smoke goal can be achieved in Phase II with in-depth development of improved fuel/air mixing components. Combustion efficiency, pattern factor, and pressure drop met or approached program goals. The NO_x value for Concept 2-5 with ERBS fuel (see Table 9-2), 8.5 g NO_x /kg fuel, is the NO_x emissions measured at the “knee” or “bucket” of the NO_x versus fuel/air data plot. Although this minimum NO_x value did not occur at the baseload fuel/air ratio of the MS7001E cycle, adjustment of the rich-stage equivalence ratio to richer conditions to shift the NO_x minimum to the baseload fuel/air ratio of 0.0235 could be achieved by redistributing combustor airflow.

Table 9-2
SUMMARY OF RICH/LEAN EMISSIONS
FOR MS7001E BASELOAD CYCLE CONDITION

Concept	NO_x Emissions (g NO_x /kg fuel)			Smoke (SAE No.)	CO UHC	Pressure Drop (%)
	ERBS	Residual	SRCH			
1A-1	Over Goals—Attributed Rich-to-Lean Dilution Geometry			46	Meets Program Goals	6-7
2-5	8.5	10.7*	11.8	37	Meets Program Goals	7.8
3-1	7.8*	10.0*	12.7*	20†	Meets Program Goals	6
Program Goals	7.0	10.7	10.2	20		

* Estimated—see Section 9.1.2.

† Smoke data measured at 100 psia combustor pressure; smoke may increase at MS7001E cycle conditions.

The NO_x value for Concept 2-5 with SRC-11 fuel (see Table 9-2) is 11.8 g NO_x /kg fuel and was estimated by adjusting the measured data (data taken at an effective fuel/air ratio of 0.0242, i.e., on the same heating value basis as ERBS fuel) to correspond to that expected had the SRC-II data been obtained at a fuel/air ratio of 0.0282, the minimum in the NO_x versus fuel/air data curve for ERBS fuel. This adjustment was based on the assumption that the NO_x versus fuel/air curves for SRC-II and ERBS have similar shape.

The residual fuel data in Table 9-2 was estimated from the ERBS NO_x data and the fuel-bound nitrogen yield data. Recall that the residual fuel contained 0.23 weight percent fuel-bound nitrogen. Using the yield data of Figure 8-71, one can estimate a yield of NO_x from this fuel N of about 30%. Also, using the results of the calculated thermal NO_x formation rates (Figure 8-70) which showed that thermal NO_x for ERBS and residual oil should be roughly the same, the residual fuel NO_x emissions can be estimated by summing the ERBS data and the fuel N contribution. Note that these data and the residual fuel estimate were for an overall combustor fuel/air ratio of approximately 0.028, which is higher than the MS7001E rating at baseload conditions. However, the combustor performance can be adjusted to these values by redistributing the airflow, as mentioned previously. Increasing the dilution air and simultaneously decreasing the first- and second-stage airflows would shift both the rich- and lean-stage equivalence ratios for optimum performance at a lower overall combustor fuel/air ratio. Further reductions in both NO_x emissions and smoke would be required to complete the concept development.

In conclusion, Concept 2-5 has the potential for meeting program goals with residual and SRC-II fuels, i.e., with fuels having bound nitrogen contents approaching 1.0 weight percent and with hydrogen contents as low as 9.0 weight percent. The overall summary of results for Concept 2-5 is as follows:

Concept 2-5 Performance Summary

- NO_x performance
 - Within 10%–15% of goals for ERBS, residual and SRC-II fuels.
 - Low FBN yield, ~15% at bound nitrogen contents of 1%.
- Smoke at SAE 37 exceeds goals but
 - Significant improvement was achieved with only a minor swirler modification in the last test of Concept 2-5.
 - Further mixing developments in Phase II should lead to meeting the smoke goal.
- Combustion efficiency, pattern factor, and temperature profiles met program goals.
- Pressure drop was approximately 7%-8%, approaching the program goal.
- Liner metal temperatures were 1150-1200 K (1600-1700 °F); however,

- Phase I test hardware was designed to maximize program resources in developing and defining the aerodynamic design, not to achieve the heat-transfer requirements of a production combustor.
- Phase II hardware will be designed for satisfactory heat transfer, and these considerations are reflected in the conceptual design of the Phase II combustor (Section 10).

Concept 3 (Rich/Lean Combustor with Narrow Passage Quench)

Also shown in Table 9-2 are the projected NO_x emissions for Concept 3-1. All three NO_x values tabulated were estimated from the test data because of limited testing at reduced pressure. The NO_x values were based on the 0.69 MPa (100 psia) ERBS fuel combustor data presented in Figure 8-24 of Section 8.1.3. To correct to full-cycle pressure, the data were multiplied by the pressure effect measured for Concept 2-5 from 0.69 MPa (100 psia) and 1.14 MPa (166 psia) combustor testing. Combustor Concept 2-5 was run on ERBS fuel, and data were obtained (see Figure 8-4 of Section 8.1.2) for a fuel/air ratio of about 0.027 at both 0.69 MPa and the full-cycle value of 1.14 MPa combustor pressure. The Concept 3-1 NO_x data taken at 0.69 MPa (Figure 8-24) were multiplied by the ratio of the Concept 2-5 1.14 MPa NO_x measurement to the Concept 2-5 0.69 MPa NO_x measurement. This factor is about 1.3 and was used to adjust low-pressure data to full-pressure cycle conditions for the MS7001E.

The estimates for Concept 3-1 NO_x emissions burning residual oil and SRC-II (tabulated in Table 9-2) were based on the ERBS value determined as above and the yield data presented in Figure 8-71. Only one yield measurement was made for Concept 3-1 (at bound nitrogen content of 0.45 weight percent N), and this point falls within the general trend for all the rich/lean liners tested. Note that although the different concepts produced somewhat different yield (Figure 8-71), these differences are of the same order as the expected data scatter. This suggests that all the rich/lean concepts tested (including Concept 3-1) follow approximately the same yield curve. Consequently, the yield of NO_x from fuel N for Concept 3-1 was assumed equal to that in Concept 2-5, and the Concept 2-5 incremental NO_x emissions index adjustment was applied to the base Concept 3-1 ERBS full-pressure NO_x estimate to account for the fuel N in the high-nitrogen fuels. Similar to Concept 2-5, this procedure implicitly assumes equal thermal NO_x for ERBS, residual, and SRC-II fuels, which was predicted analytically and verified experimentally (recall that ERBS doped with pyridine, residual doped with pyridine, and ERBS/SRC-II blend data for NO_x versus FBN formed essentially one curve).

The smoke data reported in Table 9-2 for Concept 3-1 were measured at 0.69 MPa (100 psia), and smoke may increase with pressure. The smoke data at 0.69 MPa (100 psia) met the program goal. An estimate of this increase would be very difficult because of limited data. However, note that the combustor was not modified for smoke improvements. Possibly restricting the swirler air to improve mixing, as was done for Concept 2-5, could offset any increase in smoke due to increased combustor operating pressure.

Comparing the combustor performance with the program goals, it can be seen that Concept 3-1 was within about 10% of the goal for ERBS fuel, lower than the goal

for residual fuel, and slightly above the goal for SRC-II. Additional improvement in all three NO_x emissions levels may be possible by adjusting the rich-to-lean quench-airhole patterns. Note that Concepts 2-5 and 3-1 were run with about the same rich- and lean-stage fuel/air ratios, but Concept 3-1 showed about 10% lower clean fuel NO_x emissions which was attributed to the improved rich-to-lean mixing provided by the narrow-passage quench zone. Since only one geometry of Concept 3-1 was tested, a reasonable assumption is that additional NO_x reductions are feasible by modifying the rich-to-lean quench holes to improve mixing.

In conclusion, Concept 3-1 has the potential for meeting program goals with high nitrogen fuels (1 weight percent nitrogen) and with hydrogen content as low as 9%. Concept 3-1 had thermal NO_x performance superior to that of Concept 2-5, and this is attributed to the excellent rich-to-lean transition accomplished by the narrow-passage quench zone which requires reduced quench air jet penetration distance. Note also that Concept 3-1 had lower pressure drop than Concept 2-5 (6% versus 7%—8%). The narrow-passage quench zone of Concept 3-1 enables rich-to-lean transition with lower pressure drop, which is of key importance since

- Reduced pressure drop improves cycle efficiency.
- The narrow-passage quench zone enables effective rich-to-lean transition in commercial-size combustors [35.6 cm (14 in.) diameter for the MS7001E] without requiring excessive pressure drop to provide jet penetration, as might be the case for Concept 2-5 scaled to production size.

The excellent thermal NO_x performance, low yield of NO_x from FBN, and the superior rich-to-lean quench characteristics of Concept 3-1 are the basis for the conceptual design of the Phase II combustor described in Section 10, which embodies the best features of Concepts 3-1 and 2-5.

The overall summary of results for Concept 3-1 is as follows.

Concept 3-1 Performance Summary

- NO_x performance
 - Approaches the ERBS goal.
 - Projected to meet the residual and SRC-II goals.
 - Low FBN yield, as for Concept 2-5.
- Smoke
 - SAE 20 at 0.69 MPa (100 psia).
- Combustion efficiency, pattern factor, and temperature profiles met all program goals.
- Liner metal temperatures were excessive, as for Concept 2-5, but are addressed in the Phase II conceptual combustor design.

Summary of Key Parameter Effects

Evaluation of the emissions data has led to several conclusions with regard to the effect of key rich/lean combustor parameters on emissions performance. These key parameters are

- Rich stage equivalence ratio
- Rich stage residence time
- Rich-to-lean quench zone configuration and mixing effectiveness

The data are largely based on the results obtained from successive modification of multinozzle rich/lean Concept 2 (six configurations all told) and the results of the narrow passage quench zone design, Concept 3. The summary of key parametric effects is as follows:

- (1) Rich stage equivalence ratio, ϕ_r
 - NO_x bucket at $\phi_r \approx 1.7-1.8$
 - dependence on fuel type
 - insufficient parametric data
 - smoke increases from SAE 10-20 to SAE 50-60 as ϕ_r increased from 1.5 to 1.8
- (2) Rich stage residence time, τ_r , rich stage length varied from 38.1 cm (15 in.) to 25.4 cm (10 in.)
 - lower NO_x peak at near stoichiometric conditions in the rich stage ($f/a \approx .012$)
 - effect on organic NO_x yield
 - reduced τ_r led to increased yield
- (3) Quench zone configuration/mixing effectiveness
 - Upstream facing quench holes vs perpendicular quench pattern
 - results in lean stoichiometry in rich stage aft section, higher thermal NO_x
 - Quench air admitted perpendicular to gas flow (as in Concepts 2, 3) leads to flat exhaust profile, confirms good jet penetration/mixing
 - Narrow passage quench zone of Concept 3
 - Led to improved NO_x , CO, and smoke performance
 - Inadequate R-L quench results in
 - Higher NO_x
 - Higher CO
 - Higher smoke

9.1.3 Problem Areas/Required Development for Rich/Low Combustors

As noted in 9.1.1, NO_x emissions may be improved by development of the rich-to-lean quench zone. A second path to lower emissions may be changing the air distribution to increase the rich-stage fuel/air ratio. Note that the NO_x emissions should reach a local minimum as the fuel flow increases (fuel/air ratio for constant airflow as in the current case), but these combustor tests did not show this clearly. The amount of NO_x control possible with this method will be limited by the smoke formation in a richer first stage. Since the smoke approaches or exceeds program goals, the amount of NO_x reduction achievable will be paced by decreasing smoke formation. The best method is to prevent smoke formation in the rich first stage through improved fuel/air mixing which minimizes locally very rich regions that have a high smoke formation rate. Improved swirlers, venturis, and fuel distribution are viable modifications to decrease smoke.

The final development areas are the cooling and mechanical strength of the rich stage. The classical method of film cooling the combustor walls was rejected because a region of stoichiometric mixture is formed between the film air at the wall and the fuel-rich core gases. This region would be near the peak flame temperature and generate significant thermal NO_x .

The alternative selected for Phase I tests was using a ceramic thermal barrier coating on the flame gas side of the liner and convection cooling via the combustor inlet air on the backside. In general, this method was acceptable for the purposes of the Phase I screening test program, but the metal wall temperatures are higher than conventionally cooled parts and creep and distortion were problems. Increasing the metal wall thickness helped, but long-term commercial designs will require enhanced heat-transfer schemes. For example, jet impingement cooling is very effective but at the expense of pressure drop. Induced surface roughness using wires or other turbulence-inducing devices could roughly double the heat-transfer coefficient. This would also be an effective method of locally increasing the heat transfer to generate a more uniform wall temperature.

A major overheating problem was noted with the centerbody in Concept 3-1. Modification of this concept as proposed in the conceptual design of Section 10 will eliminate this section while preserving the narrow-passage quench-zone concept.

Another modification, which will increase the rich-stage liner life, is decreasing the combustor pressure drop. This will decrease the pressure stress on the wall as well as increase the gas turbine system efficiency. Reducing the stress will reduce the buckling failures as noted on several designs.

A final mechanical consideration is the first-stage length. Independent of the beneficial NO_x considerations, a short first stage is preferred to a long first stage because for a given combustor pressure drop, the short first stage has lower stress.

In summary, the rich/lean NO_x emissions for these combustors in their tested form can probably be improved by using a modified version of Concept 3-1. However, the challenge is scaling the design to accommodate MS7000 flows and developing a design consistent with the current reverse flow combustors.

9.1.4 Conclusions

Concepts 2-5 and 3-1 are rich/lean combustors which demonstrate real potential for achieving dry low NO_x program goals with nitrogen fuels containing on the order of 1% bound nitrogen (SRC-II). Concept 3-1 was selected as the basis for the conceptual design of the Phase II combustor because of comparable-to-superior thermal NO_x performance versus Concept 2-5, low NO_x yield from FBN, and the superior rich-to-lean quench characteristics of the narrow-passage quench zone which will enable scaling this combustor to commercial size with acceptable pressure drop.

9.2 LEAN/LEAN COMBUSTOR CONCEPTS

9.2.1 Data Correlations

NO_x data from the tests of lean/lean combustor Concepts 4, 4-1, 5, and 6 were fit to correlation equations which include the major functional dependences, as for the rich/lean correlation fits presented in Section 9.1.1. The data obtained in the lean/lean combustor tests were correlated in the same functional format as Equation 1 of Section 9.1.1, i.e.,

$$E\text{INO}_x = K \left(\frac{P_3}{A} \right)^a \left(\frac{\Phi_p}{B} \right)^b \left(\frac{\Phi_s}{C} \right)^c \left(\frac{D}{V_r} \right)^d \exp \left(\frac{T_3 - E}{f} + \frac{6.33 - H_o}{52.63} \right) \quad (1)$$

Concept 4 (Series-Staged Lean/Learn)

The constants in Equation 1 were evaluated using the data from Table 8-13. The temperature correlation factor, f , was assumed to be 350 based on correlations derived for other programs. The NO_x correlations (also shown in Figure 9-3) for ERBS and residual fuels are as follows.

For ERBS fuel:

$$E\text{INO}_x = 7.5 \left(\frac{P_3}{166} \right)^{0.4} \left(\frac{\Phi_p}{0.34} \right)^{0.4} \left(\frac{\Phi_s}{0.56} \right) \left(\frac{114}{V_r} \right)^{0.36} \exp \left(\frac{T_3 - 630}{350} + \frac{6.33 - H_o}{52.63} \right) \quad (8)$$

For residual fuel:

$$E\text{INO}_x = 11.4 \left(\frac{P_3}{166} \right)^{0.4} \left(\frac{\Phi_p}{0.34} \right)^{0.4} \left(\frac{\Phi_s}{0.56} \right) \left(\frac{114}{V_r} \right)^{0.36} \exp \left(\frac{T_3 - 630}{350} + \frac{6.33 - H_o}{52.63} \right) \quad (9)$$

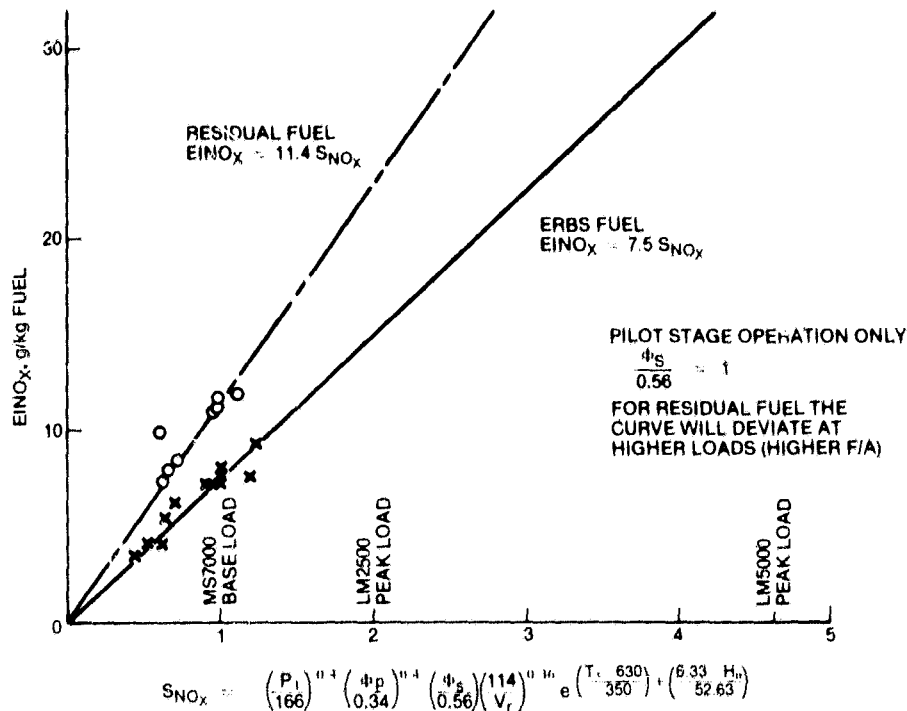


Figure 9-3. Data correlation for Concept 4

For pilot-stage operation only, Equation 8 can be used if $\left(\frac{\Phi_s}{0.56} \right)$ is assumed to be unity. However, Equation 9 cannot be used. This is because of FBN in the residual fuel. At high pilot-only load operation, the pilot dome has an equivalence ratio of about 1.8. The combustor, therefore, operates as a rich/lean design, and the FBN conversion to NO_x should be low. Gerhold*, et al. have shown that the FBN conversion increases with the equivalence ratio until $\Phi = 0.85$ and then the conversion decreases. Pilot dome equivalence ratio of 0.85 translates into $\Phi_p = 0.4$. Therefore Equation 9 is limited to $\Phi_p \leq 0.4$ and $\Phi_s \leq 0.85$.

The tests conducted later in the program showed that the hydrogen content had apparently little effect on the NO_x formation (H_2 varied from 9% to 13%). Therefore, the difference in Equations 8 and 9 is due to the nitrogen content of residual fuel. The yield Y (percent conversion of fuel-bound nitrogen into NO_x) is:

$$Y = \frac{EINO_x N=F - EINO_x N=O}{F \times 32.86} \times 100$$

where N is the percent nitrogen by weight.

* Gerhold, Fenimore, and Dederick, *Two-Stage Combustion of Plain and N Doped Oil*, Reprint 8599, General Electric Company, Corporate Research and Development, Schenectady, New York.

Therefore from Equations 8 and 9:

$$Y = 51.6 \left(\frac{P_3}{166} \right)^{0.4} \left(\frac{\Phi_p}{0.34} \right)^{0.4} \left(\frac{\Phi_s}{0.56} \right) \left(\frac{114}{V_r} \right)^{0.36} \exp \left(\frac{T_3 - 630}{350} + \frac{6.33 - H_o}{52.63} \right) \quad (10)$$

or for MS7000 cycle at baseload:

$$Y = 51.6\%$$

Equation 10 shows that the conversion of fuel bound nitrogen into NO_x is a function of the operating parameters. The same restrictions on Φ_p and Φ_s that apply to Equation 9, apply to Equation 10.

Concept 4-1

Equation 8 showed that NO_x emissions are a strong function of the effective secondary-stage equivalence ratio, i.e., the degree of mixing achieved in the second stage. Therefore, as a first modification to Concept 4, the mixing in the secondary stage was enhanced by the addition of a cone on each swirler (identified as Concept 4-1). The data obtained with Concept 4-1 is presented in Table 8-15 of Section 8.2. The data were then correlated, and the constants in Equation 1 evaluated, resulting in the following correlation equations.

For ERBS fuel:

(I) Both stages fueled:

$$E\text{INO}_x = 4.3 \left(\frac{P_3}{166} \right)^{0.4} \left(\frac{\Phi_p}{0.31} \right)^{0.4} \left(\frac{\Phi_s}{0.56} \right) \left(\frac{114}{V_r} \right) \exp \left(\frac{T_3 - 630}{350} + \frac{6.33 - H_o}{52.63} \right) \quad (11)$$

(II) Pilot stage fueled only:

$$E\text{INO}_x = 6.7 \left(\frac{P_3}{166} \right)^{0.4} \left(\frac{\Phi_p}{0.31} \right)^{0.4} \left(\frac{114}{V_r} \right) \exp \left(\frac{T_3 - 630}{350} + \frac{6.33 - H_o}{52.63} \right) \quad (11a)$$

For residual fuel:

(I) Both stages fueled:

$$EINO_x = 10.2 \left(\frac{P_3}{166} \right)^{0.4} \left(\frac{\Phi_p}{0.31} \right)^{0.4} \left(\frac{\Phi_s}{0.56} \right) \left(\frac{114}{V_r} \right) \exp \left(\frac{T_3 - 630}{350} + \frac{6.33 - H_o}{52.63} \right) \quad (12)$$

For SRC-II fuel:

(I) Both stages fueled:

$$EINO_x = 20.0 \left(\frac{P_3}{166} \right)^{0.4} \left(\frac{\Phi_p}{0.31} \right)^{0.4} \left(\frac{\Phi_s}{0.56} \right) \left(\frac{114}{V_r} \right) \exp \left(\frac{T_3 - 630}{350} + \frac{6.33 - H_o}{52.63} \right) \quad (13)$$

These correlations are shown graphically in Figure 9-4. Comparison of Equations 11 and 11a shows that the majority of the NO_x is produced in the pilot stage. Figure 9-4 also shows that for residual and SRC-II fuels, the $EINO_x$ is not a linear

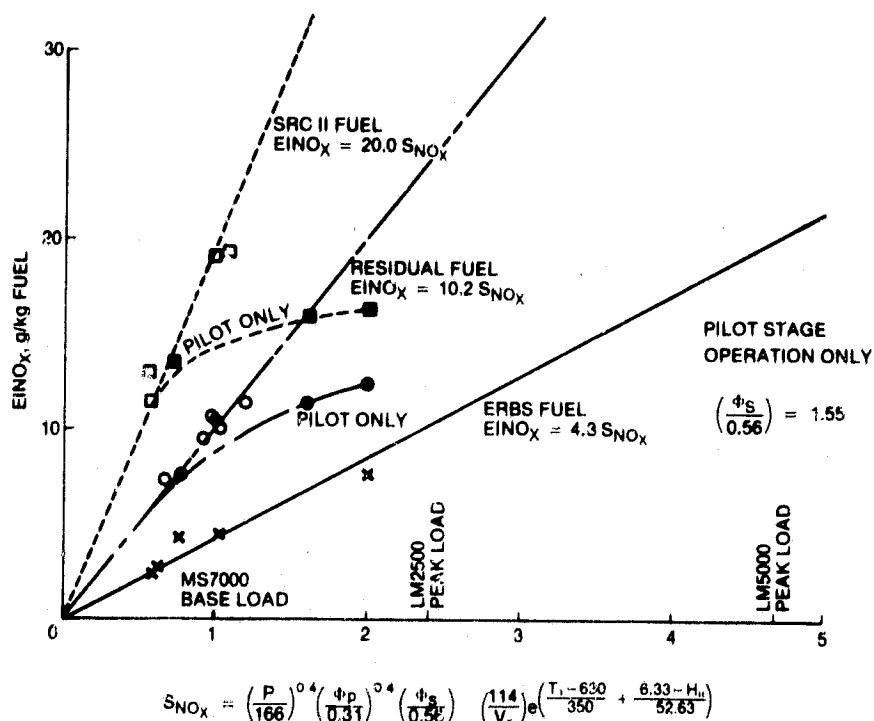


Figure 9-4. Data correlation for Concept 4-1

function for pilot-only operation. As postulated earlier in the discussion of Concept 4, the reason for this deviation is due to nitrogen content of the fuel. Therefore, both Equations 12 and 13 are limited to $\Phi_p \leq 0.45$ (pilot dome Φ of 0.85 is equivalent to Φ_p of 0.45 in this design) and $\Phi_s \leq 0.85$.

Equations 11, 12, and 13 are correlations of NO_x data for ERBS, residual, and SRC-II fuels, respectively. The difference is due to the nitrogen content of the fuels. Work done at NASA* has shown that the conversion of FBN into NO_x decreases as the amount of nitrogen increases. Therefore, the conversion rate for residual fuel (0.23% FBN) should be higher than for SRC-II (0.87% FBN). Equations 11, 12, and 13 demonstrate this, and the deduced yield equations are ($\Phi_p \leq 0.45$, $\Phi_s \leq 0.85$)

For residual fuel:

$$Y = 78 \left(\frac{P_3}{166} \right)^{0.4} \left(\frac{\Phi_p}{0.31} \right)^{0.4} \left(\frac{\Phi_s}{0.56} \right) \left(\frac{114}{V_r} \right) \exp \left(\frac{T_3 - 630}{350} + \frac{6.33 - H_o}{52.63} \right) \quad (14)$$

For SRC-II fuel:

$$Y = 54.9 \left(\frac{P_3}{166} \right)^{0.4} \left(\frac{\Phi_p}{0.31} \right)^{0.4} \left(\frac{\Phi_s}{0.56} \right) \left(\frac{114}{V_r} \right) \exp \left(\frac{T_3 - 630}{350} + \frac{6.33 - H_o}{52.63} \right) \quad (15)$$

For the MS7001E cycle at baseload conditions, the yields are approximately 78% and 55%, respectively. Comparing Concepts 4 and 4-1, the conversion of FBN to NO_x is higher for Concept 4-1 (78% as opposed to 52%, for residual fuel). This is attributed to modifications made to improve mixing, which resulted in reduced residence time at rich stoichiometry. Improved mixing results in higher NO_x yield and lower smoke (smoke data is discussed elsewhere in this report), although it also tends to reduce thermal NO_x , as demonstrated in the superior performance of Concept 4-1 versus Concept 4.

Concept 6 (Parallel-Staged Lean/Low Combustor)

The data obtained for Concept 6 were also correlated in the same form as for the previous two concepts. The constants were evaluated using the data in Table 8-17 of Section 8.2. Correlation equations for Concept 6 (also shown graphically in Figure 9-5) are as follows.

* David A. Bittker, *An Analytical Study of Nitrogen Oxides and Carbon Monoxide Emissions in Hydrocarbon Combustion with Added Nitrogen—Preliminary Results*, DOE/NASA/2593-79/10.

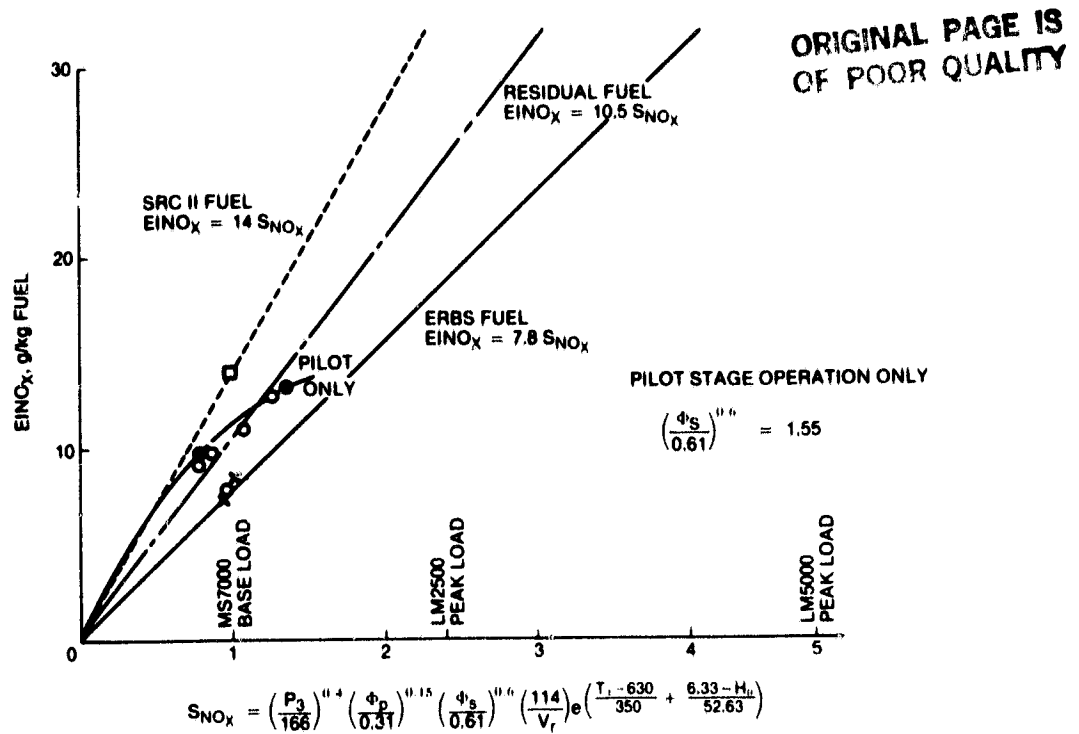


Figure 9-5. Data correlation for Concept 6

For ERBS fuel:

(I) Both stages fueled:

$$EINO_x = 7.8 \left(\frac{P_3}{166} \right)^{0.4} \left(\frac{\Phi_p}{0.31} \right)^{0.15} \left(\frac{\Phi_s}{0.61} \right)^{0.6} \left(\frac{114}{V_r} \right) \exp \left(\frac{T_3 - 630}{350} + \frac{6.33 - H_o}{52.63} \right) \quad (16)$$

For residual fuel:

(I) Both stages fueled:

$$EINO_x = 10.5 \left(\frac{P_3}{166} \right)^{0.4} \left(\frac{\Phi_p}{0.31} \right)^{0.15} \left(\frac{\Phi_s}{0.61} \right)^{0.6} \left(\frac{114}{V_r} \right) \exp \left(\frac{T_3 - 630}{350} + \frac{6.33 - H_o}{52.63} \right) \quad (17)$$

For SRC-II fuel:

(I) Both stages fueled:

$$EINO_x = 14 \left(\frac{P_3}{166} \right)^{0.4} \left(\frac{\Phi_p}{0.31} \right)^{0.15} \left(\frac{\Phi_s}{0.61} \right)^{0.6} \left(\frac{114}{V_r} \right) \exp \left(\frac{T_3 - 630}{350} + \frac{6.33 - H_o}{52.63} \right) \quad (18)$$

Figure 9-5 again shows that, for pilot-stage operation only with residual fuel, the NO_x is not a straight-line function of operating parameters. The reason for the deviation was discussed earlier. Therefore, equivalence ratios are limited to $\Phi_p \leq 0.4$ and $\Phi_s \leq 0.85$. The FBN conversion for this concept can be calculated from Equations 16, 17, and 18.

For residual fuel:

$$Y = 35.7 \left(\frac{P_3}{166} \right)^{0.4} \left(\frac{\Phi_p}{0.31} \right)^{0.15} \left(\frac{\Phi_s}{0.61} \right)^{0.6} \left(\frac{114}{V_r} \right) \exp \left(\frac{T_3 - 630}{350} + \frac{6.33 - H_o}{52.63} \right) \quad (19)$$

For SRC-II fuel:

$$Y = 21.7 \left(\frac{P_3}{166} \right)^{0.4} \left(\frac{\Phi_p}{0.31} \right)^{0.15} \left(\frac{\Phi_s}{0.61} \right)^{0.6} \left(\frac{114}{V_r} \right) \exp \left(\frac{T_3 - 630}{350} + \frac{6.33 - H_o}{52.63} \right) \quad (20)$$

For MS7001E baseload conditions, the yield values are 36% and 22% for residual and SRC-II fuels, respectively. For this lean/lean design, the conversion of FBN into NO_x is unusually low. The reason may be as discussed previously, i.e., incomplete mixing causes rich pockets to be present in the fuel/air mixture. These rich pockets result in reduced fuel-bound nitrogen conversion. If modifications to this combustor were to be made to improve NO_x by improved mixing (as for Concept 4-1), the conversion rate would probably increase as was observed for Concept 4-1.

Estimation of Lean/Lean Combustor Emissions for High Pressure Ratio Cycles

As may be noted from Equation 11 for Concept 4-1 and the discussion of lean/lean results in Section 8.2, Concept 4-1 has the potential for ultralow thermal NO_x emissions with ERBS fuel. Concept 5 demonstrates similar performance, while Concept 6 has higher thermal NO_x but lower FBN yield. The data for these combustors were extrapolated, using the correlation fits, to the 16:1 and 30:1 pressure ratio

conditions of the aircraft derivative LM2500 and LM5000 engines. Section 10.3 presents the conceptual designs of two combustors (based on lean/lean Concept 6 and rich/lean Concept 3) for application to the LM2500 16:1 pressure ratio cycle conditions. Extrapolation of the data to the LM2500 and LM5000 cycle conditions indicates considerable difficulty in meeting some of the NO_x goals. This is illustrated in Table 9-3 which shows some data for a standard combustor (without modifications for reduced NO_x), a double-annular combustor, and for the radial axial combustor. These data are from the GE/NASA Experimental Clean Combustor Program (ECCP) but have been adjusted to the hydrogen content of ERBS fuel for comparison with NASA/DOE data. The extrapolated data for Concept 4-1 agree well with those for the ECCP double-annular combustor. The Concept 6 combustor NO_x level was comparable to that of Concept 4 (i.e., they were about the same without development). It is believed that with minimum development the NO_x level for Concept 6 would be equivalent to that of Concept 4-1 or the ECCP double-annular (at the same operating conditions). Therefore, for the 16:1 pressure ratio cycle (LM2500), Concept 6 was selected as the most appropriate design. Concept 6 would have length advantages over Concept 4 and would be more adaptable to the LM2500 flow path. The NO_x goals for the LM2500 cycle are shown in Table 9-3. Although Concept 6 had a low

Table 9-3

NO_x EMISSIONS FOR HIGH PRESSURE RATIO CYCLE CONDITIONS

All data adjusted to 12.9% H_2 (ERBS)

Engine Pressure Ratio	12	16 (LM2500)	30 (LM5000)	Comments
Typical A/C Derivative Combustion System			38 g/kg	(LM5000)
ECCP Double Annular			21	Selected Configuration
			17-53	Range for 17 Configurations
Radial Axial			17	Selected Configuration
			16-40	Range Measured
NASA/DOE Concept 4 (series staged)	7.5	15	35	Extrapolated Data for P/P = 16&30
Concept 4-1	4.5	10	20	Extrapolated Data for P/P = 16&30
Concept 5 (premixed parallel staged)	5	8.7	24	Extrapolated Data for P/P = 16&30
Concept 6 (parallel staged)	8	18.5	37.6	Extrapolated Data for P/P = 16&30
Goal	7	8.06	8.28	EPA stds (75 ppm plus heat rate correction)

conversion rate of FBN, it is expected that with development for reduced NO_x this advantage would probably be lost. Concept 4 had lower FBN conversion rates before it was modified for improved fuel and air mixing in Concept 4-1. As the main-stage mixing is improved, the FBN conversion rate will probably increase. Therefore one rich/lean concept was also designed for the LM2500 engine. This concept would provide capability for handling fuels with FBN.

Inspection of Table 9-3 shows that to meet the NO_x goals for the LM5000 cycle will require all of the most advanced techniques available. The best NO_x levels demonstrated in programs conducted to date are more than twice the goals. Therefore the selected design for the 30:1 pressure ratio cycle has two stages, variable geometry and premixing of the fuel and air. Preliminary design sketches, flow splits, operating parameters, and performance predictions for the higher pressure ratio cycle combustors are presented in Section 10.3 of this report.

9.2.2 Summary and Conclusions, Lean/Lean Combustor Concepts

Figure 9-6 presents a summary of the NO_x emissions data for lean/lean combustor Concepts 4, 4-1, 5, and 6. As may be seen, Concept 4-1 has the potential of meeting all program goals with ERBS and possibly a residual fuel with less than 0.25 weight percent fuel nitrogen. In fact, with fuels with low nitrogen content (i.e., ERBS), this concept would meet the NO_x emission level with considerable margin,

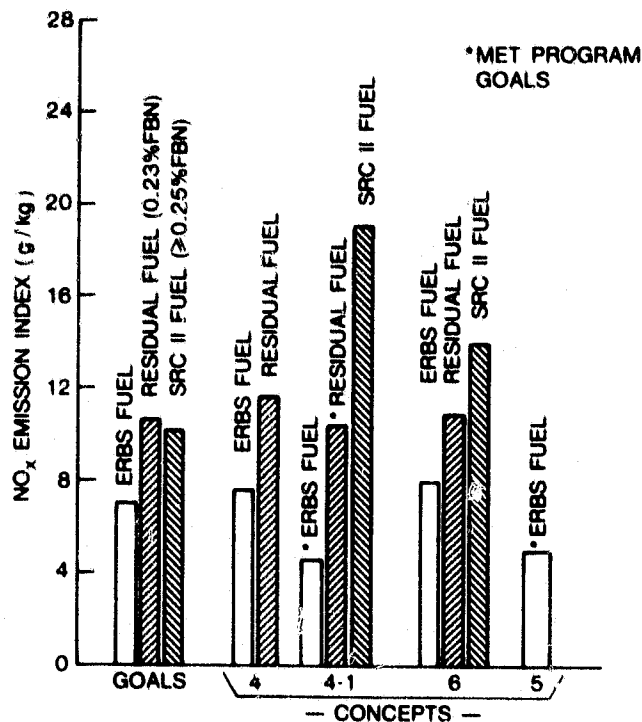


Figure 9-6. NO_x summary of lean/lean combustors

having clean fuel NO_x emissions of approximately 5 g/kg fuel. The two deficiencies observed, smoke at high pilot fuel/air ratios and low efficiency at lean operating conditions could most likely be overcome with some development including flow-split adjustments, additional swirl-cup changes, and possible additional pressure drop. All other performance parameters including pattern factors, liner temperature, and carbon deposits were met on the initial testing. This combustor concept does not appear to have the potential for meeting NO_x emission goals with fuels with nitrogen contents much in excess of 0.25%.

Consequently, Concept 4-1 is not recommended as the primary vehicle for Phase II development for application to high nitrogen fuels. The rich/lean combustor concept (based on Concept 3-1) is the recommended vehicle for development to meet dry low NO_x emissions for high-nitrogen liquid fuels and for low and intermediate Btu coal-derived gas fuels, particularly with organic nitrogen in the form of ammonia contamination of the coal-derived gas. However, Section 10.2 presents the conceptual design of a lean/lean combustor (based on Concept 4-1) for consideration in Phase II development in the interest of providing a full assessment of potential applications of the generated Phase I low NO_x combustor technology. Similarly, Section 10.3 of this report presents conceptual designs, based on the lean/lean combustor concepts, of combustors which may be considered for application to a 16:1 pressure ratio LM2500 cycle.

9.2.3 Problem Areas/Required Development for Lean/Lean Combustors

As noted above, the lean/lean combustor concept recommended for consideration during Phase II is Concept 4-1, since this configuration produced very low levels of NO_x with ERBS fuel. Problems that remain for this concept, based on the test program, are high smoke and NO_x from the pilot stage just before switchover to pilot and main stage operation, and low combustion efficiency at FSNL and just after switchover to the main stage. Two approaches are presented to resolve these problems. One method is to enrich the pilot stage dome and to move the transition point from pilot to dual operation to a lower power condition where fuel/air ratios are lower and smoke and NO_x levels would be acceptable. In order to avoid low local fuel/air ratios (low efficiency) after switchover, only a portion of the main-stage nozzles (approximately half) would be fueled. All of the nozzles would be fueled at full power.

The other approach to resolve the Concept 4-1 problems is to enrich the pilot-stage dome for FSNL operation and use variable-geometry pilot swirlers to increase the airflow to the pilot before switchover to two-stage operation. Details of the design and operational characteristics of conceptual designs which address these features are contained in Section 10.2.

Section 10

CONCEPTUAL DESIGNS OF PHASE II COMBUSTORS

As discussed in Section 9.0, rich/lean combustor Concept 3-1 has the potential for achieving dry low NO_x emissions with high nitrogen liquid fuels (SRC-II). The combination of good thermal NO_x performance and low NO_x yield from FBN also make this combustor an excellent candidate for the combustion of low and intermediate Btu coal-derived gas fuels with organic nitrogen in the form of NH_3 contamination. Section 10.1 presents the conceptual design of this prime combustor concept recommended for full-scale development in Phase II for combustion of liquid and gas fuels.

Section 10.2 presents the conceptual design of a lean/lean combustor, based on Phase I Concept 4-1, which has potential for ultra-low NO_x emissions on clean fuels. Although not recommended for high-nitrogen fuels applications (meets NO_x goals for ≤ 0.25 weight percent FBN) it is included to provide a full assessment of the application of the derived Phase I technology. Similarly, Section 10.3 presents the conceptual design of combustor concepts which could be applied to high-pressure-ratio cycles.

10.1 RICH/LEAN COMBUSTOR DESIGN RECOMMENDED FOR PHASE II

The Phase I program tested scaled combustors by using a typical through-flow gas turbine test apparatus. However, the General Electric heavy duty gas turbines use a different flow geometry that eventually impacts the design. Figure 10-1 is a schematic of the General Electric Heavy Duty combustion system. As shown, the combustors are located at a larger radius from the machine centerline than the compressor and turbine wheels. Also, the combustors are cantilevered outside the compressor. This design necessitates a reverse flow combustion system. The airflow leaves the compressor and turns 180° (hence "reverses flow") and actually flows toward the compressor inlet before entering the combustion system.

As the air flows toward the combustor head end, small portions are bled off for cooling and major portions are extracted for dilution air and combustion air. The only air that flows near the combustor head end is that required for the fuel nozzle swirler which is typically 5 to 10% of the total airflow. This geometry is distinctly different from that tested under the current Phase I Program (to simplify the test rig and reduce hardware costs) which used an aircraft type flow path where all the combustor airflow must pass the liner head end. This difference will have a marked influence in cooling the rich stage of a rich/lean combustor by using backside convection (current program designs) because the amount of cooling air may be reduced by a factor of about five if only the rich stage is used.

Table 10-1 lists some of the key design criteria that were considered in the proposed conceptual Phase II design, along with the ultimate impact of the parameter. Scaling the design to a larger diameter to handle the required machine airflow and decreasing the combustor pressure drop will decrease the rich-to-lean mixing rate.

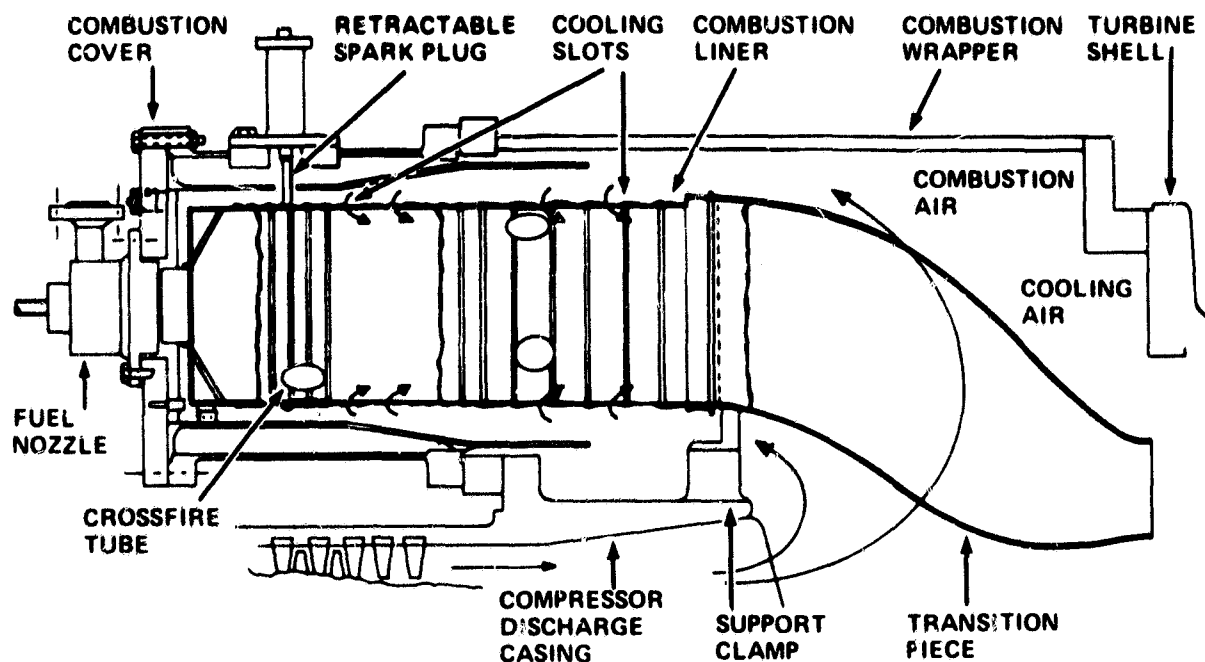


Figure 10-1. General Electric heavy-duty reverse-flow combustion system

Table 10-1

**RICH/LEAN COMBUSTOR DESIGN CONSIDERATIONS
FOR FULL-SCALE PRODUCTION MS7001E HARDWARE**

Design Criteria	Effect	Impact	Design Action
Lower Combustor Pressure Drop with Larger Combustor Diameter and Higher Flow	Slower Rich/Lean Mixing	NO _x	Minimum Rich-to-Lean Jet Penetration
Reverse Airflow Rich-Stage Area	Rich-Stage Cooling	Metal Temperature	Augment Turbulence, Use Centerbody so Rich-to-Lean Quench Air Is Available for Coolant
Mechanical Strength	Liner Failure	Parts Life	Increase Metal Thickness, Short First Stage

The combustor pressure drop can be considered as the driving force which supplies the mixing energy while the larger combustor diameter increases the length required for rich-to-lean jet penetration and mixing. As noted from the test results from modifications of Concept 2 and comparing Concepts 2-5 and 3-1, the rich-to-lean mixing time is key in determining the thermal NO_x formation (refer to the discussion in Section 9.1). Slow mixing allows some of the gas to remain at near stoichiometric equivalence ratios where the NO_x formation is excessive. As demonstrated by Concept 3-1, one method of decreasing the mixing time is to decrease the rich-to-lean jet penetration length. This feature will be used in the proposed conceptual design.

The reverse airflow geometry can potentially limit the amount of cooling available for backside convection cooling of the rich stage. Consequently, the design should maximize the airflow around the head end. An approach to accomplish this is to duct all the air from the compressor exit to the combustor head end to make the heavy duty system similar to an aircraft design. However, the extra 180° flow reversals would induce pressure drop that could be much better spent by improving the mixing energy in the combustor. An alternative is to increase the airflow past the combustor head end by making a centerbody in the rich stage (for example Concept 3-1) so that in a reverse flow system, at least a portion of the rich-to-lean quench air flows around the rich stage stage and into the centerbody where it is injected into the rich flame gases. The pitfall in this scheme is to avoid excessive rich-stage metal surface area. Note that the centerbody structure of Concept 3-1 was thermally damaged during the test program. Also, the rich-stage convection cooling could be augmented to make better use of the available air. Jet impingement cooling and artificial surface roughness (trip wires, fins, grooves) can double the heat-transfer coefficient.

The final entry in Table 10-1 is the rather broad category of mechanical strength. Actually, this consideration is tied closely with the wall cooling, since strength at operating temperature is the important parameter. The mechanical problem can be eased by proper mechanical design. For example, thicker metal walls will increase the strength and a short rich stage is more resistant to buckling than a long section. Also, as noted above, a short rich stage (Concepts 3-1, and 2-3) showed a lower mid load NO_x peak with very little, if any, penalty.

Figure 10-2 is a schematic of the proposed rich/lean design for Phase II development, suitable for a heavy-duty reverse-flow combustion system. The design uses concepts developed during the current program (based on Concept 3-1) and was developed to be interchangeable with the production MS7001E combustion system, i.e., retrofittable to the MS7001E machine. The rich stage is an annular section formed by two concentric cones. The walls are coated with a thermal barrier coating and cooled only by backside convection. The annular rich stage was selected to minimize the jet penetration distance for the rich-to-lean quench region. Comparing Concepts 3-1 and 2-5 demonstrated the benefits of this feature. Also, since the quench air is added from both sides of the annulus, a large portion of the rich-to-lean quench air is used for rich-stage cooling. Fuel is injected through eight nozzles spaced uniformly around the rich stage annulus. Each nozzle will have an air swirler to produce rapid fuel and air mixing.

ORIGINAL PAGE IS
OF POOR QUALITY.

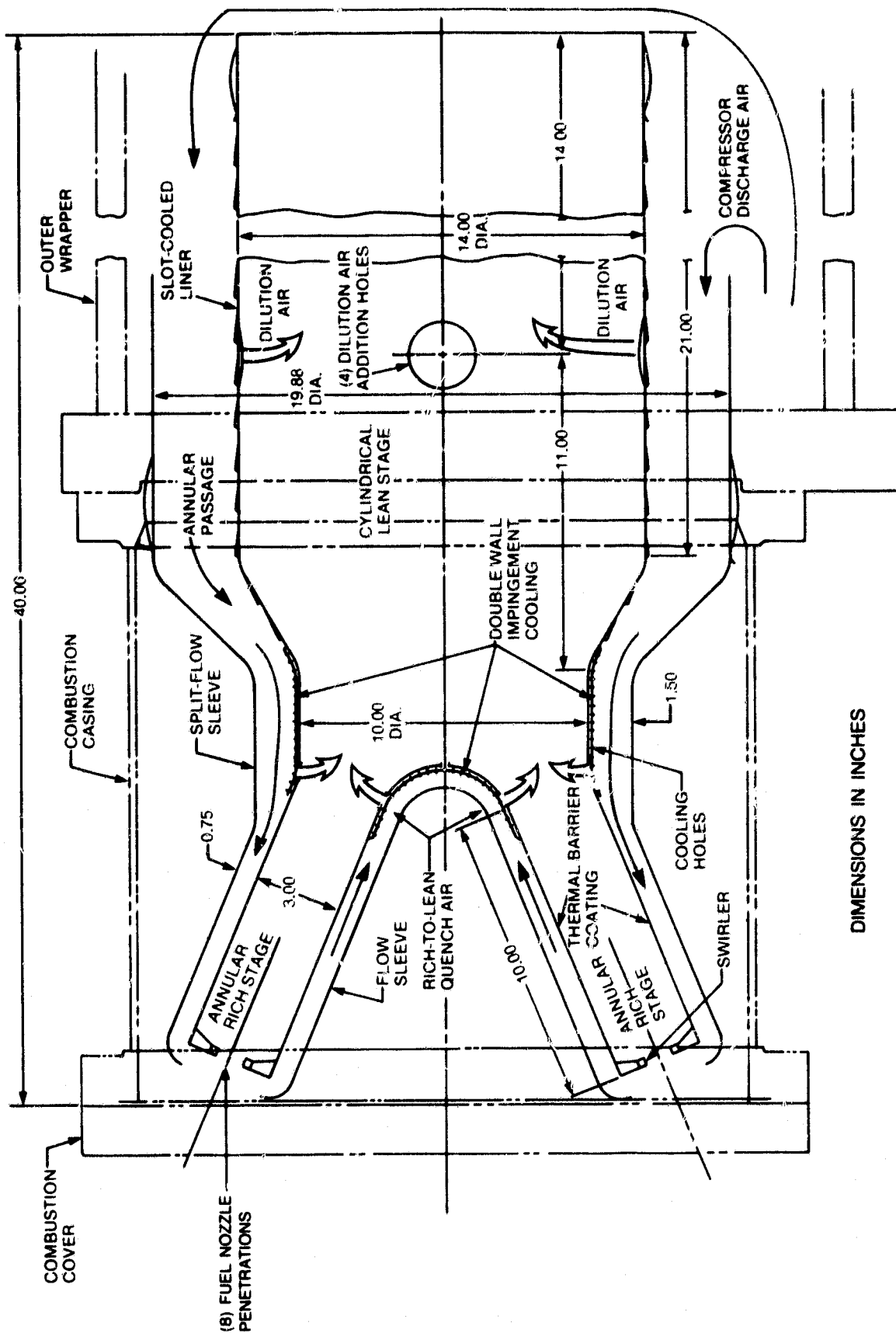


Figure 10-2. Rich-lean combustor for MS7001E application

The rich stage is encased in a flow sleeve to guide the airflow and to maintain sufficient backside air velocity to adequately cool the liner. The portion of the flow sleeve inside the annulus is a cone. The outside flow sleeve must be made in two parts and mechanically assembled in the proper position with respect to the liner. As shown, the flow sleeves form guide passages for the air but after more detailed design, the flow sleeve may be a portion of an impingement cooling design.

The annular rich stage provides a method for minimizing the jet penetration distance for the rich-to-lean quench air. This critical process is accomplished near the annulus exit. In Figure 10-2, only one row of quench holes is shown, but in the actual design multiple rows will be used to optimize the mixing. Also, note that this transition region uses a double wall impingement cooled structure. The local gas and metal temperature gradients induced by the air jets would probably cause spalling of a thermal barrier coating. An alternative, which could be explored during the test program, is the use of slot cooling. However, adding cooling air immediately establishes a stoichiometric flame region near the wall. This would be detrimental to both cooling and NO_x . Attempting to establish a rather thick film and minimizing mixing of the rich gas may be an effective method to handle this critical area.

The annular rich stage section discharges into a throat followed by a step increase to a 35.5 cm (14 in.) diameter which is the production MS7001E size. The sudden expansion establishes recirculation zones to aid in the lean zone flame stability. This flame zone is similar to many conventional combustors, and film (slot) cooling will be used in the walls.

The dilution holes are located 35.5 cm (14 in.) from the end of the liner. This location is identical to current production and was used here to ensure that the combustor exit pattern and pressure factors will be within machine limits. Current design practice is to operate with a pattern factor of about 0.12 in the heavy duty machines compared with the 0.25 or higher factor for aircraft.

The above discussion reviewed a new conceptual design for a full-scale rich/lean heavy-duty combustion system that is compatible with current MS7001E production hardware and cycle conditions, and should meet dry low NO_x goals with high nitrogen content fuels. This design includes only a 4% pressure drop while increasing the liner size to accommodate the machine flows. Predicting the NO_x emissions would be a rough estimate at best but, based on the excellent NO_x performance of Concept 3-1 and with careful detailed design and testing optimization, the combustor has the potential for meeting program goals in actual hardware.

10.2 CONCEPTUAL DESIGN OF LEAN/LEAN COMBUSTOR FOR MS7001E CYCLE

10.2.1 Introduction

The lean/lean series staged combustor Concept 4 was tested at MS7001E conditions. The data obtained was very encouraging and NO_x goals were met at most of

the load conditions for fuels with nitrogen content up to 0.25 weight percent. Some problems still remaining for this design are low combustion efficiencies at low load and just after transition, and high NO_x and smoke at medium load (pilot-only operation). In Section 9.2.1 it was shown that the majority of the NO_x was generated in the pilot stage. The two designs presented here should resolve the above problems and also have features to improve the emissions and smoke further. In the previous design, the pilot stage operated very lean at low loads and very rich at medium loads. The lean burning produced low combustion efficiency, and rich burning produced high smoke. In one of the designs presented, the pilot stage (mainly pilot dome) operates at about constant equivalence ratio ($\Phi = 0.6$). In the other design, the transition point is shifted to lower power and the main stage fuel flow is staged.

10.2.2 Discussion

The lean/lean design for the MS7001E cycle is a series staged combustor. The main stage uses hot gases from the pilot stage for sustaining combustion. The proposed design has a very short pilot stage and main stage (see Figure 10-3). This avoids excessive residence time, but provides adequate length for complete combustion. The pilot stage uses four variable geometry swirlers. However, an alternate version is presented which employs fuel staging of the second stage.

Variable Area Pilot Swirler Design

At lightoff and low power conditions, all of the fuel is introduced into the pilot stage. With the variable geometry feature, the pilot stage can be made to operate lean ($\Phi = 0.6$) for reduced NO_x and smoke. A dome equivalence ratio of $\Phi = 0.6$ should also produce very high combustion efficiency and good flame stability. As the fuel flow in the pilot stage is increased, the pilot swirler area is increased so that the equivalence ratio remains essentially constant.

At high-power conditions, fuel is injected into the main stage. At these conditions, the fuel flow to the pilot stage is reduced. The pilot swirler area is also reduced to maintain constant equivalence ratio. Both stages are always operated with lean fuel/air mixtures. The pilot dome Φ is maintained at approximately 0.6. Table 10-2 and Table 10-3 present the flow splits and the equivalence ratios for this design.

The pilot swirler used for this design is an axial-radial type. The axial flow primary swirler is fixed while the secondary radial flow swirler has a variable area. At no-load and high-power conditions, the swirler area is at a minimum. The area is increased for medium loads. Because of this increase in area, the pressure drop is reduced, as shown in Table 10-2.

Fixed Pilot Swirler Design

At lightoff and low-power conditions, all of the fuel is introduced into the pilot stage. The pilot dome equivalence ratio is approximately 0.6 for the no-load condition. This produces very high combustion efficiency and good flame stability. As the load is increased, the pilot dome becomes richer. To avoid very high equivalence

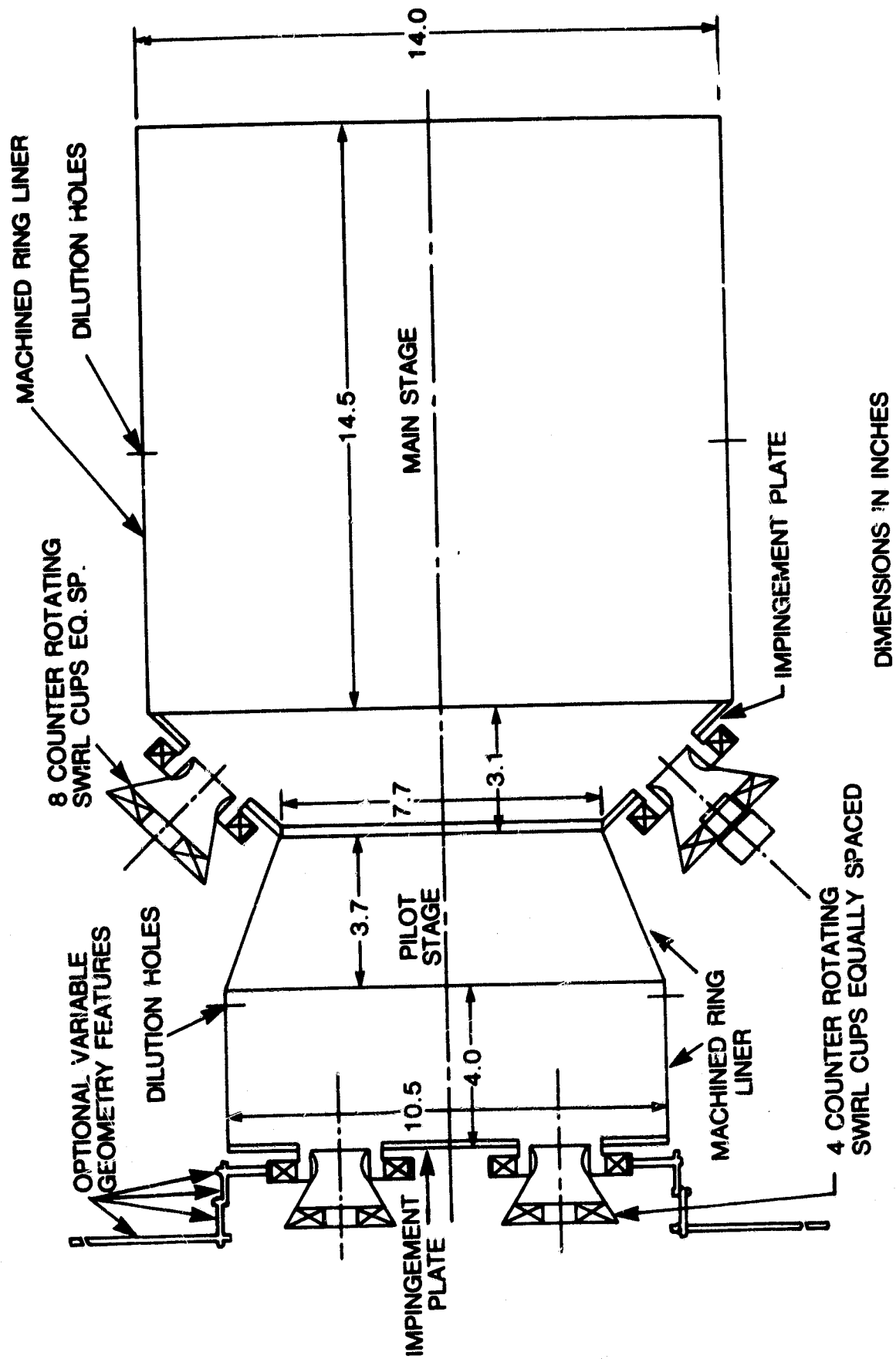


Figure 10-3. Conceptual design of lean/lean combustor, MS7001E cycle

Table 10-2
MS7000 COMBUSTOR – LEAN/LEAN DESIGN
(Variable Geometry Pilot Swirler)
FLOW SPLIT (Percentage of W_c)

Load (%)	0	50	70	70	90	100
Pilot Swirler	9.0	30.0	38.0	9.0	9.0	9.0
Dome Cooling	4.2	3.2	3.0	4.2	4.2	4.2
Dilution	10.0	7.7	6.8	10.0	10.0	10.0
Liner Cooling	8.8	6.8	6.0	8.8	8.8	8.8
Total Pilot	32.0	47.7	53.8	32.0	32.0	32.0
Main Swirler	35.0	26.9	23.8	35.0	35.0	35.0
Dome Cooling	5.2	4.0	3.5	5.2	5.2	5.2
Dilution	10.0	7.7	6.8	10.0	10.0	10.0
Liner Cooling	17.8	13.7	12.1	17.8	17.8	17.8
Total Main Stage	68.0	52.3	46.2	68.0	68.0	68.0
Pressure Drop	10%	4.5%*	3.2%*	6.8%	6%	5.8%

*Pressure drops for 50% and 70% load points are 7.5% and 6.8%, respectively, for fixed geometry.

Table 10-3
MS7000 COMBUSTOR – LEAN/LEAN DESIGN
(Variable Geometry Pilot Swirler)
COMBUSTOR EQUIVALENCE RATIOS

LOAD (%)	0	50	70	70	92	100
f/a Overall	0.0054	0.0141	0.0183	0.0183	0.0235	0.0253
Percentage Pilot Fuel	100	100	100	29	23	21
Φ Overall	0.78	0.204	0.265	0.265	0.340	0.366
Φ Pilot Swirl Cup	0.867	0.680	0.697	0.854	0.869	0.854
+ Dome Cooling	0.591	0.613	0.646	0.582	0.592	0.582
+ Pilot Dilution	0.336	0.498	0.554	0.331	0.337	0.331
+ Pilot Liner Cooling	0.244	0.428	0.493	0.240	0.244	0.240
Φ Main Dome	0	0	0	0.469	0.651	0.719
Predicted NO_x (g/kg Fuel)	3.2	5.4	6.3	2.6	4.1	4.7

ratios in the pilot dome, and therefore high smoke, the main stage is fueled at lower load conditions (50% load as compared to 70% for the variable geometry design).

At transition to the main stage, only half of the main stage swirlers are fueled. This approach avoids very low main stage equivalence ratios. The combustor flow splits and the equivalence ratios are shown in Tables 10-4 and 10-5, respectively.

Both Designs

Four counter-rotating swirl cups are mounted on the dome of the pilot stage, concentric with air-atomizing fuel nozzles. The high level of mixing and turbulence (produced by counter rotating swirl cups) and small droplets (produced by the nozzles) result in very uniform fuel/air mixtures. The result is therefore, low smoke and emissions levels from the pilot stage. Tables 10-3 and 10-5 also show the predicted NO_x levels for both designs. The highest NO_x level produced from the pilot stage is predicted to be 6.3 g/kg.

In the main stage, eight swirlers are mounted around the combustor. These swirlers also employ air-atomizing fuel nozzles. At high-power conditions, a large portion of the fuel flow is introduced into the main stage. These swirl cups are also counter-rotating for good mixing. At these conditions, the overall fuel/air equivalence ratio in the main stage is very lean and with the intense mixing and turbulence caused by the main stage swirl cups, the NO_x emissions should also be very low, as shown in Tables 10-3 and 10-5.

The designs presented here are not suitable for fuels with high fuel bound nitrogen content. The conversion is expected to be of the order of 80% which is typical of lean/lean burning combustors. At this conversion rate, fuels with $\text{FBN} > 0.25$

Table 10-4
MS7000 COMBUSTOR – LEAN/LEAN DESIGN
(Fixed Geometry Pilot Swirler)
FLOW SPLIT (Percentage of W_c)

Pilot Swirler	9.0
Dome Cooling	4.2
Dilution	10.0
Liner Cooling	8.8
Total Pilot	32.0
 Main Swirler	 35.0
Dome Cooling	5.2
Dilution	12.0
Liner Cooling	15.8
Total	68.0

Table 10-5
MS7000 COMBUSTOR – LEAN/LEAN DESIGN
(Fixed-Geometry Pilot Swirler)
COMBUSTOR EQUIVALENCE RATIOS

LOAD (%)	0	50	50	70	92	100
<i>f/a</i> Overall	0.0054	0.0141	0.0141	0.0183	0.0235	0.0253
Percentage Pilot Fuel	100	100	39	29	23	21
Φ Overall	0.78	0.204	0.204	0.265	0.340	0.366
Φ Pilot Swirl Cup	0.867	2.267	0.884	0.854	0.869	0.854
+ Dome Cooling	0.591	1.545	0.603	0.582	0.592	0.582
+ Pilot Dilution	0.336	0.879	0.343	0.331	0.337	0.331
+ Pilot Liner Cooling	0.244	0.638	0.249	0.240	0.244	0.240
Φ Main Dome	0	0	0.310*	0.469	0.651	0.719
Predicted NO_x (g/kg Fuel)	3.2	6.3	3.1	2.6	4.1	4.7

*Half of main-stage swirlers fueled; therefore, effective $\Phi = 0.62$

weight percent generate very high NO_x and therefore EPA requirements for NO_x emission cannot be met. Both of these designs, however, can be used with residual fuel (FBN < 0.25% by weight). Both have features for meeting EPA emissions requirements. The NO_x emission and the smoke should be below the limit and the combustion efficiency should be over 99%. If these designs are used with clean fuels, ultra low NO_x levels can be expected.

10.3 APPLICATION OF NASA/DOE DRY LOW NO_x HEAVY FUELS PROGRAM RESULTS TO OTHER CYCLES

10.3.1 Lean/Lean Concept 6 for the LM2500 Cycle

The annular version of Concept 6, designed for the LM2500 engine, is a lean/lean parallel-staged double-annular combustor with 30 fuel injectors and 30 swirl cups in each of the two annuli. The Double Annular Dome Combustor, as illustrated in Figure 10-4, features the use of two primary combustion zones, or domes, separated by a short centerbody. In this parallel-staged combustor design concept, the outer dome is designed to operate with lower airflows than those supplied to the inner dome. Only the outer dome is fueled at idle and other low engine-power operating conditions. In this manner, near-stoichiometric fuel/air mixtures and long residence

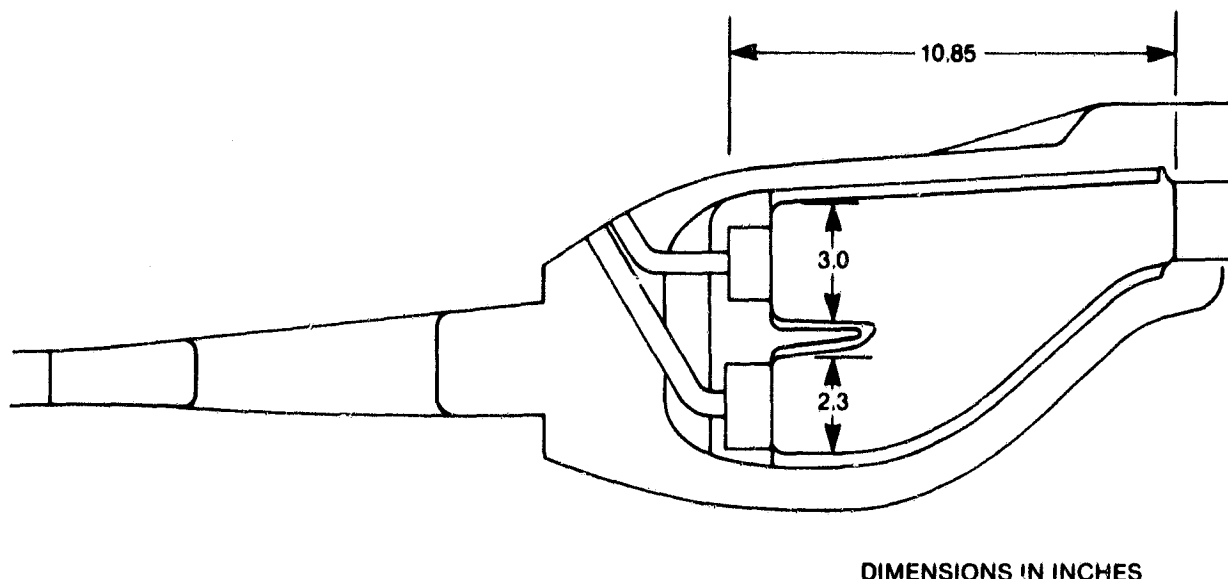


Figure 10-4. LM2500 Concept 6, double-annular parallel-staged low NO_x combustor

times, due to the low air velocities, are maintained in the outer dome at the low engine-power operating conditions. As a result, low CO and HC emission levels at these operating conditions are obtained. At high engine power operating conditions, both stages are fueled and most of the total fuel flow is supplied to the inner dome. Consequently, lean fuel/air mixtures are obtained in both domes, and very short residence times are obtained in the inner dome due to its high air velocities. As a result, low NO_x and smoke emission levels are obtained.

A list of aerodynamic design parameters for this concept is presented in Table 10-6, along with those for the NASA/GE ECCP CF6-50 double annular combustor and the NASA/GE QCSEE double annular combustor, for comparison. Airflow distribution for the LM2500 double annular concept is presented in Table 10-7 and the combustor equivalence ratios and estimated NO_x emission levels for several operating conditions are presented in Table 10-8. The first NO_x level presented in this table was based on Concept 6 with a correction made for differences in residence time between the Concept 6 as tested and the residence time for an LM2500 flowpath. An estimated NO_x emission level for full-load conditions, based on NASA/GE ECCP test results, is also presented in Table 10-8. This lower NO_x level is probably more representative of the potential of the parallel-staged double-annular system. However, some additional development would be required to achieve EPA standards at 75 ppm plus heat rate corrections.

Test data correlations for NASA/DOE Concept 6 were used to estimate NO_x emissions with SRC-II fuel and with residual fuel. However, the conversion efficiency of FBN is believed to be very configuration-dependent and these estimates for the LM2500 double annular combustor are only approximate.

Table 10-6
LM2500 LOW NO_x COMBUSTOR
NASA/DOE CONCEPT 6
COMBUSTOR AERODYNAMIC DESIGN PARAMETERS

Combustion System	CF6-50 Double Annular	QCSEE Double Annular	LM2500 Double Annular
Combustor Length cm (in.)	32.8 (12.9)	18.5 (7.3)	26.4 (10.4)
Outer Dome Height cm (in.)	6.9 (2.7)	5.6 (2.2)	7.6 (3.0)
Inner Dome Height cm (in.)	6.1 (2.4)	4.6 (1.8)	5.8 (2.3)
Length/Dome Height - Outer	12.2 (4.8)	8.4 (3.3)	8.9 (3.5)
Length/Dome Height - Inner	13.7 (5.4)	10.4 (4.1)	11.4 (4.5)
Number of Fuel Injectors	60	40	60
Reference Velocity (ft/s)	75	59	50
Space Rate MJ/hr-m ³ -atm	0.227	0.302	0.179
(Btu/hr-ft ³ -atm, ×10 ⁻⁶)	6.1	8.1	4.8
Outer Dome Velocity m/s (ft/s)	9.8 (32)	6.7 (22)	6.7 (22)
Inner Dome Velocity m/s (ft/s)	26.5 (87)	22.0 (72)	18.9 (62)
Outer Passage Velocity m/s (ft/s)	36.6 (120)	50.0 (164)	37.5 (123)
Inner Passage Velocity m/s (ft/s)	46.0 (151)	62.6 (205)	36.0 (118)

Table 10-7
AIRFLOW SPLITS
FOR LM2500 CONCEPT 6
(Lean/Lean)

Pilot Swirlers	17.0%
Dome Cooling	4.3
Dilution	<u>5.0</u>
Total Pilot Stage	26.3%
Main Swirlers	30.7%
Dome Cooling	4.0
Dilution	<u>8.0</u>
Total Main Stage	42.7%
Outer Liner Cooling	8.6%
Centerbody Cooling	6.1
Inner Liner Cooling	10.8
Aft Dilution	<u>5.5</u>
Total Aft Section	31.0%

Table 10-8
EQUIVALENCE RATIOS AND ESTIMATED NO_x EMISSIONS
FOR LM2500 CONCEPT 6

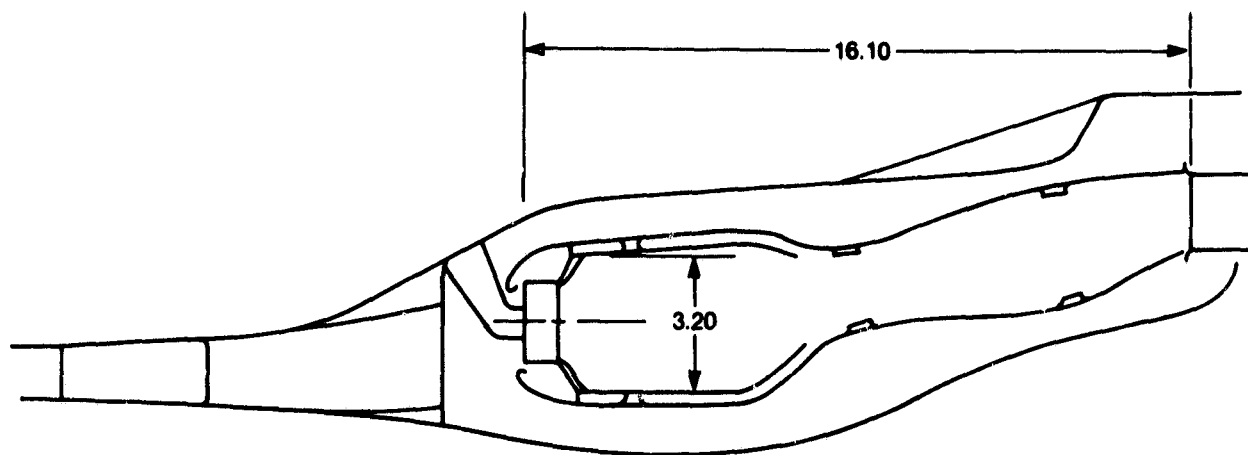
Load Condition	Idle	70%	70%	100%
<i>f/a</i> Overall	0.0122	0.0214	0.0214	0.0241
Percentage Pilot Fuel	100	100	35	35
Φ Overall	0.18	0.32	0.32	0.36
Φ Pilot Swirlers	1.06	1.86	0.65	0.74
+ Dome Cooling	0.85	1.49	0.52	0.59
+ Primary Dilution	0.69	1.21	0.42	0.48
Φ Main Swirlers	0	0	0.67	0.76
+ Dome Cooling	0	0	0.59	0.67
+ Primary Dilution	0	0	0.48	0.54
Predicted NO _x	5.2	15.0	9.7	13.0
Based on ECCP D.A.				9.4
With Residual Fuel				17.6
With SRC II Fuel				23.4

10.3.2 Rich/Lean Concept 3 for the LM2500 Cycle

Concept 3, adapted for the LM2500 engine and illustrated in Figure 10-5, is a rich/lean two-stage annular combustor with 30 fuel injectors and 30 swirl cups in the rich stage dome. The rich stage operates with a high equivalence ratio, which results in low NO_x generation and low availability of oxygen for fuel-bound nitrogen conversion. At the end of the rich stage, the area of the combustor flowpath is decreased to accelerate the flow to a high velocity and to provide a reduced mixing distance for the second-stage air jets in the quick-quench region. The quench air is introduced from the outer liner and from the inner liner through a staggered hole pattern arrangement to provide very rapid mixing with the hot gases from the rich stage. The quench air dilutes the mixture to a low equivalence ratio which results in low NO_x generation in the second stage, where the combustion process is completed.

The combustor dome and primary zone liners are impingement cooled. The dome cooling air is introduced into the primary zone through small gaps around each of the dome swirlers. The rich stage liner cooling air is introduced through wall slots immediately upstream of the quench section.

Flow splits for this design are presented in Table 10-9, and the fuel/air equivalence ratios at three engine load conditions are presented in Table 10-10. Due mainly to the short residence times for this version of Concept 3, the estimated NO_x emission levels are quite low, even with fuel containing 0.46 percent FBN.



DIMENSIONS IN INCHES

Figure 10-5. LM2500 Concept 3, rich/lean series-staged low NO_x combustor

**Table 10-9
AIRFLOW SPLITS
FOR LM2500 CONCEPT 3 (Rich/Lean)**

Dome Swirler	10.0%
Dome Cooling	5.0
Primary Zone Dilution	4.0
Total Rich Stage	19.0%
Primary Imp. Cooling	11.0%
Quench Flow	24.0
Neck Cooling	4.0
Total Quench Flow	39.0%
Aft Liner Cooling	18.0%
Secondary Dilution	24.0
Total Combustor	100.0%

Table 10-10**EQUIVALENCE RATIOS AND PREDICTED NO_x EMISSIONS
FOR LM2500 CONCEPT 3**

Load Condition	Idle	70%	100%
<i>f/a</i> Overall	0.0122	0.0214	0.0241
Equivalence Ratios:			
Rich Stage	0.95	1.67	1.88
Quench Stage	0.31	0.55	0.62
Overall	0.18	0.32	0.36
Predicted NO _x	1.1	4.3	5.0
With 0.46% FBN			9.5

10.3.3 Lean/Lean Combustor for LM5000 Application

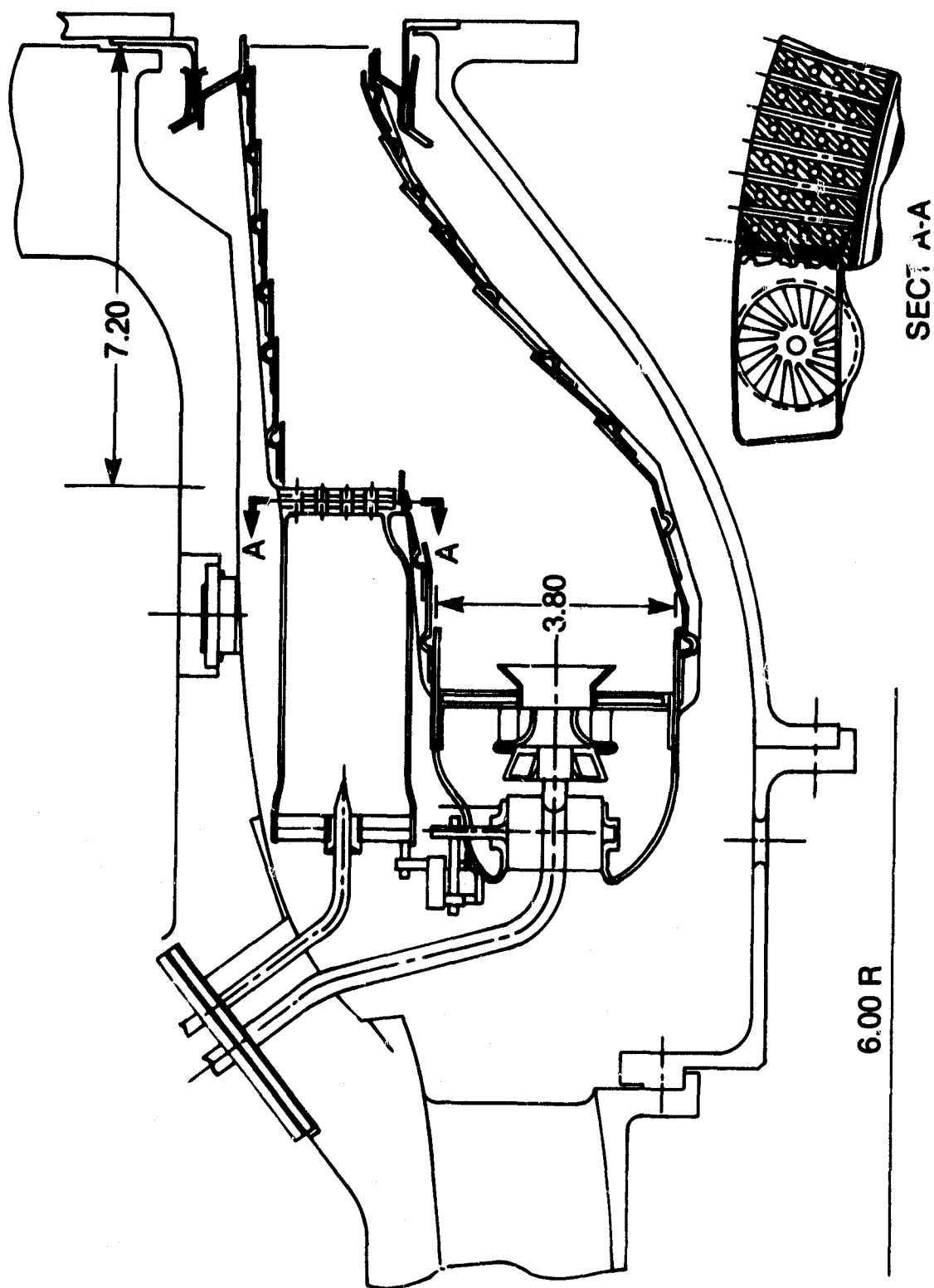
A low NO_x, lean/lean parallel-staged combustor, designed for the LM5000 engine, is illustrated in Figure 10-6. This concept has thirty cylindrical main stage premixing tubes positioned around the outside of the annular pilot stage. Variable register plates are used at the inlets of the premixing tubes to modulate the main stage airflow, and variable geometry vanes are used to modulate the pilot stage airflow. A conventional arrangement of 30 counter-rotating swirl cups and 30 fuel nozzles are used for the pilot stage. The main stage premixing tubes transition into rectangular ducts that supply the fuel/air mixture to an annular perforated plate flameholder. The flameholder is cooled by high velocity air that flows through small radial holes in the flameholder plate.

Combustor flow parameters for this concept are presented in Table 10-11 for two engine operating conditions. At idle conditions, the pilot stage variable geometry is open and the premixing tube register plates are partially closed. All of the engine fuel flow is burned in the pilot stage. At high engine power conditions the pilot stage fuel is shut off and all of the engine fuel flow is premixed and burned in the main stage. At full load conditions the premixing tube register plates are wide open and the pilot stage variable geometry is closed to reduce the pilot stage dome airflow to a very small quantity. The main stage variable geometry can be modulated to provide an equivalence ratio of about 0.55 in the main stage premixing tubes at all of the high-power and intermediate operating conditions.

Combustor fuel/air equivalence ratios and predicted NO_x emissions at the engine idle and full load conditions are presented in Table 10-12. With fuel/air premixing and with very short residence times, the predicted NO_x emission levels at full load conditions with ERBS fuel are very low. For this lean premixing combustor, with a very short burning residence time (1.3 ms), conversion efficiency of FBN is very difficult to predict.

The combustor configuration shown in Figure 10-6 has been designed under another program* and will be tested late in 1981 with Jet A fuel.

* GE/NASA Advanced Low Emissions Combustor Program — Contract NASA-22006.



DIMENSIONS IN INCHES

Figure 10-6. LM5000 Concept 6, parallel-staged low NO_x combustor with premixing and variable geometry

Table 10-11
AIRFLOW SPLITS
FOR LM5000 CONCEPT 6 (LPP + Var. Geom.)

	Idle	100%
Pilot Swirlers	17.8	7.2
Dome Cooling	4.8	1.9
Liner Cooling	<u>6.4</u>	<u>6.4</u>
Total Pilot Stage	29.0	15.5
Main Premix Duct	47.2	60.7
Outer Liner Cooling	12.3	12.3
Inner Liner Cooling	5.4	5.4
Dilution	<u>6.1</u>	<u>6.1</u>
Total Aft Section	23.8	23.8

Table 10-12
EQUIVALENCE RATIOS AND PREDICTED NO_x
for LM5000 CONCEPT 6 (LPP + Var. Geom.)

Load Condition	Idle	100%
<i>f/a</i> Overall	0.0120	0.0225
Percentage Pilot Fuel	100	0
Φ Overall	0.178	0.333
Φ Pilot Swirlers	1.00	0
+ Dome Cooling	0.79	0
Φ Premix Duct	0	0.55
Predicted NO _x	5.6	3.2

Appendix A

**LOW NO_x HEAVY FUEL COMBUSTOR CONCEPT PROGRAM
REPORT – PRELIMINARY RESULTS ON A LOW NO_x
LEAN BURN CATALYTIC COMBUSTION CONCEPT**

TEST SERIES 1

January 12, 1980

**Prepared for
General Electric Company
Gas Turbine Division
1 River Road
Schenectady, New York 12345**

**Prepared by
R. Chang, E. Chu, H. Tong
Acurex Corporation
Energy and Environmental Division
485 Clyde Avenue
Mountain View, California 94042**

Appendix A

LOW NO_x HEAVY FUEL COMBUSTOR CONCEPT PROGRAM REPORT – PRELIMINARY RESULTS ON A LOW NO_x LEAN BURN CATALYTIC COMBUSTION CONCEPT

INTRODUCTION

The objective of the present study is to examine a low NO_x, lean-burn, catalytic combustion concept for fuels containing fuel-bound nitrogen. Under lean-burn conditions, fuel NO_x formation predominates, and thermal NO_x is subdued. Suppression of fuel NO_x formation therefore becomes a primary concern.

The present concept is based on findings by various investigators^(1,2) that NO_x in combustion effluents can actually be reduced by the injection of hydrocarbon-oxygen mixtures in one case and NH₃ in another. It seems that the presence of various intermediate species of reaction (CO, CH_x, CN, NH_x), simultaneously with NO_x will sometimes reduce NO_x to N₂ given favorable temperatures and residence times. In the present study, nitrogen-doped fuel is introduced into a first-stage catalyst monolith where it is partially converted to intermediate products as well as some NO_x. The catalytic reaction is then temporarily "frozen" by introducing a small gap between the first and second stages. This enables the intermediate products of reaction to interact with the NO_x present, hopefully to reduce the NO_x to N₂. The gap is then followed by a second set of catalyst monoliths where fuel conversion is completed.

Since the concept is highly exploratory, the optimum conditions, if any exist, cannot be defined a priori. In the present study, two reactor arrangements were examined for diesel fuel doped with pyridine under various conditions by varying the fuel/air ratio and the approach velocity and monitoring the reactor effluents. If the concept is viable, there should be some combination favoring low NO_x formation.

METHOD OF APPROACH

All tests were performed in the Acurex subscale catalytic combustion test facility shown schematically in Figure A-1. The catalyst was mounted in a stainless steel test section lined with a ceramic insulating material. Visual observation of the catalyst reactor was made from the aft end of the test section through a quartz window. Bed temperatures were monitored with thermocouples located at various points in the catalyst bed. Exhaust gas composition was monitored continuously with gas analyzers. In a few studies, measurements of NH₃ and HCN concentrations were also made by absorption in solution and then reading with ion selective electrodes. No. 2 diesel fuel doped with pyridine (0.5 weight percent N) was used as the test fuel and was introduced as a fine spray with an air-atomized injector into a mixing zone above the combustor.

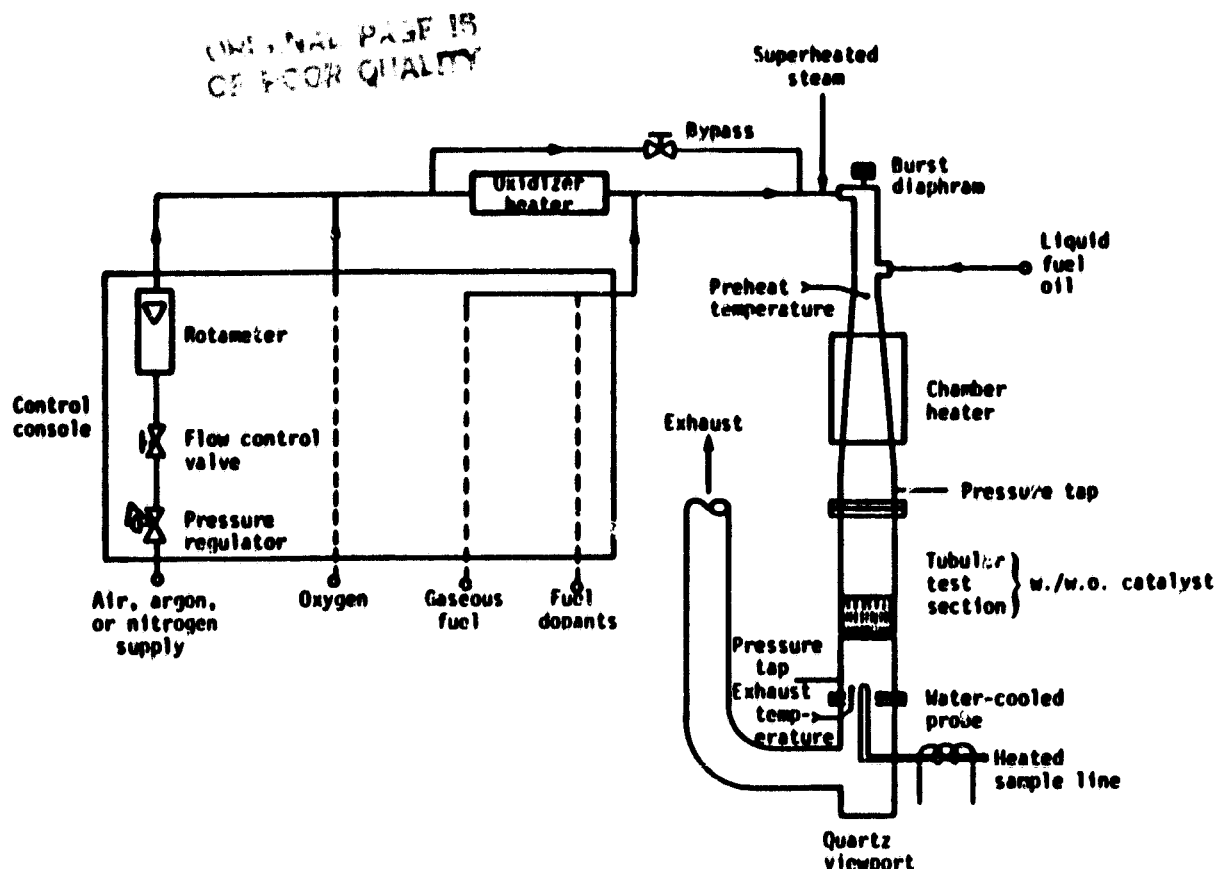


Figure A-1. Catalytic combustion test facility

The test conditions examined were:

Inlet pressure:	1 atm
Inlet temperature:	700 °F
Reference velocity:	30-80 ft/s
F/A (fuel/air) ratio:	0.02-0.035 (by weight)

Two catalyst arrangements were examined. The first (Figure A-2) consisted of two large cell monoliths (2 in. diameter, 1 in. thick, 9 cells/in.²) and one medium cell monolith (2 in. diameter, 1 in. thick, 16 cells/in.²) in series as the front section followed by a rear section made up of two small cell monoliths (2 in. diameter, 1 in. thick, 200 cells/in.²). A gap of 1.5 in. separated the two sections. In the second arrangement (Figure A-3), two large cell monoliths (2 in. diameter) made up the front section and two medium cells (2.5 in. diameter) and one small cell monolith (2.5 in. diameter) the rear section. A gap of 2.5 in. separated the two sections.

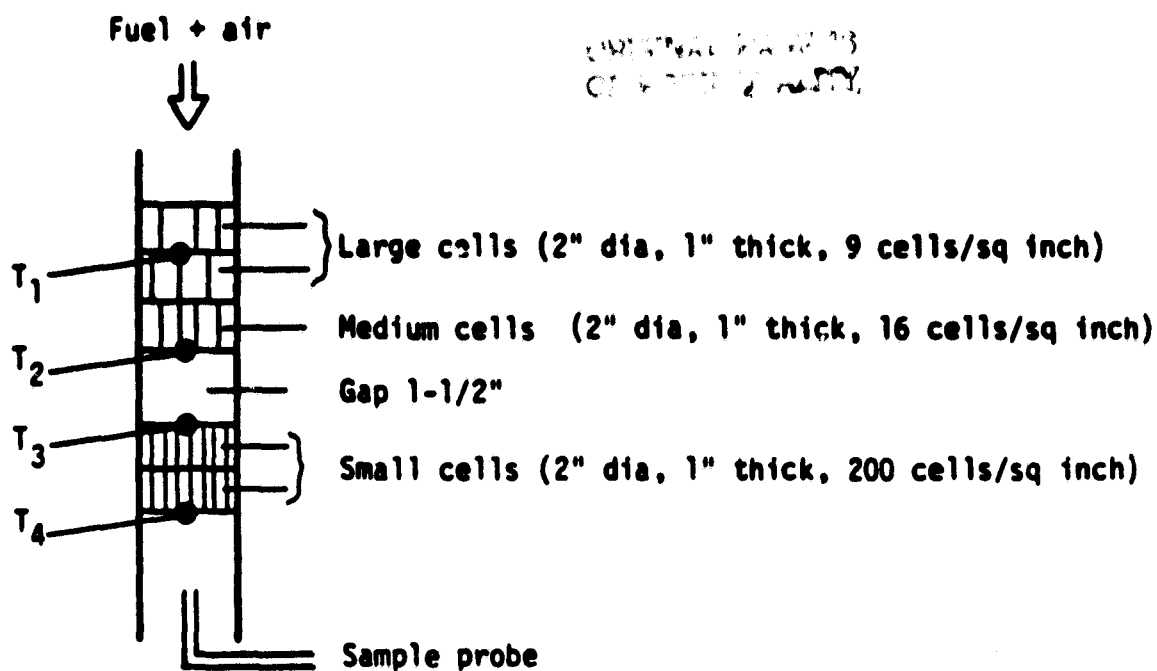


Figure A-2. Schematic of catalyst monolith arrangement 1

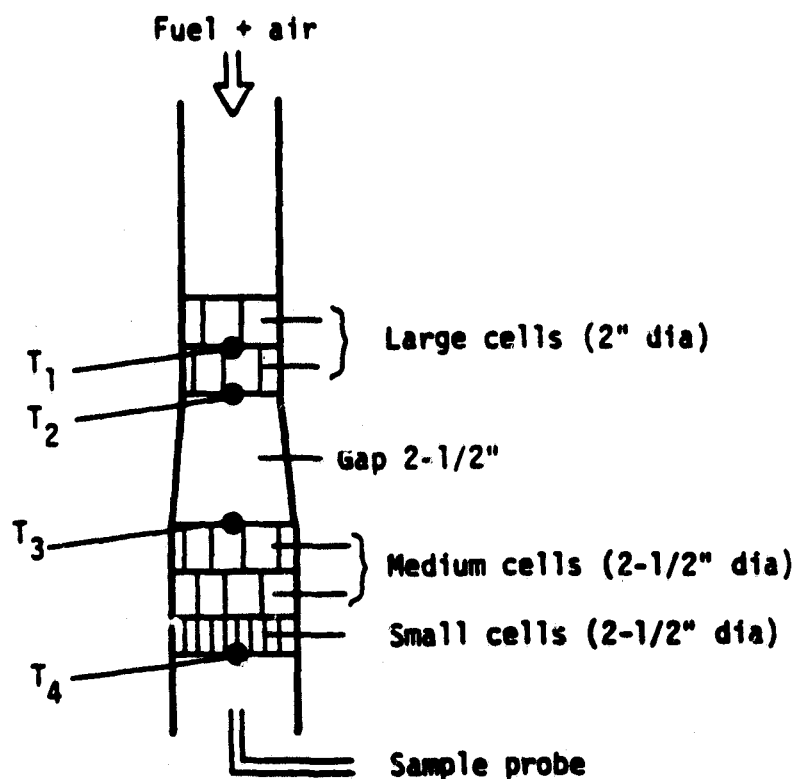


Figure A-3. Schematic of catalyst monolith arrangement 2

RESULTS AND DISCUSSION

Results are summarized in Tables A-1a, A-1b, and A-2.

Tables A-1a and A-1b summarize results with catalyst arrangement 1. Table A-1a is a baseline study using pure No. 2 diesel. As expected, NO_x emissions were low in the absence of fuel nitrogen. Table A-1b assesses the same catalyst arrangement with the pyridine-doped diesel. The first four points were preliminary studies to assess the general stability of the system. At the fuel/air ratios and approach velocities used, combustion was stable and efficient with low unburned hydrocarbon (UHC) and CO emissions. Fuel NO_x conversion, however, also approached 100%.

The next series of points summarizes the effect of changing the approach velocity at more or less constant fuel/air ratios. Again, combustion was complete, but NO_x conversions were high, averaging about 75% and remaining rather steady as the velocity changed.

The fuel/air ratio was then changed gradually at constant approach velocity. As the fuel/air mixture got leaner, the NO_x conversion also decreased, but with a corresponding rise in CO and UHC emissions. This indicated that combustion was incomplete. Unfortunately, no measurements were made on the presence of other nitrogen species, in particular ammonia and cyanide. At the temperatures encountered in the combustor, it is expected that all the pyridine would be dissociated.

The second catalyst arrangement was then studied, and results are summarized in Table A-2. The major differences in this arrangement compared to the first are:

- The gap is wider (2.5 in. versus 1.5 in.)
- The front section is less reactive (two large-cell monoliths versus two large plus one medium-cell monolith)
- The back section is more reactive (larger diameter monoliths)

The results show the same general trend: NO_x emissions were low at low fuel/air ratios. This time, however, some measurements were also made on NH_3 and HCN. For the points where NO_x emissions were low, NH_3 and HCN emissions were also low. Since NH_3 , HCN, NO_x and N_2 are the primary nitrogenous species formed in most combustion systems, our findings above are strong indications that the fuel nitrogen has probably been converted to gaseous nitrogen. The combustion in the second arrangement with the wider gap, however, seemed less stable than in the first arrangement. Bed temperatures fluctuated more in this arrangement, and it was more difficult to maintain a steady test condition. In fact, we had tried an earlier series of test runs with a catalyst arrangement similar to Figure A-2 except with a gap of 5 in. The combustion was so unstable that we failed to maintain a constant test condition. These results are therefore not reported.

In both arrangements, the systems were not operating adiabatically, as evidenced by the low temperatures in the catalyst bed. At a fuel/air ratio of 0.03 and 0.024, adiabatic bed temperatures should approach 2800 °F and 2400 °F, respectively. The gap temperatures (measured in arrangement 1 and estimated in arrangement 2

Table A-1a
COMBUSTION RESULTS ON CATALYST ARRANGEMENT 1 (Figure A-2), DIESEL

f/a	TA (%)	V (ft/s)	Temperature Distribution*					Emissions						
			Front Section		Gap	Back Section		NO_x (ppm)	$NH_3 + HCN$ (ppm)	UHC (ppm)	CO (ppm)	CO_2 (%)	O_2 (%)	
			T_1	T_2	T_G	T_3	T_4							
														Theoretical/ Actual
0.034	200	30	1325	1444	1065	1565	2196	N.A.†/20	$10 \sum XN +$	—	1	50	7	11.8
0.035	200	30	1337	1465	1090	1589	2245	N.A.†/20		—	2	50	7	11.6

*See Figure A-2 for actual location of temperature measured

†N.A. = not applicable

$\sum XN = NO_x + HCN + NH_3$

$f/a =$ fuel/air ratio, $TA =$ theoretical air, $V =$ approach velocity

Table A-1b
COMBUSTION RESULTS ON CATALYST ARRANGEMENT 1 (Figure A-2),
DIESEL + PYRIDINE

f/a	TA (%)	V (ft/s)	Temperature Distribution*					Emissions						
			Front Section		Gap	Back Section		NO _x (ppm)	NH ₃ + HCN (ppm)	UHC (ppm)	CO (ppm)	CO ₂ (%)	O ₂ (%)	
			T ₁	T ₂	T _G	T ₃	T ₄							
0.029	240	40	—	—	—	—	2266	294/300	102	—	3	50	6.7	12.4
0.029	240	36	1471	1576	(1259)†	1647	2197	294/300	102	—	—	30	6.6	12.5
0.029	240	36	1377	1681	1560	1752	2270	294/300	102	—	6	30	6.8	12.0
0.03	230	53	1404	1786	1831	1838	2227	310/300	97	—	5	40	6.9	12.0
0.034	200	53	1221	1679	1548	1634	2224	350/260	74	—	30	50	7.5	11.0
0.033	210	55	1227	1695	1650	1644	2183	334/250	75	—	20	40	7.4	11.5
0.033	210	63	1243	1744	1769	1691	2220	334/260	78	—	13	50	7.5	11.5
0.034	200	72	1271	1806	1938	1765	2229	350/250	71	—	7	30	7.2	11.5
0.035	200	82	1275	1802	1995	1750	2232	350/250	71	—	7	60	7.2	11.5
0.03	230	67	1284	1827	—	1867	2393	310/260	84	—	4	50	7.5	10.7
0.025	280	72	1225	1637	1628	1681	2010	252/235	93	—	3	70	6.3	12.3
0.023	300	72	1172	1454	1476	1552	1710	235/190	81	—	31	1540	5.5	13.5
0.021	330	70	1114	1376	1363	1432	1555	215/9	42	—	1500	1030	1.4	18.0
0.024	290	69	1163	1436	1407	1495	1636	244/8	33	—	3000	1510	2.3	17.4

*See Figure A-2 for actual location of temperature measured

†No actual gap temperature was measured, average of T_2, T_3 taken f/a = fuel/air ratio, TA = theoretical air, V = approach velocity

Table A-2
COMBUSTION RESULTS ON CATALYST ARRANGEMENT 2 (Figure A-3),
DIESEL + PYRIDINE

f/a	T_A (%)	V (ft./s)	Temperature Distribution*					Emissions						
			Front Section		Gap	Back Section		NO_x (ppm)	Percent Conversion	$NH_3 + HCN$ (ppm)	UHC (ppm)	CO (ppm)	CO_2 (%)	O_2 (%)
			T_1	T_2	T_G^+	T_3	T_4							
0.032	215	37	1374	1475	(1518)	1561	2097	326/300	92	—	5	>1200	7.1	11.5
0.031	222	38	1380	1475	(1517)	1559	2003	320/290	91	—	4	>1200	7.0	11.5
0.027	256	43	1338	1440	(1476)	1513	1860	276/260	96	—	2	510	6.4	12.0
0.026	265	40	1329	1412	(1440)	1469	1781	274/220	80	—	12	—	5.9	13.5
0.024	287	44	1300	1368	(1399)	1430	1687	247/34	14	—	19	~8000	3.5	15.5
0.022	314	46	1314	1392	(1419)	1447	1711	226/44	30	4.2 + 18.7	11	8300	—	15.2
0.027	256	59	1428	1519	(1554)	1590	1892	276/240	87	—	5	440	6.4	12.6
0.023	300	65	1386	1467	(1491)	1516	1760	236/19	17	2.8 + 18.9	25	~9000	2.7	16.5
0.025	276	61	1410	1504	(1532)	1560	1846	256/145	61	2.6 + 8	3	~4100	5.5	13.5

*See Figure A-3 for actual location of temperature measured

+No actual gap temperature was measured, average of T_2, T_3 taken

f/a = fuel/air ratio, T_A = theoretical air, V = approach velocity

due to thermocouple breakdown) should be taken as rough estimates only. Radiation from the bed on both sides of the thermocouple may cause higher temperature readings for the gas phase in the gap.

In general, however, a trend seems to be established in the tests run so far. This is summarized in Figure A-4. Fuel nitrogen to NO_x decreased with fuel/air ratios. Catalyst arrangement 1 had a higher fuel nitrogen conversion at the same fuel/air ratio compared to arrangement 2, as evidenced by the shift in the curves. This is probably due to the more reactive front section in arrangement 1 (more surface area), indicating that too much fuel conversion in the first section may not be desirable. In fact, to achieve comparable NO_x emissions, arrangement 1 required a higher approach velocity (70 ft/s versus 40 ft/s), which lowers fuel conversion, and lower fuel/air ratios which lowers bed temperatures.

The high heat loss in the reactor beds also makes the temperatures in the system generally lower than a comparable adiabatic system. For an adiabatic system, lower front section activity (less surface area or lower catalyst activity) may be more desirable for a given fuel/air to achieve low NO_x emissions. On the other hand, the front section must be sufficiently active to provide some fuel conversion. The interactions of fuel/air ratio, approach velocity, catalyst activity, and bed temperature, however, are difficult to determine from the present data. The effect of gap width cannot

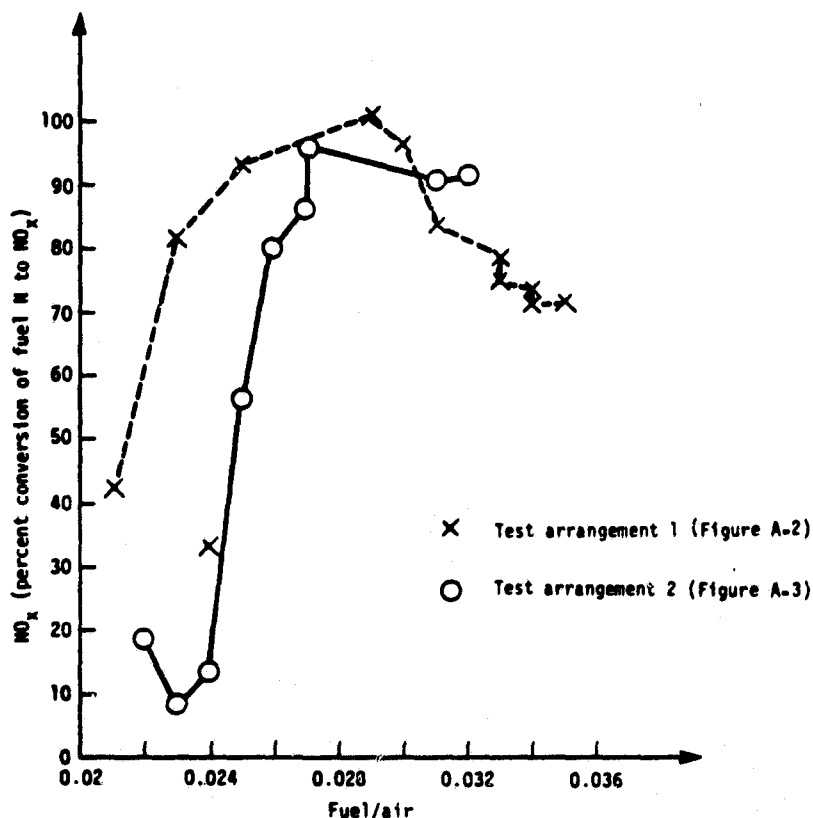


Figure A-4. Fuel nitrogen conversion to NO_x as a function of fuel/air ratio

be assessed since in both arrangements studied, low NO_x conditions were achieved. Although it may be argued that the second arrangement had lower gap residence time due to lower approach velocities and longer gap distance, the front section catalyst activities were not the same, and it is difficult to uncouple all the effects with the current data. The back section of the catalyst bed following the gap is essentially a cleanup section where the fuel and intermediates are fully converted. The high CO and UHC breakthrough seems to indicate that a more reactive second section is required for efficient cleanup under conditions favoring low NO_x .

CONCLUSIONS AND RECOMMENDATIONS

Results from our series of studies indicate that we may indeed have a viable concept for low NO_x production from fuel containing fuel-bound nitrogen. However, a large number of parameters affect system performance. The limited amount of data we have at present does not allow us to uncouple all the viable interactions among key variables. To design a full-scale system for gas turbine applications, we need to be able to scale up from bench-scale results as well as to build in the flexibility of operation required in order to respond to startup, changing loads, and shutdown. More information will therefore be needed around design conditions to see how various parameters affect the results. It is also imperative that more tests be made to confirm our present findings.

There are a number of variables which will most likely affect our system and need to be considered in greater detail, in particular around design conditions.

- Fuel/air ratios—affect system temperature and reactant concentration.
- Approach velocity—affects residence time and therefore conversion as well as temperature.
- Gap distance—determines residence time available for gas-phase reaction in the absence of catalyst.
- Catalyst activity—controls temperature and conversion, particularly important in the front section. A sufficiently active rear section is also needed for efficient cleanup under all conditions.
- System heat balance—how well the system approaches adiabatic conditions may determine how the other variables should vary since heat loss affects system temperatures.
- Others—pressure, fuel type, and nitrogen content may all affect system performance.

Given the large number of parameters that have to be examined, a more comprehensive test program will be required to provide sufficient data for performing a full-scale design.

REFERENCES

1. A.L. Myerson, "The Reduction of Nitric Oxide in Simulated Combustion Effluents by Hydrocarbon Oxygen Mixtures," *Fifteenth Symposium (International) for Combustion*, The Combustion Institute, Pittsburgh, p. 1085, 1974.
2. S.M. Banna and M.C. Branch, "NA₃-NO Reaction in the Post-Flame Region of a Flat Flame Burner," Paper No. 78-50, Fall Meeting, Western States Section, Combustion Institute, Lagunne Beach, CA, October 1978.

Appendix B

ANALYSIS OF SUBSCALE CATALYTIC REACTOR TEST SERIES 1

June 1980

ANALYSIS OF SUBSCALE CATALYTIC REACTOR TESTS

Appendix A discusses tests of a lean-burn catalytic combustor. Acurex Corporation performed the experiments discussed below and identified a two-stage catalytic combustion concept as a potential method for achieving low NO_x emissions while burning fuels containing substantial fuel bound nitrogen. As shown in Figure B-1, fuel is injected into the air upstream of a catalyst bed. This region premixes the fuel and air similar to other purposed catalytic combustion systems. The fuel/air mixture enters a graded cell catalyst bed where chemical reactions begin.

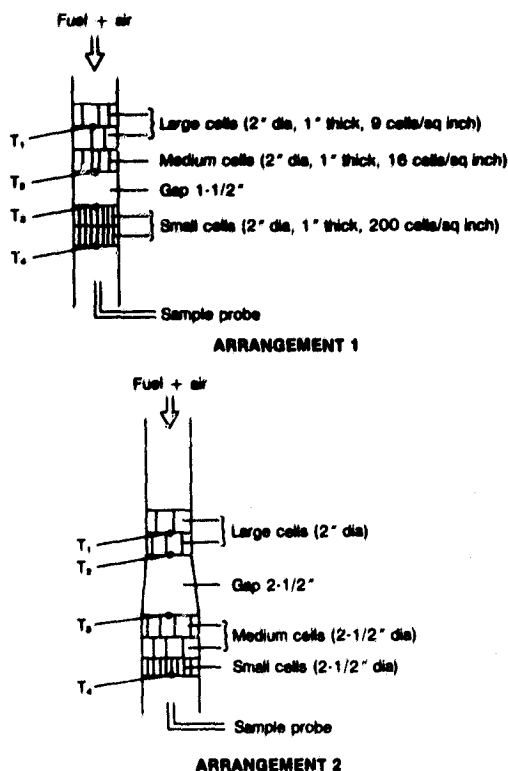


Figure B-1. Schematic of catalyst monolith arrangements 1 and 2

A unique feature of this catalytic system is the gap or homogeneous reaction zone located between the two catalysts. The fuel/air mixture, which partially burns in the upstream catalyst, is held at a high temperature in the gap, to promote homogeneous chemical reactions. This residence time temporarily isolates intermediate combustion species (NO_x , NH_3 , etc.) from a catalytic surface, and given favorable gas tem-

peratures and residence times, will promote reaction of ammonia or other single-nitrogen atom species (NH , NH_2 , HCN) with NO to form N_2 . The chemical reaction mechanism is that of the thermal deNO_x process which was reported by others. Both the NO_x and the intermediate N atom species are formed from the fuel-nitrogen species in the first-stage catalyst bed. In general, the upstream catalyst section will not completely burn the fuel, and a second catalyst bed is required downstream of the gap to consume the remaining fuel species (CO , UHC). Also note that unreacted fuel nitrogen at the downstream end of the gap enters a second catalytic stage which would probably promote conversion of fuel N into NO_x .

Figure B-1 shows two distinct configurations for the gap reactor. The overall performance and the NO_x yield from fuel N depend on the total catalyst bed residence time (gas velocity and bed size) as well as the gap width which, in fact, determines the homogeneous residence time. The fuel/air ratio is important because it controls the burned gas temperature. Acurex tested these variables burning No. 2 fuel oil doped to 0.5 weight percent N for the two catalyst arrangements shown in Figure B-1.

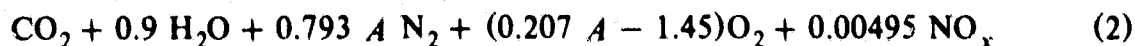
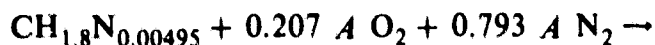
Test data from the two configurations are presented in Tables B-1, B-2 and B-3. Note that all the fuel/air ratios are very lean where one typically expects near unity conversion of fuel N into NO_x , but very low thermal NO_x because of low flame temperatures.

Table B-1 demonstrates the low thermal NO_x and, more importantly, Tables B-2 and B-3 show some operating conditions with exceptionally low yields (14%-40%). These low-yield data were encouraging and were therefore reviewed using an independent analysis to further substantiate the data.

As indicated in Table B-1 through B-3, the yield numbers were calculated by finding the theoretical NO_x for 100% yield using the reported fuel/air ratio with no allowance for thermal NO_x (i.e., thermal NO_x was assumed zero). The latter assumption is justified by the thermal NO_x data (Table B-1) which show that thermal NO_x formation produced less than 10% of the theoretical fuel NO_x . Using these assumptions, the yield is defined as

$$y = \frac{\text{NO}_x \text{ (measured)}}{\text{NO}_x \text{ (theory)}} \quad (1)$$

where NO_x (theory) was calculated from a simplified combustion equation as illustrated below for 0.5 weight percent N .



Where A is the moles of air per mole of fuel defined from the mass fuel air ratio (f/a)

$$\begin{aligned} A &= \frac{\text{mole weight fuel}}{\text{mole weight air}} \frac{1}{f/a} \\ &= \frac{0.481}{f/a} \end{aligned} \quad (3)$$

Table B-1
COMBUSTION RESULTS ON CATALYST ARRANGEMENT 1
(FIGURE B-1), DIESEL

<i>f/a</i>	<i>T</i> <i>A</i> (%)	<i>V</i> (ft/s)	Temperature Distribution*					Emissions						
			Front Section		Gap	Back Section		NO _x (ppm)		NH ₃ + HCN (ppm)	UHC (ppm)	CO (ppm)	CO ₂ (%)	O ₂ (%)
			<i>T</i> ₁	<i>T</i> ₂	<i>T</i> _G	<i>T</i> ₃	<i>T</i> ₄	Theoretical/Actual	Percent Conversion					
0.034	200	30	1325	1444	1065	1565	2196	N.A.†/20	10 XM‡	—	1	50	7	11.8
0.035	200	30	1337	1465	1090	1589	2245	N.A.†/20	—	—	2	50	7	11.6

*See Figure B-1 for actual location of temperature measured
†N.A. = not applicable
‡XM = NO_x + HCN + NH₃
 β/a = fuel/air ratio, TA = theoretical air, V = approach velocity

Table B-2
COMBUSTION RESULTS ON CATALYST ARRANGEMENT 1 (FIGURE B-1),
DIESEL + PYRIDINE

<i>f/a</i>	<i>T_A</i> (%)	<i>V</i> (ft/s)	Temperature Distribution*				Emissions								
			Front Section		Gap	Back Section		NO _x (ppm)			NH ₃ + HCN (ppm)	UHC (ppm)	CO (ppm)	CO ₂ (%)	O ₂ (%)
			<i>T₁</i>	<i>T₂</i>	<i>T_G</i>	<i>T₃</i>	<i>T₄</i>	Theoretical/Actual	Percent Conversion	Yield N/C					
0.029	240	40	—	—	—	—	2266	294/300	102	—	3	50	6.7	12.4	
0.029	240	36	1471	1576	(1259)†	1647	2197	294/300	102	—	—	30	6.6	12.5	
0.029	240	36	1377	1681	1560	1752	2270	294/300	102	—	6	30	6.8	12.0	
0.03	230	53	1404	1786	1831	1838	2227	310/300	97	—	5	40	6.9	12.0	
0.034	200	53	1221	1679	1548	1634	2224	350/260	74	—	30	50	7.5	11.0	
0.033	210	55	1227	1695	1650	1644	2183	334/250	75	—	20	40	7.4	11.5	
0.033	210	63	1243	1744	1769	1691	2220	334/260	78	—	13	50	7.5	11.5	
0.034	200	72	1271	1806	1938	1765	2229	350/250	71	—	7	30	7.2	11.5	
0.035	200	82	1275	1802	1995	1750	2232	350/250	71	—	7	60	7.2	11.5	
0.03	230	67	1284	1827	—	1867	2393	310/260	84	—	4	50	7.5	10.7	
0.025	280	72	1225	1637	1628	1681	2010	252/235	93	—	3	70	6.3	12.3	
0.023	300	72	1172	1454	1476	1552	1710	235/190	81	—	31	1540	5.5	13.5	
0.021	330	70	1114	1376	1363	1432	1555	215/90	42	—	1500	1030	1.4	18.0	
0.024	290	69	1163	1436	1407	1495	1630	244/80	33	—	3000	1510	2.3	17.4	
										EQN 6					

*See Figure B-1 for actual location of temperature measured

*See Figure B-1 for actual location of temperature measured
†The actual gap temperature was measured, average of *T₂*, *T₃* taken
f/a = fuel/air ratio, *T₁* = theoretical air, *V* = approach velocity

Table B-3
COMBUSTION RESULTS ON CATALYST ARRANGEMENT 2 (FIGURE B-1),
DIESEL + PYRIDINE

ϕ/a	TA (%)	V (ft/s)	Temperature Distribution*					Emissions								
			Front Section		Gap	Back Section		NO _x (ppm)			NH ₃ + HCN (ppm)	UHC (ppm)	CO (ppm)	CO ₂ (%)	O ₂ (%)	
			T ₁	T ₂	T _G [†]	T ₃	T ₄	Theoretical/Actual	Percent Conversion	Yield N/C						
0.032	215	37	1374	1475	(1518)	1561	2097	326/300	92	84	—	5	>1200	7.1	11.5	
0.031	222	38	1380	1475	(1517)	1559	2003	320/290	91	82	—	4	>1200	7.0	11.5	
0.027	256	43	1338	1440	(1476)	1513	1860	276/260	96	81	—	2	510	6.4	12.0	
0.026	265	40	1329	1412	(1440)	1469	1781	274/220	80	75	—	12	—	5.9	13.5	
0.024	287	44	1300	1368	(1399)	1430	1687	247/34	14	16	—	19	-8000	3.5	15.5	
0.022	314	46	1314	1392	(1419)	1447	1711	226/44	30	20	4.2 + 18.7	11	8300	—	15.2	
0.027	256	59	1428	1519	(1554)	1590	1892	276/240	87	75	—	5	440	6.4	12.6	
0.023	300	65	1386	1467	(1491)	1516	1760	236/40	17	22	2.8 + 18.9	25	-9000	2.7	16.5	
0.025	276	61	1410	1504	(1532)	1560	1846	256/145	61	50	2.6 + 8	3	-4100	5.5	13.5	
											EQN 6					

*See Figure B-1 for actual location of temperature measured.
†T_G is actual gas temperature; see measured average of T₁, T₂, T₃, and T₄.

*See Figure B-1 for actual location of temperature measured

†No actual gap temperature was measured, average of T_2 , T_3 taken ϕ/a = fuel/air ratio, TA = theoretical air, V = approach velocity

Substituting into Equation 1

$$Y = \frac{\frac{\text{NO}_x (\text{measured})}{0.00495 (f/a)}}{0.45 (f/a) + 0.481} \quad (4)$$

Consequently, the tabulated yield depends on both the measured NO_x as well as the measured fuel/air ratio which could introduce substantial error into the reported yield.

A second method for evaluating the yield was used as an independent check on the Acurex data. This method is independent of the fuel/air ratio, but uses the measured CO_2 and CO . Carbon atoms are used as a tracer species for the fuel nitrogen. The fuel analysis specifies a nitrogen atom to carbon atom ratio (Equation 2; $C=1$, $N=0.00495$) in the fuel. The fuel carbon is converted into CO and CO_2 in the burned gas, and a portion of the fuel N is converted into NO_x . Thus, in the burned gas, the nitrogen atom to carbon atom ratio is measured as

$$\frac{\text{NO}_x (\text{ppm measured})}{(\text{CO} + \text{CO}_2 + \text{UHC}, \text{ppm measured})} \quad (5)$$

where both the carbon species and the NO_x must contain the same sample moisture, i.e., either wet or dry measurements for all species. Assuming zero thermal NO_x similar to the first method, the yield of NO_x from fuel N is expressed as

$$Y = \frac{\frac{\text{NO}_x (\text{ppm measured})}{(\text{CO}_2 + \text{CO} + \text{UHC}) \text{ ppm measured}}}{\text{N/C fuel analysis}} \quad (6)$$

Thus, carbon atoms are a tracer species because both the fuel analysis and the burned gas analysis measure every carbon atom. Equation 6 is then the yield because the fuel analysis measures all fuel nitrogen and the exhaust gas measures only those N atoms converted into NO_x in the flame. Note that this method is unaffected by sample dilution because both the NO_x and the carbon species are diluted by the same factor. Consequently, air leaking into the sample line does not alter the calculated yield.

Figure B-2 is a plot of the yield reported by Acurex (Equation 4) versus that calculated using the carbon atom tracer method (Equation 6). For high yields ($Y > 50\%$), reasonable agreement was demonstrated, with the latter method (Equation 6) generally showing slightly lower yields. However, the four points with very low and encouraging yields did not follow this same trend, as shown in Figure B-2. However, all four points were found to be in agreement with the remainder of the data by checking the reported fuel/air ratio with the measured O_2 and CO_2 data (Tables B-2 and B-3) and corrected data, accordingly.

It should be noted that the UHC measurements from the tests are referenced to propane (C_3H_8) so that the number of moles of carbon atoms from the UHC measurements must be multiplied by three when used in Equation 6. Based upon the UHC ppm measured, as shown in Tables B-2 and B-3, the effect is very small except for the two test points where the UHC was very high at 1500 and 3000 ppm.

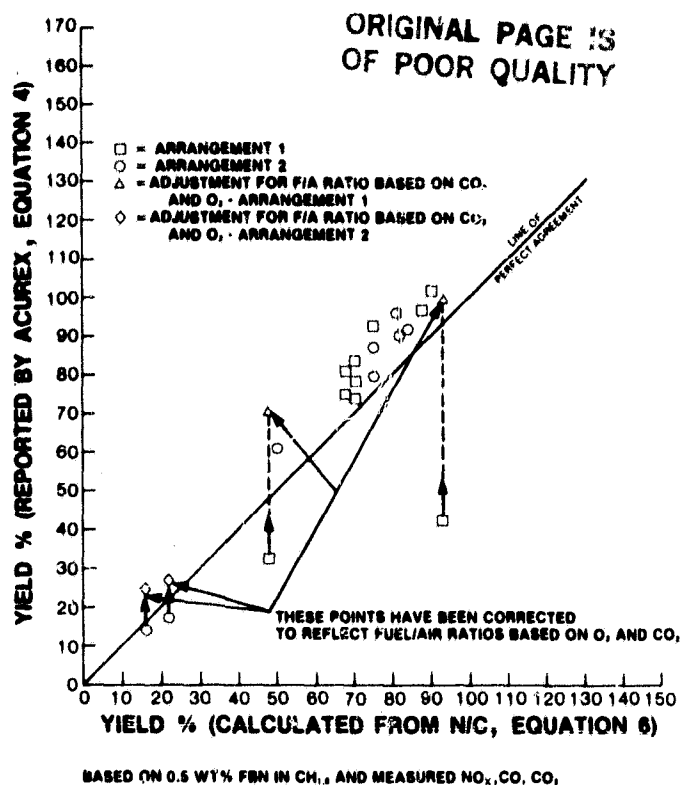


Figure B-2. Yield reported by Acurex vs. yield from N/C reported

Equation 2 was used to calculate the theoretical dry-sample mole fractions of oxygen and carbon dioxide in the burned gas as a function of the fuel/air ratio. Figure B-3 is a cross plot of O₂ and CO₂ for variable fuel/air ratios. As shown, the data (Tables B-1, B-2, B-3) fall along the curve which confirms the instrument operation and the assumed fuel composition. However, this plot does not analyze the possibility of air leaking into the sample line because excess air simply changes the fuel/air ratio which moves the points along the theoretical line.

Figure B-4 compares the reported fuel/air ratio with the reported O₂ and CO₂ values. The theoretical lines are also shown. Most of the data agree well with the theoretical lines, but the lower yield points do not. The reported fuel/air ratio is higher than that implied by the CO₂ and O₂ data. One possibility is air diluting the sample, thereby decreasing the gas sample fuel/air ratio and diluting the NO_x. This decreases the yield calculated by Equation 4, which is consistent with the deviation shown in Figure B-2. Subsequently, the yield obtained from these four points was re-calculated using Equation 6, but a fuel/air ratio consistent with the reported O₂ and CO₂. The corrections are shown in Figure B-2 and make these data consistent with the previous.

The above comparison corroborated the original catalytic yield data, which showed the potential for low NO_x. This analysis has also corrected several yields. Additional experimental work will explore catalytic operation at the low-yield conditions.

ORIGINAL PAGE IS
OF POOR QUALITY

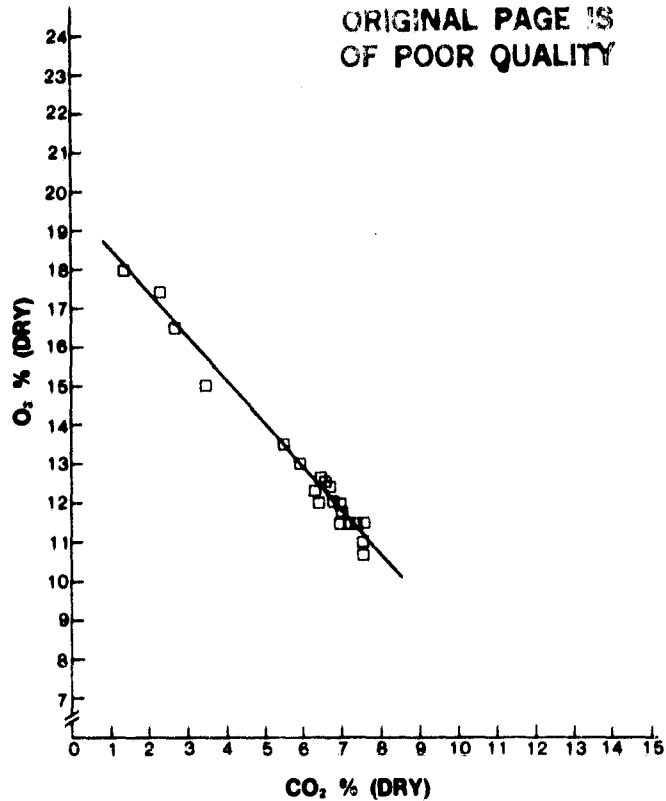


Figure B-3. Measured O_2 vs. CO_2

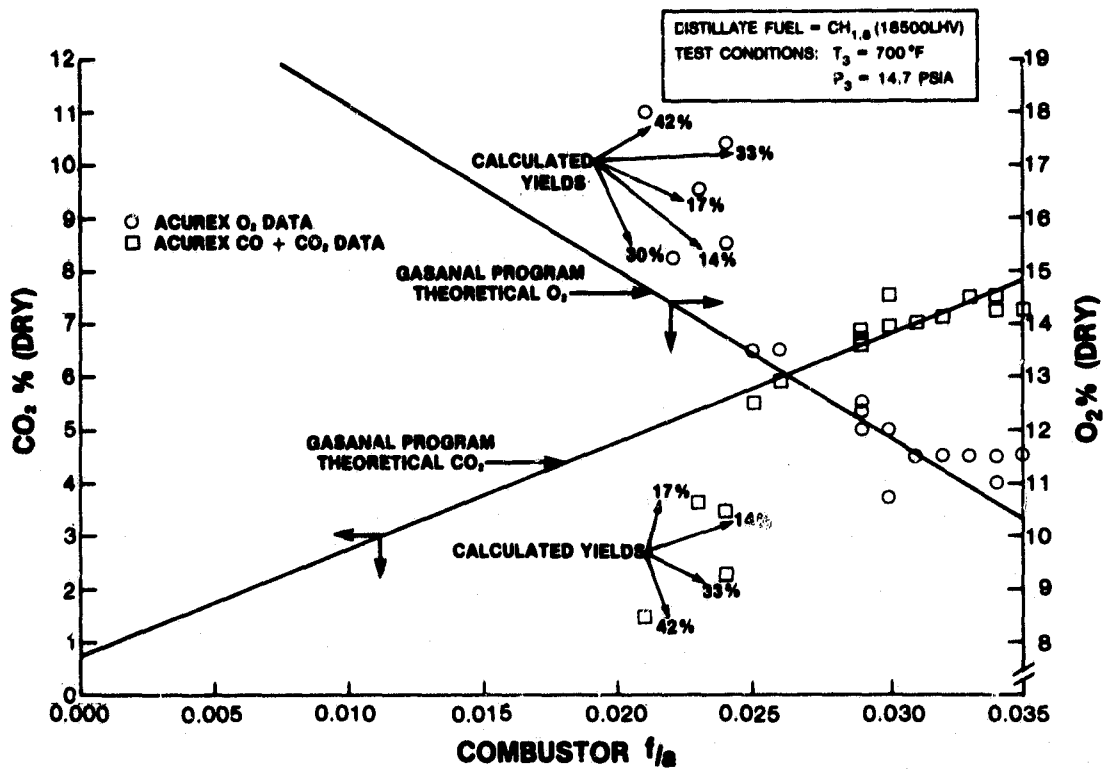


Figure B-4. Comparison of theoretical vs. measured CO_2 and O_2

Appendix C

**LOW NO_x HEAVY FUEL COMBUSTOR CONCEPT PROGRAM
REPORT - FURTHER RESULTS ON A LOW NO_x
LEAN BURN CATALYTIC COMBUSTION CONCEPT**

TEST SERIES 2

October 7, 1980

**Prepared for
General Electric Company
Gas Turbine Division
1 River Road
Schenectady, New York 12345**

**Prepared by
G. Snow and H. Tong
Acurex Corporation
Energy and Environmental Division
485 Clyde Avenue
Mountain View, California 94042**

Appendix C

LOW NO_x HEAVY FUEL COMBUSTOR CONCEPT PROGRAM REPORT - FURTHER RESULTS ON A LOW NO_x LEAN BURN CATALYTIC COMBUSTION CONCEPT

INTRODUCTION

The objective of the present program was to evaluate the effectiveness of a gapped bed, catalytic reactor concept for controlling NO_x emissions from the combustion of nitrogen-containing fuels. This appendix describes a series of tests which are a continuation of those described in an earlier memorandum.

In the earlier tests, data were obtained for two different configurations in which pyridine-doped diesel fuel was catalytically combusted. These tests showed that under certain fuel/lean conditions a gapped reactor could burn nitrogenous fuels in such a way that measured NO_x emissions were moderately low. Simultaneously with low NO_x emissions, however, generally high hydrocarbon emissions were also measured.

Since the previous test series was exploratory and the results indicated a potential for low NO_x emissions, the test series described below were conducted to verify the original low NO_x behavior and to gain some indications of the effect of pressures greater than one atmosphere. Simultaneously, it was believed that additional catalyst length would complete the hydrocarbon burnout and yield conditions of low NO_x emissions and high combustion efficiency.

METHOD OF APPROACH

The catalytic reactor test configuration was similar to that described earlier but with some adjustments. Figure C-1 is a sketch of the reactor arrangement including the thermocouple locations. Here the test section was nominally 2 in. in diameter and incorporated a 2 in. gap following two large cell segments (1 in. length for each segment). The earlier configurations used 1.5 in. and 2.5 in. gap lengths. Additional fine cell segments were installed to bring the total length of the second stage to 6 in. The extra segments were to ensure the burnoff of remaining hydrocarbons and carbon monoxide following the deNO_x reactions in the gap. Some data were also taken with only a single large cell segment in the first stage, giving a first-stage length of 1 in. This was to check the possibility that excessive oxidation in the reactor first stage would deplete the pool of intermediate species (CO, CH_x, CH, NO_x) and prevent an efficient deNO_x process in the gap.

The catalytic reactor was installed in the Acurex subscale 3 atmosphere test facility as before. Exhaust gas composition was monitored continuously with gas analyzers. A chemiluminescent analyzer was used to measure nitric oxide (NO). Comparative measurements of total NO_x (NO + NH₂) have been taken to verify the existence of NO as the only NO_x species. Some conditions at which the NO concen-

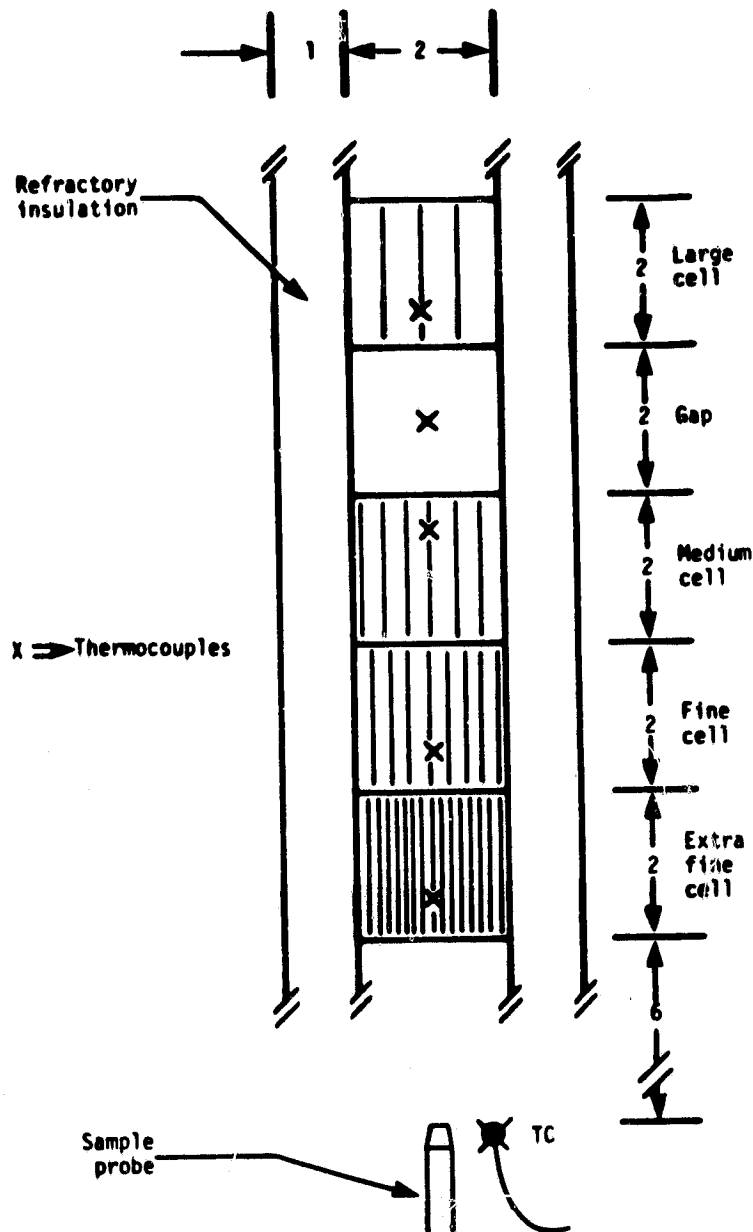


Figure C-1. Catalytic reactor arrangement

tration was low were accompanied by measurements of ammonia (NH_3) and hydrogen cyanide (HCN) using an ion-specific electrode technique.

The test fuel was No. 2 diesel that was doped with pyridine to give a total fuel nitrogen content of 0.524% by weight. The original diesel and the final mixture have the following elemental compositions:

	No. 2 Diesel	Diesel + Pyridine
C	86.52% by mass	86.22% by mass
H	12.82	12.64
N	0.025	0.524
S	0.250	0.248
O	0.38	0.37

The test conditions examined were

Combustor pressure	1.5-3 atm
Catalyst inlet temperature	700-970 °F
Actual inlet velocity	40-55 ft/s
(Fuel/air) by mass	0.016-0.034

The minimum housing test pressure was 8 psig due to the back pressure imposed by the exhaust heat exchanger and valve hardware necessary for 3 atmosphere operation.

RESULTS AND DISCUSSION

The catalytic reactor configuration was very stable in operation and gave combustion efficiencies in excess of 99.9% except at the leanest conditions ($f/a < 0.022$). Unfortunately, the desired low fuel nitrogen conversion to NO_x could not be achieved simultaneously with high combustion efficiency. The test results are summarized in Tables C-1, C-2, and C-3. Table C-1 gives some of the data from the earlier testing that was described in Appendix A. Here, those data have been reduced in a manner identical to the present data so that comparisons may be made on an equal basis. The results of the present testing are presented in Tables C-2 and C-3, the latter being the single-segment first-stage configuration.

Data were collected over wide ranges of preheat temperatures, reference or approach velocities, and fuel/air ratios as shown in the data tables. Fuel nitrogen conversion to NO remained high ($\sim 80\%$) in all cases except where overall combustion efficiency was low. Generally, at fuel/air ratios below 0.021, combustion was unstable and incomplete. At this condition, the combination of low NO, high unburned hydrocarbon, and near-zero levels of NH_3 and HCN concentrations led to the conclusion that much of the pyridine nitrogen passed through the reactor essentially unchanged or at least bound to some form of hydrocarbon, either of which is measured by the hydrocarbon analyzer. Every attempt to fully consume the carbon monoxide and unburned hydrocarbons through variation of the available parameters resulted in the high conversion of this nitrogen to NO.

Figures C-2 through C-6 illustrate the fuel nitrogen behavior and combustion efficiency over the test matrix. Figure C-2 gives the nominal test condition of 700 °F preheat and 52 ft/s actual approach velocity. Since the test section pressure was 8 psig, 52 ft/s corresponds to 80 ft/s at 1 atmosphere. Both combustion efficiency and

ORIGINAL PAGE IS
OF POOR QUALITY

Table C-1
PREVIOUS TEST RESULTS (1-12-80)

Data Point	Date	Housing Press (mg)	V _{ref} at Actual Conditions (l/s)	Air (scfm)	Percent T ₄	(f/a) _m	NO Measured (ppm)	NO Theoretical (ppm)	FN Conversion (%)	NH ₃ (ppm)	HCN (ppm)	Carbon Conversion to CO ₂ (%)	Combustion Efficiency %	T _{gap} (%)	T _{avg} Across Gap (°F)	T _{max} (°F)	T _{ad} (°F)	Preheat T _p (°F)
13B	1-12	0	70		501	0.014	90	131	68	•	•	94.8	47.17	1363		1555	•	700-800
14B			69		443	0.016	80	149	54			73.1	7.6	1407		1636		
10B			67		201	0.035	260	334	77.8			100	99.94			2393	2781	
4B			53		218	0.032	300	307	97.6			100	99.90			2227		
4C			40		254	0.028	259	263	83.7			99.9	99.80		1440	1781	2425	
5C			44		346	0.020	34	192	17.7			99.9	90.91		1399	1687		
8C			65		412	0.017	19	161	11.8	3	19	99.8	87.69		1491	1760		

*Note: Blank table entries indicate unmeasured or uncalculated parameters

Table C-2
PRESENT TEST RESULTS, TWO SEGMENT FIRST STAGE

Data Point	Date	Housing Press (psig)	V_{ref} at Actual Conditions (ft/s)	Air (scfm)	$(f/a)_m$	NO Measured (ppm)	NO Theoretical (ppm)	FN Conversion (%)	NH ₃ (ppm)	HCN (ppm)	Carbon Conversion to CO, CO ₂ (%)	Combustion Efficiency η (%)	T_{gap} (°F)	T_{avg} Across Gap (°F)	T_{max} (°F)	T_{ad} (°F)	Preheat T_p (°F)
2	8-18	7	39	32	0.025						99.9	99.65	1500	1766	2259		800
3		7	39	32	0.024						100	99.81	1600	1838	2273		800
4		7	39	32	0.024						100	99.81	1500	1875	2261		790
5		8	52	48	0.025						100	99.88	1060	1480	2250		700
6		8	52	48	0.025						100	99.88	1007	1444	2250		694
1	8-19	9	52	48	0.024	230	271	84.7	0	0	100	99.97	1140	2230	2230		755
2			51	48	0.023	220	260	84.5	0	0	100	99.96	1067	2280	2280		726
3			50	48	0.023	210	251	83.7	0	0	100	99.86	960	2040	2111		711
4			50	48	0.023	210	251	83.7	0	0	100	99.91	953	2000	2000		712
5			50	48	0.028	260	308	84.5	0	0	100	99.97	996	2380	2380		706
6			51	48	0.028	270	313	86.4	0	0	100	99.98		2394	2394		718
7			50	48	0.030	300	339	88.5	0	0	100	99.98		2540	2540		712
8			50	48	0.033	300	365	82.2			100	99.99		2630	2630		738
9			51	48	0.033	310	365	84.9			100	99.98		2662	2662		
1	8-22	8	52	48	0.028	260	308	84.5			100	99.98	1170	2330	2330	2388	706
2			52	48	0.027	235	303	77.6			100	99.97	1140	2322	2322	2375	708
3			52	48	0.028	245	308	79.5			100	99.97	1130	2250	2250	2388	702
4			52	48	0.027	245	297	82.5			100	99.97	1130	2290	2290	2350	699
5			52	48	0.022	200	241	83.1			100	99.73	1130	2026	2026		718
6			52	48	0.021	195	237	82.3			100	99.51	1120	1970	1970		718
7			52	48	0.022	195	241	80.9			100	99.61	1130	1980	1980		720
8			52	48	0.016	16	180	8.9			84.4	78.79	1010	1680	1680		696
9			58	48	0.023	205	252	81.4			99.6	99.53	1160	1870	1870		824
10			58	48	0.022	205	246	83.3			99.7	99.62	1160	1920	1920		828
11			58	48	0.020	76	222	34.3	3	8	97.5	88.28	1130	1750	1750		827
12			58	48	0.020	96	219	43.9			98.0	90.40	1120	1760	1760		829
13			58	48	0.019	40	212	18.8			94.0	83.91	1110	1700	1700		828
14			58	48	0.019	207	207	12.6	2	11	92.4	81.74	1105	1700	1700		826
15			58	48	0.019	32	207	15.4			92.5	81.65	1104	1700	1700		826
16			64	48	0.017	94	186	50.4			97.4	92.00	1210	1800	1800		960
17			64	48	0.017	86	183	47.0	1	3	97.1	91.24	1197	1750	1750		966
18			64	48	0.016	100	182	55.0			97.9	93.28	1208	1830	1830		970

Continued

ORIGINAL PAGE IS
OF POOR QUALITY

Table C-2
PRESENT TEST RESULTS, TWO SEGMENT FIRST STAGE (Cont'd)

Data Point	Date	Housing Press (psig)	V_{ref} at Actual Conditions (ft/s)	Air (scfm)	$(f/a)^2_m$	NO Measured (ppm)	NO Theoretical (ppm)	FN Conversion (%)	NH ₃ (ppm)	HCN (ppm)	Carbon Conversion to CO ₂ (%)	Combustion Efficiency η (%)	T_{gap} (N)	T_{avg} Across Gap (°F)	T_{max} (°F)	T_{ad} (°F)	Preheat T_p (°F)
1	8-29	8	32	28	0.026	235	292	80.4			100	99.95	1782	1932	2271	2343	749
2			30	28	0.023	205	261	78.5			100	99.89	1290	1528	2020		695
3			31	28	0.020	175	226	77.3			100	99.50	1160	1485	1780		727
4			32	28	0.020	20.5	219	9.4			95.5	79.23	1100	1345	1540		748
5			32	28	0.025	115	284	40.6			98.9	91.25	1146	1414	1670	2313	768
6			29	25	0.022	195	246	79.3				99.77	1220	1530	2020		773
7			27	23	0.019	165	211	78.1				99.27	1140	1443	1770		775
8			27	23	0.019	98	208	47.2			98.5	90.13	1100	1355	1630		790
9			20	17	0.021	200	238	83.9				99.81	1300	1504	1987		776
10			15	13	0.022	205	240	85.5			99.97	99.89	1450	1580	1983		758
11			15	13	0.019	160	206	77.8				99.37	1160	1387	1787		753
12			16	14	0.023	200	251	79.7				99.84	1743	1662	2063		760
13			23	20	0.024	225	266	84.7				99.91	1800	1841	2158		786
14			23	20	0.029	280	323	86.6				99.97	2200	2085	2380	2488	792
15			54	45	0.027	260	298	87.2				99.97	1500	1740	2335	2438	834
16		30	28	45	0.026	245	292	83.8				99.94	2270	2098	2355		870
17			27	44	0.030	290	333	87.0				99.94	2400	2320	2450	2613	858
18			28	44	0.030	280	333	84.1				99.95	2300	2260	2400	2613	860
19			25	44	0.022	200	245	81.6				99.93	1600	1710	2057		716
20			26	44	0.022	195	241	81.0				99.92	1600	1685	2003		802
21			26	44	0.018	140	202	69.2			99.95	98.91	1200	1387	1760		800
22			26	44	0.020	60	223	26.9			98.2	84.50	1100	1345	1550		786

Table C-3
PRESENT TEST RESULTS, SINGLE SEGMENT FIRST STAGE

Data Point	Date	Housing Press (psig)	V_{rel} at Actual Conditions (ft/s)	Air (scfm)	$(f/a)_m$	NO Measured (ppm)	NO Theoretical (ppm)	FN Conversion (%)	NH_3 (ppm)	HCN (ppm)	Carbon Conversion to CO, CO_2 (%)	Combustion Efficiency %	T_{gap} (%)	T_{avg} Across Gap (°F)	T_{max} (°F)	T_{ad} (°F)	T_p (°F)	Preheat T_p (°F)
1	9-2	8	20	17	0.022	190	247	77.0			99.93	99.49	1650	1698	2163	2463	782	782
2			20	17	0.028	235	313	75.2			99.96	96.33	2100	1939	2325	2463	772	772
3			20	17	0.038	250	429	58.3			99.95	86.46	2300	2120	2470	2950	781	781
4			19	17	0.021	130	233	55.7			99.16	92.72	1043	1361	1691	2950	759	759
5			15	13	0.026	235	291	80.7			52.97	99.10	1928	1816	2263	2338	741	741
6			15	13	0.033	260	370	70.2			99.98	93.77	2293	1935	2365	2713	760	760
7			14	13	0.022	190	242	78.5			99.97	99.47	1060	1389	2122	2363	727	727
8			30	26	0.026	240	288	83.4			99.98	99.69	2000	1914	2300	2363	792	792
9			30	26	0.034	290	378	76.8			99.99	94.28	2300	2115	2500	2763	796	796
10			30	26									1000	1310	1500		793	793
11			36	32	0.027	300	304	98.7			99.97	99.68	2002	2016	2280		900*	900*
12			36	32	0.031	320	345	92.7			100.00	99.68	1900	2045	2433	2588	751	751
13			47	40	0.033	290	367	79.0			99.84	99.74	2100	2063	2578	2719	800	800
14		11	48	45	0.031	270	345	78.2			99.91	99.85	2120	2075	2532	2650	835	835
15		14	55	57	0.030	260	335	77.7			99.94	99.87	1900	2023	2490	2608	837	837
16		30	36	57	0.031	270	344	78.6			99.97	99.95	2340	2213	2555	2675	875	875
17		30	36	57	0.033	300	365	82.2			99.98	99.96	2569	2350	2640	2775	883	883
18		30	35	57	0.023	150	254	59.0			99.14	75.48	1095	1448	2000		852	852

*Upstream flameholding

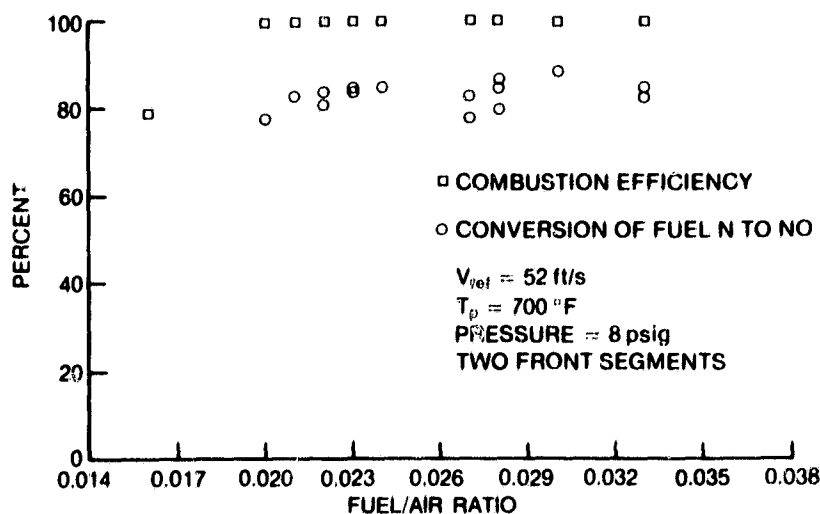


Figure C-2. Fuel N conversion and combustion efficiency vs fuel/air—two first-stage segments

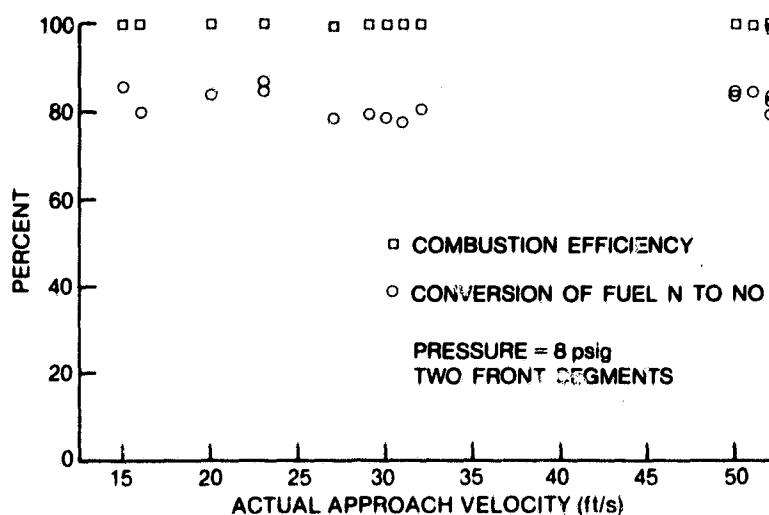


Figure C-3. Fuel N conversion and combustion efficiency vs approach velocity at actual conditions—two first-stage segments

nitrogen conversion are high over the range of fuel/air ratios shown. Note also that these parameters are independent of the fuel/air ratio except at the lean limit. The highest fuel/air ratio is bound by the maximum temperature capability of the catalytic reactor. Figure C-3 indicates that the actual approach velocity has little effect on the conversion of reactants over the range investigated. At the leanest test conditions where combustion is incomplete, the effect of preheat temperature is shown in Figure C-4. As expected, both combustion efficiency and nitrogen conversion show a monotonic increase with preheat.

ORIGINAL PAGE IS
OF POOR QUALITY

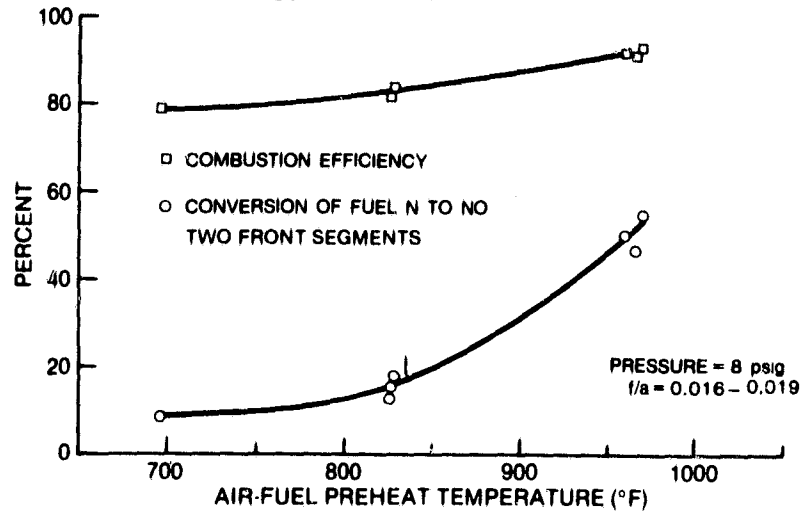


Figure C-4. Fuel N conversion and combustion efficiency vs preheat temperature at lean limit of combustor stability—two first-stage segments

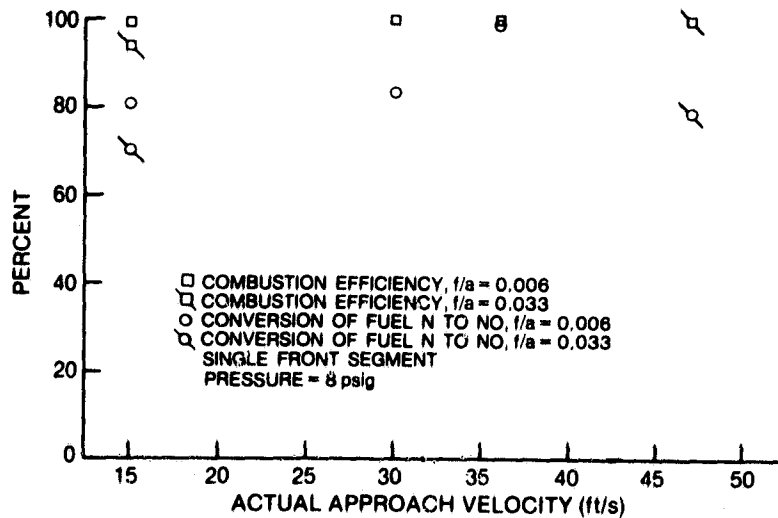


Figure C-5. Fuel N conversion and combustion efficiency vs approach velocity at actual conditions—single first-stage segment

Data taken on the reactor with only a single first-stage segment are plotted in Figures C-5 and C-6. Many of the same observations are applicable here as well. However, both combustion efficiency and nitrogen conversion appear to be slightly lower than the first configuration. This may be due to an insufficient length of large-cell monolith to effectively preheat the bulk reactant stream, or it may be attributed simply to catalyst aging and/or deactivation. Data taken at 1.75, 1.95, and 3.0 atmospheres combustor pressure are also shown in Figure C-6. This variation in combustor pressure has little effect on the results.

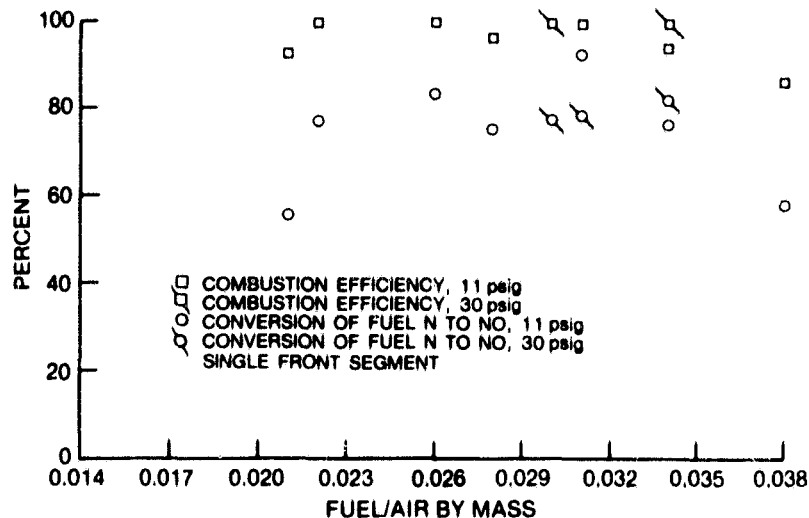


Figure C-6. Fuel N conversion and combustion efficiency vs f/a—single first-stage segment

CONCLUSIONS AND RECOMMENDATIONS

The present reactor configuration was shown to be unsuccessful in significantly reducing NO emissions from fuel-bound nitrogen while simultaneously achieving high combustion efficiency. It is probable, however, that a successful demonstration of the concept will follow after a thorough investigation of such factors as gap residence time, gap temperature, amount of catalyst surface area available in the first stage, and possibly catalyst type.

In reviewing the data taken earlier and reported January 12, 1980, it is apparent that those points at which the NO measurement was low were accompanied by high concentrations of unburned hydrocarbons or carbon monoxide. This is consistent with the current results. Two of the earlier data points did show a low unburned hydrocarbon concentration simultaneously with a low NO level which cannot be fully explained. It seems unlikely that the fuel-bound nitrogen has been converted to N_2 since many other data points at near identical conditions do not verify this. Two possibilities are that the nitrogen is contained in some unmeasured compound, or that the nitrogenous hydrocarbons were removed along with condensables in the emissions bench gas conditioner.

Although the present results were not positive, the constraints of time and budget did not allow a thorough evaluation of the concept. Suggestions for further work include supplementing the experimental effort with an analytical study to help define those conditions under which the $deNO_x$ process is favored. The Acurex PROF and PROF-HET computer codes may be useful if the proper chemical kinetic constants for the nitrogen mechanism are available. Further experimental work should include gas sampling from various distances behind the first-stage catalyst coupled with variable first-stage configurations. This would be followed by the

identification of the second-state catalyst to complete the energy release from the fuel. Finally, some studies should be conducted with real nitrogenous fuels instead of pyridine-doped diesel to determine the effect of nitrogen binding or conversion to NO_x .